WCIO 2015

NEW YORK CITY | 6-9 MAY

CONFERENCE PROGRAM

6–9 MAY 2015 | HILTON NEW YORK
NEW YORK CITY
#WCIO2015

Brought to you by
WCIO
Advancing Interventional Oncology

COVIDIEN

positive results for life™

Emprint™ Ablation System
with Thermosphere™ Technology

Learn more about the breakthrough technology that is only a part of this ablation system at Booth #103

FIELD CONTROL + THERMAL CONTROL + WAVELENGTH CONTROL = THERMOSPHERE™ TECHNOLOGY

Visit Covidien at Booth 103.

http://surgical.covidien.com/products/ablation-systems

CONTENTS

Welcome to New York City for WCIO 2015.

The WCIO Conference Program Committee has worked alongside session moderators, WCIO leadership, and staff to prepare the leading interventional oncology (IO) meeting, bringing together medical experts from around the world for a multidisciplinary approach.

WCIO 2015 is a unique conference developed by a global team of experts from multiple specialties, to further the goal of cross-disciplinary collaboration and education. The meeting provides remarkable educational opportunities that span private practice, hospital, and institutional settings.

WCIO 2015 highlights include:

- Expanded Tumor Boards
- HCC Part I and II: Best of APSCVIR
- Palliative Care/Symptom Management Session
- Old Cancers, New Treatments Session
- Comparative Effectiveness in Interventional Oncology Session
- Program for Early Career Interventional Oncologists
- Selected Abstracts Presented at Plenary Sessions
- Hands-On Scientific Workshops

Medical students, residents and fellows, advanced practice providers, IO experts, and less experienced operators alike are participating in this truly dynamic learning and networking experience. We look forward to engaging with you to discuss available and emerging therapies in the field.

This is your opportunity to explore best practices as well as new discoveries. Leave WCIO 2015 with insights and strategies for the fight against cancer in your own practice, hospital, or institution.

Please visit **www.io-central.org** to join our interventional oncology community if you are not already a community member. We look forward to meeting with you this week and are excited you have joined us for this extraordinary event.

Welcome to New York!

The WCIO 2015 Program Committee

Hyun S. "Kevin" Kim, MD
Program Chair
University of Pittsburgh
Pittsburgh, Pennsylvania, USA

Constantinos T. Sofocleous, MD, PhD
Scientific Chair
Memorial Sloan Kettering Cancer Center
New York, New York, USA

Matthew Callstrom, MD, PhD
Workshop Chair
Mayo Clinic
Rochester, Minnesota, USA

Matthew Kennedy
Allied Health Program Chair
Memorial Sloan Kettering Cancer Center
New York, New York, USA

Riccardo A. Lencioni, MD
Early Career Program Chair
Pisa University School of Medicine
Pisa, Italy

J. F. Geshwind, MD
Yale University School of Medicine
New Haven, Connecticut, USA

Christiane Kuhl, MD
Klinikum Aachen (University Hospital Aachen)
Aachen, Germany

Robert Lewandowski, MD
Northwestern University
Chicago, Illiinois, USA

David C. Madoff, MD
Weill Cornell Medical College
New York, New York, USA

The WCIO Program Committee would like to thank all those who participated in the abstract review process. Without your diligent work, WCIO 2015 would not be possible.

Muneeb Ahmed, MD
Ed Boas, MD, PhD
Matthew Callstrom, MD, PhD
Sohail Contractor, MD
Jacob Cynamon, MD
Alban Denys, MD
Christos Georgiades, MD, PhD
S. Nahum Goldberg, MD
Kelvin Hong, MD
Tobias F. Jakobs, MD
Nadine Abi Jaoudeh, MD
Alexis Kelekis, MD, PhD
Hyun S. "Kevin" Kim, MD
Christiane Kuhl, MD
Fred Lee, MD
Riccardo A. Lencioni, MD
David C. Madoff, MD
Todd Schlachter, MD
Constantinos T. Sofocleous, MD, PhD
Michael C. Soulen, MD
Robert Suh, MD
Hooman Yarmohammadi, MD

If there was an award, we'd win it.

The Acculis Microwave Tissue Ablation System is the only single applicator system to complete a spherical 5 cm ablation in six minutes.†

Watch an animation of the Acculis MTA System
at www.angiodynamics.com

acculis
Microwave Tissue Ablation System

angiodynamics

†Based on 140 W, 6 min. ex-vivo bovine study—liver; +/- 0.5 cm. Bench Test results may not necessarily be indicative of clinical performance.

Hoffmann R, Rempp H, Erhard L, Blumenstock G, Pereira PL, Claussen CD, Clasen S. Comparison of four microwave ablation devices: an experimental study in ex-vivo bovine liver. Radiology. 2013 Jul;268(1):89-97.

Acculis Accu2i pMTA 510-245

INDICATIONS FOR USE: The Accu2i pMTA Applicator with Sulis VpMTA Generator Software release 2.1.0 is indicated for intraoperative coagulation of soft tissue.

CONTRAINDICATIONS: The Accu2i pMTA Applicators are contraindicated in patients with heart pacemakers and other electronic device implants.

CAUTION: Federal (USA) law restricts this device to sale by or on the order of a physician.

Refer to instructions provided with product for all contraindications, warnings and potential complications.

IO University

On-Demand Education for the IO Professional

Discover the in-depth IO curriculum, best practices, and industry advances for every stage of your career in Interventional Oncology.

- Access industry hot topics through live and recorded webinars
- Earn CME credit and develop your career
- Access recorded proceedings of past WCIO events
- Gain insights from expert faculty within the field
- Participate in the IO curriculum to gain insights into the fundamentals of oncology

Introducing the IO Curriculum

Advance your understanding of the fundamentals of oncology as it applies to IO through the IO Curriculum. Incorporate IO into existing treatment offerings and modalities within various oncology settings, including academic institutions and community clinical settings.

Try our first module, “Language of Oncology” for **free!**

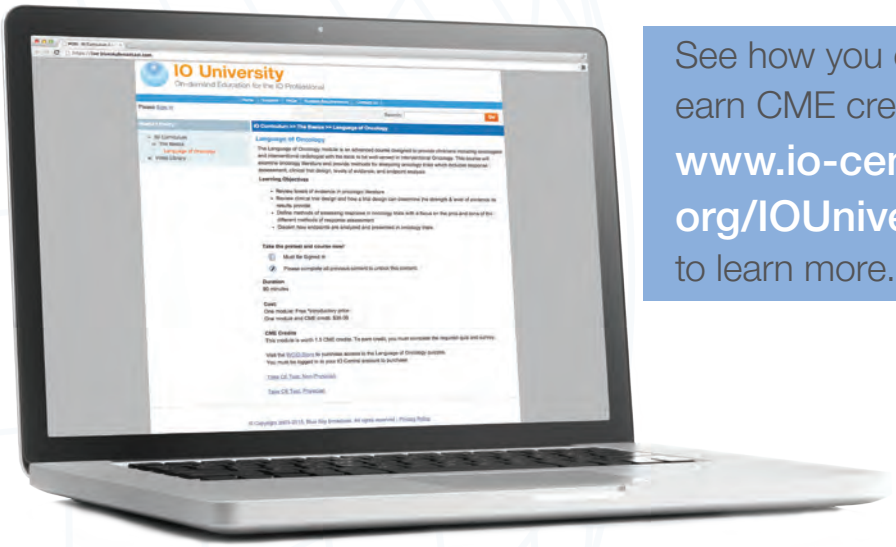

See how you can earn CME credit. Visit **www.io-central.org/IOUniversity** to learn more.

GENERAL INFORMATION

WCIO Board of Directors 2014 – 2015

Riccardo A. Lencioni, MD, *Chair*
Pisa University School of Medicine
Pisa, Italy

J. F. Geschwind, MD, *Vice Chair*
Yale University School of Medicine
New Haven, Connecticut, USA

Michael C. Soulen, MD, *Past Chair*
Hospital of the University of Pennsylvania
Philadelphia, Pennsylvania, USA

Afshin Gangi, MD, PhD
NHC, University Hospital
Strasbourg, Bas-Rhin, France

S. Nahum Goldberg, MD
Hadassah Hebrew University Medical Center
Jerusalem, Israel

David Lu, MD
University of California, Los Angeles
Los Angeles, California, USA

William S. Rilling, MD
Medical College of Wisconsin
Milwaukee, Wisconsin, USA

Riad Salem, MD, MBA
Northwestern University
Chicago, Illinois, USA

Stephen Solomon, MD
Memorial Sloan Kettering Cancer Center
New York, New York, USA

New York Hilton Midtown

1335 Avenue of the Americas
New York, NY 10019

Registration

Ballroom Promenade

Wednesday, 6 May	8:00 – 18:00
Thursday, 7 May	6:30 – 18:00
Friday, 8 May	7:30 – 18:00
Saturday, 9 May	7:30 – 12:00

Exhibit Hall

Ballroom Promenade & Foyer

Wednesday, 6 May	8:30 – 19:00
Thursday, 7 May	9:30 – 16:30
Friday, 8 May	9:30 – 16:30

Speaker Ready Room

Midtown Suite

Wednesday, 6 May	6:30 – 18:00
Thursday, 7 May	6:30 – 18:00
Friday, 8 May	6:30 – 18:00
Saturday, 9 May	6:30 – 12:00

Posters

Americas Hall 1

Wednesday, 6 May	13:00 – 19:00
Thursday, 7 May	8:00 – 18:00
Friday, 8 May	8:00 – 19:30
Poster Presentation Reception	18:00 – 19:30
Saturday, 9 May	8:00 – 10:00

Internet Access

Sponsored by Guerbet

Network: **Guerbet**
Password: **WeSupportWCIO**

Connect with @WCIO on Twitter and share your experience at the conference via social media using #WCIO2015.

WCIO 2015 On Demand – Share Sessions with Your Colleagues

WCIO 2015 On Demand provides you web access to WCIO 2015 sessions,* including speaker slides, videos, and pointer movements so you can follow along with the recorded presentation from the convenience of your home or office. Your purchase includes the conference session library and sessions for online download. WCIO 2015 On Demand is available for purchase at the registration desk for a discounted price of $100.

**Abstract and Allied Health sessions are not included.*

Case of the Week: Meet the Experts

This interactive session is the perfect opportunity to explore a case and discuss with colleagues and experts.

IO Around the World

Wednesday, 6 May
17:30 – 19:00

Grand Ballroom Promenade & Foyer

Network with collagues and experts from around the globe! Kick off WCIO 2015 and join fellow participants for WCIO Around the World, a reception designed to connect you with thought leaders and industry partners. Go "around the world" enjoying international food and beverages as you mingle with conference participants and build relationships.

FACULTY

Nasser Altorki, MD
Weill Cornell Medical College
New York, New York, USA

Yasuaki Arai, MD
National Cancer Center
Tokyo, Japan

Thomas D. Atwell, MD
Mayo Clinic
Rochester, Minnesota, USA

Alain Botczuk, MD
Columbia University
New York, New York, USA

J. Philip Boudreaux, MD
Oschner Medical Center
Baton Rouge, Louisiana, USA

Arthur Braat, MD
UMC Utrecht
Utrecht, Netherlands

D.J. Breen, MD
Consultant, Abdominal Radiologist
United Kingdom

Michael C. Brunner, MD
University of Wisconsin Madison & Madison VA Hospital
Madison, Wisconsin, USA

Matthew Callstrom, MD, PhD
Mayo Clinic
Rochester, Minnesota, USA

Cherng Chao, MD
University of Pittsburgh
Pittsburgh, Pennsylvania, USA

Julius Chapiro, MD
Charité University Hospital
Berlin, Germany

Jin Wook Chung, MD
Seoul National University Hospital
Seoul, South Korea

Deidre Cohen, MD
NYU Langone Medical Center
New York, New York, USA

Alban Denys, MD
University Hospital of Lausanne
Lausanne, Switzerland

Frederic Deschamps, MD
Gustave Roussy
Villejuif, Val de Marne, France

Damian Dupuy, MD
Rhode Island Hospital, Brown University
Providence, Rhode Island, USA

Jeremy Durack, MD
Memorial Sloan Kettering Cancer Center
New York, New York, USA

Jean Emond, MD
Columbia University
New York, New York, USA

Andrew Evans, MD
Mount Sinai Health System
New York, New York, USA

David J. Finley, MD
Dartmouth-Hitchcock Medical Center
Hanover, New Hampshire, USA

Afshin Gangi, MD, PhD
NHC, University Hospital
Strasbourg, Bas-Rhin, France

Julien Garnon, MD
University Hospital of Strasbourg
Strasbourg, Alsace, France

Bernhard Gebauer, MD
Charité University Hospital
Berlin, Germany

Ben George, MD
Medical College of Wisconsin
Milwaukee, Wisconsin, USA

Debra Gervais, MD
Massachusetts General Hospital
Boston, Massachusetts, USA

J. F. Geschwind, MD
Yale University School of Medicine
New Haven, Connecticut, USA

Alice Gillams, MD
The London Clinic
London, England

Michelle S. Ginsberg, MD
Memorial Sloan Kettering Cancer Center
New York, New York, USA

S. Nahum Goldberg, MD
Hadassah Hebrew University Medical Center
Jerusalem, Israel

Tim Greten, MD
National Cancer Institute
Bethesda, Maryland, USA

Tobias F. Jakobs, MD
The Hospital of the Order of St. John of God, Munich
Munich, Bavaria, Germany

Jack Jennings, MD, PhD
Washington University Saint Louis
Missouri, USA

Ahmad Kaseb, MD
MD Anderson Cancer Center
Houston, Texas, USA

Alexis Kelekis, MD, PhD
Attikon University Hospital
Athens, Haidari, Greece

Hyun S. "Kevin" Kim, MD
University of Pittsburgh
Pittsburgh, Pennsylvania, USA

T. Peter Kingham, MD
Memorial Sloan Kettering Cancer Center
New York, New York, USA

Christiane Kuhl, MD
Klinikum Aachen (University Hospital Aachen)
Aachen, Germany

Matthew Kulke, MD
Dana Farber Cancer Institute
Boston, Massachusetts, USA

A. Nick Kurup, MD
Mayo Clinic
Rochester, Minnesota, USA

Sharon Kwan, MD
University of Washington
Seattle, Washington, USA

Riccardo Lencioni, MD
Pisa University School of Medicine
Pisa, Italy

Robert Lewandowski, MD
Northwestern University
Chicago, Illinois, USA

David C. Madoff, MD
Weill Cornell Medical College
New York, New York, USA

Kieran Murphy, MD
University of Toronto
Toronto, Ontario, Canada

Govindarajan Narayanan, MD
University of Miami
Miami, Florida, USA

Albert A. Nemcek, Jr., MD
Northwestern Memorial Hospital
Chicago, Illinois, USA

Lt. Commander Daniel Nicastri, MD
Icahn School of Medicine at Mount Sinai
New York, New York, USA

William S. Rilling, MD
Medical College of Wisconsin
Milwaukee, Wisconsin, USA

Peter Rose, MD
Mayo Clinic
Rochester, Minnesota, USA

Riad Salem, MD, MBA
Northwestern University
Chicago, Illinois, USA

Constantinos T. Sofocleous, MD, PhD
Memorial Sloan Kettering Cancer Center
New York, New York, USA

Luigi Solbiati, MD
General Hospital of Busto Arsizio
Busto Arsizio, Varese, Italy

Stephen Solomon, MD
Memorial Sloan Kettering Cancer Center
New York, New York, USA

Michael C. Soulen, MD
Hospital of the University of Pennsylvania
Philadelphia, Pennsylvania, USA

Alda Tam, MD
MD Anderson Cancer Center
Houston, Texas, USA

Kiang Hiong Tay, MD
Singapore General Hospital
Singapore

R. Houston Thompson, MD
Mayo Clinic
Rochester, Minnesota, USA

Sean Tutton, MD
Medical College of Wisconsin
Milwaukee, Wisconsin, USA

Sarah B. White, MD
Medical College of Wisconsin
Milwaukee, Wisconsin, USA

Bradford Wood, MD
National Institutes of Health
Bethesda, Maryland, USA

David Woodrum, MD, PhD
Mayo Clinic
Rochester, Minnesota, USA

Abraham Wu, MD
Memorial Sloan Kettering Cancer Center
New York, New York, USA

Koichiro Yamakado, MD, PhD
Mie University
Tsu, Mie, Japan

Thomas Yau, MD
The University of Hong Kong
Pok Fu Lam, Hong Kong

Simon Chun Ho Yu, MD
The Chinese University of Hong Kong
Hong Kong

Etay Ziv, MD, PhD
Memorial Sloan Kettering Cancer Center
New York, New York, USA

Allied Health Program

Laura Ardizzone, DNO, CRNA, DCC
Memorial Sloan Kettering Cancer Center
New York, New York, USA

Deborah Fleischer, NP
Memorial Sloan Kettering Cancer Center
New York, New York, USA

Majid Maybody, MD
Memorial Sloan Kettering Cancer Center
New York, New York, USA

Heeralau Mohabir, RT (R)
Memorial Sloan Kettering Cancer Center
New York, New York, USA

Piera Robson, MSN, CNS, NP
Memorial Sloan Kettering Cancer Center
New York, New York, USA

Wesley Shay, RA, RT
Memorial Sloan Kettering Cancer Center
New York, New York, USA

David Silva, RA, RT
Memorial Sloan Kettering Cancer Center
New York, New York, USA

CME INFORMATION

WCIO
Advancing Interventional Oncology

This activity has been submitted to the Oncology Nursing Society (ONS) for approval to award contact hours. ONS is accredited as an approver of continuing nursing education by the American Nurses Credentialing Center's COA.

Learning Objectives

- Utilize new technologies presented to help select the appropriate therapies in the treatment of patients;
- Integrate multidisciplinary treatment options into a comprehensive patient care program; and
- Apply proven interventional techniques into current practice.

Who Should Attend?

WCIO 2015 is specifically designed to meet the educational needs of:

- Clinical Researchers
- Diagnostic Radiologists
- Interventional Oncologists
- Interventional Radiologists
- Medical Oncologists
- Radiation Oncologists
- Scientists
- Surgical Oncologists
- Interventional Radiology Nurses
- Interventional Oncology Nurses
- Medical Students
- Residents
- Interventional Radiology Physician Assistants
- Interventional Oncology Physician Assistants
- Oncology Nurses
- Oncology Physician Assistants
- Hepatology Nurses
- Hepatology Physician Assistants
- Liver Transplant Nurses/ Coordinators
- Nursing Students
- Fellows

"SAM"s – Qualification

WCIO will submit this activity to the ABR for SA-CME qualification. Maintenance of Certification (MOC) is for ABR-certified diplomats who are required to participate in order to maintain certification, or for lifetime certificate holders who voluntarily enroll to participate. A minimum of 75 AMA Category 1 CME credits are required every three years. At least 25 of the 75 Category 1 CME credits must be self-assessment CME (SA-CME).

Society of Interventional Radiology
The vision to heal™

Accreditation Statement

This activity has been planned and implemented in accordance with the Essentials and Standards of the Accreditation Council for Continuing Medical Education (ACCME) through joint sponsorship of the Society of Interventional Radiology (SIR) and WCIO. SIR is accredited by the ACCME to provide continuing medical education for physicians.

Disclosure Policy

In accordance with the ACCME's Standards for Commercial Support of Continuing Medical Education, all faculty and planning partners must disclose any financial relationship(s) or other relationship(s) held within the past 12 months. We have implemented a mechanism to identify and resolve all conflicts of interest prior to delivering the educational activity to learners.

CNE Accreditation Statement

Allied Health Program – The Collaborative IO: A Symposium from the Nursing or Allied Health Perspective

This activity is approved for credit by the ASRI.

WCIO 2016

BOSTON, MA | 9-12 JUNE

WCIO 2016 is Heading to Boston

Join us in *The City on the Hill* to learn about all things IO and network with colleagues and industry experts. June is an ideal time to visit Boston and with so many direct flights, getting there will be easy!

What to Expect in 2016

- A multidisciplinary approach to IO
- Earn CME, SAMS, CNE and AART credits
- Access the scientific information and up-to-date findings needed to stay current in the field
- Exciting and interesting tumor boards and debates amongst the world's leading physicians
- Helpful information on how to start an IO program, gain referrals, and help more patients
- Access to the latest technology designed by our corporate sponsors to help you care for patients

WCIO

Advancing Interventional Oncology

9-12 JUNE 2016

BOSTON, MASSACHUSETTS

SEAPORT BOSTON HOTEL & WORLD TRADE CENTER

WWW.WCIOEVENTS.ORG

WCIO 2016 details will be highlighted and updated throughout the year at www.wcioevents.org.

ACKNOWLEDGEMENTS

WCIO gratefully acknowledges the generous support and participation of our industry supporters:

Educational Grants Providers

BTG · Cook Medical · Guerbet Contrast for Life · Lilly

WCIO Hands-on Workshop Participants

angiodynamics · BENVENUE MEDICAL · Boston Scientific Advancing science for life™ · COVIDIEN · DFINE · EDA Technology · endocare extending life every day · GALILMEDICAL Leading Through Innovation · GE · Medtronic · NeuWave Medical Minimally Invasive. Maximum results. · perseon SCIENCE FOR HUMANITY · PHILIPS

WCIO In-Training Scholarship Program Supporters

Boston Scientific Advancing science for life™ · BTG · COVIDIEN · DFINE · endocare extending life every day · GALILMEDICAL Leading Through Innovation · Guerbet Contrast for Life · MERIT · NeuWave Medical Minimally Invasive. Maximum results. · PharmaCept · SIRTeX

Exhibitors

angiodynamics · BARD Biopsy · ONYX PHARMACEUTICALS An Amgen subsidiary · Boston Scientific Advancing science for life™ · BTG · CareFusion · CELO NOVA BIOSCIENCES · Celsion Corporation · Cook Medical · DFINE · EDA Technology · endocare extending life every day · GALILMEDICAL Leading Through Innovation · Guerbet Contrast for Life · HS · INTERVENTIONAL NEWS · Medtronic · Medtronic & COVIDIEN Covidien is joining Medtronic · MedWaves, Inc. · MERIT MEDICAL · NeuWave Medical Minimally Invasive. Maximum results. · perseon SCIENCE FOR HUMANITY · PharmaCept · PHILIPS · RadioMed/IBA · SIRTeX · Vison Medical

Sponsors and exhibitors listed at time of print. For more information about the WCIO Corporate Partner program, please contact Beverlee Galstan at **bgalstan@wcioonline.org**.

Corporate Partners

Platinum

BTG · COVIDIEN · Guerbet Contrast for Life

Partners

endocare extending life every day · SIRTeX

EXHIBITORS

AngioDynamics, Inc.
Booth 401
14 Plaza Drive
Latham, New York 12110 USA

Bard Biopsy
Booth 117
1415 West 3rd Street, Suite 109
Tempe, Arizona 85281 USA

Bayer HealthCare & Onyx Pharmaceuticals
Booth 305
P.O. Box 915
Whippany, New Jersey 07981 USA

Boston Scientific
Booth 100
300 Boston Scientific Way
Barlborough, Massachusetts 01752 USA

BTG
Booth 114
300 Barr Harbor Drive, Suite 800
West Conshohocken, Pennsylvania 19428 USA

CareFusion
Booth 404
75 North Fairway Drive
Vernon Hills, Illinois 60061 USA

Celonova Biosciences
Booth 109
18615 Tuscany Stone, Suite 100
San Antonio, Texas 78258 USA

Celsion
Booth 201
997 Lenox Drive, Suite 100
Lawrenceville, New Jersey 08648 USA

Cook Medical Inc.
Booth 111
P.O. Box 4195
Bloomington, Indiana 47402 USA

DFINE
Booth 400
3047 Orchard Parkway
San Jose, California 94134 USA

EDDA Technology
Booth 504
5 Independence Way
Princeton, New Jersey 08540 USA

Endocare, Inc.
Booth 110
9825 Spectrum Drive, Building 3
Austin, Texas 78717 USA

Galil Medical
Booth 300
4364 Round Lake Road West
Arden Hills, Minnesota 55112 USA

Guerbet LLC
Booth 104
120 West 7th Street, Suite 108
Bloomington, Indiana 47404 USA

HS Medical
Booth 302
4521 North Dixie Highway
Boca Raton, Florida 33431 USA

Interventional News
Booth 124
526 Fulham Road
Fulham, London SW6 5NR England

Medtronic Pain Therapies
Booth 203

Medtronic/Covidien
Booth 103

MedWaves, Inc.
Booth 115
16760 West Bernardo Drive
San Diego, California 92127 USA

Merit Medical Systems, Inc.
Booth 402
1600 West Merit Parkway
South Jordan, Utah 84095 USA

NeuWave Medical
Booth 301
3529 Anderson Street
Madison, Wisconsin 53704 USA

Perseon
Booth 502
2188 West 220 South
Salt Lake City, Utah 84119 USA

PharmaCept
Booth 500
Bessemerstr 82
Berlin-Schöneberg 12103 Germany

Philips
Booth 113

RadioMed Corporation/IBA
Booth 303

Sirtex Medical Inc.
Booth 403
300 Unicorn Park Drive
Woburn, Massachusetts 01801 USA

Vison Medical USA Inc.
Booth 107
Unit 40, 3350 Scott Boulevard
Santa Clara, California 95051 USA

INDUSTRY SYMPOSIA

Wednesday, 6 May
13:00 – 13:40
Presented by Covidien

New Technologies in Tumor Ablation Treatment: Thermosphere™ and Predictability

Moderator: Matthew Callstrom, MD, PhD, *Mayo Clinic*
Presenters: Joseph Brannan, *Covidien* and Donna D'Souza, MD, *University of Minnesota*

Wednesday, 6 May
13:40 – 14:20
Presented by Medtronic

Tips and Tricks in Embolization

Michael Cohn, MD, *Services Memorial Healthcare System* and *Florida Atlantic University Medical School* and Vladimir Sheynzon, MD, *Columbia University College of Physicians* and *Surgeons New York Presbyterian Hospital*

Thursday, 7 May
7:00 – 7:40
Presented by PharmaCept

DSM-TACE EmboCept® S: An Effective Therapy with Biodegradable Microspheres in Liver Tumors

Prof. Christiane Kuhl, *University Hospital Aachen* and Federico Collettini, MD, *Charite University Hospital Berlin*

Thursday, 7 May
12:00 – 12:40
Presented by NeuWave Medical

Microwave Ablation Summit: Breakthroughs in Lung, Bone and Kidney

Presenters: Dr. Rob Su, Dr. Roger Williams, and Dr. Aaron Fischman

Thursday, 7 May
12:40 – 13:20
Presented by Siemens (Three Topics)

Advance Cancer Care: New Possibilities with MIYABI Angio-CT and Artis zeego with syngo DynaCT

Moderator: Dr. Wieland Voigt, *Siemens AG, Healthcare*

Expanding the field of Interventional Oncology through Advanced Technology

Götz Martin Richter, MD, PhD, *Clinic for Diagnostic and Interventional Radiology, Katharinenhospital*

Making Routine Cases Easier and Complex Cases Possible – Angio-CT Miyabi

Constantinos T. Sofocleous, MD, PhD, *Memorial Sloan Kettering Cancer Center*

Friday, 8 May
12:00 – 12:40
Presented by BTG and Philips Healthcare

New Pathways in Imaging and Navigation for Liver-Directed Therapies

Prof. G. Narayanan MD, *University of Miami* and Assistant Prof. Edward Kim, MD, *Icahn School of Medicine at Mount Sinai*

Friday, 8 May
12:40 – 13:20
Presented by GE

Optimize Cone-Beam CT in Interventional Oncology – Applications, Workflow, and Settings

Abe Levitin, MD, *Cleveland Clinic* and Dr. Muneeb Ahmed, *Beth Israel Deaconess Medical Center* and *Harvard Medical School*

DOWNLOAD THE WCIO 2015 MOBILE APP TO ACCESS WCIO 2015 IN THE PALM OF YOUR HAND!

The WCIO 2015 mobile app gives you one stop access to everything the conference has to offer. Through the app, you can

- Search the conference schedule and add sessions to your personal agenda
- Participate in polls, send questions to moderators, and provide real-time feedback on sessions
- Sort by speaker and view all the sessions in which he/she will be presenting
- View all WCIO exhibitors and favorite the ones you are most interested in meeting
- Find fun things to do in New York City!

How to download:

Apple and Android devices: Search for "WCIO 2015" in the Apple App Store or Google Play Store.

All other devices: point your browser to: **www.wcioevents.org/mobileapp**

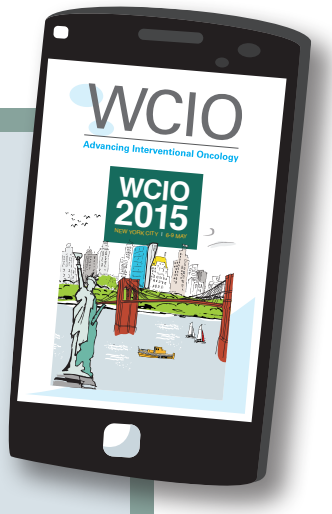

Get Involved!

Interact with our expert speakers and engage in real-time discussions during education sessions all through the mobile app.

SCIENTIFIC PROGRAM

Schedule subject to change.

Wednesday, May 6

8:30-9:30	Breakfast and Exhibitor Time — *Ballroom Promenade & Foyer*	
Time	**East Ballroom**	
9:00-11:00	**HCC, Part 1 — *Moderators: David C. Madoff, MD, Riad Salem, MD, and Jin Wook Chung, MD***	
	9:00-9:15	**Welcome** — *Hyun S. "Kevin" Kim, MD*
	9:15-9:27	**Staging and Guidelines for HCC: NCCN, Barcelona, or Hong Kong?** — *Thomas Yau, MD*
	9:27-9:39	**Surgical Options for HCC: When and Why?** — *Jean Emond, MD*
	9:39-9:51	**Role of Ablation: Should It Be Used As Primary Therapy For Early Stage HCC?** — *David Madoff, MD*
	9:51-10:03	**Transarterial Therapies for HCC: Should It's Role Be Limited To Just The Unresectable?** — *Riad Salem, MD*
	10:03-10:15	**Systemic Treatments for HCC: Is There Really A Significant Benefit?** — *Ahmad Kaseb, MD*
	10:15-11:00	**Tumor Board** — *All Speakers*
11:00-11:30	Break with Exhibitors — *Ballroom Promenade & Foyer*	
11:30-13:00	**MSK — *Moderators: Matthew Callstrom, MD, PhD and Afshin Gangi, MD, PhD***	
	11:30-11:40	**Featured Abstract — Best Abstract Paper 33: Improved Cytotoxicity with a Novel Mitochondria - Targeted Doxorubicin Prodrug in Colorectal Carcinoma Cells** — *Jemianne Jia, MS4*
	11:40-11:50	**MSK Interventions: Palliation, Ablation, Consolidation** — *Afshin Gangi, MD, PhD*
	11:50-12:00	**Treatment of Spine Metastases with RFA: New Approaches** — *Jack Jennings, MD, PhD*
	12:00-12:10	**Role of Ablation in Orthopedic Oncology: A Surgeon's Perspective** — *Peter Rose, MD*
	12:10-12:20	**Hardware and Ablation in the Pelvis** — *Sean Tutton, MD*
	12:20-12:30	**Ablation Treatment of Desmoids: Is It More Effective Than Traditional Treatments?** — *Julien Garnon, MD*
	12:30-12:40	**Avoiding Complications in MSK Ablation** — *Anil "Nick" Kurup, MD*
	12:40-12:50	**Tips and Tricks with MSK Ablation** — *Matthew Callstrom, MD, PhD*
	12:50-13:00	**Tumor Board** — *All Speakers*
13:00-14:20	Lunch and Exhibitor Time — *Ballroom Promenade & Foyer*	
13:00-13:40	Industry Symposium presented by Covidien — New Technologies in Tumor Ablation Treatment: Thermosphere™ and Predictability — Moderator: Matthew Callstrom, MD, PhD; Presenters: Joseph Brannan and Donna D'Souza, MD — *East Ballroom*	
13:40-14:20	Industry Symposium presented by Medtronic — Tips and Tricks in Embolization – Michael Cohn, MD and Vladimir Sheynzon, MD— *East Ballroom*	
14:20-15:00	**Review of Guidelines for HCC and Best Staging System* — *Moderators: J. F. Geschwind, MD and Hyun S. "Kevin" Kim, MD***	
	14:20-14:28	**HCC in the Era of Advanced Hepatitis C Therapies** — *Hyun S. "Kevin" Kim, MD*
	14:28-14:36	**HCC Treatment Guidelines: The Best Staging Systems and the Best Practices Based on Best Clinical Evidence - AASLD/EASL/NCCN/ESMO** — *William S. Rilling, MD*
	14:36-14:44	**HCC Transcatheter Therapies for BCLC C Patients** — *Michael C. Soulen, MD*
	14:44-14:52	**Novel Drug Delivery Platforms for HCC from the Laboratory** — *Sarah White, MD*
	14:52-15:00	**HCC in the Era of Advanced Hepatitis C Therapies** — *Hyun S. "Kevin" Kim, MD*
15:00-16:00	**Old Cancers, New Treatments — *Moderators: Christiane Kuhl, MD, Simon Yu, MD, and Yasuaki Arai, MD***	
	15:00-15:20	**Selective Internal Radiation Therapy for Cholangiocarcinoma** — *Simon Yu, MD*
	15:20-15:40	**IO in Palliative Care for Old Cancer Patients** — *Yasuaki Arai, MD*
	15:40-16:00	**IO in Breast Cancer Patients** — *Christiane Kuhl, MD*
16:00-16:30	Break with Exhibitors — *Ballroom Promenade & Foyer*	
16:30-17:30	**Palliative Care/Symptom Management — *Moderators: Sean Tutton, MD, and Alexis Kelekis, MD, PhD***	
	16:30-16:42	**Medical Management of Pain: What An Astute Interventional Oncologist/Radiologist Can Do** — *Sean Tutton, MD*
	16:42-16:54	**Percutaneous Nerve Blocks and Neurolysis** — *Alexis Kelekis, MD, PhD*
	16:54-17:06	**Percutaneous Techniques for Pleural Effusion, Malignant Ascites, and Outlet Obstruction** — *Alda Tam, MD*
	17:06-17:18	**Palliative Embolization: Pain and Bleeding** — *Albert A. Nemcek, MD*
	17:18-17:30	**Percutaneous Ablation and Bone Augmentation for Pain Management** — *Kieran Murphy, MD*
17:30-19:00	**IO Around the World Reception** — *Ballroom Promenade & Foyer*	
18:30-20:00	**Early Career Interventional Oncologists Program *(invitation only)* — *Moderator: Robert Lewandowski, MD***	
	18:30-18:35	**Welcome and Introduction** — *Hyun S. "Kevin" Kim, MD, and Robert Lewandowski, MD*
	18:35-18:45	**Top 5 Practice Development Tips** — *William S. Rilling, MD*
	18:45-19:20	**Best Case Presentation**
		18:45-18:50 — **RFA** — *Riccardo Lencioni, MD*
		18:50-18:55 — **MWA** — *Matthew Callstrom, MD, PhD*
		18:55-19:00 — **Cryo** — *Matthew Callstrom, MD, PhD*
		19:00-19:05 — **Navigation & Ablation** — *Tobias F. Jakobs, MD*
		19:05-19:10 — **cTACE** — *Michael C. Soulen, MD*
		19:10-19:15 — **DEB-TACE** — *J. F. Geschwind, MD*
		19:15-19:20 — **Y90** — *Riad Salem, MD*
	19:20-20:00	**Tumor Board** — *Robert Lewandowski, MD*

*Supported by an educational grant from Guerbet

Thursday, May 7

6:45-8:15	Breakfast — *Ballroom Promenade & Foyer*
7:00-7:40	Industry Symposium presented by PharmaCept - DSM-TACE EmboCept® S: An Effective Therapy with Biodegradable Microspheres in Liver Tumors — *Prof. Christiane Kuhl and Federico Collettini, MD — West Ballroom*

Time	East Ballroom	Time	West Ballroom
	Workshop 1 – Didactic/Video		**Abstract Presentations – HCC** Moderators: Anne Covey, MD and John Sangjoon Park, MD *Full Details and Descriptions on Page 18*
8:00-9:30	**Embolization: Bland to Y90** — *Julius Chapiro, MD; Yasuaki Arai, MD; and Bernhard Gebauer, MD*	**8:00**	**Paper 1 —** Repetitive Superselective cTACE as a Bridge To Therapeutic Treatments In Patients With Unresectable Solitary HCC Tumor Larger Than 8 cm. A Single Center Experience
		8:09	**Paper 2 —** Is Radioembolization without 99mTc-macroaggregated Albumin Injection Possible: A Retrospective Review of 39 Patients with Hepatocellular Carcinoma
		8:18	**Paper 3 —** Transarterial Chemoembolization for the Treatment of Advanced Hepatocellular Carcinoma: a Large Retrospective Cohort Study with 508 Patients
		8:27	**Paper 4 —** Contrast Enhancement Kinetics of the Hepatic Arterial Vasculature After Drug Eluting Bead Trans-Arterial Chemoembolization
		8:36	**Paper 5 —** Transcathether Arterial Chemoembolization Plus Radiotherapy is Superior to Chemoembolization Alone for Hepatocellular Carcinoma: A Comprehensive Systematic Review and Meta-analysis
		8:45	**Paper 6 —** Development and Validation of an Endovascular Chemotherapy Filter Device to Enable High Dose Transarterial Hepatic Doxorubicin Therapy: In Vitro Proof of Concept in Human Serum
9:30-10:00	Break with Exhibitors — *Ballroom Promenade & Foyer*		

	Molecular Oncology *Moderators: J. F. Geschwind, MD, Riccardo Lencioni, MD, and Bradford Wood, MD*		**Allied Health Program**	
10:00-12:00	**10:00-10:15**	**Oncogenic Pathways & Their Relevance To Interventional Oncology** — *S. Nahum Goldberg, MD*	**10:00-10:30**	**Interventional Radiology and Anesthesiology: Collaborative Approaches to Quality Patient Care** — *Laura L. Ardizzone, DNP, CRNA, DCC*
	10:15-10:30	**Pathologic Changes & Prognostic Biomarkers in Tumor Ablation** — *Constantinos Sofocleous, MD, PhD*		
	10:30-10:45	**Image Guided Drug Delivery** — *Riccardo Lencioni, MD*		
	10:45-11:00	**HSP90 As Therapeutic Targets in Combination Ablation Therapies & Molecular Mechanisms of Cell Survival After Themal Ablation** — *David Woodrum, MD, PhD*	**10:45-11:15**	**Radiology Assistant Practice Model: An ASK Perspective** — *David Silva, RA, RT*
	11:00-11:15	**Angiogenesis** — *Julius Chapiro, MD*		
	11:15-11:30	**Glycolysis & Its Importance In Cancer** — *J. F. Geschwind, MD*		
	11:30-11:45	**Pathological Changes Prognostic Biomarkers in Arterially Directed Therapies: SIRT/TACE** — *Hyun S. "Kevin" Kim, MD*	**11:30-12:00**	**Venous Access Placements: Strategies to Help Lower Infection Rates** — *Wesley Shay, RA, RT*
	11:45-12:00	**Clinical & Translational Research Pathways for Molecular Therapies & Immunotherapies in HCC** — *Tim Greten, MD*		
12:00-14:00	Lunch and Exhibitor Time — *Ballroom Promenade & Foyer*			
12:00-12:40	Industry Symposium presented by NeuWave Medical — Microwave Ablation Summit: Breakthroughs in Lung, Bone and Kidney — Dr. Rob Su, Dr. Roger Williams, and Dr. Aaron Fischman — *East Ballroom*			
12:40-13:20	Industry Symposium presented by Siemens — Advance Cancer Care: New Possibilities with MIYABI Angio-CT and Artis zeego with syngo DynaCT — Dr. Wieland Voigt, Götz Martin Richter, MD, PhD, and Constantinos T. Sofocleous, MD, PhD — *East Ballroom*			

	Comparative Effectiveness *Moderators: Hyun S. "Kevin" Kim, MD and Michael C. Brunner, MD*		**Allied Health Program**	
14:00-14:30	**14:00-14:07**	**Science of CER** — *Michael C. Brunner, MD*	**14:00-14:30**	**Critical Complications in the IO Patient** — *Deborah Fleischer, NP*
	14:07-14:18	**CER in Procedural Oncology** — *Sharon Kwan, MD*		
	14:18-14:25	**Resources for CER Research in IO** — *Cherng Chao, MD*		
	14:25-14:30	**Funding Opportunities for CER in Oncology** — *Hyun S. "Kevin" Kim, MD*		
14:00-16:00	WCIO Residents' and Fellows' Exhibit Hall Walk Through — *Ballroom Promenade & Foyer*			

Thursday, May 7 (continued)

Time	East Ballroom	
	Primary Lung Cancer *Moderators: Steve Solomon, MD, and Koichiro Yamakado, MD, PhD*	
14:30-16:00	14:30-14:40	**Lung Cancer Screening** — *Michelle Ginsberg, MD*
	14:40-14:50	**Progression of Atypical Adenoma to Lung Adenocarcinoma** — *Alain Borczuk, MD*
	14:50-15:00	**Sublobar Resection Versus Lobectomy for Primary Lung Cancer: Has the Standard Changed?** — *Nasser Altorki, MD*
	15:00-15:10	**SBRT Clinical Trial Update** — *Andrew Evans, MD*
	15:10-15:20	**Lung Cancer Ablation** — *Damian Dupuy, MD*
	15:20-15:30	**Management of Multifocal Stage I Lung Cancer** — *David Finley, MD*
	15:30-15:40	**Local Therapy in the Setting of Metastatic Lung Cancer** — *Abraham Wu, MD*
	15:40-15:50	**Biopsy of Lung Cancer in the World of Personalized Medicine** — *Etay Ziv, MD, PhD*

16:00-16:30	Break with Exhibitors — *Ballroom Promenade & Foyer*

Time	America's Hall	Time	West Ballroom
	Workshop 2 – Hand On/Video		**Abstract Presentations – Liver Mets** Moderators: Joshua Weintraub, MD and Luigi Solbiati, MD *Full Details and Descriptions on Pages 18-19*
16:30-18:00	**MSK/Spine** — *Jack Jennings, MD, PhD, and Frederic Deschamps, MD*	16:30	**Paper 7** — Comparison of Changes in Liver and Spleen Volume and Hepatosplenic Function After Chemoembolization Versus 90Y Radioembolization in Patients with Metastatic Neuroendocrine Tumor
		16:39	**Paper 8** — Association of Three Common Proto-oncogene Mutations to the Response of Radioembolization for Hepatic Colorectal Metastasis
		16:48	**Paper 9** — EASL and mRECIST Better Predict Survival After Yttrium-90 Radioembolization Therapy Compared to RECIST and WHO in Metastatic Unresectable Colorectal Cancer in the Liver
		16:57	**Paper 10** — Prospective Evaluation of Transarterial Chemoembolization Using a New Generation of Doxorubicin Eluting Beads for the Treatment of Chemorefractory Liver Metastases from Breast Cancer
		17:06	**Paper 11** — Efficacy of Aggressive Antibiotic Prophylaxis to Prevent Abscess Following Percutaneous Hepatic Ablation in Patients with Biliary Enteric Anastomosis
		17:15	**Paper 12** — Transradial Arterial Access for Intra-Arterial Liver Directed Therapy: A Single Center Initial Experience
		17:24	**Paper 13** — The Post-SIR-Spheres Surgery Study (P4S): Outcomes Following Liver Resection or Transplantation in 100 Patients Previously Treated with Selective Internal Radiation Therapy (SIRT) using Y-90 Resin Microspheres
		17:33	**Paper 14** — A Comparison of Response By 4 FDG-PET Metrics of Metabolic Activity and RECIST 1.1 as Predictors of Overall Survival After Selective Internal Radiation Therapy (SIRT) of Colorectal Liver Metastases.
		17:42	**Paper 15** — *KRAS* Status as an Independent Prognostic Factor for Survival of Unresectable Colorectal Cancer after Yttrium-90 Radioembolization Therapy
		17:51	**Paper 16** — Survival Differences in Glass Versus Resin Radioembolization of Hepatic Malignancies
18:00-19:30	**Corporate Advisory Council Meeting *(Invitation Only)*** — *Executive Lounge - 44th Floor*		

Friday, May 8

7:30-9:00	Breakfast — *Promenade & Foyer*		
Time	**America's Hall**	**Time**	**West Ballroom**
	Workshop 3 - Hands On		**Abstract Presentations – Guidance and Technology** Moderators: Muneeb Ahmed, MD and Eric Lis, MD *Full Details and Descriptions on Page 19*
8:00-9:30	**Guidance, Navigation, Assessment, and Robotics** — *Bradford Wood, MD and Luigi Solbiati, MD*	**8:00**	**Paper 17** — Radiation Map Fusion Guided Combination of External Beam Radiation with Thermal Ablation for Up to 10 cm Liver Tumors
		8:09	**Paper 18** — Exact Detection of Ablative Margin and Local Tumor Progression in Liver Tumors: Preliminary Follow-up Results
		8:18	**Paper 19** — Greyscale, Color Doppler, and B-Flow Ultrasound Guidance for Tissue Hydrodissection: Modality Impact on Injection Localization
		8:27	**Paper 20** — CT-Guided Screw Fixation Plus Cementoplasty in the Treatment of Painful Bone Metastases
		8:36	**Paper 21** — Intraprocedural 3D Quantification of Lipiodol Deposition on Cone-Beam CT Predicts Tumor Response After Transarterial Chemoembolization in Patients with Hepatocellular Carcinoma
		8:45	**Paper 22** — Thermal Ablation of Benign Thyroid Disease: A Prospective Multi-Center Study
		8:54	**Paper 23** — Cement Leakage in Balloon Kyphoplasty for Spinal Metastasis and Myeloma A Retrospective Evaluation of Incidence and Risk Factors
		9:03	**Paper 24** — Portal Vein Embolization Via a Percutaneous Transsplenic Access
		9:12	**Paper 25** — The Immediate Elevation of Serum Tumor Marker After Irreversible Electroporation Implies Technique Success
9:30-10:00	Break with Exhibitors — *Ballroom Promenade & Foyer*		
Time	**East Ballroom**	**Time**	**West Ballroom**
	WCIO Meets APSCVIR: HCC, Part 2 *Moderators: J. F. Geschwind, MD and Hyun S. "Kevin" Kim, MD*		**Allied Health Program**
10:00-11:30	**Interventional Oncology Management of Hepatocellular Carcinoma – The Evidence from Asia**		
	10:00-10:15 **Local Ablation** — *Koichiro Yamakado, MD, PhD*	**10:00-10:30**	**Image Guided Lung Biopsies: Pleural Puncture Plugging** — *Majid Maybody, MD*
	10:15-10:30 **Chemoembolization** — *Jin Wook Chung, MD*		
	10:30-10:45 **Radioembolization** — *Kiang Hiong Tay, MD*		
	10:45-11:00 **Management of HCC in the West** — *Riccardo Lencioni, MD*	**10:45-11:15**	**Venous Access: Potential Nightmares** — *Dave Silva, RA, RT*
	11:00-11:15 **Is There A Role For Combination Therapies in HCC** — *J. F. Geschwind, MD*		
	11:15-11:30 **Trial Design in HCC: Principle and End Points** — *Riad Salem, MD*		
		11:30-12:00	**Impact of Palliative Catheter Placement on the Quality of Life of Patients with End-Stage Cancer and Refractory Ascites** — *Piera M. Cote Robson MSN, CNS, NP*
12:00-14:00	Lunch and Exhibitor Time — *Ballroom Promenade & Foyer*		
12:00-12:40	Industry Symposium presented by BTG and Philips Healthcare — New Pathways in Imaging and Navigation for Liver-Directed Therapies — Prof. G. Narayanan, MD and Prof. Edward Kim, MD — *East Ballroom*		
12:40-13:20	Industry Symposium presented by GE – Optimize Cone-Beam CT in Interventional Oncology – Applications, Workflow, and Settings — Abe Levitin, MD and Dr. Muneeb Ahmed — *East Ballroom*		

SCIENTIFIC PROGRAM

Schedule subject to change.

Friday, May 8 (continued)

Time	East Ballroom		Time	West Ballroom
Renal Ablation *Moderators: Thomas Atwell, MD, and Jeremy Durack, MD*			**Allied Health Program**	
14:00-15:00	14:00-14:10	**Choosing Your Device and Knowing the Outcomes** — *D.J. Breen, MD*	14:00-14:30	**Scheduling Strategies in a Complex IR Department** — *Heeralall Mohabir RT (R), MBA*
	14:10-14:20	**Lessons Learned from the Dark Side of Renal Ablation** — *Thomas Atwell, MD*		
	14:20-14:30	**If Surgery Is the Standard, Where Does Ablation Fit In?** — *R. Houston Thompson, MD*		
	14:30-15:00	**Renal Tumor Board** — *All Speakers*		
mNET *Moderators: Michael Soulen, MD*				
15:00-16:00	15:00-15:10	**Assessment and Triage of NETs in the IO Clinic** — *Michael C. Soulen, MD*		
	15:10-15:20	**Systemic Drug Therapies: Which One When?** — *Matthew Kulke, MD*		
	15:20-15:30	**When Is Surgery Beneficial In Metastatic NETs?** — *J. Philip Boudreaux, MD*		
	15:30-15:40	**PRRT: Integration with Liver-Directed Therapies** — *Arthur Braat, MD*		
	15:40-15:50	**Embolotherapy: Is There A Best Technique?** — *Sarah White, MD*		
	15:50-16:00	**Radioembolization of mNET** — *Tobias F. Jakobs, MD*		
16:00-16:30	Break with Exhibitors — *Ballroom Promenade & Foyer*			

Time	America's Hall	Time	West Ballroom
Workshop 4 – Video/Hands On		**Abstract Presentations – HCC + Basic Science** Moderators: Jacov Cynamon, MD and Uei Pua, MBBS *Full Details and Descriptions on Pages 19-20*	
16:30-18:00	**Ablation: Kidney and Lung** — *Debra Gervais, MD and Stephen Solomon, MD*	16:30	**Paper 26** — The Analysis for the Causes of Delayed Hospitalization after Transcatheter Arterial Chemoembolization in Patients with Unresectable Hepatocellular Carcinoma
		16:39	**Paper 27** — Superselective Transcatheter Arterial Embolization of Adrenal Metastases from Hepatocellular Carcinoma is Feasible and Safe
		16:48	**Paper 28** — The Effect of Anti-Reflux Catheters on Pulmonary Shunt Fraction in Patients with Hepatocellular Carcinoma
		16:57	**Paper 29** — The Effect of Sociodemographics on Survival in Hepatocellular Carcinoma Patients Undergoing Orthotopic Liver Transplantation: UNOS Population Study
		17:06	**Paper 30** — Development of the New Prognostic Staging System and Proposal of Treatment Algorithm Based on the Multivariate Survival Analyses (MVA) After Doxorubicin Drug Eluting Beads Trans-Arterial Chemoembolization (DEB TACE) in Patients with Unresetable Hepatocellular Carcinoma (HCC)
		17:15	**Paper 31** — Analysis of *In Vitro* Growth Inhibition of Human Colorectal Cancer and Hepatocellular Carcinoma Cells by Anti-Angiogenic Drug-Eluting Beads
		17:24	**Paper 32** — SVP ^{90}Y PET/CT Dosimetry After Radioembolization in Rabbit VX2 Liver Tumor Model: Comparisons to MIRD Calculations and Ex Vivo Microsphere Uptake
		17:33	**Paper 33** — Improved Cytotoxicity with a Novel Mitochondria-Targeted Doxorubicin Prodrug in Colorectal Carcinoma Cells
18:00-19:30	**Poster Presentation Reception** — *America's Hall*		
18:00-19:30	**Case of the Week: Meet the Experts** — *America's Hall*		

Saturday, May 9

7:30-8:30 Breakfast — *Promenade & Foyer*

Time	America's Hall	Time	West Ballroom
	Workshop 5 – Hands On		**Abstract Presentations – Thoracic and Genitourinary** *Moderators: Debra Gervais, MD and Robert Suh, MD* *Full Details and Descriptions on Page 20*
8:00-9:30	**RFA/MW/Cryo/IRE** — *Govindarajan Narayanan, MD and D. J. Breen, MD*	8:00	**Paper 34** — Comparative-Effectiveness analysis of Surgery vs. Ablation for Stage T1a Renal Cell Carcinoma in the SEER population
		8:09	**Paper 35** — Percutaneous Microwave Ablation of T1a Renal Cell Carcinoma: Interval Update with Median 11-Month Imaging Follow-Up
		8:18	**Paper 36** — Cryoablation of Prostate Adenocarcinoma Recurrences: 2 Year Follow-Up
		8:27	**Paper 37** — Scaled Signal Intensity of Uterine Fibroids based on T2-weighted MR Images: A Potential Objective Method to Determine the Suitability for Magnetic Resonance-Guided Focused Ultrasound Surgery of Uterine Fibroids
		8:36	**Paper 38** — Adjunctive Techniques to Allow for Percutaneous Cryoablation of Renal Masses in Difficult Anatomic Locations
		8:45	**Paper 39** — Thermal Ablation of Metastatic Adrenocortical Carcinoma: Long-Term Results
		8:54	**Paper 40** — Percutaneous Cryoablation for the Treatment of Primary and Metastatic Lung Tumors
		9:03	**Paper 41** — Image Guided Treatment of Chylous Effusions in Oncologic Patients: Single Center Experience
		9:12	**Paper 42** — Estrogen Receptor Alpha in Lung Cancer Development and Growth, A Novel Therapeutic Target
		9:21	**Paper 43** — Radiofrequency Ablation Versus Surgery for the Treatment of Lung Metastases

9:30-10:00 Break — *Ballroom Promenade & Foyer*

Time	East Ballroom	
	Metastatic Colorectal Cancer *Moderators: Constantinos Sofocleous, MD, William Rilling, MD and Alban Denys, MD*	
10:00-12:30	**Resectable or Potentially Resectable Disease (Debate: Surgery vs. Ablation) — *William Rilling, MD***	
	10:00-10:15	**Surgery Remains the Gold Standard for All CLM** — *T. Peter Kingham, MD*
	10:15-10:30	**Ablation Should Replace Surgery For Selected CLM That Can Be Treated With Margins** — *Constantinos Sofocleous, MD, PhD*
	10:30-10:45	**Role of PVE and Other Techniques As Bridge To Resection** — *Alban Denys, MD*
	Non-Resectable Disease — *Alban Denys, MD*	
	10:45-11:00	**What is New in Systemic Treatment for Stage IV CRC?** — *Deirdre Cohen, MD*
	11:00-11:15	**Locoregional Therapy in CRC Mets: Timing and Results** — *William Rilling, MD*
	11:15-11:30	**The Case for Integration of Locoregional Therapy with Systemic Therapy** — *Ben George, MD*
	Pulmonary Mets — *Constantinos Sofocleous, MD, PhD*	
	11:30-11:45	**Resectable Pulmonary Mets Should Only Be Treated By Surgery** — *Lt. Commander Daniel Nicastri, MD*
	11:45-12:00	**SBRT Is All You Need For Pulmonary Mets** — *Abraham Wu, MD*
	12:00-12:15	**Ablation Is The Best Option For Selected Pulmonary Metastases** — *Alice Gillams, MD*
	12:15-12:30	**Tumor Board** — *All Speakers*

Abstract Index

Paper 1: Repetitive Superselective cTACE as a Bridge to Therapeutic Treatments in Patients with Unresectable Solitary HCC Tumor Larger than 8 cm.: A Single Center Experience

I. Dedes, A. Drevelegas, *Interventional Radiology Department, Interbalkan European Medical Center, Thessaloniki, Greece.*

Paper 2: Is Radioembolization Without 99mTc-macroaggregated Albumin Injection Possible: A Retrospective Review of 39 Patients With Hepatocellular Carcinoma

R. Gurajala[1], E. Nasr[1], S. Shrikanthan[1], K. Karuppasamy[2], [1]*Nuclear Medicine, Cleveland Clinic, Beachwood, Ohio, United States,* [2]*Intervention Radiology, Cleveland Clinic, Cleveland, Ohio, United States.*

Paper 3: Transarterial Chemoembolization for the Treatment of Advanced Hepatocellular Carcinoma: A Large Retrospective Cohort Study with 508 Patients

Y. Zhao[1], J. Sohn[1], F. Fleckenstein[1], S. Sahu[1], R. Duran[1], R. Schernthaner[1], H. Lee[1], J. Geschwind[1], M. Lin[2], [1]*Interventional Radiology, Johns Hopkins Hospital, Baltimore, Maryland, United States,* [2]*Philips Research North American, U/S Imaging and Interventions (UII), Briarcliff Manor, New York, New York, United States.*

Paper 4: Contrast Enhancement Kinetics of the Hepatic Arterial Vasculature after Drug Eluting Bead Trans-Arterial Chemoembolization

W. Lea[1], S. Dybul[1], S.B. White[1], P. Patel[1], R. Hieb[1], S. Tutton[1], W. Rilling[1], E. Hohenwalter[1], R. Setser[2], [1]*Vascular and Interventional Radiology, Medical College of Wisconsin, Milwaukee, Wisconsin, United States,* [2]*Siemens Healthcare, Forchheim, Germany.*

Paper 5: Transcathether Arterial Chemoembolization Plus Radiotherapy is Superior to Chemoembolization Alone for Hepatocellular Carcinoma: A Comprehensive Systematic Review And Meta-Analysis

Y. Huo[1], G.D. Eslick[2], [1]*Surgery, UNSW Australia, Kensington, New South Wales, Australia,* [2]*Department of Surgery, University of Sydney, Penrith, New South Wales, Australia.*

Paper 6: Development and Validation of an Endovascular Chemotherapy Filter Device to Enable High Dose Transarterial Hepatic Doxorubicin Therapy: In Vitro Proof of Concept in Human Serum

A.S. Patel[1], C. Sze[1], J. Yang[1], M. Saeed[1], A.D. Losey[1], B. Thorne[1], S.W. Hetts[1], **M. Wilson[1],** A. Chin[2], [1]*Radiology, University of California, San Francisco, San Francisco, California, United States,* [2]*ChemoFilter, Inc., Burlingame, California, United States.*

Paper 7: Comparison of Changes in Liver and Spleen Volume and Hepatosplenic Function after Chemoembolization Versus 90Y Radioembolization in Patients with Metastatic Neuroendocrine Tumor

V. Etezadi, T. Larrea, M.C. Soulen, W.S. Stavropoulos, J. Mondschein, M. Dagli, *Interventional Radiology, Hospital of University of Pennsylvania, Philadelphia, Pennsylvania, United States.*

Paper 8: Association of Three Common Proto-Oncogene Mutations to the Response of Radioembolization for Hepatic Colorectal Metastasis

R. O'Hara, N.N. Davis, R.L. Hardman, *Radiology, University of Utah, Salt Lake City, Utah, United States.*

Paper 9: EASL and mRECIST Better Predict Survival After Yttrium-90 Radioembolization Therapy Compared To RECIST and WHO In Metastatic Unresectable Colorectal Cancer in the Liver

M.J. Magnetta[1], L. Steven[1], M. Xing[1], D. Zhang[2], K. Kim[3], [1]*Interventional Radiology, University of Pittsburgh School of Medicine, Pittsburgh, Pennsylvania, United States,* [2]*Graduate School of Public Health, University of Pittsburgh, Pittsburgh, Pennsylvania, United States,* [3]*Cancer Therapeutics Program, University of Pittsburgh Cancer Institute, University of Pittsburgh School of Medicine, Pittsburgh, Pennsylvania, United States.*

Paper 10: Prospective Evaluation of Transarterial Chemoembolization Using a New Generation of Doxorubicin Eluting Beads for the Treatment of Chemorefractory Liver Metastases from Breast Cancer

M.P. Kohi[1], A. Taylor[2], K.P. Koll[2], J. LaBerge[2], R. Kerlan[2], N. Fidelman[2], [1]*Radiology & Biomedical Imaging, University of California, San Francisco, San Francisco, California, United States,* [2]*University of California, San Francisco, San Francisco, California, United States.*

Paper 11: Efficacy of Aggressive Antibiotic Prophylaxis to Prevent Abscess Following Percutaneous Hepatic Ablation in Patients with Biliary Enteric Anastomosis

M.D. Richter[1], S.Y. Huang[1], S. Gupta[1], B.C. Odisio[1], T.A. Aloia[2], C. Conrad[2], J. Vauthey[2], [1]*Interventional Radiology, The University of Texas MD Anderson Cancer Center, Houston, Texas, United States,* [2]*Surgical Oncology, The University of Texas MD Anderson Cancer Center, Houston, Texas, United States.*

Paper 12: Transradial Arterial Access for Intra-Arterial Liver Directed Therapy: A Single Center Initial Experience

R.M. Linville, **M. Woods,** R.A. Holayter, P. Dalvie, McDermott, O. Ozkan, J. Pinchot, J. Fallucca, *Interventional Radiology, University of Wisconsin, Madison, Wisconsin, United States.*

Paper 13: The Post-SIR-Spheres Surgery Study (P4S): Outcomes Following Liver Resection Or Transplantation In 100 Patients Previously Treated With Selective Internal Radiation Therapy (SIRT) Using Y-90 Resin Microspheres

D.A. Iannitti[1], J. Bilbao[2], B. Sangro[3], M. Schon[4], K. Kouladouros[4], R. Lee[5], D. Manas[6], R. Jeyarajah[7], G. Katsanos[8], G. Maleux[9], A. Pinna[10], L. Bester[11], D. Morris[12], P. Chow[13], R. Stubbs[14], P. Gow[15], C. Vivaldi[16], K. Fisher[17], W. Lau[18], V. Donckier[19], G. Ercolani[20], F. Pardo[21], [1]*HPB Surgery, Carolinas Medical Center, Charlotte, North Carolina, United States,* [2]*Radiology, Clínica Universidad de Navarra, Pamplona, Spain,* [3]*Liver Unit, Clínica Universidad de Navarra and Centro de Investigacion Biomedica en Red de Enfermedades Hepaticas y Digestivas (CIBEREHD), Pamplona, Spain,* [4]*Klinikum Karlsruhe, Karlsruhe, Germany,* [5]*Radiology, Taipei Veterans General Hospital and National Yang-Ming University School of Medicine, Taipei, Taiwan,* [6]*Liver Unit, Freeman Hospital, Newcastle, United Kingdom,* [7]*Methodist Dallas Medical Center, Dallas, Texas, United States,* [8]*Hôpital Erasme , Université Libre de Bruxelles, Brussels, Belgium,* [9]*University Hospitals Leuven, Leuven, Belgium,* [10]*University of Bologna, Bologna, Italy,* [11]*St. Vincent's Hospital, Sydney, New South Wales, Australia,* [12]*St. George Hospital, Kogarah, New South Wales, Australia,* [13]*National Cancer Center Singapore, Singapore, Singapore,* [14]*Wakefield Gastro Clinic Ltd, Wellington, New Zealand,* [15]*Austin Hospital, Burgundy st Heidelberg, Victoria, Australia,* [16]*Ospedale Santa Chiara, Pisa, Italy,* [17]*Surgical Associates, Inc., Tulsa, Oklahoma, United States,* [18]*The Chinese University of Hong Kong, Shatin, New Territories, Hong Kong,* [19]*Hôpital Erasme & Institut Jules Bordet, Brussels, Belgium,* [20]*University of Bologna, Sant'Orsola Hospital, Bologna, Italy,* [21]*HPB and Transplant Surgery, Clinica Universidad de Navarra, Pamplona, Spain.*

Abstract Index

Paper 14: A Comparison of Response by 4 FDG-PET Metrics of Metabolic Activity and RECIST 1.1 as Predictors of Overall Survival after Selective Internal Radiation Therapy (SIRT) of Colorectal Liver Metastases

W. Shady[1], Brody[1], W. Alago[1], R.H. Siegelbaum[1], H. Yarmohammadi[1], F.E. Boas[1], C. Sofocleous[1], S. Kishore[2], N. Pandit-Taskar[2], J.A. Carrasquillo[2], J.R. Osborne[2], M. Gonen[3], R.K. Do[4], N.H. Segal[5], N.E. Kemeny[5], [1]*Interventional Radiology, Memorial Sloan Kettering Cancer Center, New York, New York, United States,* [2]*Nuclear Medicine, Memorial Sloan Kettering Cancer Center, New York, New York, United States,* [3]*Epidemiology-Biostatistics, Memorial Sloan Kettering Cancer Center, New York, New York, United States,* [4]*Radiology, Memorial Sloan Kettering Cancer Center, New York, New York, United States,* [5]*Medicine, Memorial Sloan Kettering Cancer Center, New York, New York, United States.*

Paper 15: *KRAS* Status as an Independent Prognostic Factor for Survival of Unresectable Colorectal Cancer after Yttrium-90 Radioembolization Therapy

S.J. Lahti, M. Xing, D. Zhang, **K. Kim,** *Interventional Radiology, Department of Radiology, University of Pittsburgh School of Medicine, Pittsburgh, Pennsylvania, United States.*

Paper 16: Survival Differences in Glass Versus Resin Radioembolization of Hepatic Malignancies

R. Morgan, A. Robinson, T.R. James, S. DeBacker, M. Smith, K. Werth, T. Brown, J. Hill, Z. Collins, *Radiology, University of Kansas Medical Center, Kansas City, Kansas, United States.*

Paper 17: Radiation Map Fusion Guided Combination of External Beam Radiation with Thermal Ablation for Up to 10 cm Liver Tumors

L. Jiang[1], V.P. Krishnasamy[1], H. Amalou[1], S. Xu[1], B.J. Wood[1], D. Citrin[2], R. Miller[2], H. Ning[2], [1]*Center for Interventional Oncology, Radiology and Imaging Sciences, National Institutes of Health, Bethesda, Maryland, United States,* [2]*Radiation Oncology Branch, National Cancer Institute, National Institutes of Health, Bethesda, Maryland, United States.*

Paper 18: Exact Detection of Ablative Margin and Local Tumor Progression in Liver Tumors: Preliminary Follow-Up Results

M. Trakymas, *Radiology, National Cancer Institute, Vilnius, Lithuania.*

Paper 19: Greyscale, Color Doppler, and B-Flow Ultrasound Guidance for Tissue Hydrodissection: Modality Impact on Injection Localization

A. Moreland, M. Ledwidge, A. Munoz Del Rio, S. Wells, D. Kitchin, J. Hinshaw, T. Ziemlewicz, M. Lubner, F. Lee, C. Brace, *University of Wisconsin - Madison, Madison, Wisconsin, United States.*

Paper 20: CT-Guided Screw Fixation Plus Cementoplasty in the Treatment of Painful Bone Metastases

C. Pusceddu, N. Ballicu, B. Sotgia, R. Fele, L. Melis, *Department of Oncological Radiology, Oncological Hospital "A. Businco", Cagliari, CA, Italy.*

Paper 21: Intraprocedural 3D Quantification of Lipiodol Deposition on Cone-Beam CT Predicts Tumor Response after Transarterial Chemoembolization in Patients with Hepatocellular Carcinoma

Y. Zhao[1], M. Lin[2], **Z. Wang[3],** R. Chen[4], R. Duran[5], G. Yenokyan[6], J. Chapiro[7], R. Schernthaner[8], J. Geschwind[9], [1]*Radiology, Johns Hopkins Hospital, Baltimore, Maryland, United States,* [2]*Radiology, Johns Hopkins Hospital, Baltimore, Maryland, United States,* [3]*Radiology, Johns Hopkins Hospital, Baltimore, Maryland, United States,* [4]*Radiology, Johns Hopkins Hospital, Baltimore, Maryland, United States,* [5]*Radiology, Johns Hopkins Hospital, Baltimore, Maryland, United States,* [6]*Radiology, Johns Hopkins Hospital, Baltimore, Maryland, United States,* [7]*Radiology, Johns Hopkins Hospital, Baltimore, Maryland, United States,* [8]*Radiology, Johns Hopkins Hospital, Baltimore, Maryland, United States,* [9]*Radiology, Johns Hopkins Hospital, Baltimore, Maryland, United States.*

Paper 22: Thermal Ablation of Benign Thyroid Disease: A Prospective Multi-Center Study

P. Liang, Chinese PLA General Hospital, Beijing, China.

Paper 23: Cement Leakage in Balloon Kyphoplasty for Spinal Metastasis and Myeloma: A Retrospective Evaluation of Incidence and Risk Factors

B. Richioud, H. Beji, A. Kalenderian, M. Cuinet, *Interventional Radiology, Centre Léon Bérard, Lyon, France.*

Paper 24: Portal Vein Embolization via A Percutaneous Transsplenic Access

K. Han, **G. Ko,** H. Ko, D. Gwon, K. Sung, H. Yoon, *Radiology, Asan Medical Center, Seoul, The Republic of Korea*

Paper 25: The Immediate Elevation of Serum Tumor Marker After Irreversible Electroporation Implies Technique Success

K. Huang, *Department of Surgery, National Taiwan University Hospital, Taipei, Taiwan.*

Paper 26: The Analysis for the Causes of Delayed Hospitalization after Transcatheter Arterial Chemoembolization in Patients with Unresectable Hepatocellular Carcinoma

H. Jung, *Seoul National University Hospital , Seoul, The Republic of Korea*

Paper 27: Superselective Transcatheter Arterial Embolization of Adrenal Metastases From Hepatocellular Carcinoma is Feasible and Safe

P.F. Laeseke, M. Ginsburg, J.D. Louie, D.Y. Sze, *Radiology, Stanford University Medical Center, Menlo Park, California, United States.*

Paper 28: The Effect of Anti-Reflux Catheters on Pulmonary Shunt Fraction in Patients with Hepatocellular Carcinoma

R. Stanborough, A.C. Bourgeois, Y.C. Bradley, J. McElmurray, A. Pasciak, *Radiology, University of Tennessee Medical Center Knoxville, Knoxville, Tennessee, United States.*

Abstract Index

Paper 29: The Effect of Sociodemographics on Survival in Hepatocellular Carcinoma Patients Undergoing Orthotopic Liver Transplantation: UNOS Population Study

M. Xing[1], K. Kim[2], [1]*Interventional Radiology, Department of Radiology, University of Pittsburgh School of Medicine, Pittsburgh, Pennsylvania, United States,* [2]*Cancer Therapeutics Program, University of Pittsburgh Cancer Institute, University of Pittsburgh School of Medicine, Pittsburgh, Pennsylvania, United States*

Paper 30: Development of the New Prognostic Staging System and Proposal of Treatment Algorithm Based on the Multivariate Survival Analyses (MVA) after Doxorubicin Drug Eluting Beads Transarterial Chemoembolization (DEB TACE) in Patients with Unresetable Hepatocellular Carcinoma (HCC)

H.J. Prajapati[1], K. Kim[2], [1]*Interventional Radiology and Image Guided Medicine, Emory University School of Medicine, Atlanta, Georgia, United States,* [2]*Interventional Radiology, Department of Radiology, University of Pittsburgh School of Medicine, Pittsburgh, Pennsylvania, United States.*

Paper 31: Analysis of *In Vitro* Growth Inhibition of Human Colorectal Cancer and Hepatocellular Carcinoma Cells by AntiAngiogenic Drug-Eluting Beads

S.J. Lahti[1], J.B. Jia[1], M. Xing[1], K. Kim[1], D. Zeng[2], [1]*Interventional Radiology, Department of Radiology, University of Pittsburgh School of Medicine, Pittsburgh, Pennsylvania, United States,* [2]*Molecular Imaging Laboratory, Department of Radiology, University of Pittsburgh School of Medicine, Pittsburgh, Pennsylvania, United States.*

Paper 32: SVP ^{90}Y PET/CT Dosimetry After Radioembolization in Rabbit VX2 Liver Tumor Model: Comparisons to MIRD Calculations and Ex Vivo Microsphere Uptake

A.C. Gordon[1], V.L. Gates[1], K.R. Harris[1], D. Procissi[1], J. Nicolai[1], S.K. Mouli[1], K.T. Sato[1], R. Salem[1], R.R. Lewandowski[1], A.C. Larson[1], S.B. White[2], R.A. Omary[3], R.R. Ryu[4], [1]*Radiology, Northwestern University, Chicago, Illinois, United States,* [2]*Radiology, Medical college of Wisconsin, Milwaukee, Wisconsin, United States,* [3]*Radiology and Radiological Sciences, Vanderbilt University, Nashville, Tennessee, United States,* [4]*Radiology, University of Colorado, Aurora, Colorado, United States.*

Paper 33: Improved Cytotoxicity with a Novel Mitochondria-Targeted Doxorubicin Prodrug in Colorectal Carcinoma Cells

J.B. Jia[1], M. Xing[1], K. Kim[1], X. Ling[2], M. Bai[2], [1]*Interventional Oncology Translational Laboratory, Department of Radiology, University of Pittsburgh School of Medicine, Pittsburgh, Pennsylvania, United States,* [2]*Molecular Imaging Laboratory, Department of Radiology, University of Pittsburgh School of Medicine, Pittsburgh, Pennsylvania, United States.*

Paper 34: Comparative-Effectiveness Analysis of Surgery vs. Ablation for Stage T1a Renal Cell Carcinoma in the SEER population

N. Kokabi[1], J.C. Camacho[1], M. Xing[2], R. Duszak[3], K.E. Applegate[3], D.H. Howard[4], K. Kim[5], [1]*Interventional Radiology and Image Guided Medicine, Emory University Hospital, Atlanta, Georgia, United States,* [2]*Interventional Radiology, Department of Radiology, University of Pittsburgh School of Medicine, Pittsburgh, Pennsylvania, United States,* [3]*Radiology and Imaging Sciences, Emory University School of Medicine, Atlanta, Georgia, United States,* [4]*Rollins School of Public Health, Emory University , Atlanta, Georgia, United States,* [5]*Cancer Therapeutics Program, University of Pittsburgh Cancer Institute, University of Pittsburgh School of Medicine, Pittsburgh, Pennsylvania, United States.*

Paper 35: Percutaneous Microwave Ablation of T1a Renal Cell Carcinoma: Interval Update with Median 11-Month Imaging Follow-Up

A. Moreland[1], M. Klapperich[1], S. Wells[1], E. Abel[1], M. Lubner[1], J. Hinshaw[1], F. Lee[1], S. Nakada[1], S. Best[1], S. Hedican[1], C. Brace[1], T. Ziemlewicz[1], J. Horn[2], A.M. Fischman[2], [1]*University of Wisconsin - Madison, Madison, Wisconsin, United States,* [2]*Icahn School of Medicine at Mount Sinai, New York, New York, United States.*

Paper 36: Cryoablation of Prostate Adenocarcinoma Recurrences: 2 Year Follow Up

D.A. Woodrum, K. Kinsman, S.M. Thompson, Gorny, M.R. Callstrom, L. Mynderse, *Mayo Clinic, Rochester, Minnesota, United States.*

Paper 37: Scaled Signal Intensity of Uterine Fibroids Based on T2-Weighted MR Images: A Potential Objective Method to Determine the Suitability for Magnetic Resonance-Guided Focused Ultrasound Surgery of Uterine Fibroids

S. Yoon, *Diagnostic Radiology, CHA Bundang Medical Center, Gyunggi-do, The Republic of Korea*

Paper 38: Adjunctive Techniques to Allow for Percutaneous Cryoablation of Renal Masses in Difficult Anatomic Locations

S. Sayegh[1], A. Fadl[1], O. Shoaib[1], A. Baadh[1], J.C. Hoffmann[1], D. Phung[2], [1]*Radiology, Winthrop-University Hospital, Mineola, New York, United States,* [2]*State University of New York at Stony Brook School of Medicine, Stony Brook, New York, United States.*

Paper 39: Thermal Ablation of Metastatic Adrenocortical Carcinoma: Long-Term Results

G.M. Varano[1], **L. Jiang[1],** V.P. Krishnasamy[1], N. Jain[1], H. Amalou[1], N. Abi Jaoudeh[1], A. Venkatesan[1], E.B. Levy[1], B.J. Wood[1], M. Edgerly[2], M. Velarde[2], A. Fojo[2], [1]*Center for Interventional Oncology, National Institutes of Health, Bethesda, Maryland, United States,* [2]*National Cancer Institute, National Institutes of Health, Bethesda, Maryland, United States.*

Paper 40: Percutaneous Cryoablation for the Treatment of Primary and Metastatic Lung Tumors

J.L. McDevitt, S.K. Mouli, K.T. Sato, *Radiology, Northwestern University Feinberg School of Medicine, Chicago, Illinois, United States.*

Paper 41: Image Guided Treatment of Chylous Efussions in Oncologic Patients: Single Center Experience

E.G. Santos Martin, K.M. McCluskey, C. Friend, R. Varma, *Radiology, UPMC, Pittsburgh, Pennsylvania, United States.*

Paper 42: Estrogen Receptor Alpha in Lung Cancer Development and Growth, A Novel Therapeutic Target

G.G. Chen, M. Li, A.W. Kong, M.J. Underwood, *Surgery, The Chinese University of Hong Kong, Shatin, Hong Kong.*

Paper 43: Radiofrequency Ablation versus Surgery for the Treatment of Lung Metastases

L. Tselikas[1], F. Deschamps[1], A. Hakime[1], C. Teriitehau[1], T. de Baere[1], E. Fadel[2], O. Mercier[2], L. Lamrani[2], P. Dartevelle[2], A. Auperin[3], [1]*Interventional Radiology, Gustave Roussy, Villejuif, France,* [2]*Thoracic surgery, Centre Chirugicale Marie Lannelongue, Plessis-Robinson, France,* [3]*Statistics department, Gustave Roussy, Villejuif, France.*

World Conference on Interventional Oncology (WCIO) 2015

May 6-9, 2015, New York, New York

Paper 1: Repetitive Superselective cTACE as a Bridge to Therapeutic Treatments in Patients with Unresectable Solitary HCC Tumor Larger than 8 cm.: A Single Center Experience

I. Dedes, A. Drevelegas

Objectives: This retrospective study includes 18 patients with unresectable solitary HCC tumor larger than 8 cm, who were treated with repetitive superselective conventional chemoembolization (cTACE), from 2003 to 2013. The primary objective was to investigate whether patients who had undergone repetitive cTACE for palliative reasons became candidates for therapeutic liver treatments. Mean overall survival, safety and tolerance were also endpoints of interest.
Methods: Thirteen male and five female patients with unresectable solitary HCC tumor larger than 8 cm were included. At the time of initial diagnosis 15 patients were classified as Child-Pugh A while 3 patients as Child-Pugh B. Sixteen patients had a cirrhotic liver, while fourteen patients had chronic hepatitis B, two had alcoholic liver disease and one had chronic hepatitis C. No patient had extrahepatic metastases or portal vein invasion. Overall, the mean radiological initial tumor size per patient (CT, MRI, DSA) was 10,46±2,16 cm. In all cases the tumor was solitary while in 16 patients the tumor was within capsule or pseudocapsule. Total number of cTACE sessions performed was 65 and the mean TACE session per patient was 3,61.
Results: All cTACE procedures were well tolerated and no major complications occurred. Post embolic syndrome presented in all patients. Mean overall survival was 44,50±26,70 months. After repetitive superselective cTACE one patient underwent liver transplantation (overall survival 50 months), 3 patients underwent hepatectomy (mean overall survival 17,0±4,24 months), 12 patients underwent RF or MW ablation (mean overall survival 46,16±25,29 months) while 2 patients underwent both hepatectomy and percutaneous RF and MW ablation (mean overall survival 73,0±24,0 months). Ten out of eighteen patients are still alive.
Conclusions: Superselective cTACE is a safe and efficient method for patients with unresectable solitary HCC tumor larger than 8 cm. Repetitive cTACE can be used in these patients as a bridge to therapeutic liver treatments, such as surgical methods like transplantation and hepatectomy or percutaneous RF and MW ablation. Large trials are needed to assess the overall survival benefit.

Paper 2: Is Radioembolization without 99mTc-macroaggregated Albumin Injection Possible: A Retrospective Review of 39 Patients with Hepatocellular Carcinoma

R. gurajala, E. nasr, S. shrikanthan, K. karuppasamy

Objectives: To present our experience with Technetium 99m labeled macroaggregated albumin (TcMAA) injection into right hepatic artery in assessing lung shunt fraction (LSF)and extrahepatic distribution in patients with hepatocellular carcinoma (HCC) prior to right lobe selective internal radiation therapy (SIRT) using Yttrium-90 glass microspheres (TheraSphere).
Methods: Between December 2007 and November 2014, 39 patients (34 males, 5 females; mean age-64 years (SD 11; range 45-84)) had planning angiograms with right lobe TcMAA injections (37 lobar and 2 segmental) and TcMAA distribution was assessed using SPECT/CT. 40 right lobe SIRT were performed; in 21, post treatment microspheres distribution was assessed (SPECT/CT=1, PET-CT=20). Excluding second SIRT in one patient (271 days after TcMAA), the mean interval between TcMAA and SIRT was 24 days (SD 12; range 7 to 67). Two-sample Wilcoxon test was used to compare LSF between different groups and Fisher's test was used to compare the frequency of prophylactic embolizations after Jan 2012 vs. before. TheraSphere treatment window illustrator tool was used to assess hypothetical radiation dose scenarios.
Results: 62% (n=24) had C-arm cone-beam computed tomography (CBCT) during planning angiogram. Hepatic arterio-portal venous shunt was seen in 4 patients and there was no hepatic arterio-hepatic venous shunt. 16 patients (41%) had no prophylactic embolization and in 23 patients prophylactic embolization of following arteries was performed prior to TcMAA injection: 18 – Gastroduodenal artery; 10 – Right gastric artery; 3 - Cystic artery; 1 – Left gastric artery. In 72% (n=28), there was no extrahepatic uptake in TcMAA SPECT-CT; among the 3 with extrahepatic uptake (duodenum/pancreas=2, abdominal wall=1; 1 of these 3 had CBCT), none had prophylactic embolization on the day of SIRT and 2 had Y90 PET-CT with no extrahepatic uptake. Uptakes seen in kidneys (n=2), spleen (n=1) and stomach distant from liver (n=1) were due to free pertechnetate. The mean TcMAA LSF was 5.9% (SD 0.03%; range 0.5 to 12.1%). There was no significant difference in the LSF among patients with (n=7) and without (n=32) extrahepatic distribution of TcMAA (median 5.5 and 4.5%; P-value 0.5) and between patients who had CBCT (n=24) and those who did not (n=15) (median 4.6 and 3.6%; P-value 0.77). Prophylactic embolization was less often after Jan 2012 (33%, n=5), compared to before (75%, n=18) (P-value 0.02) and there was no significant difference in the LSF between these two groups (median 5.5 and 4.3%; P-value 0.42). No patient died or was hospitalized with radioembolization induced liver disease within 30-days. At the maximum lung shunt fraction measured (12.1%), an SIRT dose of 120 Gy to a lobe measuring 1000 cc would result in 17.1 Gy to the lungs. For 1000 cc of liver measured on CT/MRI, radiation delivered using 6 Gq of TheraSphere on a given day would range from 138 Gy to 122 Gy based on 0 to 12% lung shunt fraction (1% waste is assumed).
Conclusions: Lung shunt fraction measured after right lobe TcMAA injection is within a small range. Extrahepatic uptake of TcMAA is rare and appears to have no impact on SIRT dosimetry. Using pre-known target liver volume, single-session planning angiogram followed by SIRT without TcMAA injection might be feasible using a patient specific dose that is pre-ordered (TheraSphere) or drawn on that day (SIR-Spheres). A prospective controlled study is required to assess the safety and adequacy of SIRT without TcMAA injection.

Paper 3: Transarterial Chemoembolization for the Treatment of Advanced Hepatocellular Carcinoma: A Large Retrospective Cohort Study with 508 Patients

Y. Zhao, J. Sohn, F. Fleckenstein, S. Sahu, R. Duran, R. Schernthaner, H. Lee, M. Lin, J. Geschwind

Objectives: The efficacy of transarterial chemoembolization (TACE) for Barcelona Clinic Liver Cancer (BCLC) class C remains controversial. The purpose of this study was to evaluate the efficacy of TACE in advanced (BCLC C) stage hepatocellular carcinoma (HCC) patients over the last 15 years in a single center.
Methods: Between November 1998 and December 2013, 508 HCC patients with BCLC C, Child-Pugh class A/B and Eastern Cooperative Oncology Group (ECOG) performance status 0-2 were consecutively enrolled in this retrospective cohort study. Last follow-up was on December 2014. The overall survival (OS) was calculated from the date of the first TACE until death. Univariate and multivariate analyses were conducted using Cox proportional hazards model to examine risk factors affecting survival. Only variables having $P<0.1$ on univariate analysis were included in the multivariate model. Risk scores for individual patients were calculated. The concordance (c)-statistic [to the receiver operating characteristic (ROC) curve] was used to assess the model's validity. Cut-off values for the risk score were determined according to ROC curves.
Results: Median patient age was 63 (range, 19-90 years) and 79.3% of patients were male. Hepatitis C was the predominant cause of HCC (45.3%). 303 patients (59.6%) were Child-Pugh A class. 221 patients (43.5%) had portal vein tumor thrombosis (PVTT), 84 patients (16.5%) had extrahepatic metastasis and 395 patients (77.8%) had ECOG performance score ≥1. The median number of TACE sessions per patient was 2 (range, 1-10) for a total of 906 procedures. In the entire cohort, 296 (58.3%) patients received conventional TACE, 153 (30.1%) patients received drug-eluting beads TACE (DEB-TACE) and 59 (11.6%) received both. In addition, 104 received

sorafenib combined with TACE. The median duration of follow-up was 9.3 months (range 0.1-153.6). At the last follow-up, 377 (74.2%) patients had died. The median overall survival was 11.9 months (95%CI 10.12-13.68). Multivariate analysis defined that PVTT (HR=1.77, 95%CI 1.39-2.26), extrahepatic spread (HR=2.17, 95%CI 1.57-3.01), number of tumor nodules (HR=1.58, 95%CI 1.24-2.00), Child-Pugh (HR=1.37, 95%CI 1.09-1.73) and tumor size (HR=1.31, 95%CI 1.02-1.68) were significantly associated with survival. The c-statistic associate with the model in the prediction of 1 year survival was 0.73 (95%CI 0.68-0.78). The patients whose scores were <3 had a significantly longer survival than patients whose scores were >3 (26.2 vs. 9.7 months, respectively, P<0.001). In patients treated without (n=404) and with (n=104) sorafenib, the median OS was 11.2 months (95% CI 9.73-12.67) and 18.5 months (95% CI 13.37-23.63), respectively. Sorafenib was not associated with longer survival (HR=0.83, 95%CI 0.64-1.06, P=0.133).

Conclusions: PVTT, extrahepatic spread, the number of tumor nodules, Child-Pugh class and tumor size were significantly associated with overall survival in BCLC C patients who underwent TACE treatment. These findings can be used as a valuable guide for designing prospective studies in identifying the subgroup that could benefit from TACE in the BCLC C population. Tumor burden should be taken into consideration for further stratifying BCLC stage C.

Paper 4: Contrast Enhancement Kinetics of the Hepatic Arterial Vasculature after Drug Eluting Bead Trans-Arterial Chemoembolization

W. Lea, S. Dybul, R. Setser, S.B. White, P. Patel, R. Hieb, S. Tutton, W. Rilling, E. Hohenwalter

Objectives: Liver directed therapy is a safe and effective treatment option for patients with hepatocellular carcinoma. Often times, patients undergo multiple treatments to the same vascular territory. Our purpose was to evaluate longitudinal changes in vascular characteristics at followup imaging following drug-eluting bead trans-arterial chemoembolization (DEB-TACE).

Methods: IRB approval was obtained for this retrospective review of 7 patients who underwent a single session of DEB-TACE for hepatocellular carcinoma (HCC) and had subsequent angiographic imaging. A prototype software program (Siemens Healthcare (Forchheim, Germany)) was used to analyze the angiograms to evaluate changes in hepatic arterial flow before and after therapy. Regions of interest (ROIs) were placed within higher order hepatic arteries supplying tumor(s) and surrounding parenchyma in each patient. Kinetic contrast enhancement parameters were measured at baseline, immediately following treatment, and at next angiographic evaluation and included time to peak enhancement (TTP), time of ½ maximum enhancement (THM), time of maximal slope of enhancement (TMS), and slope of enhancement. These parameters were compared using a paired t-test analysis.

Results: No significant difference was present in the kinetic contrast enhancement parameters between those at baseline and immediately following DEB-TACE (TTP P=0.24, THM P=0.62, TMS P=0.77, slope P=0.47). Additionally no significant difference was present in the kinetic contrast enhancement parameters between those at baseline and at subsequent angiographic imaging (mean 88 days; TTP P=0.13, THM P=0.32, TMS P=0.43, slope P=0.30).

Conclusions: Single session drug-eluting bead chemoembolization for HCC likely does not result in persistent significant changes in vascular flow beyond 3 months to the treated vascular bed.

Paper 5: Transcathether Arterial Chemoembolization plus Radiotherapy is Superior to Chemoembolization Alone for Hepatocellular Carcinoma: A Comprehensive Systematic Review and Meta-Analysis

Y. Huo, G.D. Eslick

Objectives: To evaluate the efficacy and safety of transcatheter arterial chemoembolization plus radiotherapy (TACE+RT) compared to TACE alone for unresectable hepatocellular carcinoma (UHCC) using meta-analytical techniques.

Methods: A search of Medline, EMBASE, PubMed, Cochrane and Google Scholar databases was done. Meta-analysis of overall survival (OS), complete response (CR) and adverse events (AEs) were performed. Subgroup analysis on study design, anticancer drug, radiotherapy type, embolization type, presence of portal venous thrombosis (PVT) and duration between TACE and RT was done.

Results: There were 25 trials (11 RCTs) involving 2,577 patients. TACE+RT showed significantly better 1 year overall survival (OR:1.36, 95% CI 1.19-1.54) and CR (OR:2.73, 95% CI 1.95-3.81) compared to TACE alone. The survival benefit progressively increased for 2, 3, 4 and 5 year overall survival (respectively: OR:1.55, 95% CI 1.31-1.85; OR:1.91, 95% CI 1.55-2.35; OR:3.01 95% CI 1.38-6.55; OR:3.98 95% CI 1.86-8.5). There was an increased incidence of gastroduodenal ulcers, alanine transaminase elevation and total bilirubin elevation in TACE+RT compared to TACE alone. Subgroup analyses showed non-significant trends where overall survival was greater for TACE+RT in patients with PVT compared to those without PVT.

Conclusions: TACE+RT was more therapeutically beneficial than TACE alone for UHCC.

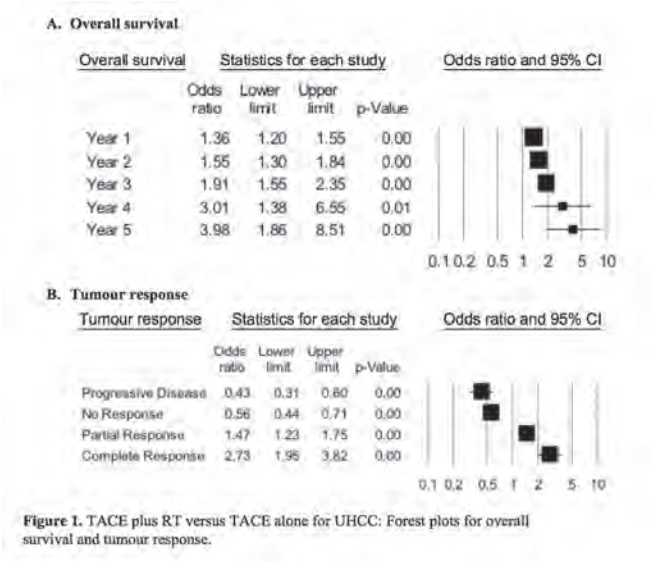

Figure 1. TACE plus RT versus TACE alone for UHCC: Forest plots for overall survival and tumour response.

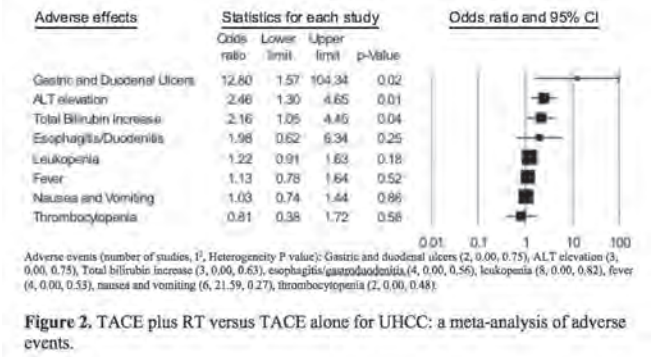

Figure 2. TACE plus RT versus TACE alone for UHCC: a meta-analysis of adverse events.

Paper 6: Development and Validation of an Endovascular Chemotherapy Filter Device to Enable High Dose Transarterial Hepatic Doxorubicin Therapy: In Vitro Proof of Concept in Human Serum

A.S. Patel, C. Sze, J. Yang, M. Saeed, A.D. Losey, B. Thorne, A. Chin, S.W. Hetts, M. Wilson

Objectives: A novel temporary endovascular chemotherapy filter (CF) device with active resin material was developed to remove doxorubicin (Dox) from the blood via an ionic mechanism. This could potentially enable high-dose Dox intra-arterial therapy while limiting Dox toxicity. Previous proof-of-concept established high-capacity rapid Dox binding of the resin in both phosphate buffered saline (PBS) and swine serum in vitro. Promising preliminary results have also been demonstrated in vivo in swine. In this study, we aim to determine resin Dox binding rate and capacity in human serum and swine whole blood in vitro.

Methods: Research grade swine whole blood was collected and mixed with heparin to form a heparinized solution at 10 IU/ml. Dox was introduced and equilibrated into either 200 ml of research grade human serum at 37°C or 50 ml of swine whole blood at a concentration 0.05 mg/ml (10 mg total for human serum, 2 mg total for swine whole blood). Resin (Dow Chemical Co.) was then introduced and mixed at a concentration of 2.5 ml/L of solution (1.9 g/L). Dox concentrations were measured over 60 minutes via fluorescence spectrophotometry, and compared to controls without resin. Human serum and swine whole blood results were compared to PBS and swine serum results from previous studies, where similar methods were employed.

Results: Fig. 1 illustrates and compares binding kinetics PBS, swine serum, human serum, and swine whole blood. Controls for human serum showed 8% and 12% reduction in Dox concentration at 30 and 60 minutes, respectively. Controls for swine whole blood showed 32% and 40% reduction in Dox concentration at 30 and 60 minutes.

Conclusions: Proof of concept and feasibility of rapid high-capacity binding of Dox from human serum and swine whole blood by resin was successfully demonstrated in vitro. Human serum experiments demonstrate slightly slower kinetics compared to

PBS and swine serum solution, but nonetheless bind at a high capacity after 30 mins. Swine whole blood experiments demonstrate rapid kinetics compared to PBS and swine serum, and also bind at high capacity after 30 mins. The high degree of binding by a small amount of resin paves way for a pre-clinical swine study testing in vivo Dox binding by CF catheters containing over 10x more resin than these experiment.

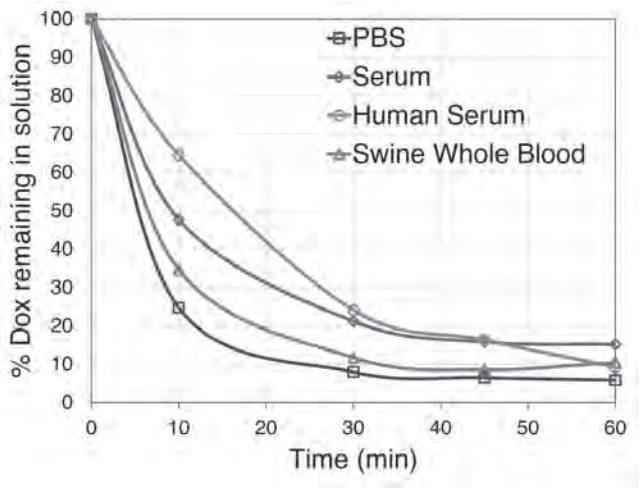

Figure 1 - Percent of total dox remaining in solution over time in physiologic solutions.

Paper 7: Comparison of Changes in Liver and Spleen Volume and Hepatosplenic Function after Chemoembolization Versus 90Y Radioembolization in Patients with Metastatic Neuroendocrine Tumor

V. Etezadi, T. Larrea, M.C. Soulen, W.S. Stavropoulos, J. Mondschein, M. Dagli

Objectives: To compare changes in markers of liver injury/synthetic function and portal hypertension, after chemoembolization (TACE) vs. radioembolization (TARE) in patients with metastatic neuroendocrine tumor (NET).
Methods: A retrospective review of a prospectively acquired database of patients undergoing either 90Y TARE with resin microspheres or TACE for metastatic hepatic NET over a 5-year period was performed. Patients treated with hepatotoxic systemic chemotherapy were excluded. Collected data included liver/spleen volumes on CT/MR, platelet count, INR, albumin, total protein, AST, ALT, bilirubin, and creatinine before therapy and approximately 1-3 and 4-6 months after.
Results: Of 47 patients, 22 patients (11M; age 62 ±12 y) underwent TARE and 25 patients (16M; age 58 ±12 y) underwent TACE. The two groups had similar baseline demographics, pretreatment spleen and liver volumes and lab data. After TARE, mean splenic volume showed a non-significant increase of 9% at 3 months post treatment (P=0.3), which increased to 15% at 6 months compared with the pretreatment volumes (P=0.008). Mean liver volume showed no significant change at 3 months post treatment (avg. decrease of 1%) but showed a significant decrease of 11% at 6 months (P=0.01). After TACE, at 1-3 months there was transient increase in mean splenic volume of 40% (P=0.03). Splenic volume subsequently normalized at the 4-6 month follow-up to a 4% increase from baseline (P=0.6). Mean liver volume showed a decreasing trend of 8% at 3 months (P=0.6) and 10% at 6 months (P=0.08). There was a significant 12.8% decrease in platelet count at 6 months in the TACE group (P=0.02) and a trend toward a decreased platelet count of 12.6% in the TARE group at 6 months (P=0.1). Changes in all other serologic data were not statistically significant.
Conclusions: In chemo-naive patients with metastatic NET both TACE and TARE appear to cause splenic enlargement although the change appears to be earlier and more transient after TACE. With the exception of a decrease in platelet values, there appears to be no significant change in major markers of hepatic injury/function within 6 months after either treatment.

Paper 8: Association of Three Common Proto-Oncogene Mutations to the Response of Radioembolization for Hepatic Colorectal Metastasis

R. O'Hara, N.N. Davis, R.L. Hardman

Objectives: Mutations in KRAS, b-RAF, and PIK3CA have been implicated as proto-oncogenes in the development of several cancers including colorectal cancers and may imply a poor prognosis. Mutations in these genes also have implications on the applications of certain chemotherapeutics. PIK3CA and KRAS mutations, for example, predict a poor response to the anti-EGFR drugs panitumumab and cetuximab. The BRAF V600E mutant is the target of specific tyrosine kinase inhibitors and suggests and invulnerability to certain proteasome inhibitors. Radioembolization with Yttrium-90 labeled resin microspheres has been FDA-approved for the treatment of unresectable hepatic metastases from colorectal cancer. However, little is known about the response of this therapy in patients harboring one or more of the above oncogenes. The purpose of this study was to compare the tumor response and survival of patients with metastatic colorectal cancer with and without mutations in three proto-oncogenes after radioembolization with Yttrium-90 labeled resin microspheres.
Methods: 26 patients with liver-dominant colorectal metastasis were evaluated that underwent radioembolization at our institution from 2011-2014. Follow up data at 3 months was available in 20 patients. All patients were evaluated for KRAS mutation. 15 were evaluated for b-RAF mutation, and 13 for PLK3CA. Odds ratio of disease progression was evaluated by logistic regression (Stata, College Station TX). Liver imaging was performed by board certified abdominal radiologists according to m-recist criteria.
Results: Among patients with wild type KRAS, PIK3CA, and b-RAF three patients had progressive disease (21.4%), 7 had partial response (50%), 2 had stable disease (14.3%) and 2 had complete response (14.3%). The patients with mutated KRAS, PIK3CA, or b-RAF had a much higher rate of progressive disease after liver directed radioembolization. Four patients had progressive disease (66.7%), one had partial response (16.7%), and one had stable disease (16.7%) (P =0.161 by Kolmogorov-Smirov test). No patient had complete response with the tested genetic mutations. There was no statistical increased risk with KRAS mutation by logistic regression in this small sample (OR 0.527, CI: 0.006-48.9).
Conclusions: Proto-oncogene testing is playing an increasing role in the chemotherapeutic treatment of metastatic colorectal cancer. Proto-oncogenes may also predict therapy response in liver directed therapy. Our results of disease progression by m-recist criteria show that patients with KRAS, PIK3CA, or b-RAF mutations are much more likely than wild type patients to have progressive disease after Y90 resin radioembolization. Given the low event rate of some of these mutations, pooled data among many institutions will likely be needed to fully investigate the association of proto-oncogenes on radioembolization outcomes.

Paper 9: EASL and mRECIST Better Predict Survival after Yttrium-90 Radioembolization Therapy Compared to RECIST and WHO in Metastatic Unresectable Colorectal Cancer in the Liver

M.J. Magnetta, D. Zhang, L. Steven, M. Xing, K. Kim

Objectives: The best imaging response criteria as a surrogate biomarker for clinical outcomes after Yttrium-90 Radioembolization (Y-90) therapy is largely unknown. The purpose of this study was to establish imaging tumor response using the modified RECIST, RECIST, WHO and EASL criteria in correlation with survival for unresectable colorectal cancer (CRC).
Methods: 132 patients with unresectable CRC liver metastases treated with Y90 from 2000-2013 were studied. Imaging was obtained a median of 36 days (range 6-731 days) prior and 83 days post Y90 (range 20-439 days). WHO, RECIST, mRECIST and EASL criteria were studied and applied to target tumors. Portal venous peripheral contrast enhancement was accounted for in mRECIST and EASL. Distribution of tumors, portal hypertension (PHT) and portal venous thrombosis (PVT) were studied. Patient characteristics including Child Pugh and CEA were studied. SPSS was used for statistical analysis. Sign's test, order logistic regression analysis, Kaplan-Meier curve, log-rank test and Cox proportional model was employed.
Results: There were strong correlations between the responders and overall survivals after Y-90 therapy in all response criteria (mRECIST P=0.002, RECIST P=0.012, WHO P=0.026, EASL P=0.002) (Fig. 1). Overall survival hazard ratios demonstrated EASL and mRECIST as better prognosticators than RECIST or WHO to predict overall survivals (Table 1). The presence of multiple lesions on pre-Y90 images using EASL and mRECIST and Child Pugh Class using EASL were associated with an increased risk of progressive disease.
Conclusions: EASL and mRECIST are better prognosticators for survival than RECIST or WHO after Y90 therapy for unresectable CRC.

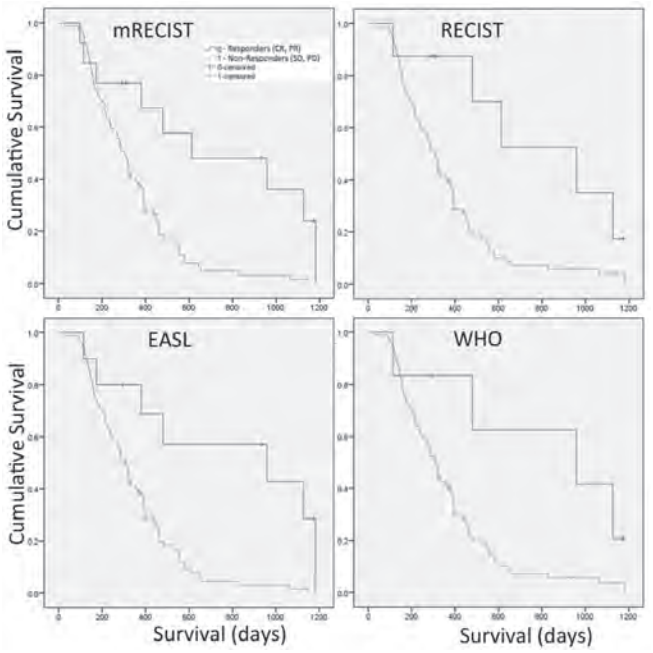

KM curves showing survival of responders versus non responders as measured by tumor response methods.

Target Lesion Response

Target lesion response	Number of Patients	Median Survival (days, 95% CI)	Mean Survival (days, 95% CI)	P-value by log-rank test	Overall Survival (Hazard Ratio, 95% CI)	P-value by Cox Model
mRECIST						
Nonresponders	110	304 (255.61, 352.39)	340 (291.61, 388.58)	0.002	Reference	0.003
Responders	20	613 (0, 1266.38)	706 (450.71, 961.92)		0.310 (0.145, 0.663)	
RECIST						
Nonresponders	120	304 (262.36, 345.64)	359 (302.54, 414.80)	0.012	Reference	0.017
Responders	12	959 (429.69, 1488.31)	776 (501.82, 1049.78)		0.325 (0.129, 0.816)	
WHO						
Nonresponders	123	311 (271.54, 350.50)	364 (307.90, 419.37)	0.026	Reference	0.034
Responders	9	959 (0, 1958.47)	798 (466.46, 1129.37)		0.329 (0.118, 0.920)	
EASL						
Nonresponders	113	304 (255.24, 352.76)	343 (294.46, 390.63)	0.002	Reference	0.003
Responders	17	959 (0, 2104.73)	763 (471.10, 1054.65)		0.266 (0.112, 0.633)	

Univariate Kaplan-Meier survival and multivariate analyses with Cox model of responders and non-responders of target and overall response according to WHO, RECIST, mRECIST and EASL guidelines.

Paper 10: Prospective Evaluation of Transarterial Chemoembolization Using a New Generation of Doxorubicin Eluting Beads for the Treatment of Chemorefractory Liver Metastases from Breast Cancer

M.P. Kohi, A. Taylor, K.P. Kolli, J. LaBerge, R. Kerlan, N. Fidelman

Objectives: To report the safety and efficacy of transarterial chemoembolization (TACE) using 70-150μm LC beads coated with doxorubicin for the treatment of chemorefractory liver-dominant metastases from breast cancer.
Methods: We performed a prospective evaluation of DEB TACE for the treatment of chemorefractory liver metastases from breast cancer in ten women with chemorefractory liver metastases. All patients had progressed following at least three separate lines of systemic chemotherapy. DEB TACE was performed in a lobar fashion using 37.5mg doxorubicin/1ml of 70-150 μm LC beads (BTG, Inc.) for a total lobar dose of 150mg of doxorubicin. Tumor response was evaluated according to mRECIST criteria based on contrast enhanced imaging performed one month following the last planned DEB TACE. Adverse events (AE) following DEB TACE were documented.
Results: A total of 20 lobar DEB TACE administrations were performed. Seven out of ten patients (70%) had partial response, one patient demonstrated stable disease (10%), and two patients (20%) experienced disease progression resulting in death. The patients who died had infiltrative liver metastases with pseudocirrhosis or portal hypertension. Both patients experienced grade 3 hepatobiliary AE within 24-hours of the DEB TACE in addition to progressive hyperbilirubinemia, which continued until death. Death occurred 3 and 6 weeks following DEB TACE, respectively.
Conclusions: DEB TACE using 70-150um LC beads may be an effective therapy for chemorefractory liver metastases from breast cancer. However, in the setting of infiltrative metastases with pseudocirrhosis, or portal hypertension, DEB TACE may result in hyperbilirubinemia, liver failure, and death.

Paper 11: Efficacy of Aggressive Antibiotic Prophylaxis to Prevent Abscess following Percutaneous Hepatic Ablation in Patients with Biliary Enteric Anastomosis

M.D. Richter, S.Y. Huang, T.A. Aloia, C. Conrad, J. Vauthey, S. Gupta, B.C. Odisio

Objectives: The current rates of liver abscess following percutaneous hepatic ablation (PHA) in patients with biliary enteric anastomosis (BEA) range between 44%-100%. To date, there is no established role for the use of a prophylactic antibiotic regimen in this setting. The present study was performed to evaluate the efficacy of an aggressive prophylactic antibiotic regimen for the prevention of liver abscess formation following PHA in patients with BEA.
Methods: A single-institution retrospective analysis was performed over a period of 56 months on 222 patients submitted to 266 PHA sessions. Eight patients (3.6%) had a prior history of BEA (hepaticojejunostomy post whipple, n=7; and liver transplant, n=1) and received a prophylactic antibiotic regimen consisting of oral levofloxacin 500mg and metronidazole 500 mg twice daily (48 hours prior to 2 weeks after the PHA), and neomycin 1g plus erythromycin base 1g orally (1pm, 2pm and 11pm on the day prior the PHA). Post-treatment clinical and imaging follow-up were utilized to identify and classify adverse events (AE) accordingly to the CTCAE classification.
Results: Each patient had one session of PHA. The median imaging follow up time was 382 days (range, 77-1025 days). Mean time from EBA creation and PHA was 1778 days. Mean tumor size treated with PHA was 1.6 cm (95% CI ± 0.35). Microwave (MW) and radiofrequency ablation (RFA) were utilized in 6 and 3 of the patients, respectively. One patient had MW and RFA utilized in two distinct lesions. None of the patients treated with hepatic ablation developed abscess following the procedure. One patient developed a grade 1 segmental biloma after PHA and was treated conservatively. No adverse events related to the prophylactic antibiotic regimen were observed.
Conclusions: Our results indicate that the risk of liver abscess following PHA in patients with BEA can be significantly reduced through the use of an aggressive antibiotic regimen when compared with other series with similar number of patients.

Paper 12: Transradial Arterial Access for Intra-Arterial Liver Directed Therapy: A Single Center Initial Experience

R.M. Linville, R.A. Holayter, P. Dalvie, J. McDermott, O. Ozkan, J. Pinchot, J. Fallucca, M. Woods

Objectives: Transradial arterial access (TRA) has become well established in interventional cardiology as first line access for cardiac catheterization due to its lower bleeding complications, improved patient satisfaction, decreased cost, and decreased time to ambulation and discharge compared to transfemoral arterial access (TFA). Limited published experience with TRA exists for interventional radiology procedures, specifically intra-arterial liver directed therapies. The purpose of this study is to report initial technical success and complication rates for TRA during Y-90 radioembolization and chemoembolization (TACE) in a single center.
Methods: All intra-arterial liver directed therapy cases with TRA were retrospectively reviewed. This access option was initially offered to patients in September 2014. Appropriateness for TRA was assessed with a Barbeau test and ultrasound evaluation of the left radial artery. Left radial artery access was performed under sonographic guidance with a single wall puncture technique. A 5 Fr Glidesheath was subsequently placed and a solution containing 3,000 units unfractionated heparin, 200 mcg nitroglycerin, and 2.5 mg verapamil was infused utilizing the hemodilution technique. A 5 Fr 110 cm Jacky Radial Optitorque catheter was used to catheterize the visceral arteries with one exception — a 4 Fr 120 cm non-taper angled Glidecath was required for additional length to reach the celiac artery. A TR band was utilized for hemostasis. Technical success, radial artery size, 30-day major and minor complications, and patient preference were evaluated. Fluoroscopy time and dose-area-product (DAP) were compared to matched controls (TFA intra-arterial liver directed therapy cases performed during the same time period).
Results: During a 4-month period there were 16 attempted liver directed therapy cases via TRA in 13 patients (10 males, 3 females; mean age of 61.8). Procedures were: Y-90 mapping (n = 7), Y-90 treatment (n = 3), and TACE (n = 6). TRA was unsuccessful once: a Y-90 mapping procedure in a 50 year old female patient with a radial artery diameter of 2.1 mm. Failure was due to inability to advance wire on initial needle access secondary to vasospasm. TRA technical success was 93.8%. Mean radial artery diameter was 2.2 mm (range 1.6 - 3.1 mm). No access site or major procedural complications occurred. One patient had mild arm pain during the pro-

cedure. This was relieved with intravenous analgesics and completely resolved with catheter removal. Five patients previously had TFA for endovascular procedures and 5/5 (100%) reported preference after the procedure for TRA. Mean fluoroscopy time (TRA: 21.6 min, TFA: 19.1 min; P=0.526) and DAP (TRA 44,383 cGycm^2, TFA: 36,103 cGycm^2; P=0.533) were not statistically significantly different between TRA and TFA matched procedures.
Conclusions: TRA for intra-arterial liver directed therapy is safe and well-tolerated. There is no significant difference in patient radiation doses when compared to matched TFA procedures. All patients who had previous TFA preferred TRA.

Paper 13: The Post-SIR-Spheres Surgery Study (P4S): Outcomes following Liver Resection or Transplantation in 100 Patients Previously Treated with Selective Internal Radiation Therapy (SIRT) using Y-90 Resin Microspheres

D.A. Iannitti, J. Bilbao, B. Sangro, M. Schon, R. Lee, D. Manas, R. Jeyarajah, G. Katsanos, G. Maleux, A. Pinna, L. Bester, D. Morris, P. Chow, R. Stubbs, P. Gow, C. Vivaldi, K. Fisher, W. Lau, K. Kouladouros, V. Donckier, G. Ercolani, F. Pardo

Objectives: SIRT (or radioembolisation) is primarily used as palliative treatment for inoperable primary or metastatic liver tumours, and as bridge-to-liver transplantation in hepatocellular carcinoma (HCC). Reports show that SIRT may downsize inoperable liver tumors, but no robust studies on post-surgical safety outcomes exist.
Methods: P4S is an international, multicenter, retrospective study to assess outcomes associated with liver resection or transplantation following SIRT using Y-90 resin microspheres (SIR-Spheres; Sirtex Medical Ltd). Primary endpoints were peri-operative and 90-day post-operative morbidity (Clavien-Dindo [CD] scale) and mortality. Analysis used standard statistical methods.
Results: Data were captured on SIRT, surgery (between 08/1998-05/2014) and follow-up on 100 patients with either primary liver cancer or secondary hepatic metastases. **Resection:** SIRT followed by resection was performed in 71 patients including 30 (42% of resection cohort) with colorectal cancer (mCRC), 23 (32%) hepatocellular carcinoma (HCC), 7 (10%) intra-hepatic cholangiocarcinoma (ICC), 4 (6%) neuroendocrine tumours (mNET) and 7 (10%) other cancers. Resection was classified as minor (<3 segments: 28.2%), major/not-extended (3-4 segments: 45.0%) or extended (≥5 segments: 26.8%). More mCRC patients had extended resection (40% vs. 17%). Baseline characteristics were otherwise similar in each cohort, and 50.0%/26.8% received chemotherapy pre-/post-SIRT, respectively. Median time from last SIRT to minor, major/not-extended and extended resection was 7.0, 5.6 and 3.5 months, respectively. Median post-operative stay was 9 days. CD grade 3+ peri-/post-operative complications were: liver failure: 7 (10%); wound-specific: 4 (6%); cardiovascular: 0 (0%); pulmonary-specific: 8 (11%); renal-specific: 2 (3%); other: 11 (15%). The 90-day readmission rate was 21%. Cumulative 90-day all-cause mortality from first hepatic surgery was 4 (6%). These 4 cases were all trisectionectomies (mCRC: 3; ICC: 1) and typically had ≥1 prior chemotherapy line, pre-surgical co-morbidities and suffered post-hepatectomy multi-organ failure including liver failure. Future liver remnant was targeted with SIRT in 1 of the 4 cases. Median survival post-resection has not been reached at a median follow-up of 30.7 months. **Transplantation:** SIRT followed by liver transplantation was performed in 29 patients, 26 (90% of transplantation cohort) HCC and 3 (10%) mNET. The HCC patients were mainly cirrhotics (92%). Median time from last SIRT to transplantation was 8.3 months. Median post-operative stay was 10 days. The incidence of complications CD grade ≥3 was 4 (14%; all other). Any grade pulmonary-specific complication occurred only in 1 patient (grade 2) and was not potentially related to prior SIRT. Any grade liver failure was observed in 3% (1 grade 2). The 90-day readmission rate was 31%, while no 90-day all-cause mortality was observed. Median survival from date of liver transplantation has not been reached with median post-surgical follow up of 40.2 months.
Conclusions: The safety profile of post-SIRT resection and transplantation appears in line with published studies of hepatic resection and transplantation. No deaths appear to be directly related to SIRT.

Paper 14: A Comparison of Response by 4 FDG-PET Metrics of Metabolic Activity and RECIST 1.1 as Predictors of Overall Survival after Selective Internal Radiation Therapy (SIRT) of Colorectal Liver Metastases

W. Shady, S. Kishore, N. Pandit-Taskar, J.A. Carrasquillo, J.R. Osborne, M. Gonen, L. Brody, W. Alago, R.H. Siegelbaum, H. Yarmohammadi, F.E. Boas, R.K. Do, N.H. Segal, N.E. Kemeny, C. Sofocleous

Objectives: There are 2 main systems of response assessment after SIRT of colorectal liver metastases (CLM): by anatomic imaging using the largest lesion diameter as by RECIST 1.1 or metabolically on FDG-PET imaging with several proposed metrics. The aim of this study was to evaluate the prognostic value of response by RECIST 1.1 and 4 metrics of metabolic activity on FDG-PET as predictors of overall survival.
Objectives: There are 2 main systems of response assessment after SIRT of colorectal liver metastases (CLM): by anatomic imaging using the largest lesion diameter as by RECIST 1.1 or metabolically on FDG-PET imaging with several proposed metrics. The aim of this study was to evaluate the prognostic value of response by RECIST 1.1 and 4 metrics of metabolic activity on FDG-PET as predictors of overall survival.
Methods: We preformed a retrospective review of our prospectively created HIPPA compliant SIRT database for the time period: December 2009 till March 2013. We included patients treated for CLM who had both imaging modalities, contrast enhanced CT and FDG-PET, available at baseline and post SIRT. Up to 5 target lesions were chosen on baseline CT. Using RECIST 1.1 patients were classified into 2 groups: any response (partial response and stable disease) or progression. On FDG-PET, 4 metabolic metrics were measured: SUVmax, SUVpeak, total lesion glycolysis (TLG), and functional lesion volume (FLV) for the same target lesions chosen on CT. For each metric a mean value of the target lesions was calculated, and patients were classified into 2 groups according to the percentage change in the metric post SIRT: responders (≥30% decrease) and non-responders; if new lesions appeared on the FDGPET post SIRT the patient was classified as a non-responder. Overall survival was calculated from time of SIRT until the latest available follow-up using Kaplan-Meier methodology. Log rank test was used to compare survival between responding and non-responding patients.
Methods: We preformed a retrospective review of our prospectively created HIPPA compliant SIRT database for the time period: December 2009 till March 2013. We included patients treated for CLM who had both imaging modalities, contrast enhanced CT and FDG-PET, available at baseline and post SIRT. Up to 5 target lesions were chosen on baseline CT. Using RECIST 1.1 patients were classified into 2 groups: any response (partial response and stable disease) or progression. On FDG-PET, 4 metabolic metrics were measured: SUVmax, SUVpeak, total lesion glycolysis (TLG), and functional lesion volume (FLV) for the same target lesions chosen on CT. For each metric a mean value of the target lesions was calculated, and patients were classified into 2 groups according to the percentage change in the metric post SIRT: responders (≥30% decrease) and non-responders; if new lesions appeared on the FDG-PET post SIRT the patient was classified as a non-responder. Overall survival was calculated from time of SIRT until the latest available follow-up using Kaplan-Meier methodology. Log rank test was used to compare survival between responding and non-responding patients.
Results: This study enrolled 42 consecutive patients with 103 target lesions; a median of 2 (range: 1-5) target lesions per patient. The median time from baseline FDG-PET imaging to SIRT was 3.5 (range: 0.4-11) weeks, while the median time from SIRT until the response assessment FDG-PET imaging was 7.4 (range: 3-16) weeks. By RECIST 1.1, 23 patients were classified as showing any response (1 patient with partial response, 22 patients with stable disease), and 19 patients were classified as progressive disease. The numbers of responders according to the FDG-PET metrics were: (12/42) by SUVmax, (14/42) by SUVpeak, (15/42) by TLG, and (14/42) by FLV. The median overall survival after SIRT was 12.7 months (95% CI: 7.1-16.3). The difference in survival between responders and non-responders was significant when using TLG (P=0.038) and FLV (P=0.036), but not reaching significance when using SUVmax (P=0.08) or SUVpeak (P=0.15). As for RECIST 1.1, there was no difference in survival between patients showing any response versus progression (P=0.80).
Results: This study enrolled 42 consecutive patients with 103 target lesions; a median of 2 (range: 1-5) target lesions per patient. The median time from baseline FDG-PET imaging to SIRT was 3.5 (range: 0.4-11) weeks, while the median time from SIRT until the response assessment FDG-PET imaging was 7.4 (range: 3-16) weeks. By RECIST 1.1, 23 patients were classified as showing any response (1 patient with partial response, 22 patients with stable disease), and 19 patients were classified as progressive disease. The numbers of responders according to the FDG-PET metrics were: (12/42) by SUVmax, (14/42) by SUVpeak, (15/42) by TLG, and (14/42) by FLV. The median overall survival after SIRT was 12.7 months (95% CI: 7.1-16.3). The difference in survival between responders and non-responders was significant when using TLG (P=0.038) and FLV (P=0.036), but not reaching significance when using SUVmax (P=0.08) or SUVpeak (P=0.15). As for RECIST 1.1, there was no difference in survival between patients showing any response versus progression (P=0.80).
Conclusion: Anatomic imaging response assessment by RECIST 1.1 showed poor sensitivity in detecting response post SIRT of CLM, and failed to predict overall survival. All FDG-PET metabolic activity metrics showed higher sensitivity in detecting response. Both total lesion glycolysis (TLG) and functional lesion volume (FLV) reached statistical significance as predictors of patients survival post SIRT of CLM.
Conclusions: Anatomic imaging response assessment by RECIST 1.1 showed poor sensitivity in detecting response post SIRT of CLM, and failed to predict overall survival. All FDG-PET metabolic activity metrics showed higher sensitivity in detecting response. Both total lesion glycolysis (TLG) and functional lesion volume (FLV) reached statistical significance as predictors of patients survival post SIRT of CLM.

Paper 15: *KRAS* Status as an Independent Prognostic Factor for Survival of Unresectable Colorectal Cancer after Yttrium-90 Radioembolization Therapy

S.J. Lahti, M. Xing, D. Zhang, K. Kim

Objectives: To determine the significance of *KRAS* mutation status as a predictor of response to Yttrium-90 radioembolization (Y90) of colorectal cancer (CRC) liver metastases.
Methods: Consecutive patients with unresectable CRC liver metastases and documented *KRAS* exon 2 mutation status who were treated with Y90 from 2002-2014 were studied. Patient demographics, lab and molecular markers, disease stages, tumor distribution, therapy regimens, treatment parameters, and OS from first Y90 were compared between patients with *KRAS* wt and mutant. Kaplan-Meier estimation and Cox proportional hazard models were used for survival analysis and to assess independent prognostic factors for OS.
Results: One hundred and six patients underwent *KRAS* exon 2 mutation analysis prior to receiving Y90, of these, 42 (39.6%) were identified as *KRAS* mutant. *KRAS* wt and mutant groups were similar in age, sex, race, Child-Pugh class, % receiving Y90 as third-line therapy, carcinoembryonic antigen expression, target mass, and lung-shunt fraction (P>0.05 for all). The mean time from liver metastasis to first Y90 was significantly shorter for the mutant group, 18.6 vs 29.0 months (P=0.003). A greater % of wt patients received anti-EGFR chemotherapy prior to Y90, 65.1% vs 7.0% (P<0.001), and additional chemotherapy after Y90, 53.1% vs 30.0% (P=0.021). Median OS from first Y90 was significantly greater in wt than in mutant patients, 9.5 vs 4.4 months (P=0.008). There was no difference in the incidence of toxicity (P=0.51) or CEA response (P=0.724) between *KRAS* groups. Univariate analysis identified pre-Y90 Child-Pugh score>5, pre-Y90 Child-Pugh score>6, pre-Y90 CEA>250, post-Y90 chemotherapy, grade ≥2 toxicity, and *KRAS* status as prognostic factors for OS. On multivariate analysis, elevated Child-Pugh score and *KRAS* status were the only pre-treatment variables shown to be independent prognostic factors for OS.
Conclusions: *KRAS* mutations and elevated Child-Pugh score independently predict poor overall survival after Y90 radioembolization of CRC liver metastases.

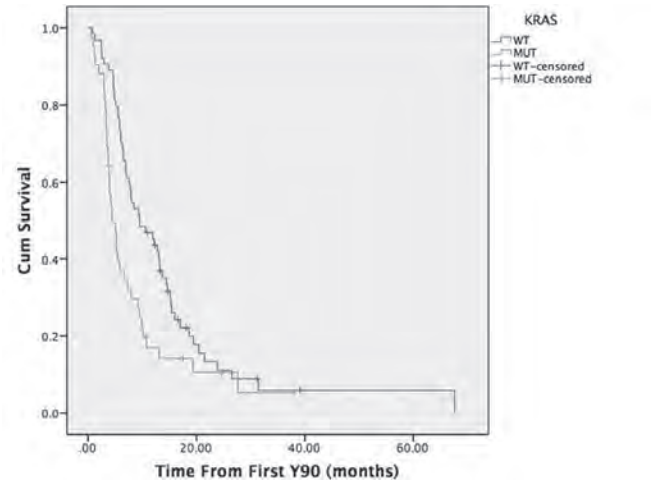

Parameters Compared	Univariate Analysis, HR (95% CI)	Univariate Analysis, p-value	Multivariate Analysis, HR (95% CI)	Multivariate Analysis, p-value
Age, >65 vs. ≤65 years	0.947 (0.623-1.440)	0.799	1.03 (0.66-1.61)	0.884
Gender, Male vs. Female	1.081 (0.699-1.670)	0.727	0.91 (0.57-1.45)	0.668
Race, White vs. Other	0.703 (0.255-1.936)	0.495	1.51 (0.92-2.47)	0.100
Child-Pugh Score, >5 vs. ≤5	0.525 (0.346-0.797)	0.003	1.74 (1.08-2.80)	0.023
Child-Pugh Score, >6 vs. ≤6	1.952 (1.100-3.465)	0.022	1.81 (1.09-3.14)	0.041
Lung Shunt Fraction, >2.5% vs. ≤2.5%	0.688 (0.453-1.047)	0.081	1.38 (0.88-2.16)	0.168
Pre-Y90 CEA, >250 vs. ≤250	0.625 (0.398-0.981)	0.041	0.72 (0.44-1.17)	0.184
Post-Y90 Chemotherapy, Yes vs. No	3.094 (2.009-4.763)	<0.001	0.63 (0.26-1.54)	0.313
KRAS, WT vs. Mutant	0.571 (0.374-0.870)	0.009	1.76 (1.14-2.73)	0.011
Portal Vein Thrombosis, Present vs. Absent	0.963 (0.630-1.471)	0.861	0.31 (0.09-1.12)	0.075
Tumor Size, >10 vs. ≤10 cm	1.253 (0.702-2.236)	0.445	1.86 (0.74-4.68)	0.186
Tumor Volume, >1000 vs. ≤1000 cc	0.856 (0.475-1.541)	0.604	1.95 (0.50-7.62)	0.338
Tumor Extent, Unilobar vs. Bilobar	1.030 (0.635-1.670)	0.905	3.37 (1.05-9.92)	0.052
Tumor Extent, Solitary vs. Multifocal	1.646 (0.315-8.606)	0.781	0.39 (0.04-4.04)	0.428
Portal Hypertension, Present vs. Absent	0.589 (0.430-1.614)	0.589	2.49 (0.53-11.62)	0.246
All Grade Toxicity, Present vs. Absent	0.871 (0.574-1.322)	0.517	0.002 (0.000-0.170)	0.007
Grade ≥2 Toxicity, Present vs. Absent	0.419 (0.191-0.920)	0.030	0.000 (0.000-0.054)	0.005
Anti-EGFR Treatments prior to Y-90, Yes vs. No	1.395 (0.916-2.123)	0.121	1.22 (0.41-3.63)	0.722

Paper 16: Survival Differences in Glass versus Resin Radioembolization of Hepatic Malignancies

R. Morgan, A. Robinson, T.R. James, S. DeBacker, M. Smith, K. Werth, T. Brown, J. Hill, Z. Collins

Objectives: To compare one-year survival differences between glass and resin yttrium-90 (Y-90) microspheres radioembolization of hepatocellular carcinoma (HCC) or hepatic metastases.
Methods: A retrospective analysis was conducted on 126 patients with unresectable primary HCC, colorectal, neuroendocrine, or other metastases who received radioembolization with glass- or resin-based Y-90 microspheres between 2008 and 2013 at a tertiary care academic medical institution. Survival analyses were conducted to compare time-to-death outcomes between glass-and resin-based Y-90 treatment types. Time-to-death was defined as days between first Y-90 treatment and death due to any cause within 365 days. Survival time for subjects alive at the end of the follow-up period was censored at 365 days. Subjects lost to follow-up were censored based on the date of last contact. Case-wise deletion was used to address missing data, as subjects with incomplete data were excluded from analyses. Kaplan-Meier curves, log-rank tests, and hazard ratios were used to compare and describe survival between groups.
Results: A total of 217 treatments were performed on 126 patients with 136 (63%) using glass particles and 81 (37%) using resin particles. Forty-six (37%) patients had metastatic colorectal cancer, 51 (40%) had primary HCC, while 11 (9%) had neuroendocrine and 18 (14%) had other primary liver metastasis. Two-thirds of all patients were male with a median age of 62 years at first treatment. Of the 126 patients, 77 (61.1%) received glass-based Y-90 treatments, of which 52 (67.5%) died prior to one year, 18 (23.4%) were lost to follow-up, and seven (9.1%) were alive at one year. Of the 49 (38.9%) patients who received resin-based Y-90 treatments, 12 (24.5%) died prior to one year, 24 (49%) were lost to follow-up, and 13 (26.5%) were alive at one year. Subjects receiving resin-based treatment were 62% less likely to die within one year when compared to subjects receiving glass-based (HR = 0.38, 95% CI = 0.2, 0.7, P < 0.01). Mean time-to-death for glass-based Y-90 treatments was 257.6 days (SE = 7.0 days) compared to 301.5 days (SE = 8.8 days) in resin-based. Volume of liver replaced by tumor and size of two dominant lesions were not significantly different (P>0.05) between the two groups.
Conclusions: While both glass- and resin-based Y-90 microspheres have demonstrated efficacy as treatment options for unresectable primary HCC and hepatic metastatic disease, there is limited research on direct comparison of survival between the two treatments. Our study demonstrates a statistically significant survival advantage of resin- over glass-based Y-90 during the first year after treatment.

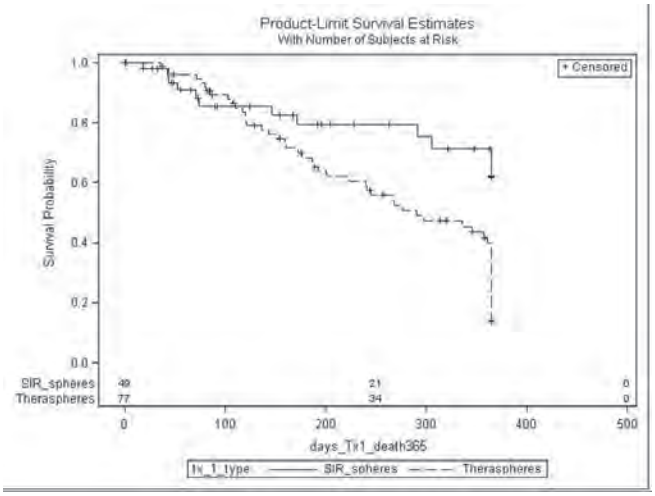

Kaplan-Meier survival curves for resin-based (solid, *n* = 49) and glass-based (dashed, *n* = 77) Y-90. The *x*-axis is survival time post-initiation of treatment (in days) up to one year. The *y*-axis is the probability of survival to time *x*. Subjects were censored at date of last contact if within 365 days of treatment or at 365 days, whichever occurred first.

Paper 17: Radiation Map Fusion Guided Combination of External Beam Radiation with Thermal Ablation for Up to 10 cm Liver Tumors

L. Jiang, V.P. Krishnasamy, H. Amalou, S. Xu, D. Citrin, R. Miller, H. Ning, B.J. Wood

Objectives: External beam radiation therapy (XRT) and thermal ablation (radiofrequency and microwave ablation) have complementary risk profiles and synergistic mechanisms. XRT works well with perfusion to generate free radicals in oxygenated tissue, but ablation is impaired by perfusion due to convective heat loss. XRT is safer in the porta hepatis, but ablation with hydrodissection is safer adjacent to bowel than XRT. Ablation is less effective for liver lesions over 3 cm, and XRT is typically not given for liver lesions larger than 6 cm due to integral radiation dose toxicities. Although speculative, XRT and ablation may interact to enhance ablation volumes. Fusion software guidance combines XRT with ablation for potentially synergistic treatment of large and/or multiple liver tumors. This trial allows us to respect the limitations, and take advantage of the strengths, of each modality by combining them for the same or different lesions.
Methods: Inclusion criteria for enrollment into the trial include unresectable hepatic neoplasms up to 5 in number and up to 10 cm each in diameter. Patients were treated with 5 total fractions (50 Gy total) of XRT over 2 weeks, and radiofrequency or microwave ablation was done between fractions 3 and 4. To accomplish this potentially synergistic tumor coverage, a navigation system for ablation was developed fusing radiation dose map, multiple imaging modalities, and probe location. Following multi-modality liver registration, the software populated a planned ablation treatment volume by overlapping the expected ablation zone of each probe to define tumor coverage.
Results: The clinical trial has enrolled and treated 3 patients thus far. The included image illustrates an example of multi-modality registration for one patient that overlays CT images, radiation dose map, planned ablation probe insertion paths, and expected overlapping ablation treatment volumes from multiple probes. Two patients received spatially synergistic treatment, using XRT and ablation to achieve an overall larger lesion coverage compared to what each modality could achieve alone. One patient received temporally synergistic treatment (RFA and radiation to same volume), which resulted in an ablation volume of 58.69 cm^3 after 12 minutes of RFA, (nearly 3 times greater than the expected volume of 20.5 cm^3 derived from in vitro porcine studies). On recent follow-up, no definite local tumor recurrence was seen in any patient, although one patient had suspected marginal recurrence one year post treatment of an almost 10 cm lesion.
Conclusions: Fusion navigation guided by radiation dose map input may combine the complementary therapies of XRT and thermal ablation, thus potentially enhancing coverage and increasing indications. We have demonstrated that both spatial and temporal synergy is feasible, with possibly different effects to target tissue. Although speculative, a larger ablation volume was seen in our early experience in tissue exposed to both XRT and RFA than otherwise expected from RFA alone, warranting additional investigation into the interaction of the two treatment modalities.

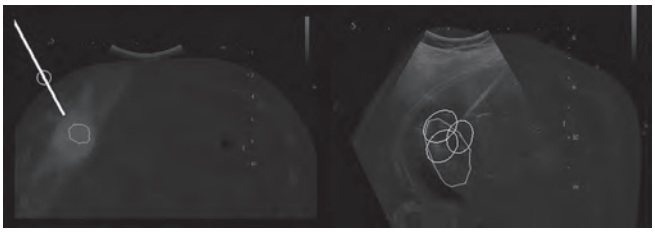

CT, US, and radiation dose map fusion (left); CT and US fusion (right). Red with green outline: lesion. Yellow line: ablation probe entry path. White circles: expected ablation volumes from multiple probes.

Paper 18: Exact Detection of Ablative Margin and Local Tumor Progression in Liver Tumors: Preliminary Follow-Up Results

M. Trakymas

Objectives: To assess the benefit of exact detection of ablative margin using implanted fiducial markers in liver tumors on local tumor progression rate.
Methods: Each of 107 metastatic and primary liver tumors (mean size 23 mm, 95% CI 20-25) was marked with minimum three titanium fiducial markers before radiofrequency ablation. The three phase contrast enhanced MDCT scan was performed for each patient after the implantation of fiducials. All the tumors were treated with US and virtual CT fusion guided RFA using perfused and multipolar internally cooled electrodes. The control contrast enhanced MDCT scan was performed next day after ablation. The evaluation of ablative margin was made by fusing CT scans according to each fiducial. The follow up data of patients were collected and analyzed for local tumor progression.
Results: RFA was technically successful in all cases. The median detected minimal ablative margin was 8 mm (ranged from 0 to > 10 mm). 32 (29%) cases required repeated ablation since the ablative margin was less than 5 mm. Reablation in 14 (13%) cases was not feasible; in 18 cases (16%) it was repeated with US and virtual CT fusion guidance and resulted in a sufficient ablative margin >= 5 mm of particular region. 30 tumors were excluded from final analysis because of follow-up shorter than 18 months. On follow-up (median 29 months, range 18-46 months) 10 local tumor progressions were detected. In these cases the final ablative margin was 0-6 mm.
Conclusions: The results of our study show importance of exact detection of ablative margin when predicting the success of ablation treatment. Fiducial markers allow detecting ablative margin with high accuracy as well as helps to perform a precise reablation.

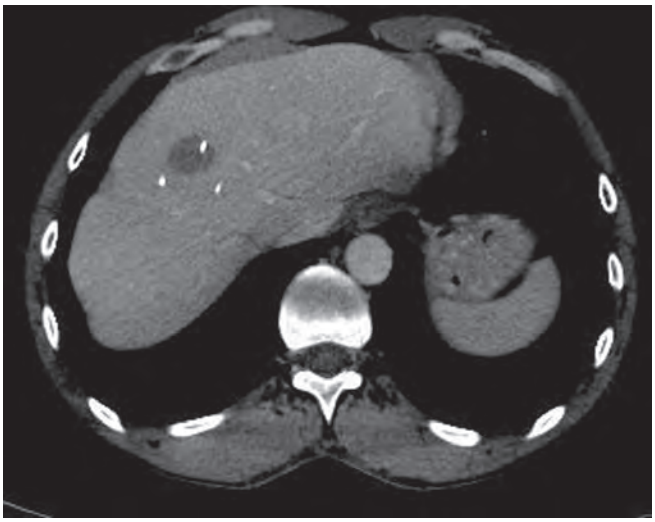

CT image of liver tumor with implanted fiducial markers

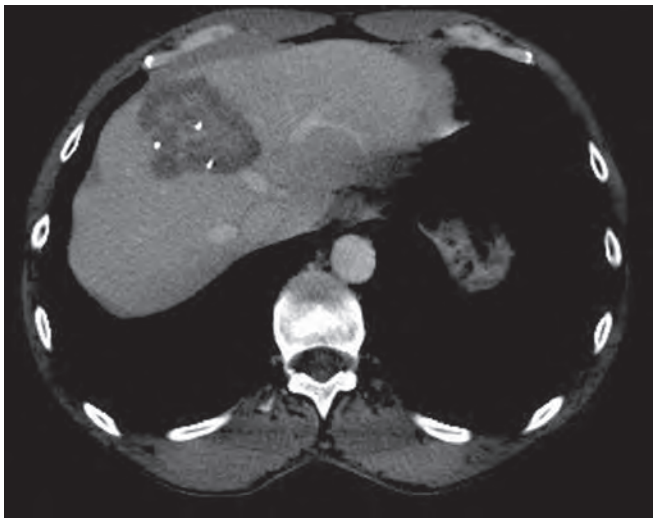

CT image of the ablation zone

Paper 19: Greyscale, Color Doppler, and B-Flow Ultrasound Guidance for Tissue Hydrodissection: Modality Impact on Injection Localization

A. Moreland, M. Ledwidge, A. Munoz Del Rio, S. Wells, D. Kitchin, J. Hinshaw, T. Ziemlewicz, M. Lubner, F. Lee, C. Brace

Objectives: Color Doppler and B-Flow are ultrasound (US) modalities with potential for use in guiding injection of tissue hydrodissection fluid instead of conventional Greyscale. B-Flow is a flow visualization technique displayed with a range of grey intensities assigned according to reflector speed and dynamics. The encoding methods employed by this proprietary technique are designed to suppress artifactual signals and emphasize fluid flow signals. Purported benefits over Color Doppler include direct visualization of fluid dynamics without requirement for overlay technique, decreased influence of scanning angle, and improved temporal and spatial resolution. The purpose of this study was to evaluate the utility of Color Doppler and B-Flow as compared to conventional Greyscale as US modalities for guidance during tissue hydrodissection.

Methods: In compliance with guidelines for the care and use of animals, 12 iohexol-doped saline injections were performed on two swine post mortem. Injections were performed under US guidance by a technologist experienced in percutaneous hydrodissection. Paired injections were performed at the interface of subcutaneous tissue with the peritoneum: at each location, one injection in the subcutaneous tissue (SQ) and one in the peritoneum (IP) was performed. Each injection delivered 30 mL of saline doped with iohexol at a rate of 1 mL/second through an 18-gauge needle and was recorded under each of 3 modalities: Greyscale, Color Doppler, and B-Flow. Cone Beam CT was performed to confirm injection location. Randomized, de-identified cines were then shown to 6 board certified radiologists experienced in hydrodissection under Greyscale guidance. Radiologists were asked to assess injection location (SQ vs. IP) as well as their level of confidence in this assessment (in the form of a numeric probability). Respondents were also asked to document presence, type, and consequence of any imaging artifact. Survey results were analyzed using Dunn's Multiple Comparison test and chi square analysis.

Results: Radiologists accurately interpreted injection locations in a mean of 81% of Greyscale, 69% of Color Doppler, and 74% of B-Flow cines with no significant difference in accuracy between modalities ($P > 0.05$). Mean sensitivities and specificities, respectively, were: 81% and 81% for Greyscale, 72% and 67% for Color Doppler, 81% and 61% for B Flow with no statistically significant differences between modalities. For accurately-interpreted cines, mean certainty in assessing injection location was similar at 78% with Greyscale, 75% with Color Doppler, and 77% with B-Flow ($P>0.05$). Among incorrectly interpreted cines, mean certainty was also similar across modalities at 64% with Greyscale, 78% with Color Doppler, and 69% with B-Flow ($P>0.05$). The rates of helpful imaging artifacts were significantly different ($P<0.05$) at 0% with Greyscale, 17% with Color Doppler, and 67% with B-Flow. The rates of detrimental artifacts were also significantly different ($P<0.05$) at 1% with Greyscale, 56% with Color Doppler, and 1% with B-Flow. Specifically, bowel gas artifacts commonly interfered with interpretation of Color Doppler cines, while flash artifacts were helpful for interpretation in B-Flow cines, per qualitative radiologist report.

Conclusions: Accuracy, sensitivity, specificity, and certainty in injection localization are similar when using Greyscale, Color Doppler, and B Flow for US guidance during hydrodissection in an ex vivo swine model. Greyscale remains the clinical gold standard modality for this application, but further investigation into the use of B Flow may be warranted in light of its helpful flash artifact.

Paper 20: CT-Guided Screw Fixation Plus Cementoplasty in the Treatment of Painful Bone Metastases

C. Pusceddu, N. Ballicu, B. Sotgia, R. Fele, L. Melis

Objectives: To retrospectively evaluate the feasibility and effectiveness of CT-guided percutaneous screw fixation plus cementoplasty (PSFPC) in patients with painful bone metastases with fractures or to prevent pathological fracture.

Methods: Twenty patients (10 men and 10 women, median age 57 years) with 22 metastatic bone lesions (11 breast cancer, 4 NSCLC, 4 multiple myeloma, 1 thymoma and 2 renal cell carcinoma) with fractures or high risk for fracture underwent CT–guided PSFPC. Twelve metastases were located in the vertebrae, 8 in the pelvis and 2 in the femurs.Five patients underwent to tumor ablation before the osteosynthesis. We analyzed the feasibility and complications of the procedure, the decrease in pain (Visual Analog Scale, VAS) and length of hospital stay.

Results: All sessions were completed and all procedures were well tolerated. PSFPC was performed under local anesthesia and conscious sedation in all patients. Only 2 out of 20 (10%) experienced moderate pain in the first 12-24 hours after the procedure, which was resolved with mild analgesics. There were no complications related to incorrect positioning of the screws or leakage of cement. All patients were able to walk within 6 hours after the procedure. The average length of hospital stay was 2 days. VAS score decreased from 7.1 (range, 4-9) before treatment to 1.6 (range, 0–5) 6 months after. No new bone fracture occurred during a median follow-up of 8 months.

Conclusions: Our results suggest that PSFPC is a safe and effective procedure which allows to stabilize the fracture and prevent the pathological fractures with a significant pain relief and good recovery of walking ability. PSFPC seems to be a promising alternative for patients who are not candidates to surgery. Further studies are required to confirm this preliminary experience.

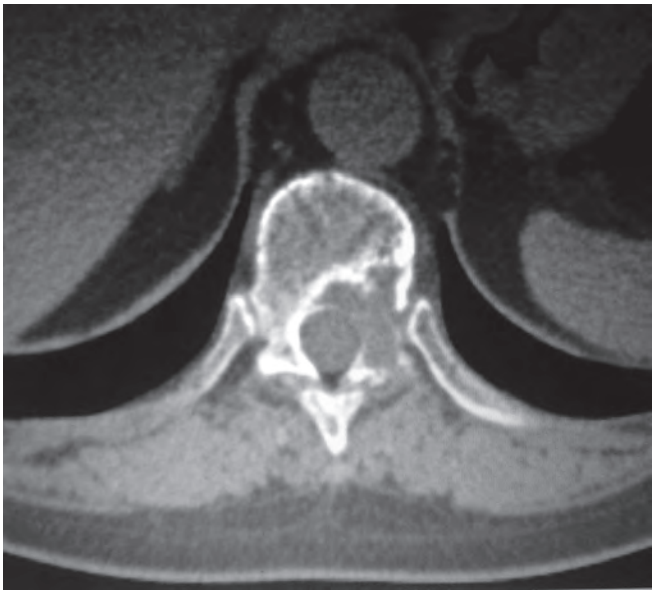

CT scan shows large osteolysis of the left pedicle of T12.

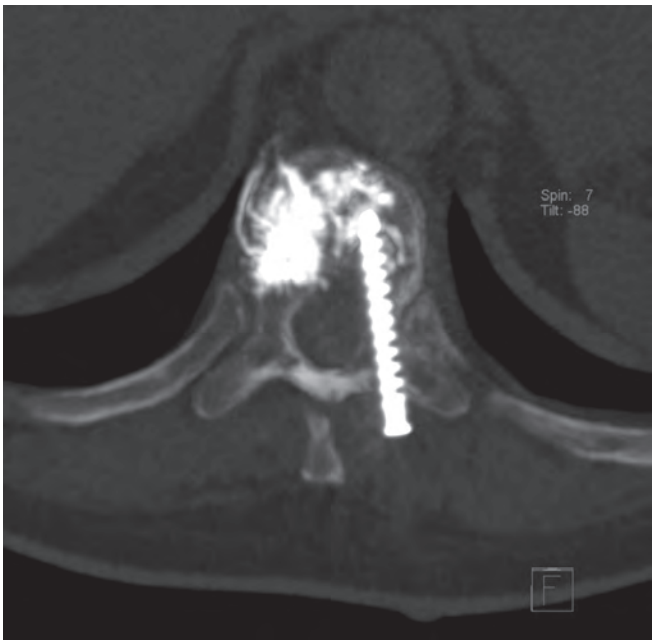

CT scan performed after screw fixation and vertebroplasty

Paper 21: Intraprocedural 3D Quantification of Lipiodol Deposition on Cone-Beam CT Predicts Tumor Response after Transarterial Chemoembolization in Patients with Hepatocellular Carcinoma

Z. Wang, R. Chen, R. Duran, Y. Zhao, G. Yenokyan, J. Chapiro, R. Schernthaner, M. Lin, J. Geschwind

Objectives: To evaluate whether intraprocedural 3D quantification of Lipiodol deposition on cone-beam computed tomography (CBCT) can predict tumor response on follow-up contrast-enhanced magnetic resonance imaging (CE-MRI) in patients with hepatocellular carcinoma (HCC) treated with conventional transarterial chemoembolization (cTACE).

Methods: This IRB approved, retrospective analysis included 36 patients with 51 HCC target lesions, who underwent cTACE with CBCT. CE-MRI was acquired at baseline and 1 month after cTACE. Overall tumor volumes as well as intra-tumoral Lipiodol volumes on CBCT were measured and compared with the overall and necrotic (non-enhancing) tumor volumes on CE-MRI using the paired student's *t*-test. Tumor response on CE-MRI was assessed using modified Response Evaluation Criteria in Solid Tumors (mRECIST). A linear regression model was used to correlate tumor volumes as well as Lipiodol volumes and the percentage of Lipiodol deposition on CBCT with the corresponding parameters on CE-MRI. Nonparametric spearman rank order correlation and trend test were used to correlate the percentage of Lipiodol deposition in the tumor with tumor response.

Results: A strong correlation between overall tumor volumes on CBCT and CE-MRI was observed (R^2=0.986). In addition, a strong correlation was obtained between the volume of Lipiodol deposition on CBCT and tumor necrosis (in cm^3) on CE-MRI (R^2=0.960); and between the percentage of Lipiodol deposition and tumor necrosis (R^2=0.979). Importantly, the extent of Lipiodol deposition (in percentage of total tumor volume) correlated strongly with tumor response on CE-MRI (Spearman rho=0.84, P<0.001).

Conclusions: Intraprocedural 3D quantification of Lipiodol deposition on CBCT can be used to predict tumor response on follow-up CE-MRI.

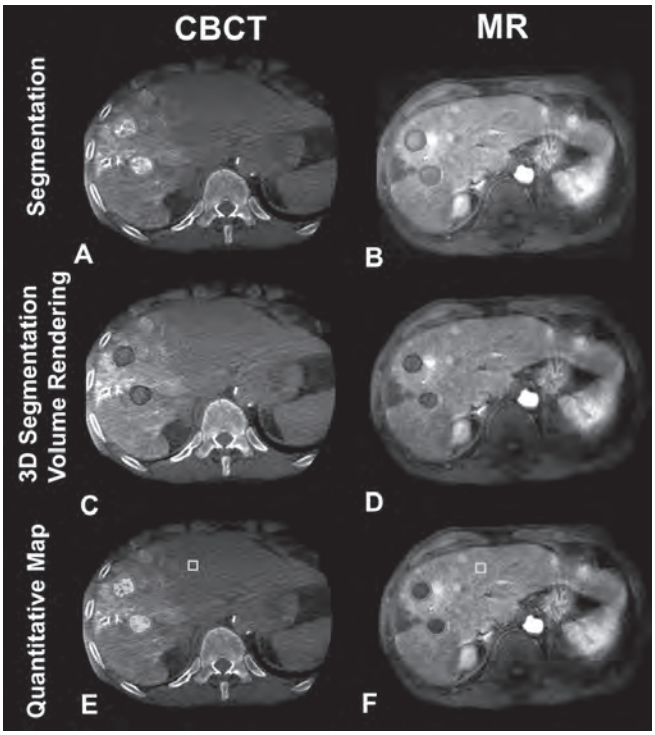

3D volumetric semi-automatic evaluation of Lipiodol deposition *(Complete Response according to mRECIST criteria)* in HCC on a representative case. Segmentation of the tumor (red circle) on CBCT at corresponding slice level as on MR (A, B). 3D segmentation volume rendering on the same slice (C, D). Quantitative color map of Lipiodol deposition on CBCT (E) and tumor viability on follow-up MRI (F). The box represents the location of the background ROI. For the anterior target lesion: the tumor volume on CBCT and on MRI was 4.69cm^3 and 4.60 cm^3, respectively; the volume of Lipiodol on CBCT and non-enhancement on MRI was 4.66cm^3 and 4.60 cm^3, respectively. For the posterior target lesion: the tumor volume on CBCT and on MRI was 4.58cm^3 and 4.51 cm^3, respectively; the volume of Lipiodol on CBCT and non-enhancement on MRI was 4.55cm^3 and 4.51 cm^3, respectively.

Paper 22: Thermal Ablation of Benign Thyroid Disease: A Prospective Multi-Center Study

P. Liang

Objectives: To analyze efficacy, safety, reliability and clinical application of the main technique of thermal ablation (MWA and RFA), prospective multi-center study with a large sample were conducted.

Methods: From February 2013 to May 2014, a total of 337 patients (mean age, 46.2 ± 12.5 years) with 435 benign thyroid lesions (mean diameter, 2.7±1.4cm) received ultrasound-guided thermal ablation in 12 hospitals in China. Patients were divided into two groups by the ablation technique (RFA and MWA) that they are performed. We assessed the initial size and microcirculation of lesions through ultrasound and drew up the ablation plan before the procedure. Patient's clinical symptoms (neck pain, dysphasia, foreign body sensation, discomfort, and cough), lesion's ultrasound imaging feature (size and vascularity) and thyroid function were brought into observation. The variance of those parameters and the complications were recorded carefully during the whole therapy(preoperative, intra-operative and postoperative period) and follow-up time(regularly in1, 3, 6, 12, 24 months). To evaluate objectively, symptom score, cosmetic score and vascularity scale as the quantitative methods were performed in our study. We calculated the volume-reduction ratio (VRR) of the lesions by measuring its initial volume and volume at follow-up endpoint. It can be calculated according to the formula of ellipsoid volume. Related index were analyzed and compared by using paired sample t-test.

Results: The number of lesions in the two groups (RFA and MWA) were 236 and 199, respectively. During the follow-up periods ranging from 1 to 12months, the VRR of thyroid lesion is 63.72% totally. Vascularity scale, symptom score and cosmetic score of all the patients between pre-ablation and post-ablation were reduced significantly (P<0.01) in the follow up period. Thyroid functional indicators changed in a transient period (about 1 to 3 days) after therapy, including T3, fT4 increasing, and TSH decreasing, which had statistical significance compared with those of pre-ablation (P <0.01). Compare between the two groups, MWA is obtained the shorter treatment time, and higher VRR (P <0.05).

Conclusions: Thermal ablation is a safe and effective new method in treating benign thyroid lesions. Interim results showed the progress of this research has basically met the initial expectations.

Paper 23: Cement Leakage in Balloon Kyphoplasty for Spinal Metastasis and Myeloma: A Retrospective Evaluation of Incidence and Risk Factors

B. richioud, H. Beji, A. Kalenderian, M. Cuinet

Objectives: Although rare, complications of vertebroplasty can be severe. They generally come from cement leakage outside the vertebral body. In spinal metastasis and myeloma, the procedural risk is generally increased due to cortical bone destruction and neoangiogenesis. Creating a free space within the vertebral body allowing cement injection at low pressure, Balloon Kyphoplasty (BKP) could limit the risk of extra corporeal leakage compared to vertebroplasty alone. This potential has never been investigated so far. We retrospectively studied cement leakage incidence and risk factors for BKP in spinal metastasis and myeloma using univariate and multivariate analyses.
Methods: 53 vertebrae (42 cancer patients, 20 females, 22 males; age 19-83 yo) were treated in 42 sessions under CT guidance. All procedures were performed by experienced radiologists on lytic lesions. Cement leakage (CL) were split into vascular (vCL) and cortical (cCL). The following items were assessed for occurrence of each kind of leakage: vertebral collapse (degree and kind of), cement filling, timing of the procedure, prior radiotherapy or antiangiogenic treatment, primary tumor site.
Results: CL, vCL and cCL rates were 57%, 17%, and 55%. Early realization of BKP, within 3 months after the collapse, appeared to be a risk factor for CL (P=0.01). cCL increased when breast was the primary tumor site (P=0.01). Discal cCL were associated with endplate lytic lesions (P=0.04).
Conclusions: Breast cancer, early BKP and endplate lesions appeared as risk factors for cement leakage. Further studies are needed, but those items may prove to be useful for therapeutic decisions.

Paper 24: Portal Vein Embolization via a Percutaneous Transsplenic Access

K. Han, G. Ko, H. Ko, D. Gwon, K. Sung, H. Yoon

Objectives: To evaluate the feasibility and safety of percutaneous transsplenic portal vein embolization.
Methods: During the recent one year, 11 patients (8 hepatocellular carcinoma, 2 cholangiocellular carcinoma, and 1 sarcomatoid carcinoma) underwent right (n = 10) or left (n = 1) portal vein embolization via a percutaneous transsplenic access. Seven of the 11 patients had huge or multiple masses in the right lobe of the liver, which hindered transhepatic access via a right portal vein. In the remaining 3 patients, transsplenic access was performed intentionally. A splenic venous branch was punctured using a 21-G chiba needle and a 0.016" micro-guide wire under ultrasound and fluoroscopy guidance. Right portal branches were embolized using gelatin sponge particles followed by histoacryl, vascular plugs, or coils to prevent recanalization. Postembolization portogram was obtained in all patients. Pressures in the main portal vein before and after the embolization were measured. Following completion of the portal vein embolization, transsplenic access routes were embolized using coils followed by histoacryl.
Results: Portal vein embolization was successfully achieved in all patients. Procedure-related complication did not occur in any patient except various degree abdominal pain during or after the embolization. Median pressures in the main portal vein before and after the embolization were 8 (range, 3-17), and 14 (range, 7-21) mmHg, respectively. Follow-up CT obtained at a median of 21 (range, 14-33) days after embolization demonstrated sufficient hypertrophy of the future liver remnants without recanalization or puncture site complications. Nine patients underwent right hemihepatectomy or trisegmentectomy at a mean of 28 (range, 21-35) days after embolization, and no patient experienced postoperative hepatic failure. One patient refused surgery owing to complete remission of hepatocellular carcinoma on follow-up CT scan. In the other patient, surgery could not be performed owing to rapid tumor progression following portal vein embolization.
Conclusions: Portal vein embolization via a percutaneous transsplenic access is a safe and feasible alternative technique in patients with an unfavorable transhepatic route.

Paper 25: The Immediate Elevation of Serum Tumor Marker after Irreversible Electroporation Implies Technique Success

K. Huang

Objectives: Irreversible electroporation (IRE) is a novel, non-thermal ablation technique that uses high-voltage DC current to induce irreversible disruption of cell membrane integrity. The technique success of IRE for tumor ablation is still difficult to be verified immediately after procedure. We present the initial experience to estimate the possible technique success by elevation of serum tumor marker within 24 hours after IRE in the treatment of liver and pancreatic cancers.
Methods: The prospective study was performed at National Taiwan University Hospital during 2012-2014. 32 consecutive patients (21 male, 11 female), age 35-77, with 20 unresectable hepatocellular carcinoma and 12 locally advance pancreatic adenocarcinoma of 2.5-5.5 cm in diameter were treated by IRE under general anesthesia. All procedures were performed with ultrasound guidance. High serum level of tumor-specific biomarker including alpha-fetoprotein (AFP) or Carbohydrate Antigen 19-9(CA 19-9) was noted in these patients. Clinical examination and laboratory assay were performed at baseline, 6 hours, 1st and 28th day after procedure. The ablation effect was evaluated by contrast-enhanced CT/MRI.
Results: Complete target tumor ablation was achieved in 29 tumors. Massive residual viable parts were noted in 2 pancreas cancer and 1 liver cancer. These patients were treated in the very early period, and then repeated IRE ablation was performed again successfully. In the patients received successful IRE, CA19-9 level in pancreas cancer patients and AFP level in HCC patients were increased significantly 6 hours after ablation, and then reached as high as 2.4±0.5 times of baseline value 24 hours later. However, for the three case with incomplete ablation, no tumor marker increase in 6 hours, and only 1.2±0.2 times increase of baseline value 24 hours later was noted.
Conclusions: IRE is a feasible and safe modality for treating locally advanced liver and pancreatic cancer in our experience. Successful ablation will result in significant increase of tumor-specific protein due to disruption of cancer cell membrane, and this phenomenon will help to monitor the therapeutic effect.

Paper 26: The Analysis for the Causes of Delayed Hospitalization after Transcatheter Arterial Chemoembolization in Patients with Unresectable Hepatocellular Carcinoma

H. Jung

Objectives: To analysis for the causes of delayed hospitalization (over 7 days) after transcatheter arterial chemoembolization (TACE) in patients with unresectable hepatocellular carcinoma (HCC) and related factors for delayed hospitalization.
Methods: We analyzed the total hospitalization period after patients with unresectable HCC received TACE, and these patients were treated during the recent 12 month at our hospital. 2554 sessions showed a short term hospital stay (less than 7 days) and 427 sessions showed a prolonged hospital stay (more than 7 days), so a total of 2981 sessions were analyzed. The hospital stay less than seven days was set for the control group and this was correlated with the patient's age, gender, the level of bilirubin and albumin, the platelet counts, the AST/ALT ratio, the a-FT, the presence of portal vein thrombosis and ascites, several scoring systems (Child-Pugh, CLIP, and OKUDA score) and the need for additional embolization at the time of the procedure.
Results: Compared with that of the control group, ascites (P=0.002), portal vein thrombosis (P=0.001), a platelet count below the hundred thousand (P=0.008), a Child-Pugh score more than B (P=0.031), a CLIP score more than 2 (P=0.001) and a OKUDA score more than II (P=0.001) showed significant differences
Conclusions: The evaluation of patients' factors would be useful to predict extended post-procedural hospitalization after hepatic chemoembolisation.

Paper 27: Superselective Transcatheter Arterial Embolization of Adrenal Metastases from Hepatocellular Carcinoma is Feasible and Safe

P.F. Laeseke, M. Ginsburg, J.D. Louie, D.Y. Sze

Objectives: To retrospectively evaluate the feasibility and safety of superselective transcatheter arterial chemoembolization (TACE) or bland embolization (TAE) for the treatment of metastatic hepatocellular carcinoma (HCC) to the adrenal glands.
Methods: A retrospective chart review was performed on six patients (5 male, 1 female; mean age 62 y, range 44-73 y) who underwent superselective TACE (n=6) or TAE (n=1) for 7 HCC metastases to the adrenal glands. One patient had bilateral metachronous adrenal metastases treated in four separate sessions. The remainder had a single isolated adrenal metastasis (right, n=4; left, n=1) treated in a single session. Two patients underwent TACE with drug eluting beads (DEB-TACE) and doxorubicin; 1 patient underwent conventional TACE with doxorubicin and lipiodol; 1 patient underwent conventional TACE with doxorubicin, cisplatin, and lipiodol; 1 patient underwent conventional TACE with doxorubicin, lipiodol, and gelatin sponge; and 1 patient underwent TAE with 40 μm and 100-300 μm microspheres. Demographics, procedural details, and outcomes were analyzed.
Results: Maximum tumor diameter was 4.6 ± 1.8 cm (mean ± SD). Mean number of treated arteries per metastasis was 1.6 (range, 1-3). Treated arteries included the inferior phrenic (right, n=2; left, n=2), superior adrenal (right, n=3; left, n=1), inferior adrenal (right, n=3; left, n=1), and renal capsular (right, n=1; left, n=1) arteries. One patient developed an intrahepatic abscess requiring drain placement and intravenous antibiotics after concurrent embolization of the liver and a right adrenal metastasis. No complications specific to treatment of the adrenal metastases occurred, including no hypertensive crises. Median length of hospital stay was 1 day (range, 0-2 days). One patient was treated as an outpatient and 1 patient stayed 2 days for management

of persistent abdominal pain. Imaging followup was available for 4 patients, including the patient with bilateral metastases. Based on mRECIST criteria, 1 patient had progressive disease at 3 months; 2 patients had stable disease at 3 and 8 months, respectively; and 1 patient had a partial response at 3 months.
Conclusions: Superselective TACE/TAE is a safe and feasible treatment option for metastatic HCC to the adrenal glands. However, the technique is technically difficult given the variable type and number of arteries supplying the metastases.

Paper 28: The Effect of Anti-Reflux Catheters on Pulmonary Shunt Fraction in Patients with Hepatocellular Carcinoma

R. Stanborough, A.C. Bourgeois, Y.C. Bradley, J. McElmurray, A. Pasciak

Objectives: Anti-reflux catheters were initially designed to limit retrograde flow of infused particles in liver directed embolotherapy. Recent preclinical research suggests that these devices may produce increased concentrations of infused microparticles within the target area of infusion. One suggested mechanism for this effect is increased downstream arterial pressure during infusion, increasing microsphere penetration. This study evaluated whether the increased downstream arterial pressure created by an anti-reflux catheter has an effect on lung-shunt fraction (LSF). LSF is an important pre-treatment safety consideration in yttrium-90 (90Y) radioembolization.
Methods: This study was conducted with informed consent and IRB approval. The 90Y pretreatment simulation was performed with two sequential, same day infusions of 100MBq and 600MBq 99mTc–MAA. Using near-identical techniques and catheter positions, infusion was performed with both anti-reflux (Surefire Medical, Denver, CO) and endhole catheters. Planar and SPECT imaging was performed following each infusion and the LSF compared.
Results: 4 patients with biopsy proven HCC and 3 patients with metastatic liver disease were evaluated using this method. The average LSF was 10.1% using the anti-reflux catheter, while the average LSF was 8.8% with the endhole catheter. This difference was not statistically significant ($p > 0.25$). In 6 out of 7 patients, the total difference in LSF did not exceed 2.5%, however, in one patient with an 18 cm HCC, LSF increased from 13.34% to 20.50% using end hole and anti-reflux catheters respectively.
Conclusions: Preliminary data cannot confirm that there is any difference in LSF when an anti-reflux catheter is used. However, for patients likely to have a large LSF, such as those with a substantial HCC burden, it may be prudent to perform the 99mTc–MAA simulation study with anti-reflux catheter, if that catheter will be used in the patient's eventual 90Y treatment.

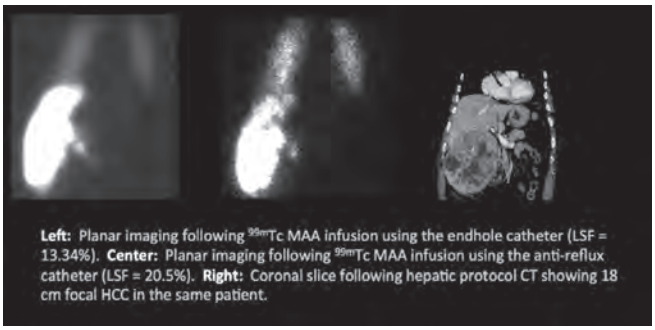

Left: Planar imaging following ^{99m}Tc MAA infusion using the endhole catheter (LSF = 13.34%). **Center:** Planar imaging following ^{99m}Tc MAA infusion using the anti-reflux catheter (LSF = 20.5%). **Right:** Coronal slice following hepatic protocol CT showing 18 cm focal HCC in the same patient.

Paper 29: The Effect of Sociodemographics on Survival in Hepatocellular Carcinoma Patients Undergoing Orthotopic Liver Transplantation: UNOS Population Study

M. Xing, K. Kim

Objectives: The effect of sociodemographic factors on overall survival (OS) in patients with hepatocellular carcinoma (HCC) undergoing orthotopic liver transplantation (OLT) has not been evaluated in large-scale population studies.
Methods: The United Network for Organ Sharing (UNOS) database was used to identify patients with HCC who were listed for OLT between 2002 and 2013. Patients within Milan Criteria for whom an HCC Model for End-Stage Liver Disease (MELD) exception was approved were included. Mean OS from OLT was stratified via age, gender, ethnicity, BMI, year of transplant, region, and insurance status. Kaplan-Meier estimation was used for survival analysis with log-rank test and Cox proportional hazard models to assess independent prognostic factors for OS. Chi-square tests were used to assess categorical variables and t-tests were used to analyze continuous variables.
Results: Of 17291 patients with HCC who were listed for OLT, 14511 received OLT, mean age 57.4 years, 76.8% male. Mean overall OS was significantly correlated with younger age <65, ethnicity, UNOS Region 4-5, post-college education and private insurance. Stratified survival sub-analysis demonstrated significantly prolonged survival in those who underwent bridging LRT, had higher wait times and more favorable sociodemographic factors. Patients with more favorable socio-demographic factors had significantly higher mean bridging LRT rates (30.7% vs. 21.1%, P=0.02) and significantly longer mean wait times (324.1 vs. 270.4 days, P=0.01).
Conclusions: In patients with HCC undergoing OLT, higher LRT bridging rates and higher wait times correlate with favorable socio-demographic factors, which are independent predictors of prolonged survival from OLT.

Sociodemographic Factors		Mean OS (95% CI) mo.	Univariate Analysis HR (95% CI)	Univariate Analysis p-value	Multivariate Analysis HR (95% CI)	Multivariate Analysis p-value	% Receiving Locoregional Therapy	p-value	Mean Wait Time (days)	p-value
Age	<65 years	112.5	1.13 (1.06-1.22)	0.001	0.89 (0.85-0.91)	<.001	27.4%	0.003	311.0	0.001
	≥65 years	99.9					26.3%		299.5	
Ethnicity	Caucasian	111.1	0.92 (0.90-0.94)	<.001	0.95 (0.93-0.97)	<.001	27.7%	<.001	297.6	<.001
	African American	109.9					29.5%		255.7	
	Others	98.2					23.4%		340.6	
UNOS Regions	1-3	102.9	0.88 (0.82-0.93)	<.001	0.97 (0.95-0.98)	<.001	23.5%	0.03	280.1	<.001
	4-5	108.1					25.7%		336.5	
	6-8	101.3					21.4%		393.1	
	9-11	98.3					33.7%		269.2	
Education Level	High School	72.8	1.07 (1.02-1.19)	<.001	0.89 (0.85-0.93)	<.001	25.6%	<.001	417.7	<.001
	Some College	105.7					26.5%		302.3	
	Bachelor	108.4					27.7%		305.9	
	Post-College	110.7					31.3%		281.4	
Insurance Status	Private	113.2	1.21 (1.13-1.35)	<.001	0.91 (0.88-0.93)	<.001	28.7%	<.001	325.3	<.001
	Public – Medicare, Medicaid	100.2					26.1%		322.9	
	Unknown	80.4					25.6%		252.8	

Paper 30: Development of the New Prognostic Staging System and Proposal of Treatment Algorithm Based on the Multivariate Survival Analyses (MVA) after Doxorubicin Drug Eluting Beads Transarterial Chemoembolization (DEB TACE) in Patients with Unresetable Hepatocellular Carcinoma (HCC)

H.J. Prajapati, K. Kim

Objectives: To develop the survival prognostic staging system (SS) from MVA in patients (pts) with HCC treated with DEB TACE and to compare with other SSs.
Methods: Consecutive unresectable and non-tranplantable pts with HCC, who received DEB TACE were studied. 420 pts (mean age, 61.4 yrs) were included in the study. Survivals were analyzed according to different parameters from the time of the 1st DEB TACE. Kaplan Meier and Cox Proportional Hazard model were used for survival analysis. The SS was constructed from MVA, and named as CIS (Clinical, Imaging and Serum) SS. Uno's C-statistic and time-dependent ROC curve were used to internally validate and compare prediction performance of the CIS SS with Child-Turcotte-Pugh (CP), Okuda, CLIP, BCLC and Hong Kong Liver Cancer (HKLC) SS.
Results: Overall median survival (OS) was 20m. Pts with CP class A (54.5%), B (40.2%) and C (5.3%) had OSs of 28m, 12.9m and 4.1m respectively (P<0.0001). In HCC pts with venous thrombosis (VT) of large vein (main PV, right or left PV, HV, IVC) (72.7%) versus (vs) small vein (segmental/subsegmental PV) had OSs of 5.8m versus 17.3m accordingly (P=0.008). On MVA, the significant independent prognostic factors (PFs) of survival were CP, ECOG PS, size of the index HCC, number (no) of the HCC, PVT, extra-hepatic metastases, serum (s) creatinine and s.alpha-feto protein (AFP). Based on these PFs, the SS was constructed (Table 1). The OSs CIS stages are shown in table 1. The survivals according to CIS scores are shown in the Figure 1a. The concordance indices of CIS, Okuda, CLIP, BCLC and HKLC SS were 0.608, 0.598, 0.586, 0.571 and 0.602 respectively. The area under the curve of CIS, Okuda, CLIP, BCLC and HKLC SS were 0.84, 0.69, 0.74, 0.72 and 0.79 respectively. The HCC treatment algorithm based on the proposed SS is shown in the figure 1b.
Conclusions: We propose the new CIS prognostic SS and treatment algorithm for advanced HCC from the MVA of survival after DEB TACE in pts with unresectable HCC. The CIS was the most informative SS in predicting survival.

Figure 1a. The OS according to the CIS scores

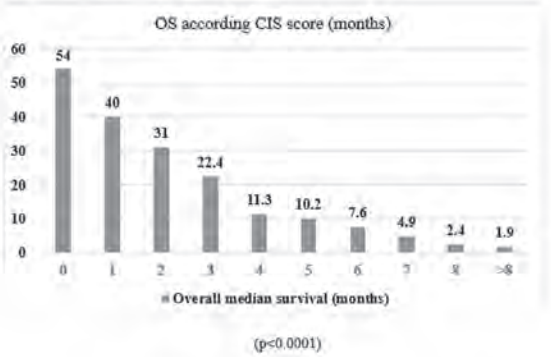

Figure 1b. CIS staging treatment algorithm for unresectable HCC after DEB TACE.

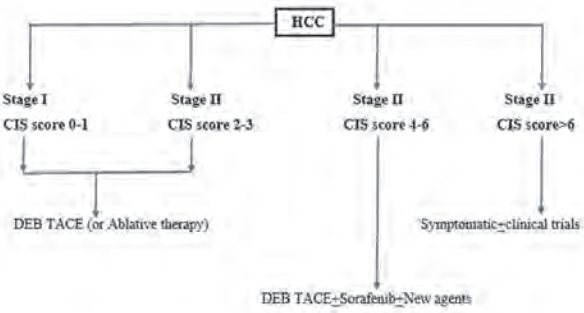

Figure 1a and Figure 1b

Table 1 – CIS staging system and survivals.

No	Variables	CIS score 0	CIS score 1	CIS score 2
1	Child Pugh Class	A	B	C
2	ECOG PS	0	1	>1
3	Index HCC size (cm)	<4	4-8	>8
4	No of HCC tumor	3 or <3	>3	
5	Venous thrombosis (VT) of Portal vein (PV)/Hepatic vein (HV)	Absent	Small vein VT	Large vein VT
6	Extra-hepatic metastasis	Absent	Present	
7	S.Creatinine (mg/dl)	<1.2	1.2 or >1.2	
8	S.AFP (ng/dl)	<400	400 or >400	
CIS STAGINGS AND SURVIVALS				
Stages	CIS Scores	%	OS (months)	P value
I	0 or 1	26.7	40.4	<0.0001
II	2 or 3	40.2	24	
III	4 to 6	25	10.6	
IV	>6	8.1	2.6	

Small VT - segmental/subsegmental PV, Large VT- main PV, right or left PV, HV, IVC.

Paper 31: Analysis of *In Vitro* Growth Inhibition of Human Colorectal Cancer and Hepatocellular Carcinoma Cells by Anti-Angiogenic Drug-Eluting Beads

S.J. Lahti, D. Zeng, J.B. Jia, M. Xing, K. Kim

Objectives: Drug-eluting bead transarterial chemoembolization (DEB-TACE) induced tumor ischemia stimulates the physiologic response to hypoxia, resulting in activation of vascular endothelial growth factor receptor (VEGFR) pathways that drive endothelial cell proliferation, migration, and reconstitution of the tumor vasculature. Recently, two anti-angiogenic DEB preparations capable of releasing the small molecule kinase inhibitors sunitinib and sorafenib have been synthesized. While these inhibitors are thought to act primarily against tumor associated pericytes and endothelial cells, they have activity against a broad range of signaling pathways. The purpose of the present study was to evaluate the direct growth inhibitory potential of sunitinib and sorafenib DEBs against human colorectal cancer and hepatocellular carcinoma cells *in vitro*.
Methods: LC Bead® 300-500μm (Biocompatibles UK Ltd.) microspheres were incubated with sunitinib-HCl and sorafenib-HCl in water. Drug loading was quantified using high performance liquid chromatography (HPLC) of drug-depleted supernatant. Viability of HCT116 and HT29 human colorectal and HepG2 hepatocellular carcinoma cells 24 and 48 hours after exposure to 5μL sunitinib DEB, sorafenib DEB, or bland DEB was quantified using the CellTiter-Glo® Cell Viability Assay (Promega Inc.). Viability of DEB treated cells was expressed as a fraction of that of time-matched untreated controls. 95% confidence intervals for viability were determined from the results of 3 replicates for each condition and were used to compare the biologic efficacy of the 3 DEB preparations.
Results: HPLC analysis of drug-depleted supernatant demonstrated DEB loading with sunitinib and sorafenib at concentrations of approximately 1 and 10 mg/mL hydrated bead, respectively. The assay results showed the 95% CI for viability after exposure to bland DEB to include the value of 1 for all conditions tested, demonstrating the lack of a direct effect of unloaded DEB on cell viability. Sunitinb DEB significantly decreased viability of HCT116 and HepG2 cells relative to unloaded bland DEB after 24 hours. After 48 hours, sunitinib DEB also demonstrated a significant inhibition of HT29 viability compared to bland DEB. Sorafenib DEB only demonstrated significant inhibition of HCT116 cells after 48 hours of exposure. The 95% CIs for viability under all other time and cell type conditions overlapped with the corresponding estimates for the bland DEB.
Conclusions: Sunitinib and sorafenib anti-angiogenic DEB can directly inhibit the proliferation of human colorectal cancer and hepatocellular carcinoma cells *in vitro*. The results suggest that these DEB preparations may have direct anti-tumor effects in addition to their putative anti-angiogenic properties.

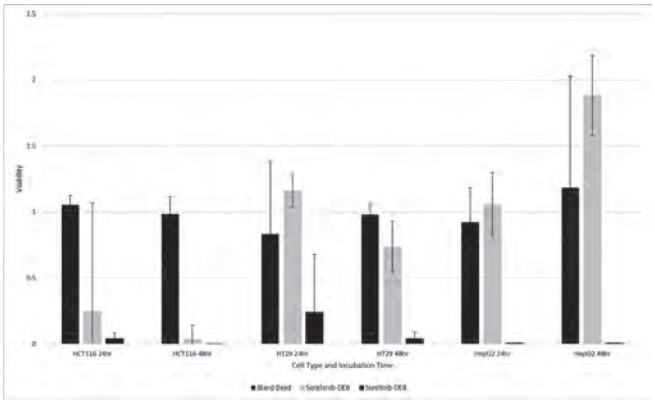

Paper 32: ^{90}Y PET/CT Dosimetry after Radioembolization in Rabbit VX2 Liver Tumor Model: Comparisons to MIRD Calculations and Ex Vivo Microsphere Uptake

A.C. Gordon, V.L. Gates, S.B. White, K.R. Harris, D. Procissi, J. Nicolai, S.K. Mouli, K.T. Sato, R.R. Ryu, R.A. Omary, R. Salem, R.R. Lewandowski, A.C. Larson

Objectives: To compare voxel-wise ^{90}Y PET/CT measurements after radioembolization to conventional Medical Internal Radiation Dose (MIRD) dosimetry approaches with tissue uptake of microspheres serving as a gold standard. Our hypothesis is that post-procedural ^{90}Y PET/CT more accurately correlates with intratumoral ^{90}Y microsphere uptake than MIRD dosimetry, which includes homogeneous dosing assumptions.
Methods: Studies were IACUC approved. VX2 tumors were implanted into the liver of New Zealand White rabbits. Whole-liver treatment volumes were calculated based on manually drawn regions of interest (ROIs) with 3D surface rendering for MIRD dosimetry calculations. Hepatic arteriography followed by radioembolization was performed. Residual activity was then measured, and PET/CT imaging (Siemens Biograph 40) was completed with TrueX reconstruction (3 iterations, 21 subsets, 4mm FWHM, 168x168 matrix, 5mm thickness), scatter correction, and attenuation correction. 3D ellipsoid ROIs were drawn to encompass tumors on fused PET/CT images while viewing side-by-side T2w MRI for anatomical correlation. Tumor necrotic volume fractions were calculated from MR images. Livers and lungs were explanted for ICP-OES analysis of microsphere content within tumor, normal hepatic, and lung tissues.
Results: Thirteen VX2 rabbits provided 26 tumors. Whole-liver radioembolization resulted in a median infused activity of 0.70mCi. Voxel-wise ^{90}Y PET/CT measurements of tumor dose were poorly correlated with conventional MIRD (Spearman r=0.41, P=0.039). Preferential tumor uptake was observed with T:N ratio of 1.77 (P=0.036). Correlations between ^{90}Y PET/CT measurements and ICP-OES measured whole tumor dose or viable tumor dose were r=0.62 (P=0.001) and r=0.64 (P=0.001), respectively. MIRD calculations were not significantly correlated with tumor ICP-OES measurements (P=0.440).
Conclusions: ^{90}Y PET/CT methods provided tumor uptake measurements of ^{90}Y activity that were correlated with tumor tissue dosing. Conventional MIRD

approaches, while proven safe for prescribing ^{90}Y activity, were not predictive of tumor microsphere content.

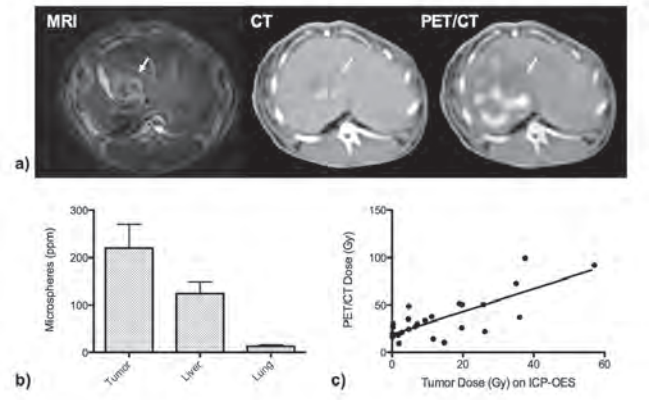

Figure 1. a) Baseline T2w MRI, non-contrast CT, and fused ^{90}Y PET/CT images demonstrating 31% necrotic tumor adjacent to the gallbladder with heterogeneous distribution of intrahepatic ^{90}Y microspheres. The activity distribution shows a region of incomplete tumor coverage (arrow). **b)** Microsphere concentration in parts-per-million for tumor, liver, and lung tissues. **c)** Voxel-wise ^{90}Y PET/CT measurements correlated with whole tumor doses on ICP-OES.

Paper 33: Improved Cytotoxicity with a Novel Mitochondria-Targeted Doxorubicin Prodrug in Colorectal Carcinoma Cells

J.B. Jia, M. Xing, X. Ling, M. Bai, K. Kim

Objectives: The 18-kDa translocator protein (TSPO) is a proapoptotic protein present in the mitochondrial membrane that is upregulated in colorectal (CRC), brain, breast, oral cavity, and prostate cancers. The purpose of this study was to formulate a mitochondria-targeted doxorubicin prodrug (**1**) by functionalizing the chemotherapy with a TSPO ligand and to evaluate its toxicity in CRC cell lines (TSPO positive) and hepatocellular carcinoma (HCC) cell lines (TSPO negative).
Methods: **1** was synthesized by conjugation of a functional TSPO ligand with doxorubicin via an enzyme-cleavable linkage. Fluorescence cell viability assays in HT29 and HCT116 CRC cell lines and HepG2 and Hep3B HCC cell lines incubated with a bolus of 10, 25 or 50μM of **1** or doxorubicin were performed using the CellTiter-Glo® Luminescent Cell Viability Assay (Promega, Madison, MI, USA) at 24, 48, 60, and 72 hours. T-tests were used for all comparisons (significance <.05) and experiments were performed in triplicate.
Results: Results are presented in Figure 1. Significant time and concentration dependent cell toxicity in all cell lines with both **1** and doxorubicin versus controls was observed (P<0.05). In the HT29, HepG2, and Hep3B cell lines, 1 caused a significant loss of cell viability at earlier time points than doxorubicin. There was a significant loss of viability in cells incubated in 10 μM of **1** at 24 hours with doxorubicin not causing a significant loss until 48 hours (P<0.05 for all). No difference in onset of cytotoxicity was seen at the other concentrations. In the HCT 116 cell line at all concentrations both **1** and doxorubicin caused a significant decrease in cell viability at 24 hours (P<0.05). In the HCT116 cell line at 48, 60, and 72 hours and in the HT29 cell line at 24 and 72 hours, **1** resulted in significantly higher cytotoxicity versus doxorubicin at all concentrations (P<0.05 for all). In HT29, 10 μM of **1** also had significantly superior cytotoxicity to doxorubicin at 48 and 60 hours and 50 μM at 60 hours (P<0.05). In cell lines with a low expression of TSPO, a consistent increased cytotoxicity of **1** was also found at 24, 48, and 60 hours with a plateau in effect at 72 hours for all concentrations in the HepG2 cell line (P<0.05 for all), however a consistent difference in cytotoxicity between the 2 drugs was not observed in the Hep3B line.
Conclusions: Our novel mitochondria-targeted doxorubicin prodrug demonstrated superior cytotoxicity compared to doxorubicin in human HCT116 and HT29 CRC cell lines and the human HepG2 HCC cell line and similar cytotoxicity to doxorubicin in the human Hep3B HCC cell line.

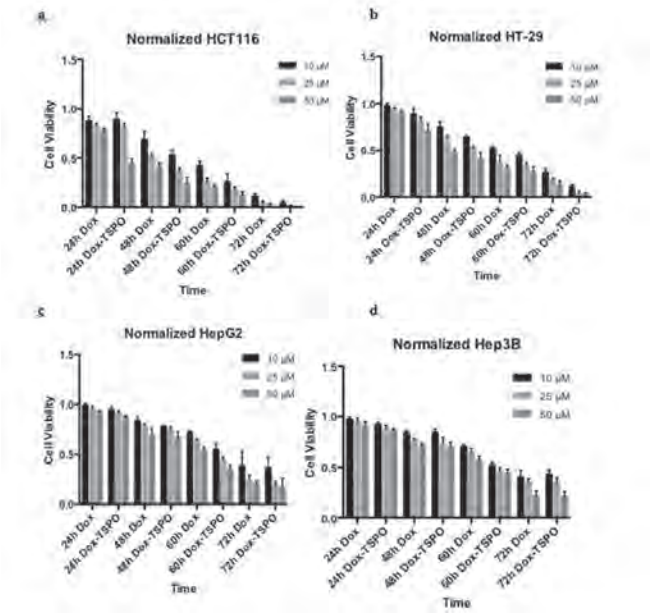

Figure 1. Viability of cell lines following incubation with **1** or free Doxorubicin presented as number of cells in relation to the control (mean ± Standard Error) **a** HT29 **b** HCT116 **c** HepG2 **d** Hep3B

Paper 34: Comparative-Effectiveness Analysis of Surgery vs. Ablation for Stage T1a Renal Cell Carcinoma in the SEER

Population

N. Kokabi, M. Xing, R. Duszak, K.E. Applegate, J.C. Camacho, D.H. Howard, K. Kim

Objectives: The annual economic burden of management of renal cell carcinoma (RCC) to the US healthcare system is up to $5 billion USD according to the literature. The purpose of this study is to investigate national practice trends in the use of thermal ablation (TA) versus surgical resection for the management of stage T1aN0M0 (≤4cm) renal cell carcinoma (RCC), associated outcomes and comparative cost effectiveness of ablative versus surgical therapeutic modalities.
Methods: Using Survival Epidemiology and End Results database, we identified patients with stage T1aN0M0 RCC (≤4cm) diagnosed in 2004 to 2011 and followed through to 2012. Patients with RCC as 1st primary were included to prevent confounding bias. Cost effectiveness estimation were performed using Markov modeling for percutaneous thermal ablation (radiofrequency ablation (RFA) and Cryoablation), laprascopic ablation (LA), partial (PN) and radical nephrectomies (RN) as well as no treatment (active surveillance). Survival was estimated using Kaplan-Meier from the time of diagnosis. Using RCC-related mortality, Cox proportional hazards models were used to compute to mean life years survived for each therapy modality adjusting for patients' demographics. Average RCC related Medicare costs attributed to each modality were also estimated using generalized least square methods.
Results: Of 28351 patients with T1a lesion on SEER database, 2133 (7.5%) did not receive curative therapy. Of 26218 patients who received curative therapy, the majority underwent surgical resection: 24992 (95.3%) surgical resection, 671(2.6%) Cryoablation, and 553(2.1%) RFA (P<0.001). When sub analyzing for patients ≥65 years, 11,493 patients (41%) were older than 64 years. Mean overall survival was similar between the surgery (81.1 months) and Thermal (81.0 months) group (P=0.48). There was no difference in survival between RFA and Cryoablation groups (80.9 months vs. 81.1 months for RFA and Cryoablation (P=0.451)). There was no significant difference among patients ≥65 years of age who received TA (80.4 months) vs. surgery (80.6 months) (P=0.35) (Figure 1). Those who did not receive curative therapy had a significantly shorter mean OS (70.4 mo; P<0.001) when compared to curative group as a whole. Cost estimation related to each therapeutic modality demonstrated significant cost savings for the ablation groups.
Conclusions: Economic burden of RCC, particularly in ≥65 years, is significant. Survivals are similar between surgery vs RFA vs Cryoablation at significant cost savings with RFA/Cryoablation. Cost effective treatments with enhanced patient experiences for T1a RCC in ≥65 years are RFA/ Cryoablation.

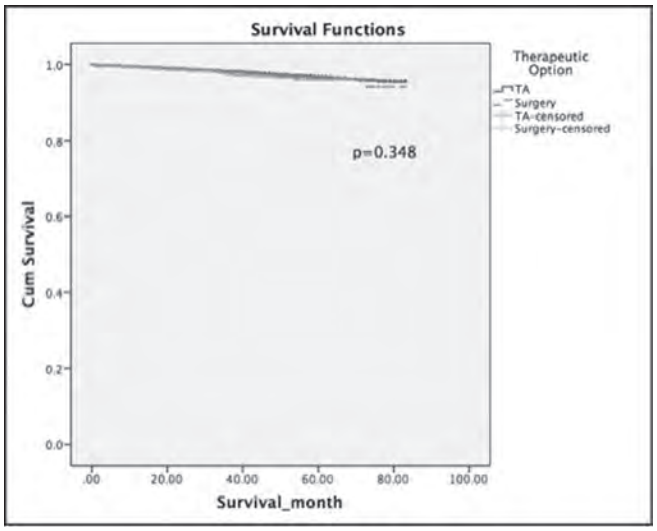

Kaplan-Meier estimation demonstrating similar survival between TA and Surgical groups for patients ≥65 years (p=0.348).

Paper 35: Percutaneous Microwave Ablation of T1a Renal Cell Carcinoma: Interval Update with Median 11-Month Imaging Follow-Up

A. Moreland, J. Horn, A.M. Fischman, M. Klapperich, S. Wells, E. Abel, M. Lubner, J. Hinshaw, F. Lee, S. Nakada, S. Best, S. Hedican, C. Brace, T. Ziemlewicz

Objectives: To evaluate feasibility, safety, and preliminary efficacy of percutaneous microwave ablation for the treatment of clinical T1a renal cell carcinoma.
Methods: Retrospective case review of an IRB-approved, HIPAA-compliant multi-institutional database was performed. All clinical T1a, biopsy-proven renal cell carcinomas treated with percutaneous microwave ablation at two academic medical centers between 03/2011 and 11/2014 were included. All patients were treated under general anesthesia in a single primary treatment session. A combination of US and CT guidance was used. Antenna type/number and time/power were at the discretion of the operator to achieve no residual enhancing tumor on immediate post-ablation CECT. Complications were categorized according to Clavien Dindo classification. Follow-up CT or MR was performed at target intervals of 6, 12, and 24 months post ablation. Kaplan-Meier method was used for survival analyses.
Results: 132 tumors among 129 patients were treated during the inclusion period. Median tumor diameter was 2.3 cm (IQR: 1.8-3.0). Mean number of antennas used was 1.2 for tumors up to 3 cm in diameter, and 1.9 for tumors 3 to 4 cm in diameter. All ablation procedures were technically successful as defined by lack of residual enhancement on immediate post ablation CECT. The rate of minor complications was 5.4% with n=6 Grade 1 complications (urinary retention, bacterial cystitis, fluid overload, atrial fibrillation) and n=1 Grade 2 complication (hemorrhage requiring transfusion). One case (0.8%) involved a major complication: renal artery pseudoaneurysm requiring coil embolization. Median length of imaging follow-up was 11 months among the 102 patients with follow-up studies internal to the institutions, and 25 of these patients had imaging follow-up at 18 months post-procedure or greater. Metastatic disease was not noted in any case, while local recurrence was identified in n=2/102 cases (1.2%). Both patients have been retreated: One with radical nephrectomy and the other with repeat microwave ablation—with neither demonstrating local recurrence to date. The overall primary treatment effectiveness was therefore 98.1% and secondary treatment effectiveness was 99.0%. Median length of clinical follow-up was 8 months (IQR: 3-15) with RCC-specific survival of 98.4% and overall survival of 97.7% (with 3 deaths unrelated to the procedure or the malignancy).
Conclusions: Percutaneous microwave ablation of T1a renal cell carcinoma was technically successful in all cases in this series. Complication rates are comparable to those for alternative thermal ablation modalities. Oncologic efficacy and survival outcomes are promising as case numbers and follow-up durations for this series increase.

Paper 36: Cryoablation of Prostate Adenocarcinoma Recurrences: 2 Year Follow Up

D.A. Woodrum, K. Kinsman, S.M. Thompson, K. Gorny, M.R. Callstrom, L. Mynderse

Objectives: To examine the 2 year followup of MR guided cryoablation in patients with biopsy proven local recurrence of prostate adenocarcinoma
Methods: Retrospective review of seventeen men(55-72yo) with biopsy-proven recurrent prostate adenocarcinoma treated with MR-guided cryoablation(Galil Medical,Minneapolis,MN). Of 17 patients, 16 had primary surgery and 1 had primary external beam radiation. After primary treatment, 9 patients underwent secondary treatment with external beam radiation. Afterward patients presented for additional therapy with MR guided cryoablation due to ongoing recurrences localized in the prostate bed identified by rising PSA and dynamic contrast MRI. Under general anesthesia, patients were brought into a wide-bore 1.5T MRI(Siemens Medical,Malvern,PA). Under MRI guidance, 2-10 cryotherapy probes were placed in/around the recurrence. A urethral warming catheter was used to protect from urethral damage. Saline displacement was used to displace the rectum from the prostate cancer recurrence for better margins. The cryoablation technique consisted of a 0.5cm probe separation with 3 freeze-thaw cycles.
Results: The average pre-procedure PSA was 1.35ng/dL and average 3 month post-procedure PSA was 0.07ng/dL(P<0.01). At the 3 month followup, 65% of patients had undetectable PSA. At the 6 month followup, the average PSA was 0.15ng/dL with 41% of patients having undetectable PSA. At 1 year, 13 of 17 patients had followup PSA with an average of 0.30ng/dL with only four patients having completely undetectable PSA. At the one year time point 3 patients had identifiable recurrence on MRI which was retreated with MR guided cryoablation. At the 2 year followup, 9 of 17 patients returned with an average PSA of 0.34ng/dL. At 2 years, two patients went on to have a recurrence identifiable by MRI with one choosing repeat cryoablation and the other choosing radiation. Complications included mild worsening of incontinence in several patients.
Conclusions: MR guided cryoablation of prostate cancer recurrences is feasible. The two year data indicates that the effect is sustainable over time, but there are patients that do go on to recur within the time frame which necessitates close interval followup with PSA measurements. Five year data is still needed to assess which patients do best over time.

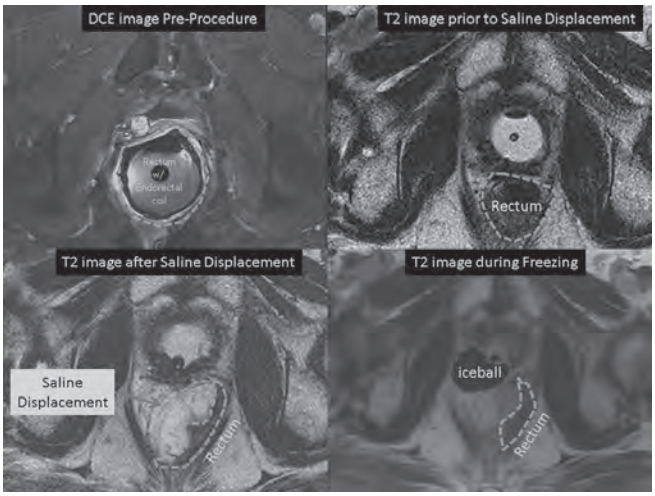

Paper 37: Scaled Signal Intensity of Uterine Fibroids Based on T2-Weighted MR Images: A Potential Objective Method to Determine the Suitability for Magnetic Resonance-Guided Focused Ultrasound Surgery of Uterine Fibroids

S. Yoon

Objectives: Magnetic resonance-guided focused ultrasound surgery (MRgFUS) is a novel method to treat uterine fibroids non-invasively. We assessed the efficacy of scaled signal intensity (SSI) of uterine fibroids in T2-weighted MR images (T2WI) as an objective parameter to determine the suitability for MRgFUS.
Methods: Forty three uterine fibroids in 40 premenopausal women were included in this retrospective study. SSI in each fibroid was measured at T2WI by standardizing its mean signal intensity to a 0-100 scale, using reference intensities of skeletal muscle (0) and fat (100), respectively. Pretreatment SSI was transformed with square root (sqrt) for normal distribution and analyzed according to the non-perfusion volume (NPV) ratio.
Results: Pre-treatment sqrt SSI of uterine fibroids showed a significant inverse-correlation with NPV ratio ($P < 0.05$). In the setting of dichotomizing treatment response at 45% of NPV ratio, the optimal cut off value of SSI (16.0) exerted an excellent diagnostic performance such as area under ROC curve (AUC) = 0.950 (95% CI, 0.837-0.993).
Conclusions: A Fibroid with SSI value 16.0 or less can be expected to have optimal responses. SSI of uterine fibroids in T2WI can be suggested as the objective parameter for the patient selection in MRgFUS.

Paper 38: Adjunctive Techniques to Allow for Percutaneous Cryoablation of Renal Masses in Difficult Anatomic Locations

S. Sayegh, A. Fadl, D. Phung, O. Shoaib, A. Baadh, J.C. Hoffmann

Objectives: The purpose of this exhibit is to describe and demonstrate adjunctive techniques that improve safety and technical success rates of percutaneous cryoablation of renal masses in difficult anatomic locations.
Methods: Management strategies for the treatment of small renal masses include active surveillance, percutaneous ablation, or nephron-sparing surgery. The decision is made based on age of patient, medical history, surgical comorbidities, mass size and location, rate of growth, and patient preference. Percutaneous image-guided cryoablation is a well-accepted, minimally invasive therapy to treat small renal masses, particularly in patients who are poor surgical candidates due to multiple comorbidities, multiple tumors, or renal failure. Lesions typically considered more difficult to ablate include central lesions, size larger than 3 centimeters, upper pole location, endophytic, and adjacent to ureter, colon, or other organs. This educational exhibit highlights the role of adjunctive techniques in ablation of renal masses in difficult anatomic locations.
Results: Some renal lesion locations have been classically described as more difficult to treat with percutaneous cryoablation due to risk of damaging adjacent critical structures, such as the ureter, renal pelvis, or adjacent bowel. Retrograde pyeloperfusion, hydrodissection, and angioplasty balloon interposition are three techniques that can be used to safely perform cryoablation in these difficult anatomic locations. In addition, choosing a patient position on the procedure table to create the safest treatment window is critical. These techniques can be used individually or in combination to improve safety when ablating renal masses in challenging anatomic locations.
Conclusions: Maximizing patient positioning, retrograde pyeloperfusion, hydrodissection, and angioplasty balloon interposition are critical adjunctive techniques that can be used to improve safety when performing percutaneous image-guided cryoablation of small renal masses in difficult anatomic locations.

Paper 39: Thermal Ablation of Metastatic Adrenocortical Carcinoma: Long-Term Results

G.M. Varano, L. Jiang, V.P. Krishnasamy, N. Jain, H. Amalou, M. Edgerly, M. Velarde, N. Abi Jaoudeh, A. Venkatesan, E.B. Levy, A. Fojo, B.J. Wood

Objectives: Adrenocortical carcinoma (ACC) is a rare but aggressive malignancy with few therapeutic options outside of complete surgical resection. Aggressive local surgical resection of ACC has been shown to improve outcomes. However, therapeutic thermal ablation has emerged over the past decade as a minimally invasive option in the treatment of metastatic disease, particularly in patients who are poor surgical candidates. It is possible, although unproven, that aggressive local control with thermal ablation may also improve outcomes. The aim of this single center retrospective review is to characterize thermal ablation for metastatic ACC and report the long-term clinical outcome.
Methods: A retrospective review was performed on patients who underwent radiofrequency, microwave, and cryo-ablation for metastatic ACC at a single tertiary care center from February 1999 to September 2014 after IRB approval was obtained. Radiographic and clinical data were evaluated longitudinally. Survival analyses from the date of percutaneous ablation were evaluated with Kaplan-Meier estimation.
Results: Thirty patients with a total of 70 ACC metastatic lesions were treated with ablation. Fourteen men and 16 women between 24 and 73 years of age (average 46 years) with a mean follow-up of 35 months (median 16, range 2 to 186) were evaluated. Lesions were located in the adrenal bed, liver, retroperitoneum, peritoneal cavity, bone, lung, and extra abdominal soft-tissues. Mean lesion diameter was 31.8 millimeters (median 24, range 6 to 103). Technical success, defined as the absence of enhancement in the tumor bed on initial follow up imaging, was achieved for 53 of 62 lesions (85%) treated for local control, including 36 of 43 liver lesions (84%). Eight lesions were treated only for pain palliation and excluded from statistical analysis. At 6 months, 1 year, and 2 years following treatment, 97%, 94%, and 94% (respectively) of initially technically successful treatments were free of local progression. Patients' median overall survival and progression-free survival were 53 months and 5 months (respectively).
Conclusions: In appropriately selected patients, thermal ablation may be useful for local control in multi-staged and multi-modality approaches to metastatic ACC management.

Paper 40: Percutaneous Cryoablation for the Treatment of Primary and Metastatic Lung Tumors

J.L. McDevitt, S.K. Mouli, K.T. Sato

Objectives: Tumor ablation has gained popularity in the treatment of primary and secondary pulmonary neoplasms in recent years, as only one-third of primary tumors are amenable to surgical resection. For these lesions, percutaneous cryoablation has emerged as a potential therapy, though clinical evidence is currently limited. The purpose of this study was to test the hypothesis that percutaneous cryoablation is a safe and effective treatment for primary and metastatic lung tumors.
Methods: An IRB-approved, HIPAA-compliant retrospective review was performed to identify all patients who underwent percutaneous cryoablation from April 2007 to September 2014 at our institution. Patients with primary lung tumors deemed to be poor surgical candidates were selected for cryoablation by a multidisciplinary tumor board. Patients with metastatic disease were deemed appropriate for cryoablation if they had stable or limited lung involvement. Cryoablation was performed using the Endocare Percutaneous Cryoablation system. The number of needles used varied based on tumor size. Procedures were performed using Computed Tomography (CT) for guidance and either moderate sedation or general anesthesia. The cryoablation protocol consisted of a 15-minute initial freeze cycle followed by a 5-minute passive thaw cycle followed by a 10-minute secondary freeze cycle. Measurement of tumor size and determination of local progression were done in accordance with World Health Organization guidelines. Complications were categorized as major or minor in accordance with SIR reporting standards. The times to local progression and median survivals were calculated using Kaplan–Meier analysis and were compared using the log-rank test. All statistical analysis was performed using SPSS Statistics 22.0. P values <0.05 were regarded as significant.
Results: A total of 47 lung tumors (25 primary, 22 metastatic) were treated. 43 treated patients (19 male, 24 female), with a mean age of 73.2 years at treatment, had at least 1 follow-up CT examination. The median follow-up for the cohort was 241 days. Of treated tumors, the mean pretreatment diameter was 2.2 cm, and an average of 2.0 probes were used per procedure. There were 11 (22%) major complications (8 pneumothoraces requiring chest tube or hospitalization, 2 hospitalizations for hemoptysis, 1 hospitalization for hypoxia) and 13 (27%) minor complications (pneumothorax and pulmonary hemorrhage not requiring treatment). Seven patients (16%) exhibited local progression during the follow-up interval, with a median time to progression for the entire group of 275 days. There was not a statistically significant difference in time to local progression between primary and metastatic tumors (median of 275 days for primary, 329 for metastatic, P=0.15).
Conclusions: Percutaneous cryoablation of lung tumors is safe and feasible with a complication rate comparable to other percutaneous ablation techniques. Further study will be necessary to determine the long-term oncologic effectiveness of this procedure.

Paper 41: Image Guided Treatment of Chylous Efussions in Oncologic Patients: Single Center Experience

E.G. Santos Martin, K.M. McCluskey, C. Friend, R. Varma

Objectives: To determine the efficacy of image guided procedures in the management of chylous leaks
Methods: A retrospective review was performed of 19 oncologic patients with chylous leaks (15 patients with chylothorax and 4 patients with abdominal chylous leaks). The chylous effusion was post-operative in 16 patients (84.2%) and non-traumatic in 3 patients (15.8%). The primary tumor of the patients within post-operative group was esophageal carcinoma (62.5%), renal cell carcinoma (12.5%), lung carcinoma (12.5%), breast carcinoma (6.25%), cholangiocarcinoma (6.25%). The primary tumor in the non-traumatic group was lymphoma (66.5%) and ovarian carcinoma (33.5%). Three patients with chylothorax and esophageal ca underwent thoracic duct ligation prior to attempting percutaneous treatment. Twenty two intranodal lymphangiograms (INL) were attempted. Within the chylothorax group, 73.3% underwent thoracic duct embolization/disruption. Additional CT guided glue embolization was performed in one patient in which the thoracic duct was surgically ligated. Any patient who required additional surgery to treat the chylous leak was considered a treatment failure. INL could not be performed in one patient which was excluded from the secondary analysis.
Results: The technical success of INL was 94.7%. INL detected a leak in 13 patients (72.2%). In the post-operative group, INL and thoracic duct embolization/disruption was successful in sealing the lymphatic leak site in 13 patients (81.25%). In the non-traumatic group, INL was not therapeutic in any case. CT guided glue injection for targeted treatment was successful in 1 patient. The overall success for image-guided treatment for chylous leaks was 77.7%.
Conclusions: Image guided percutaneous treatment is safe and effective in the management of oncologic patients with chylous leaks.

Paper 42: Estrogen Receptor Alpha in Lung Cancer Development and Growth, a Novel Therapeutic Target

G.G. Chen, M. Li, A.W. Kong, M.J. Underwood

Objectives: The treatment for lung cancer is limited for the advantaged lung cancer and this is partly due to our poor understanding of lung carcinogenesis and the lack of effective treatment targets. Estrogen receptor alpha (ERa) plays a role in certain

tissues carcinogenesis. The objective of this study was to determine the level of ERa in smoking-related lung cancer and its role in treatment of lung cancer.
Methods: In this study, ERa was analyzed in the smoking carcinogen N-nitrosamine NNK-induced lung tumor in a mouse model and in human lung cancer tissues. The role of ERa in lung tumor development and growth was explored using various cellular and molecular approaches. Since cytochrome P450 1B1 (CYP1B1) is the enzyme responsible for metabolize NNK, the possible involvement of CYP1B1 in the ERa pathway was also explored.
Results: Our in vivo study demonstrated that ERa and CYP1B1 and were over-expressed at the early stage of NNK-induced lung tumorigenesis. Microarray analysis found that ERa was involved in the ERK/MAPK Pathway. NNK activated RAS/ERK/AP1 as it remarkably increased the levels of p-ERK, c-Fos and c-Jun, but inhibited multiple negative regulators of Ras/ERK/AP1, pdcd4, spry1, spry2 and Btg2 through up-regulating miR-21. Both CYP1B1 siRNA and ERK specific inhibitor suppressed NNK-mediated ERa up-regulation, suggesting that ERa is down-stream of CYP-1B1and ERK. ERK inactivation led to the accumulation of CYP1B1, indicating that CYP1B1 is up-stream of ERK activation. Inhibition of ERK or ERa decreased NNK-induced cell proliferation, and block of CYP1B1 or ERa induced apoptosis in lung cancer cells.
Conclusions: We conclude that ERa up-regulated by smoking carcinogen NNK contributes to the lung carcinogenesis. NNK-mediated ERa induction is via CYP1B1 and ERK activation. The inhibition of ERa arrests the lung cancer cell proliferation and growth, indicating that ERa is likely to be a novel therapeutic target against smoking-related lung cancer.

Paper 43: Radiofrequency Ablation Versus Surgery for the Treatment of Lung Metastases

L. Tselikas, E. Fadel, A. Auperin, F. Deschamps, O. Mercier, L. Lamrani, A. Hakime, C. Teriitehau, P. Dartevelle, T. de Baere

Objectives: To compare efficacy and tolerance of radiofrequency ablation (RFA) and surgery for the treatment of lung metastases
Methods: This retrospective, IRB approved study, included patients with up to 5 lung metastases, with à maximal diameter of 4 cm, without pleural or lymph node involvement on preoperative CT-scan. Seventy-eight patients with 130 metastases received surgery and 126 patients with 223 metastases received RFA. Patient and treatment characteristics were compared. Efficacy was assessed using overall survival, progression free survival (PFS), pulmonary progression and local recurrence rates. Complications and hospital stay were also reported.
Results: Patients were significantly older in the RFA group (P<0.0001), with more extra-thoracic locations of cancer requiring additional treatments (P=0.015). Metastases were larger in the surgery group (mean size: 17.4 vs. 15.4 mm, P =0.05), and more frequently unilateral (94% vs. 76%, p=0.0014) Overall survival at 1 and 3 years was 94.8 and 67.2% for the surgery group versus 94 and 72.1% for the RFA group, P = 0.46. One and 3-year PFS (49.4 and 26.2 vs. 38.9 and 14.8, P = 0.18), pulmonary progression (39.1 and 56% vs. 41.2 and 65.3%, P = 0.99), or local recurrence (5.4 and 10.6 vs. 14.8 and 18.6, P = 0.07), rates were not different when comparing surgery and RFA respectively. Complication rate was 29% for surgery and 32% for RFA (P = 0.8), with a significantly lower hospital stay for RFA patients (P<0.0001)
Conclusions: RFA seems efficient and safe, and have to be considered as an alternative to surgery for the treatment of lung metastases.

Poster 1: Regulation of Cell Survival by MET and EGFR Receptor Tyrosine Kinase Signaling following Sublethal Heat Stress in Hepatocellular Carcinoma

S.M. Thompson, M.R. Callstrom, D. Jondal, K. Butters, B. Knudsen, J. Anderson, D.A. Woodrum

Objectives: Tumor recurrence following percutaneous thermal ablation of hepatocellular carcinoma (HCC) remains a significant clinical problem, particularly in tumors ≥3.0cm. Prior experiments identified that various growth factor signaling pathways may be induced following sublethal heat stress. The aims of the present study were to test the hypotheses that 1) sublethal heat stress induces MET and EGFR receptor tyrosine kinase signaling in HCC cells *in vitro* and at the ablation margin *in vivo* and 2) inhibition of MET and EGFR signaling decreases HCC clonogenic survival following sublethal heat stress *in vitro*.
Methods: N1S1 (MET+) and AS30D (EGFR+) HCC cells and a panel of eight human HCC cell lines were subjected to sublethal heat stress (45.0C) or control (37.0C) for 10 minutes and assessed for phospho-MET and phospho-EGFR by western immunoblotting at 0 to 120 minutes post heat stress. Repeat experiments were performed with pre-treatment of N1S1 and AS30D cells with small molecule inhibitors to MET and EGFR, respectively. IACUC approved intentional partial laser thermal or sham ablation was performed on orthotopic N1S1 and AS30D HCC tumors under US-guidance and liver/tumor tissue assessed for phospho-MET and phospho-EGFR immunostaining at 24 hours post-ablation (N=8). The HCC cell lines N1S1 and AS30D were pre-treated with a dose-titration of small molecule inhibitors against MET or EGFR or vehicle control followed by sublethal heat stress (45.0C) or control (37.0C) for 10 minutes and assessed for colony formation at 7-10 days (N=3).
Results: Western immunoblotting demonstrated that sublethal heat stress induced MET and EGFR phosphorylation in the N1S1 and AS30D cells immediately post heat stress and this heat stress induced MET and EGFR phosphorylation was blocked with pre-treatment with small molecule inhibitors to MET and EGFR. Sublethal heat stress induced MET phosphorylation in 1 of 8 and EGFR phosphorylation in 6 of 8 human HCC cell lines, respectively. Immunohistochemical analysis of the ablation zone demonstrated markedly increased MET phosphorylation at the tumor ablation margin in N1S1 tumors and a mild increase in EGFR phosphorylation at the tumor ablation margin in AS30D tumors. There was no evidence of increased MET or EGFR phosphorylation in the tumor or at the margin between liver and tumor in the sham ablation group. Inhibition of MET resulted in a dose-dependent 55% to 74% decrease in N1S1 clonogenic survival following sublethal heat stress compared to sublethal heat stress alone (P<0.03) while inhibition of EGFR resulted in a dose-dependent 40% decrease in AS30D clonogenic survival following sublethal heat stress compared to sublethal heat stress alone (P<0.01).
Conclusions: These data demonstrate that sublethal heat stress of HCC cells induces rapid MET and EGFR receptor tyrosine kinase signaling in vitro and that thermal ablation induces MET and EGFR phosphorylation at the HCC tumor ablation margin in vivo. Inhibition of MET or EGFR blocks heat stress induced MET and EGFR signaling and significantly reduces HCC clonogenic survival following sublethal heat stress. These data not only suggest that MET and EGFR pathways may in part mediate HCC cell survival following sublethal stress in a cell-type dependent manner but also that other receptor or non-receptor tyrosine kinases may be involved in activating downstream signaling pathways and survival mechanisms. As such, thermal ablation induced tyrosine kinase (TK) signaling including MET, EGFR and other TKs warrants further investigation as a candidate mechanism for recurrence and progression following thermal ablation of HCC.

Poster 2: Biofunctionalized Hybrid Magnetic/Gold Nanostructures as Catalysts for Photothermal Ablation of Colorectal Liver Metastases

S.B. White, D. Kim, Y. Guo, W. Li, J. Chen, Y. Yang, A.C. Larson

Objectives: Nanoparticles can be tailored to serve as drug delivery vehicles or catalysts for photothermal ablation with delivery quantified using MRI techniques. We previously validated the efficacy of our anti-MG1 conjugated hybrid magnetic/gold nanostructures (HNS) during *in vitro* studies. These particles have an iron oxide core (MR imaging), a gold shell, (photothermal sensitizer), and are conjugated with monoclonal antibodies (anti-MG1) in order to hone in to the tumor. The purpose of our study was to demonstrate the feasibility of using MRI to detect *in vivo* delivery of anti-MG1 conjugated hybrid magnetic/gold nanostructures (HNS) in a rodent model of colorectal liver metastases (CRLM) and assess potential for HNS to serve as catalysts for photothermal ablation of CRLM.
Methods: Multi-functional HNS conjugated with anti-MG1 mAb were synthesized and coupling efficiency determined. Nineteen Wistar rats were each implanted with 2 tumors in their right and left hepatic lobes using 5 x 10^6 CC-531 cells (colorectal liver metastasis cell line). The rats were divided into three groups, one treated with anti-MG1 coupled HNS, one treated with HNS alone, and one group with no HNS infusion thus serving as control. Voxel-wise R2 and R2* measurements were performed using a 7.0 T MRI prior to, immediately post and 24 hours after injection. After image acquisition, photothermal ablation was performed using a fiber-coupled near infrared (NIR) (808 nm) diode-laser (BWF5, B&W Tek, Inc., DE, USA). Each rat was illuminated at laser powers of 1.2 W for 3 minutes. An infrared (IR) thermal camera (ICI7320P, Beaumont, TX, USA) was used to measure the temperature of the irradiated region. The animals were then euthanized and tumors were collected for histological assessment.
Results: The coupling efficiency of the anti–MG1 to the HNS was 55%. Six rats were treated with 1.5 mg of anti-MG1 conjugated HNS, and 6 rats were treated with 1.5 mg of HNS alone, 7 served as controls. Of the tumors treated with anti-MG1 HNS, the mean decrease in R2 was 35% and of R2* was 40% compared to the HNS alone group that had a mean decrease in R2 of 37% and R2* of 63%. Prussian blue staining confirmed delivery of anti-MG1 HNS and HNS to the tumors. Photothermal ablation resulted in mean temperatures in the anti-MG1 coated HNS treated, HNS treated and control tumors of 50.2°C (±7.8), 51°C (±4.4), 39.5°C (±2.0), respectively.
Conclusions: R2 and R2* MRI measurements permit *in vivo* detection of anti-MG1 coupled HNS and HNS delivery to tumors in the CRLM rodent model. Thus, these HNS can serve as a catalyst for photothermal ablation of CRLM.

Poster 3: Does Thermosensitive Liposomal Vinorelbine Decrease Tumor Growth follow Percutaneous Radiofrequency Ablation of Liver Tumors in a Mouse Model?

W. Yang, W. Song, X. Mei, W. Gong, J. Lee, K. Yan

Objectives: To investigate whether combining radiofrequency (RF) ablation with intravenous thermo sensitive-liposome-encapsulated Vinorelbine (Thermo-Vin) improves tumor destruction, intratumoral drug accumulation, tumor growth and end-point survival. Further, to explore the initial tumor size on long-term outcome of combined therapy.
Methods: First, antitumor efficacy of Thermo-Vin was asessed in vitro. Next, H22 liver adenocarcinomas (n = 159) were implanted in 149 mice in this animal care committee–approved in vivo study. Tumors received (a) no treatment; (b) RF ablation alone (70±2 degree, 5mins), (c) RF ablation followed by Free-Vin (RF+Free-Vin), or (d)(e)(f), RF ablation followed by Thermo-Vin (RF+Thermo-Vin) at various Vinorelbine concentration (5,10,20mg/kg). Tumor destruction area was compared in different treatments 24hr after treatment. Intratumoral Vinorelbine uptake with and without RF ablation were compared. Pathological staining revealed cell apoptosis and cellular proliferation at edge of coagulation and residual tumor. Finally, for long-term outcome analysis, tumors were divided into three classes according to tumor size. Large as 13-15 mm in diameter, medium as 10-12mm and small tumor as 7-9mm. These tumors were randomized into three treatment and one control arms for Kaplan-Meier analysis to define survival end-point (3.0-cm diameter).
Results: In vitro, at 37 degree Thermo-Vin inhibit 45% ofH22 cells viability, while at 42 degree inhibit 63% of cells viability at 24hr. Likely, in vivo, 10mg/kg Thermo-Vin increased tumor destruction over RF ablation or free-Vin (mean, 341.8±65.4 mm2vs. 157.5±51.5 mm2or 225.3±25.4 mm2, P=0.001, P=0.007).Mean intratumoral Vinorelbine accumulation for Thermo-Vin+RF increased 15 fold, compared with Free-Vin alone (1156.5±158.2 ug/ml vs. 74.7±10.5ug/ml, P=0.016). Thermo-Vin substantially increased apoptosis at coagulation margin and suppressed cellular proliferation in the residual tumor. Thermo-Vin+RF arm had better survival result than RF alone (mean, 37.6±20.1days vs. 23.4±5.0 days, p=0.015) or Free-Vin+R Farms (mean, 37.6±20.1days vs. 23.3±1.2 days, P=0.016), with corresponding slower tumor growth rates in animals with medium sized tumors. No significant different in survival among three treatment arms in large and small sized tumors.
Conclusions: Thermo sensitive liposomes selectively delivery Vinorelbine to the edge of RF coagulation and effectively increase induced tumor coagulation. End-point survival is most effected in animals with medium sized tumors, suggesting that tumor size plays important role in long-term outcome for combined RF/Liposomal therapy.

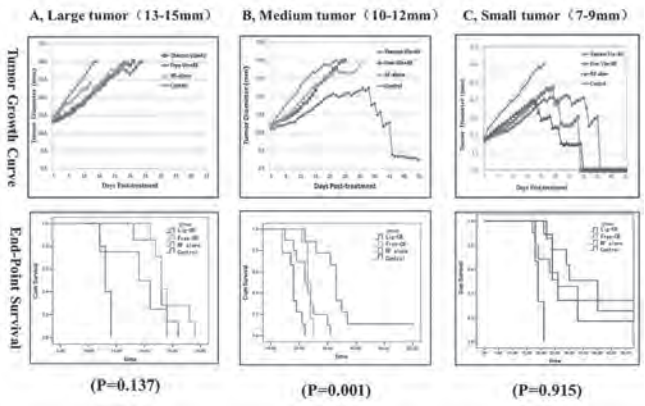

Figure. End-Point Survival and Effect of Tumor Size on Outcome
(a) There was no significant different in survival among three treatment groups in large sized tumors (P=0.137). (b) Thermo-Vin+RF group had better survival result than RF alone or Free-Vin+RF groups, with corresponding slower tumor growth rates. There was no significant difference in mean end-point survival between RF alone and Free-Vin+RF. (c) There was no significant different in survival among three treatment groups in small sized tumors (P=0.915).

Poster 4: Catheter-Related Particle Flow Dynamics May Be Critical to the Success of Intra-Arterial Radioembolization for the Treatment of Liver Tumors

A. van den Hoven, M. Lam, S. Jernigan, M. van den Bosch, G. Buckner

Objectives: Radioembolization has evolved as a viable treatment option for patients with unresectable and chemorefractory liver tumors. Remarkably, the interplay between catheter design/position and fluid-particle dynamics is still inadequately understood. The objective of this study was to investigate differences in cross-sectional catheter position, particle flow dynamics and downstream branch distribution between microsphere administrations with a standard end-hole microcatheter (SMC) and an anti-reflux catheter (ARC).
Methods: A total of 7 experiments were performed in a bench-top model of the hepatic arterial vasculature with recreated hemodynamics. Fluorescent microspheres (3 experiments) and clinically used holmium microspheres (4 experiments) were administered with the SMC and ARC positioned at the same level along the longitudinal vessel axis, but with random cross-sectional placement. Catheter-related particle flow dynamics were analyzed by reviewing video recordings of UV-light illuminated fluorescent microsphere administrations. Downstream branch distribution was analyzed by quantification of collected microspheres in separate filters for two first-order branches. Mean deviation from a perfectly homogenous distribution (DHD) was used to compare the distribution homogeneity between catheter types.
Results: The SMC administrations demonstrated a random off-centered catheter position (in 71% of experiments), and a laminar particle flow pattern with an inhomogeneous downstream branch distribution, dependent on catheter position and injection force. The ARC administrations demonstrated a fixed centro-luminal catheter position, and a turbulent particle flow pattern with a more consistent and homogenous downstream branch distribution. Quantitative analyses confirmed a significantly more homogeneous distribution with the ARC; the mean DHD was 40.85% (IQR 22.76%) for the SMC and 15.54% (IQR 6.46%) for the ARC (P = 0.047).
Conclusions: Catheter type impacts downstream microsphere distribution in an in-vitro hepatic arterial model. A clinical trial has been initiated to investigate these effects during holmium-166 radioembolization.

Fluorescent microsphere administration with a SMC. Note the off-centered SMC position, laminar outflow pattern and absence of microsphere flow towards the LHA.

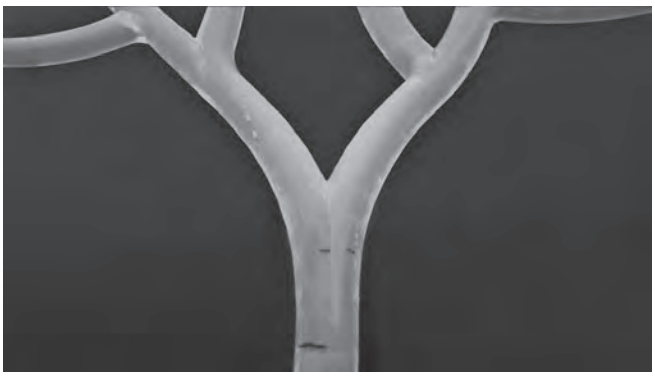

Fluorescent microsphere administration with an ARC. Note the centro-luminal ARC position, turbulent outflow pattern (an eddy current is visible adjacent tot the ARC tip) and more homogenous microsphere distribution over the LHA and RHA.

Poster 5: Evaluation of Dosimetry in Microwave Ablation (MWA) Zones in a Novel Perfused Porcine Liver Model

S. Singh, P.N. Siriwardana, E. Johnston, J. Watkins, B.R. Davidson, R. Illing

Objectives: Microwave ablation (MWA) is an increasingly popular method of thermal ablation for solid tumour deposits in the liver. Purported advantages over radiofrequency ablation (RFA) include larger ablation zones, greater speed and less heat sink effect. For the majority of MWA systems, treatment parameters used depend on a pre-defined algorithm of time and power based on an *ex vivo*, fresh non perfused animal liver model which is stated in the instruction manual with no standard deviation values. Clinical studies have shown these settings give smaller ablation zones than expected suggesting the non perfused model to be inadequate. We performed MWA of the liver comparing a novel perfused ex vivo porcine liver model with a fresh non perfused liver with an aim to generate more reliable dosimetry data.

Methods: The Acculis Microwave Tissue Ablation Sulis™ V system (Angiodynamics, Queesbury) was used to ablate three perfused ex vivo livers and three non-perfused livers at 140 W for two minutes per ablation. Porcine liver was perfused via hepatic artery and portal vein using time expired human blood oxygenated with 14% O_2, 5% CO_2 and balance N_2 at 150ml/min warmed via a heat exchanger to near 37C. Seventeen ablation zones were created under ultrasound guidance; 9 in the non-perfused arm and 8 in the perfused arm. After ablation, the livers were bisected along the path of the ablation probe, the ablation zones measured and sections were stained with H&E and NADH. The expected ablation zone size based on the instruction manual was 35 mm x 29 mm.
Results: The perfused ablation zones were smaller than the non-perfused zones. The mean of the maximum diameter of the axis perpendicular to the MW probe in the ablation zone (short axis) in the perfused and non-perfused livers were 17.8 (±2.7) mm and 21.1 (±2.3) mm respectively (P = 0.0138).The mean of the maximum lengths of the ablation zone in length with the probe (long axis) in the perfused and non-perfused livers were similar at 39.6 (±5.3) mm and 40.3 (±3.5) mm (P=0.7448). When compared to the values of ablation zone given in the instruction manual of the MTA system, there is a consistent difference of over a centimetre in the short axis measurement (17.8 (± 2.7) mm vs 29 mm). The long axis measurement however is similar 39.6 (±5.3) mm vs 35 mm. No standard deviation values are stated in the instruction manual.
Conclusions: The perfused liver model produced significantly smaller ablation zones compared to the non-perfused livers and reference values stated in the instruction manuals. The non-perfused mean ablation zone size in our experiments was closer to the instruction manual. This finding is consistent with recent clinical studies which show that the instruction manual data overestimates the ablation zone size for a particular power-time combination. An *ex-vivo* perfused model may generate more realistic dosimetry data than ex vivo non perfused models.

Poster 6: Characterization of Nanopore Formation after Irreversible Electroporation (IRE) in the Porcine Vertebral Body

T. Appleton Figueira, J. Gu, M. Gagea, J. Ensor, M. Melancon, N.M. Muñoz, K. Dixon, A. McWatters, Y. Qiao, A. Tam

Objectives: To assess the formation of nanopores and the distribution of nanoparticles in cells after nanoparticle injection and irreversible electroporation (IRE) in the porcine vertebral body.
Methods: Five thoracolumbar vertebral bodies in a single animal were subjected to intervention: IRE sham (n=1), nanoparticle injection (NPI) (n=1); NPI+IRE (n=3). Nanoparticle injection consisted of the percutaneous delivery of 2cc of a mixture of fluorescent nanospheres varying in diameter (20, 40 and 100 nm) into the vertebral body 2 minutes prior to IRE. Euthanasia of the animal was performed 18 minutes after the first NPI+IRE ablation. The vertebral bodies were harvested and processed for analyses by scanning electron microscopy and quantitative pathology imaging. A total of 300 bone marrow cells were evaluated: 60/vertebral body with 30 cells located 4 mm, and 30 located 8 mm, from the IRE probe. The presence of nanopores and nanoparticles were analyzed using a generalized mixed effects linear model.
Results: Nanopores were observed in bone marrow cells of the vertebrae treated with NPI+IRE compared to the control vertebrae (P <0.01). However, proximity to the IRE electrode did not affect nanopore formation (P=0.68). The average nanopore diameter was 163 nm (range 40-1570 nm). Both the number of cells with pores and the number of pores per cell found in each vertebral body were inversely correlated to the time of treatment before euthanasia. The 18 minutes post-IRE vertebral body had nanopores in 15% of the cells (=2.89 nanopores/cell). The 10 minutes post-IRE vertebral body had nanopores in 23% of cells =2.14 nanopores/cell), and the 4 minutes post-IRE vertebral body had nanopores in 53.3% of cells (=4.06 nanopores/cell). Nanoparticles were identifiable in every sample where they were injected. Quantitative imaging analysis indicated that after IRE treatment nanoparticles were localized to the cell membrane.
Conclusions: Nanopores were visualized in bone marrow cells after IRE. Nanoparticles were localized to the cell membrane. The findings support the feasibility of developing a nanoparticle-based IRE treatment platform in bone.

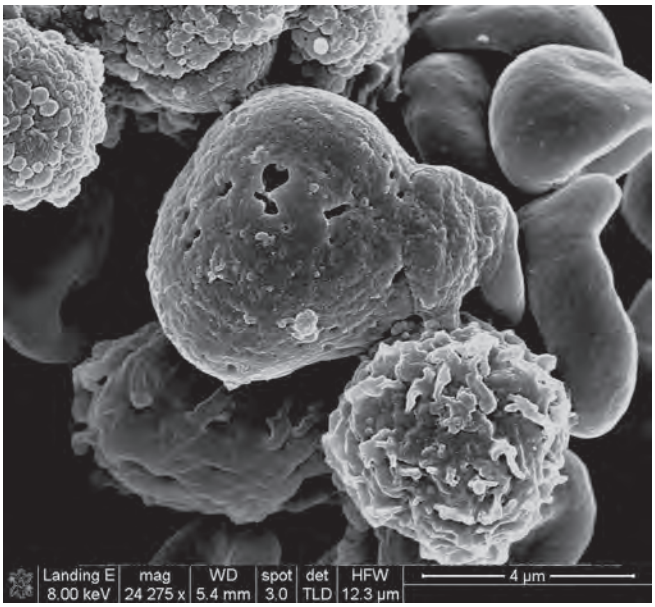

Poster 7: In-vitro Flow Distribution Characterisation of Y90 Surrogates: Density and Gravitational Effects

M. Caine, S. McGhee, P. Garcia, W. Mullett, X. Zhang, M. Hill, S.L. Willis, M.R. Dreher, A.L. Lewis

Objectives: The density of radio-embolic microspheres may influence the distribution of microspheres in tissue and resultant dose distribution. The objective of this study was to investigate the influence of radio-embolic microspheres density on flow distribution through a Vascular Flow Simulator (VFS).
Methods: Distribution of cold surrogates (Glass, TheraSphere® [Yttrium Alumino Silicate, density = 3.6 g/ml] and Resin, SIR-Spheres® [Aminex 50, density = 1.6 g/ml]) were investigated in the VFS under various injection and Blood Mimicking Fluid (BMF) flow rates. The injection solution was 0.9% saline (dyed for UV quantification). Conditions were designed to determine the distribution of injection solution (dye), microspheres and total volumetric flow following injection of surrogates. Injection of surrogates in equal volumes was performed with a syringe pump at a standard rate of 20ml/min or 10ml/min (reduced injection rate) in to BMF flow rates of 120ml/min (as described to be common hepatic flow rate [1]) or 60ml/min (reduced flow modelling embolization). The VFS (Figure 1) is composed of a series of branched channels that diminish in diameter from 4 mm to 0.9 mm and combine into 6 exit channels. The influence of gravity was investigated by placing the VFS in a horizontal (flow mediated alone) or vertical (additional influence of gravity) orientation wherein anterior (channels 1-2) and posterior (Channels 3-6) sections were defined. Distribution of spheres, dye solution and volume flow were compared as a percentage of total amounts per injection under standard and reduced flow and injection rates.
Results: It was observed that the distribution of microspheres and injection solution were well correlated (R^2= 0.9442, P=0.001); however, microsphere distribution did not correlate with total flow (R^2=0.0266, P=>0.05). In the horizontal orientation, microsphere distribution per channel was similar between glass and resin under all test conditions with no significant difference (P > 0.05). Although not significant (P=0.052), VFS orientation (horizontal vs. vertical) appeared to affect the distribution of BMF with higher flow favouring lower posterior channels in the vertical orientation. Importantly there was no statistical difference between the distribution of glass and resin microspheres in the vertical or horizontal orientation (P > 0.05). These results suggest that material density does not play a dominant role in microsphere distribution.
Conclusions: Distributions of radio-embolic microspheres appear to be mostly determined by vascular geometry, not the density of microspheres. No significant differences in distributions were observed between glass and resin surrogates under a variety of flow and injection rates. *References:* [1] Salem, R., Tech Vasc Interv Radiol. 2007 Mar;10(1):12-29.

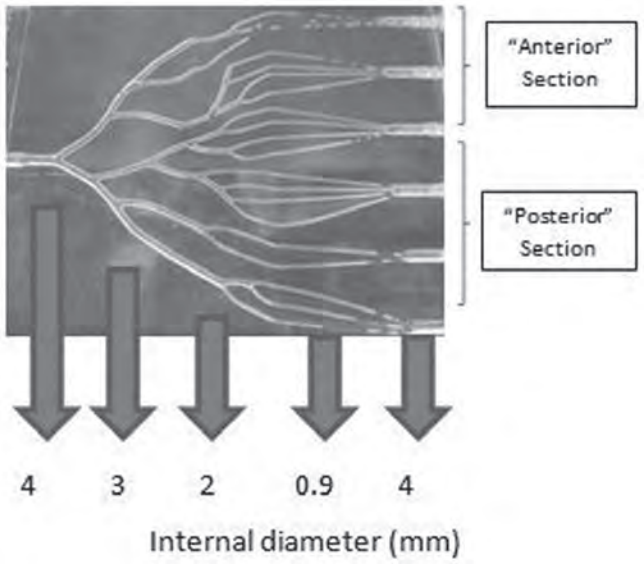

Figure 1: VFS geometry with theoretical division of anterior and posterior sections.

Poster 8: Characterization of Tissue Contraction following Microwave Ablation of Liver Lesions Using TACE Imaging as a Clinical Fiducial

C. Harari, T. Ziemlewicz, C. Brace

Objectives: Microwave (MW) tumor ablation is known to induce tissue contraction in both *ex vivo* and *in vivo* experimentation. However, a detailed quantitative analysis of clinical MW ablation contraction has not been reported. The purpose of this study was to quantitate tissue contraction due to MW ablation of hepatocellular carcinomas (HCCs) in human subjects.
Methods: Twenty-two patients with HCCs, all with cirrhosis, were treated with combination MW ablation and transarterial chemoembolization (TACE) therapy. Twelve patients received TACE immediately preceding MW ablation and 10 patients received TACE 2-4 weeks prior to MW ablation. Contrast-enhanced CT scans were obtained following both TACE and MW ablation procedures as well as just prior to 20/22 of the MW ablations. TACE samples were used because of their iodine containing ethiodol component, which served as an *in situ* fiducial in the ablation zone. All ablation procedures were preformed with a single microwave system (Certus 140 with PR antennas; NewWave Medical, Madison, WI) with one to three 17-gauge antennas. CT scans were evaluated using OsiriX 5.8.2 and measurements were made to assess tumor volume, maximum tumor diameter and CT attenuation before and after MW ablation procedures. Measurements were compared before and after ablation using matched pair t-tests.
Results: Overall, mean tumor volume was significantly smaller post-ablation when compared to pre-ablation (17.5 ± 12.8 cm^3 vs 24.1± 17.1 cm^3). Mean total contraction was therefore 27.6 ± 8.6% ($P < .001$). This value was marginally lower than contraction noted in prior *ex vivo* studies. Slightly less contraction was noted when TACE was administered 2-4 weeks in advance of MW ablation (26.9 ± 9.7%; $P < .01$) compared to immediately preceding MW ablation (29.5 ± 5.1%; $P < .05$). Similarly, maximum tumor diameter exhibited significant contraction when comparing pre- and post-ablation measurements (14.1 ± 9.6%; $P < .001$). Although the change in tumor x-ray attenuation was not significant overall, (2.0 ± 23.7%; $P = .36$), attenuation increased significantly in tumors > 4 cm post ablation (18.6 ± 12.2%).
Conclusions: Significant tissue contraction was observed immediately following MW ablation of HCC in patients with cirrhosis. In addition, an increase in CT attenuation post-ablation of larger tumors suggests consolidation of ethiodol due to contraction. Ethiodol may be a useful *in situ* fiducial to assess contraction after thermal ablation in human patients.

Poster 9: A Metastatic Hepatoma Model of Rats Using 13762-MAT-B-III Cell Line: Basic Characteristics and Potential as a Tool for Interventional Oncology Experiment

S. Hur, H. Kim, J. Chung

Objectives: To evaluate the characteristics of a 13762-MAT-B-III model in the rat liver and to assess the adequacy of the model for transarterial embolization (TAE) study.
Methods: $1x10^5$ 13762-MAT-B-III rat breast cancer cells were inoculated into the livers of 11 Fisher 344 rats. Natural course via MRI follow-up, histological characteristics, and tumor response after TAE were evaluated.
Results: The tumor induction rate of the 13762-MAT-B-III hepatoma model was 100%. Except for one tumor that started to regress after 14 days, the 13762-MAT-B-III hepatomas showed rapid growth, up to 13.1±1.4 mm, at 21 days. Peritoneal seeding was observed in all rats. TAE was conducted successfully in three rats on day 11. The TAE-treated hepatomas were significantly smaller on day 21 ($P=0.040$) and had a significantly greater apoptosis ratio ($P=0.046$).
Conclusions: The 13762-MAT-B-III hepatoma model can be useful in many interventional oncology studies by providing consistent and rapidly growing tumors.

Poster 10: Tumor Ablation Combined with Thermo-Sensitive Liposomal Doxorubicin: Effect of Treatment Time and Administration Schedule

C. Rossmann, C. Swenson, R. Reed, D. Haemmerich

Objectives: Recent studies suggest improved efficacy when combining radiofrequency ablation (RFA) with localized drug delivery by thermo-sensitive liposomal drug carriers (TSL) releasing doxorubicin (DOX) upon exposure to hyperthermic temperatures. The purpose of this study was to develop mathematical models and perform corroborating porcine studies for identification of optimal heating strategies to maximize local drug accumulation for this combination treatment strategy.
Methods: We used three dimensional computer models to simulate RFA tissue heating with a cooled needle electrode for 5 to 60 minutes, and to predict the DOX release from TSL-DOX in plasma, interstitium and cells considering temperature-dependent liposomal release. We performed three sets of porcine animal studies with a commercial TSL-DOX formulation (ThermoDox®) and a cooled RF needle electrode, where TSL-DOX was infused at a dose of 50 mg/m2 over 30 min before ablation. In a first set of animals (n=3), blood samples were obtained every 15 min, and plasma DOX concentration was quantified by LC-MS/MS. In a second set of animals (n=9), either one (n=3), three (n=3) or six (n=3) overlapping 12-min ablations were performed. In a third study, ablations were performed for 5 min (n=2) or 12 min (n=2) in one animal. In the latter two studies, liver samples were excised following ablation, frozen, thawed, and fluorescence imaging was performed in a cross section of the ablation to visualize tissue DOX concentration, and LC-MS/MS was performed on punch biopsy tissue samples.
Results: Total amount of DOX deposited within the heated tissue increased approximately linearly with ablation time for single ablations in both simulation and animal study. Increased delay between drug administration and RFA in simulations decreased amount of DOX delivered to the target site due to plasma clearance of liposomal drug carriers (59% DOX reduction for RFA 2h later administration). In both mathematical models and in vivo studies most DOX (80-95%) was delivered just outside the thermal lesion. The initial plasma half-life of ThermoDox in the porcine model was >2.25 hours. Three or six ablations delivered significantly more total DOX to the targeted tissue region compared to a single ablation.
Conclusions: DOX is primarily delivered to the margin outside the ablation zone. Increased ablation time enhances drug delivery, as predicted by computer simulations and confirmed by porcine studies. Further, multiple sequential ablations increase total amount of DOX delivered.

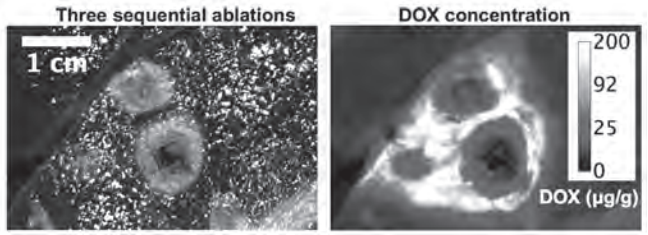

Three sequential 12-min ablations, with non-ablated tissue between gray ablated tissue (left). Fluorescence image shows delivery of high amount of DOX to insufficiently ablated tissue (right).

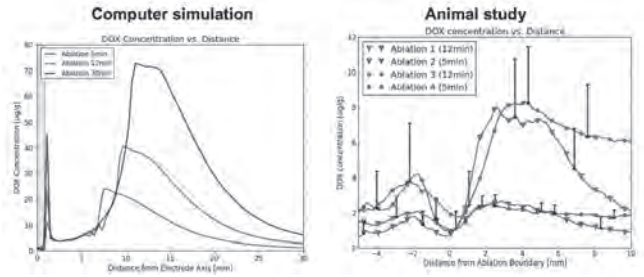

Increased ablation time enhances DOX delivery to ablation margin. Computer simulation for 5, 12 and 30 min ablations, with DOX concentration relative to distance from RF electrode (left). Porcine study confirms simulation with 5 and 12 min ablations. DOX concentration was inferred from fluorescence images, and is shown relative to visible ablation boundary (right).

Poster 11: Radioembolization Experience in the VX2 Rabbit Model: Radiation Safety, Angiography, and Factors Influencing Delivery Efficiency

A.C. Gordon, V.L. Gates, S.B. White, K.R. Harris, D. Procissi, J. Nicolai, S.K. Mouli, K.T. Sato, R.R. Ryu, R.A. Omary, R. Salem, R.R. Lewandowski, A.C. Larson

Objectives: Yttrium-90 radioembolization is increasingly utilized for the benefit of patients with hepatic malignancy; however, there are barriers to entry with few existing preclinical centers, resulting in lack of basic science reports to evaluate newly emerging concepts and therapeutic approaches in the field. The objective of this study is to describe our experience with radiation safety practices, angiographic considerations, and factors for improved microsphere delivery efficiency in the VX2 rabbit model.

Methods: Studies were approved and performed in accordance with the institutional animal care and use committee and office for research safety. Twenty-nine White New Zealand rabbits underwent ultrasound-guided implantation to create ≥ 2 VX2 tumor sites in the liver. Tumors were allowed to reach 1-2 cm confirmed with magnetic resonance imaging (MRI) prior to hepatic arterial angiography. Whole-liver radioembolization was performed with glass ^{90}Y microspheres using calibrated dose vial activities of 1, 3, or 5 GBq over a period of five quarters (Q1-5). The total exposure time, fluoroscopy time, digital subtraction angiography time, and effective dose (mSv) were recorded for each research animal. Residual activity, infusion time, infusion volume, and highest animal surface reading (mrem/hr) were measured following radioembolization.

Results: Tumor growth was confirmed on MRI in 100% of implanted rabbits (n=29). Over the study period, the average fluoroscopy time per procedure decreased from 13.1 to 4.6 minutes (Q1->Q5). Residual activity could not be accurately assessed in four cases that were excluded due to dose vial > 30 days post-calibration on the treatment day (activities <0.05 mCi). For the remaining cases (n=25), median residual activity was 22.8%. Deviations from the manufacturer's recommended infusion rate and volume for patients were often necessary due to the smaller VX2 rabbit anatomy. Decreasing dose vial size (R^2=0.1876, P=0.0306), higher infusion rates (R^2=0.1889, P=0.0299), and higher infusion volumes (R^2=0.2055, P=0.0229) were significantly correlated with increased delivery efficiency. The mean administered activity was 0.97 mCi (95% confidence interval, 0.58-1.36 mCi). The median surface reading over the right costal margin was 10 mR/hr (mean 49.0 ± 78.8 mR/hr).

Conclusions: ^{90}Y radioembolization can be safely performed in this model with short fluoroscopy times. Our optimal infusion volume and rate were in agreement with those recommendations provided in the manufacturer's package insert, suggesting these values are primarily determined by the delivery system and not the vascular bed, to which the microspheres are being infused. These approaches should permit preclinical studies to improve radioembolization.

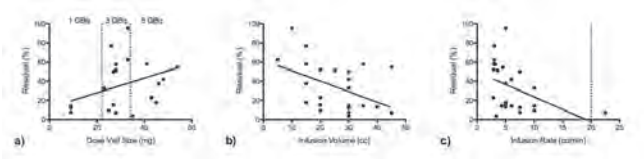

Figure 1. Residual activity as a function of **a)** dose vial size (mg), **b)** infusion volume (cc), and **c)** infusion rate (cc/min). Based on these results, optimal infusion volumes and rates exceed 56cc and 19cc/min, respectively. Delivery efficiency is also improved through the use of a smaller number of microspheres and dose vials calibrated to 1GBq may be ideal.

Poster 12: Development of a Successful and Sustainable Percutaneous Renal Mass Ablation Program in a Community Hospital Setting

A. Baadh, S. Mittal, D. Phung, A. Fadl, J.C. Hoffmann

Objectives: To describe the development of a community hospital renal tumor ablation program that is sustainable and results in excellent outcomes.

Methods: Image-guided ablation is an excellent treatment option for patients with small renal masses. However, it can be challenging to find appropriate treatment candidates, especially when not in a large academic medical center. Many physicians understand that a consistent presence at multidisciplinary tumor board is essential. However, this exhibit will provide additional details about creating a successful percutanous ablation program in a community hospital setting.

Results: Developing a renal ablation program involves multiple steps. A strong presence at multidisciplinary tumor board is essential to building the tumor ablation program. This includes interaction and discussion with diagnostic radiologists, urologists, and oncologists. Since starting a renal ablation program in September 2011, a total of 79 patients have been referred for renal mass ablation. All patients were seen in interventional radiology (IR) clinic for evaluation. Communication was maintained with referring physicians after initial clinic visit, ablation procedure, and post-procedure imaging. Of the 79 patients with renal masses evaluated in IR clinic, 71 were treated with image-guided percutaneous ablation. All procedures were performed with CT guidance. Sixty-nine were performed with moderate sedation. Two were performed with general anesthesia. Of the 71 cases, 70 were performed with cryoablation and one was performed with microwave ablation. One patient required angiography and embolization due to prolonged hematuria. No other major complications occurred. All patients are followed with contrast-enhanced cross-sectional imaging at 3, 6, 9, 12, 18, and 24 months, then annually. Long-term outcomes are presented at multidisciplinary conference. As of November 2014, no patients have evidence of recurrent or residual tumor.

Conclusions: Developing a small renal mass image-guided percutaneous ablation program at a community hospital can be done successfully, providing excellent outcomes and good quality of life for patients.

Poster 13: PERCUTANEOUS RENAL CRYOABLATION PROVIDES LONG-TERM TUMOR CONTROL

T.J. Hanson, A.J. Weisbrod, A.N. Kurup, G.D. Schmit, M.R. Callstrom, C.M. Lohse, S.A. Boorjian, R.H. Thompson, G.K. Chow, B.C. Leibovich, T.D. Atwell

Objectives: To determine the efficacy of percutaneous renal cryoablation in achieving long-term tumor control.

Methods: With IRB-approval, we reviewed our prospectively maintained renal ablation registry to include patients treated with percutaneous renal cryoablation from 2003-2011 and their data was updated through January 2014. This included 429 tumors treated during 375 procedures among 354 patients. Tumor characteristics, local tumor control, and patient survival were assessed.

Results: Mean tumor size was 3.2 cm (1.1-9.7). 239 (56%) tumors were centrally located. Of the 347 biopsies performed, RCC was confirmed in 220 (63%). Among the 391 tumors followed for at least 3 months, estimated recurrence-free survival rates (number still at risk) at 1, 3, 5, and 7 years following cryoablation were 99.2% (333), 97.4% (165), 95.6% (59), and 92.9% (14), respectively. Neither tumor size nor location were associated with time to tumor recurrence. Among the 220 biopsy-proven RCCs, 199 were followed for at least 3 months. Estimated recurrence-free survival rates (number still at risk) at 1, 3, 5, and 7 years following cryoablation for these tumors were 98.9% (165), 97.0% (78), 93.1% (29), and 88.0% (7), respectively. Estimated cancer-specific survival rates for those patients with sporadic RCC (number still at risk) at 1, 3, 5, and 7 years following cryoablation were 100% (119), 99% (66), 99% (28), and 99% (9), respectively.

Conclusions: Percutaneous cryoablation provides durable, long-term oncologic control of renal masses.

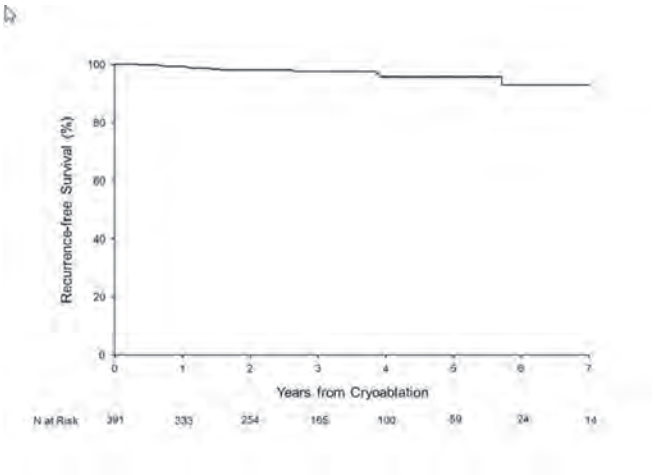

Figure 1. Kaplan-Meier curve showing local recurrence free survival for 391 tumors treated with cryoablation.

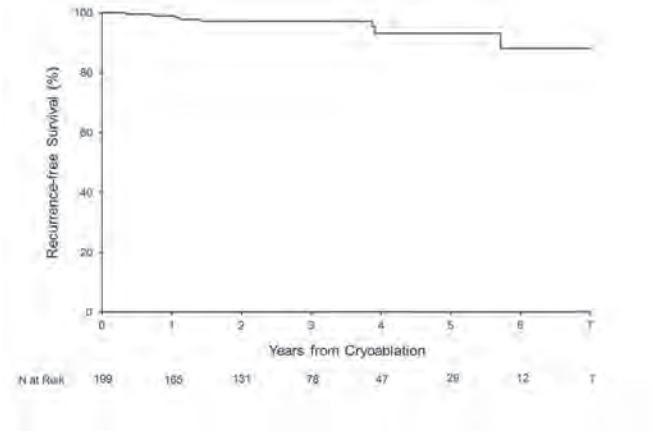

Figure 2. Kaplan-Meier curve showing local recurrence free survival for 199 renal cell carcinomas treated with cryoablation

Poster 14: Safety and Efficacy of Renal Cryoablation for Small Renal Masses: Midterm Follow-up

J.J. Zechlinski, K. Cicuto, S. Dybul, E. Hohenwalter, W. Rilling, P. Langenstroer, S. Tutton

Objectives: Small, incidental renal masses identified on advanced imaging require a thoughtful treatment strategy which preserves renal function and minimizes procedural morbidity. We report our multi-disciplinary experience with percutaneous renal cryoablation, an expanding, minimally invasive treatment modality.
Methods: We performed a retrospective review of patients undergoing percutaneous cryoablation for renal tumors from 2006-2012, excluding those having follow-up at outside institutions. Patient and tumor characteristics, cryoablation technique, complications, renal function, and pattern of recurrence were evaluated. IRB approval was obtained.
Results: One hundred thirty-nine ablations were performed on 126 patients. Mean patient age was 67 years (range 36-88). Mean tumor size was 2.3 cm (range 0.8-6.8), treated on average with 2.3 probes (range 1-6) with a technical success rate of 97.8%. There were 13 major complications (9%), including perinephric hemorrhage (5), hematuria with clot retention (3), acute kidney injury and/or dehydration (2), persistent arrhythmia (1), nerve injury (1), and post-operative pain (1). No renal collecting system injuries were observed. Retrograde pyeloperfusion was used in 4 cases to avoid such injury. There was no significant decline in renal function 3 months after ablation (P=0.86). Among 116 patients with clinical T1 disease, mean follow-up was 32.9 months with 20% of the cohort having follow-up beyond 5 years. Local recurrence was observed in 10 patients (9%), in all but one patient initially treated with repeat ablation. Early local recurrence was typically observed within 3 months of ablation, and felt to be due to inadequate margins. Delayed, local recurrence was variable, in 3 patients occurring greater than 3 years after ablation and underscoring the need for long-term radiologic follow-up. One patient required a total of 3 percutaneous cryoablations over a 5 year period, and a second patient underwent 2 percutaneous cryoablations followed eventually by laparoscopic cryoablation over an 18 month period for localized disease. One patient developed delayed local recurrence and lung metastases (occurring 32.9 months and 36.8 months after ablation, respectively), and did not undergo additional therapy due to worsening medical comorbidities, dying 5 years after initial ablation. No other patients developed metastatic disease. Seven patients (6%) died of unrelated causes.
Conclusions: Percutaneous cryoablation is a safe and effective option for the management of small renal tumors, with a low complication rate, preservation of renal function, and infrequent local recurrence. Early recurrence appears to be due to inadequate ablation margins.

Poster 15: A New Angiographic Imaging Platform Reduces Radiation Exposure for Uterine Fibroid Embolization

R. Schernthaner, S. Nguyen, R. Duran, J. Sohn, S. Sahu, J. Chapiro, Y. Zhao, J. Geschwind, K. Hong, M. Lin

Objectives: Uterine fibroid embolization (UFE) is a nonsurgical treatment option for premenopausal women with bothersome fibroid-related symptoms such as abnormal uterine bleeding or bulk-related symptoms. Because most of the women undergoing UFE are at child-bearing age, the exposition of women's genital system to radiation during UFE should be as low as reasonable achievable. The purpose of this study was to quantify the radiation exposure reduction of a new C-arm imaging platform for women with symptomatic uterine fibroids being treated using UFE.
Methods: This was a prospective, HIPAA compliant and IRB approved two-arm trial. 40 consecutive women (mean age 46 years, range 32-59 years) with symptomatic uterine fibroids who were treated using UFE either on the new C-arm imaging platform (n=25; AlluraClarity, Philips Healthcare, Best, the Netherlands) or on a standard C-arm imaging platform (n= 15; Allura, Philips Healthcare). The new system includes optimized acquisition parameters and real-time processing algorithms such as noise reduction, motion compensation and automatic pixel shift. Air Kerma (AK), dose area product (DAP) and acquisition time for digital fluoroscopy (DF) and digital subtraction angiography (DSA) were recorded. Body mass index (BMI) was also noted. The unpaired *t*-test and Wilcoxon rank-sum test were used to assess statistical differences between the platforms.
Results: There was no difference in BMI between the two patient cohorts (mean 31.8±7.8 vs. 34.6±5.7 on new and standard platforms, respectively; P=0.20). Additionally, there was no significant difference in DF or DSA time for new and standard platforms, respectively (mean DF 27.5±7.9 vs. 27.5±7.4 minutes, p=0.99, and mean DSA 70.1±22.1 vs. 66.6±20.9 seconds, P=0.62), indicating that the course of the procedure were similar between the two cohorts. Compared to the standard platform, the new platform significantly reduced the cumulative AK and DAP by 67% and 72%, respectively (median 0.53 Gy and 148.9 Gy*cm^2 vs. 1.62 Gy and 524.8 Gy*cm^2, respectively, P<0.001 for both). Specifically, DAP for DF and DSA decreased by 57% (median 77.8 vs. 179.1 Gy*cm^2, P=0.006) and 81% (median 61.6 vs. 326.5 Gy*cm^2, P<0.001), respectively.
Conclusions: The new imaging platform maintained similar procedure time while significantly reducing radiation exposure for women with symptomatic uterine fibroids being treated using UFE.

Poster 16: Percutaneous Microwave Ablation of T1a and T1b Renal Cell Carcinoma: Single Center, Single Operator Evaluation of Safety and Early Clinical Efficacy

S.A. Wells, A. Mithqal, K.M. Wheeler, J. Davilla-Aponte, M.S. Patel, N.S. Schenkmen

Objectives: To evaluate the safety and primary effectiveness of a high-powered, gas-cooled microwave ablation system for percutaneous treatment of biopsy-proven T1 renal cell carcinoma.
Methods: Between 2/2013 and 6/2014, 34 biopsy-proven renal cell carcinomas were treated in 33 patients using a high-powered, gas-cooled microwave ablation system (NeuWave Medical, Madison, WI) with US or CT-guidance at an academic medical center by a single radiologist. Mean patient age and BMI were 66.4 years (range: 46 - 87) and 30.7 (range: 20.5 - 42.8). Mean renal nephrometry score was 7 p=27, a=6, x=1 (range: 4 – 10). Preprocedure core biopsy was performed for all patients; histologic subtypes included clear cell (n=19), papillary (n=11), chromophobe (n=2) and carcinoma not otherwise specified (n=1). Of tumors graded, Fuhrman grades 1 (n=5), 2 (n=6), 3 (n=1) and 4 (n=1). Of papillary tumors subtyped, Type 1 (n=3) and Type 2 (n=1). Each patient underwent a single treatment session. Serial post-procedure imaging was performed with enhanced CT or MRI at 6-month intervals.
Results: Mean tumor diameter was 3.2 cm (range: 1.7 – 6.3); T1a (28/34) was 2.9 cm (range: 1.7-4.0) and T1b (6/34) was 5.1 cm (range: 4.1-6.3). A mean of 2.0 antennas (T1a: 1.9; T1b: 2.8) for a mean duration of 5.5 minutes (T1a: 4.7; T1b: 9.0) at a mean generator power of 58.8 W (T1a: 59.5; T1b: 54.9) was applied. Technical success (no residual tumor on immediate post-ablation CT) was achieved for all tumors. Two grade 1 complications (cystitis); two grade 2 complications (pneumonia, urinoma) were documented by Clavien-Dindo classification. There was no clinically or statistically significant change (P=0.07) in creatinine pre- (1.1 mg/dl) and post-ablation (1.2

mg/dl). Median length of hospitalization was 1 day. All patients are currently alive and without evidence of metastatic (renal cell carcinoma-specific survival of 100%). Thirty-four patients have had follow-up imaging at a mean and median of 7.25 months and 6 months post ablation, respectively (IQR: 6.0 – 12.0) with local progression [primary failure] in one case conferring an overall primary treatment effectiveness of 97%.
Conclusions: This single center, single operator study using percutaneous microwave ablation for the treatment of T1 renal cell carcinoma demonstrates that the procedure is both safe and effective at short-term follow-up. Continued follow-up and further investigation is warranted to document long-term oncologic outcomes relative to existing treatment strategies.

Poster 17: Transcatheter Arterial Embolization with Closed Renal Circuit for Huge Renal Cell Cancers

S. Onozawa, S. Murata, T. Ueda, F. Sugihara, D. Yasui, I. Miki, Y. Kondo, S. Kumita

Objectives: Purpose of this study was to evaluate the safety of transcatheter arterial embolization (TAE) with closed renal circuit (TAE-CRC), for the management of large renal cell carcinomas (RCCs).
Methods: The subjects were 33 patients with RCC who underwent a total of 35 sessions of TAE-ABOD. This TAE-CRC technique as follows: balloon occlusion of renal drainage vein and infusion of absolute ethanol into the tumor-feeding arteries during aspiration of blood via a balloon catheter to reduce leakage of ethanol into the systemic circulation. The endpoint of this study was to establish a safe regimen for high-dose ethanol injection therapy.
Results: The administered dose of ethanol ranged from 0.2 to 0.5 ml/kg [median: 0.34 (SD: 0.10) ml/kg], increased in a stepwise manner. The systemic ethanol concentration was measurable in 14 patients, and was less than 0.1 mg/ml in 12 and from 0.1 to less than 0.2 mg/ml in two. There were no major complications such as renal failure or renal abscess.
Conclusions: TAE-CRC can safely deliver a high dose of absolute ethanol for the treatment of large RCCs.

Poster 18: An Anti-Reflux Catheter as a Pressure-Directed Delivery Device: A Computational Model and Empirical Results

E.D. Durham, D.B. Jaroch, K.S. Hunter

Objectives: Tumor vasculature is typically tortuous, hypertensive and dense, resulting in heterogeneous resistivity to blood flow [1, 2, 3]. As a result, full penetration of such tumors, like hepatocellular carcinomas [4], using embolic agents and chemotherapeutics is challenging in conventional procedures that rely on blood flow alone to deliver agents. Unlike standard end-hole catheters, an anti-reflux catheter can locally increase vascular pressure, thereby increasing delivery efficiency and penetration depth. This study aims to: 1) explore the mechanism by which an anti-reflux catheter achieves elevated distal pressure in an artificial hydraulic cardiovascular model, and 2) computationally model the fluid dynamics of catheter interactions in a two-element Windkessel circuit.
Methods: An anti-reflux catheter demonstrates valve-like behavior by impeding reverse flow and minimally resisting forward flow. Infusion using such catheters allows for localized pressurization of compliant target vasculature. A physical hydraulic circuit representing physiological vasculature was utilized to empirically investigate the ability of an anti-reflux catheter to selectively pressurize distal vasculature and verify computational model predictions. The Windkessel model provides a mathematical analogue of the behavior of the system in vivo (Figure 1).
Results: Experimental Data: Standard end-hole catheters demonstrate an initial pressure drop associated with flow restriction due to the catheter profile (Fig. 2d). During infusion, the end-hole catheter demonstrates minimal ability to generate distal pressure empirically. The anti-reflux catheter also exhibits an initial pressure drop when deployed in simulated vasculature (Fig. 2b). By varying the rate of infusion, vasculature distal to the anti-reflux catheter tip could be selectively pressurized above systemic values. Computational Model: As demonstrated in the empirical model, the simulation shows that the anti-reflux catheter causes an initial drop in distal pressure when the tip is expanded (Fig. 2a). Modeled infusion demonstrates selective pressurization dependent on infusion rate and correlates closely with experimental results.
Conclusions: Anti-reflux catheters are able to selectively pressurize distal vasculature, offering a mechanism for delivery of therapeutic agents to aberrant tumor vasculature. When conventional flow-directed delivery methods cease to be effective in penetrating tumors deep enough to cause widespread tumor necrosis, pressure-directed therapy is a favorable alternative. Pressurized delivery increases tumor penetration depth and dosage delivered [5].

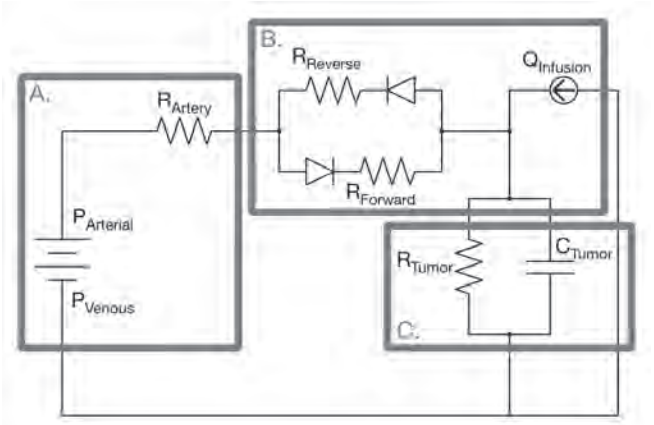

Figure 1: The 2-element Windkessel model consists of three main components: A) the pressures generated by the heart at the tumor site, B) the anti-reflux catheter, and C) the compliant tumor vasculature.

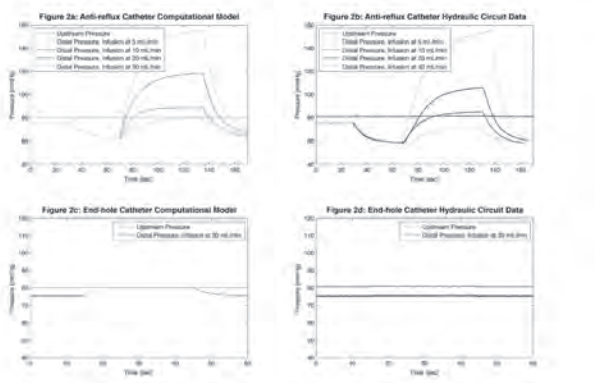

Figure 2: Comparison of hydraulic circuit data and predictive computational model.

Poster 19: Evaluation of a Quantitative 3D Navigation System for Small Lesion Biopsy in Phantom

W. Moore, P. Bhattacharji

Objectives: The purpose of this study is to evaluate the performance of a quantitative 3D navigation system for CT-guided biopsy of small lesions using phantoms.
Methods: One abdominal/pelvic phantom and one thoracic phantom, each with 6 small lesions, were used in this study. An interventional radiologist performed biopsy needle placement on each lesion under the guidance of a quantitative 3D navigation system (IQQA-Guide, EDDA Technology). First, the phantoms were CT pre-scanned to obtain fully quantified 3D anatomies by using the navigation system. Then, the physician placed sensors on phantom surface and re-CT scanned it per the CT-guided biopsy procedure. The 3D anatomies of the phantom were aligned with this CT scan by the system via deformable registration and used as a quantitative anatomy map for 3D navigation. The physician set target at lesion center and planned a needle path in 3D. When inserting needle, the physician followed the real-time 3D navigational information generated by the system, including 3D displays of the planned path and needle position/movement in the 3D anatomy map, distance to the target, hint if the needle would hit the target. Both one-pass and two-pass needle placement were performed for each nodule. Lastly, a confirmation CT scan was performed when the system indicated the target was hit. Accuracies of the 3D anatomy map registration and navigation were evaluated. Time used for the navigated procedures were recorded.
Results: The average lesion diameter in the phantoms was 13.9mm and the average distance of the lesions to surface along the planned paths was 66.9mm. Across all the procedures, the average 3D anatomy map registration error was 1.79mm. The mean needle placement accuracy was 2.87mm for one-pass and 2.65mm for two-pass. The average time of navigated needle placement was 9'21" for one-pass and 12'28" for two-pass. This was no significant difference among the thoracic and abdominal/pelvic phantom results.
Conclusions: The results suggest that the quantitative 3D navigation system could potentially facilitate physicians to perform accurate needle placement and reduce procedure time in small lesion biopsy.

Poster 20: Application of Real-Time 3D Navigation in CT-Guided Percutaneous Interventional Procedures – A Feasibility Study

W. Moore, P. Bhattacharji

Objectives: This study aims to assess the feasibility of incorporating an electromagnetic 3D navigation system in CT-guided interventional procedures under the existing workflow.
Methods: In this IRB approved study, patients scheduled for CT-guided thoracic and hepatic biopsy and ablations were recruited. The quantitative 3D navigation system (IQQA-Guide, EDDA Technology, Inc.) contains an electromagnetic tracking system and provides real-time quantitative 3D navigation information, including the tracked instrument position in a fully-quantified 3D patient-specific anatomy map generated from pre-procedural CT, and its spatial relation to target. Interventional radiologists performed CT-guided procedures as they routinely do, without following the 3D navigation display. The navigation system took as input the intra-operative CT images, and continuously tracked the needle position relative to the 3D anatomy map and the latest intra-operative CT scans. Accuracy of the system was evaluated as the distance between the final needle position on the confirmation CT scan and the needle position predicted by the navigation system. Workflow fitness of the system was also evaluated by the interventional radiologists.
Results: From Jan 2014 to August, 12 patients (9 females, 3 males, average age 57) enrolled under the IRB and underwent 13 procedures (7 lung biopsies, 2 lung cryo ablations, and 4 liver biopsies). The average diameter of targets was 12.2mm, with a mean distance from skin of 61.2±23.0mm. 18GA of biopsy needles were used for lung biopsy, 16GA for liver biopsy, and 13GA for lung ablations. Accuracy of the 3D navigation system in this passive study was 4.08±2.35mm. 9 of the 13 procedures (70%) had accuracy smaller than 5mm. Average time of the system setup was 3 min, and the system fit the existing workflow of CT-guided interventions with minimum impact.
Conclusions: The results suggest that navigation for interventional procedures using the quantitative 3D navigation system could be performed along the existing clinical workflow. The 3D navigation system has the potential to navigate precision needle placement and help reduce time in complicated procedures.

Poster 21: Liver Injury after Ablative Techniques: A Comparison of Changes in Liver Function Tests

D. Yang

Objectives: Percutaneous ablative techniques such as radiofrequency ablation (RFA) and irreversible electroporation (IRE) target malignant liver lesions with the intent of destroying tumor cells and minimizing adverse effects to adjacent normal tissue. Liver function tests (LFTs) have been used to assess the degree of liver insult after a variety of treatments to include medication, trans-arterial embolization as well as RFA. The literature comparing the quantitative effects of ablative techniques on liver function tests is largely lacking. It is the intent of this retrospective review to compare changes in LFTs before and after treatment with RFA and IRE.
Methods: A database containing the laboratory results of patients treated with percutaneous ablative techniques for primary and metastatic hepatic tumors was queried. The LFTs (AST and ALT) of 161 patients treated with RFA (n=58) and IRE (n=103) were restrospectively reviewed. The pretreatment values were within 30 days of the procedure and the posttreatment values were all obtained the day after treatment. The mean of the difference between the prereatment and post-treatment LFTs were compared in the two groups using independent t-test with SPSS software. Exclusion criteria included patients with prior percutaneous ablations or trans-arterial hepatic embolizations.
Results: Preliminary results demonstrate a statistically significant higher increase of AST after IRE ablation versus RFA ablation. The mean AST change in patients treated with IRE was an increase of 581 U/L and in patients treated with RFA 197 U/L. Similar findings were seen with changes in ALT when compared between the two groups.
Conclusions: IRE is a nonthermal ablative technique which has been shown to be less injurious to nontarget tissue when compared to thermal ablations like RFA. The greater increase in the LFTs after treatment with IRE when compared to the RFA seems inconsistent with these prior findings. Correlation with the volume of tumor treated in the two gropus as well as long term follow-up in future studies are needed to further assess the significance of the changes in LFTs seen in this study.

Poster 22: Real-time Shear Wave Elastography on the Evaluation of Radiofrequence Ablation for Liver Tumours: A Clinical Study

X. Xie

Objectives: To evaluate the elasticity change of liver tumour before and after radiofrequency ablation (RFA) and the capacity of estimating ablation extent using real-time Shear Wave Elastography (SWE).
Methods: **Methods** A total number of 57 patients (male 38female 19mean age 52.2 yearsrange 21.0 – 79.0 years) with 57 lesions (mean diameter 2.4 cmrange 1.0 – 5.4 cm)including 32 hepatocellular carcinomas4 intrahepatic cholangiocarcinomas20 metastasis liver cancer1 sarcoma underwent SWE examination before30 min after1 day after and 1 month after ablation. The maxminmean and standard deviation SWE values were measured. The colour scale was 0 – 70 kPa. The parameters at different time were compared. All parameters were expressed as kPa. The ablation zones treated with Cool-tip radiofrequency system and duration 12 min were chosen (n=12). The long and short diameters of ablation zone were measured on baseline ultrasound and SWE images. The volume was calculated according to equation V=ðXYZ/6 (V volumeX long diameterY=Z short diameter). The non-enhanced extent on CEUS at the same day was used as reference.
Results: **Results** 1The extent of ablation zone was clearly showed on SWE image. 2The max (121.80 ± 68.52)min (30.36 ± 24.96)mean (66.92 ± 24.88)and SD (20.37 ± 12.97) SWE values of 30 min after1 day after (108.20 ± 46.9931.87 ± 18.0867.12 ± 23.5319.41 ± 12.05) and 1 month after (130.40 ± 53.6832.00 ± 22.0686.88 ± 45.1835.05 ± 25.50) were higher than whose of before RFA (50.85 ± 30.6115.30 ± 8.7830.50 ± 11.567.37 ± 4.26) (P<0.001)respectively. 3No significant difference was found among elasticity parameters of 30 min1 day and 1 month after RFA. 4The long diameter (3.0 ± 0.6 cm) of ablation zone on SWE was similar with which on baseline ultrasound (2.9 ± 0.5 cm) but less than CEUS (3.4 ± 0.4 cm) (P<0.01). The short diameter (2.3 ± 0.4 cm) and volume [(9.2 ± 4.7) cm^3] of ablation zone on SWE were not significantly different compared to those on baseline ultrasound [2.4 ± 0.5 cm(9.3 ± 5.0) cm^3] and contrast enhanced ultrasound [2.2 ± 0.6 cm(9.6 ± 6.0) cm^3].
Conclusions: **Conclusions** SWE could quantitively analyze the elasticity change before and after ablation. The ablation zone became stiffer after RFAbut no changes over time. The SWE could clearly show the boundary of ablation zonebut still have a discrepancy with the actual necrosis extent.

Poster 23: Cone Beam CT with Fluoroscopic Overlay versus Conventional CT Guidance for Percutaneous Osteoid Osteoma RFA

T.J. McKay, B.C. Perry, G. Shivaram

Objectives: To compare technical success, radiation dose, and total room utilization time for osteoid osteoma radiofrequency ablation (RFA) using fluoroscopic/cone-beam CT (CBCT) with 2-axis needle guidance versus conventional CT guidance.
Methods: In this retrospective study, 11 patients who underwent fluoroscopic/CBCT guided intraosseous probe placement for osteoid osteoma RFA were compared to 11 patients undergoing probe placement via conventional CT guidance over a 2 year period. CBCT cases were performed on a Philips angiography system using Xper Guide navigation (Philips, Eindhoven, Netherlands). After a non-contrast cone-beam CT was performed, a needle trajectory for ablation was planned on a separate workstation. Needle placement was done using fluoroscopic guidance with overlay on cone-beam CT images. Orthogonal views, along the needle axis and perpendicular to the needle, were used to advance the needle into the target. Conventional CT guided procedures were performed on a 64-slice CT (Lightspeed, GE Medical Systems, Milwaukee WI), without the use of CT-fluoroscopy. Dose area product (DAP) and dose length product (DLP) were recorded for Xper Guide and conventional CT respectively and were converted to effective doses using conversion factors from the literature to allow for direct dose comparison. Technical success, radiation dose, and total room utilization time were compared between the two groups.
Results: Average tumor size was similar in the two groups. For the 11 cases performed under fluoroscopic/CBCT guidance, 8 tumors were located in the femur and 3 in the tibia. In the 11 conventional CT cases, 4 tumors were located in the femur, 4 in the tibia, and 1 each in the acetabulum, talus, and great toe. All procedures in the study were technically successful by imaging criteria and initial clinical response to ablation. 2 of the 11 conventional CT ablation patients re-presented with pain and subsequently underwent fluoroscopic/CBCT guided ablation procedures. Effective radiation doses were significantly lower with fluoroscopic/CBCT guidance compared to CT guidance (1.96 vs 9.30 mSv, P = $7.1*10^{-6}$). Total room utilization times for fluoroscopic/CBCT were longer than for conventional CT (143 vs. 108 minutes).
Conclusions: Fluoroscopic/cone beam CT guidance of percutaneous osteoid osteoma ablation yields similar technical success with significantly reduced radiation dose compared to conventional CT guidance.

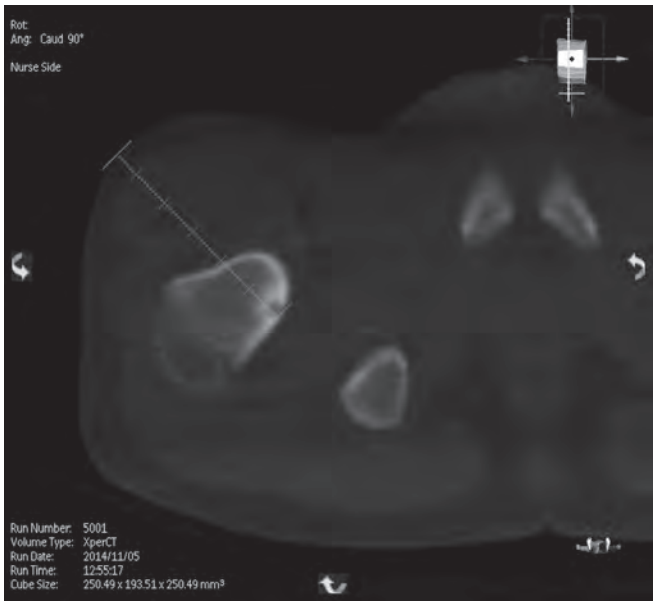

Planning of RFA probe trajectory based on initial CBCT.

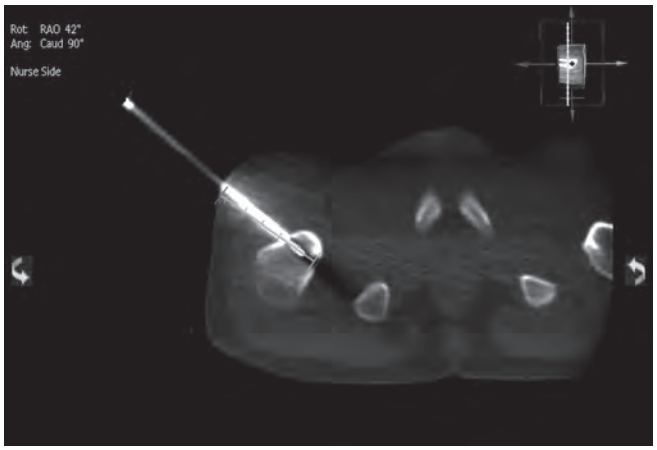

Using alternating perpendicular and along the needle views, the RFA probe is advanced into the target leison.

Poster 24: C-Arm CT During Radioembolization Requires a Specialized Protocol: Optimization for Extrahepatic Shunting and Parenchymal Enhancement

J. Prince, A. van den Hoven, S. Slijderink, B. de Keizer, E. Vonken, R. Bruijnen, H. Verkooijen, M. Lam, M. van den Bosch

Objectives: C-arm CT imaging before radioembolization can prevent repeat procedures, but reported acquisition protocols differ and none allow simultaneous vascular, extrahepatic, and parenchymal enhancement. Enhancement of extrahepatic tissue contraindicates treatment. Lack of enhancement of targeted segments indicates suboptimal treatment. In both cases, adjustments to the catheter position can be made before Tc-99m-MAA injection and SPECT/CT acquisition. Our objective was to optimize the C-arm CT protocol for radioembolization, specifically for extrahepatic shunting and parenchymal enhancement.
Methods: An initial protocol was based on a literature review and was applied in all consecutive patients undergoing a pretreatment angiography and C-arm CT (Allura Xper FD20, Philips). The injection speed was determined by maximizing the power injection on DSA without causing contrast reflux. Contrast (Visipaque 270, GE Healthcare) was diluted 1:1 with a NaCl solution to prevent streak artefacts. Image quality and diagnostic accuracy were reviewed before each of three protocol adjustments. In total, 28 patients were included with unresectable and chemorefractory liver-dominant malignancies. Two raters retrospectively evaluated anonymized scans for extrahepatic deposition, parenchymal enhancement and motion artefacts. A third rater assessed the subsequent SPECT/CT after Tc-99m-MAA injection which was used as reference standard.
Results: The first protocol was applied in 5 patients (n=5) and used a scan time of 10 seconds after a delay of 6 seconds. Parenchymal enhancement was deemed insufficient and in the second protocol (n=10), the delay increased by timing the liver enhancement on DSA (median 8 s, range 4-10 s). More motion artefacts were seen (27% of scans vs. 0%). A third protocol with a scan time of 5 seconds (n=7) reduced these artefacts, but also the subjective image quality. After reverting to the second protocol, another 7 patients were scanned. Retrospective analyses showed that discrimination between perfused and non-perfused liver parenchyma was highest in the second protocol compared with the first and third (86% vs. 60% and 73%). Of 21 patients who did not show extrahepatic shunting on C-arm CT, one showed shunting on Tc-99m-MA SPECT/CT near the implanted coils (NPV 95%). Out of the 7 patients who showed non-perfused target liver parenchyma on C-arm CT, 5 were confirmed on Tc-99m-MA SPECT/CT (PPV 71%).
Conclusions: Radioembolization benefits from a custom C-arm CT protocol for detection of extrahepatic deposition and optimal parenchymal enhancement. Shunting to extrahepatic tissue is predicted accurately, however, coil-embolization of the gastroduodenal artery may limit diagnostic accuracy.

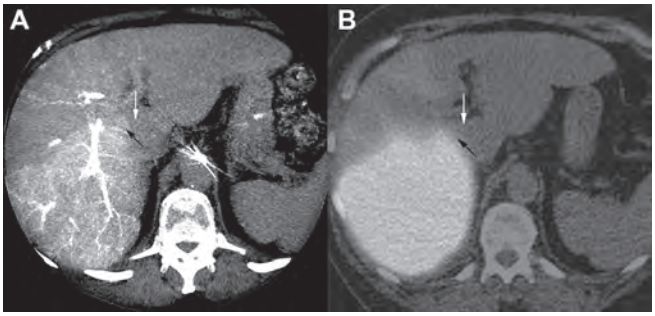

C-arm made after contrast injection in the right hepatic artery (A). Parenchymal enhancement corresponds with the subsequent SPECT/CT after Tc-99m-MAA injection (B). The black arrow indicates enhancement, whereas the white arrow shows the lack thereof in segment I.

Poster 25: A Novel Vascular Flow Simulator for Evaluation of Embolic Agent Administration

M. Caine, X. Zhang, M. Hill, P. Garcia, S.L. Willis, T. Chung, A.L. Lewis, M.R. Dreher, T. de Baere

Objectives: To develop a vascular flow simulator (VFS) that is a useful tool for both evaluating flow characteristics of particulate and liquid embolic agents through a vascular phantom network and for training of Interventional Radiologists (IR) on handling and administration of different product formulations.
Methods: The VFS is a compact self-contained unit consisting of a fluid recirculating system that feeds flow through a transparent silicone vascular phantom that is directly visualized by the operator (Figure 1). The vascular network bifurcates into 6 vascular subunits consisting of a 20 total 1 mm diameter model blood vessel. Each vascular subunit converges into one outlet channel which can be set to full flow or pass through a fine filter by operation of a dial. The fine filters act as separate embolizable "organs" that become occluded with the embolic agent resulting in concurrent flow changes in the vascular subunit. Catheterization is via a hemostatic valve at the inlet and allows for proximal or selective catheterization of the 2nd and 3rd order branches of the vascular phantom. The VFS allows the physician to explore such parameters as the effect of catheter tip placement, blood flow rate and injection rate, embolic concentration and embolic type. Coloured dye may be used as a mock iodinated contrast agent. The viewing window allows the physician to observe first-hand the effects of embolization on the flow in the targeted subunit as well as reflux and non-target embolization by direct visualization of the embolic agent and model blood flow.
Results: Both Lipiodol and microspherical embolics were evaluated on the VFS and digitally recorded. This was compared to fluoroscopic recordings of the same formulations delivered in a healthy swine liver embolization model. There was an excellent correlation between the observed flow dynamics of the embolic formulations in the VFS (Figure 2(a)) and that captured on fluoroscopy (Figure 2(b)) for lipiodol and microspherical embolics.
Conclusions: The VFS provides the IR with a tool to observe directly the effects of administration technique and formulation variation on the flow behaviour of embolic agents predictive of the in vivo situation.

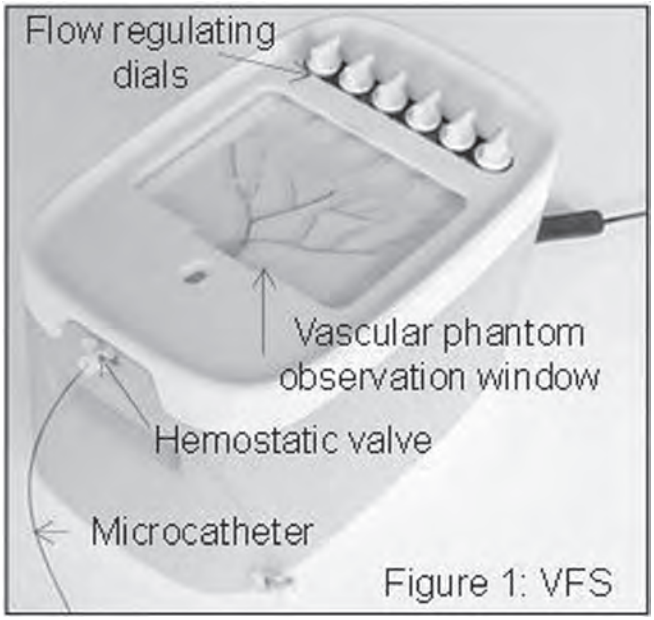

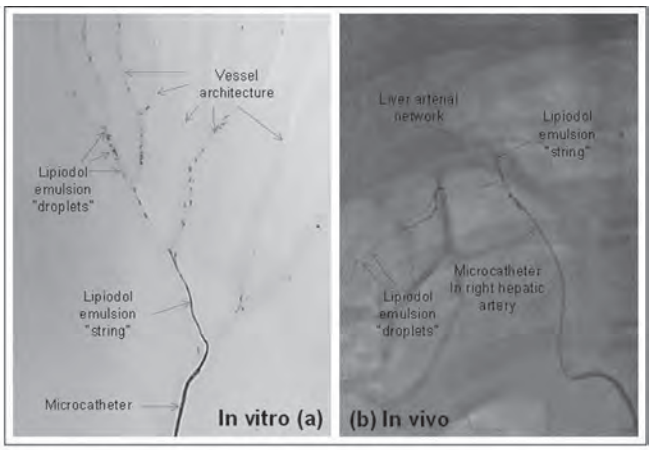

Figure 2 (a): Video still image of cTACE formulation delivered into the VFS and (b) fluoroscopy still image of the same formulation delivered into the right hepatic of a healthy swine

Poster 26: Utilization of an Electromagnetic Navigation System for CT-Guided Biopsy of Thoracic Lesions

J. Mammarappallil, J. Christensen

Objectives: Electromagnetic navigation (EMN) is a newly available option for percutaneous thoracic biopsy. The purpose of this study was to evaluate the utility and efficacy of EMN in CT-guided biopsy of thoracic lesions.

Methods: Over a 9-week period EMN-guided percutaneous CT biopsy was performed on 6 patients (Veran Medical Technologies, ig4™ IR system, St. Louis, MO). Patients were scheduled prospectively based upon EMN system availability. After application of EMN markers, a low dose expiratory planning chest CT was obtained and loaded into the EMN system. The lesions were localized utilizing EMN guidance with a spot CT-fluoroscopy image obtained prior to biopsy. 20-gauge core biopsy specimens were obtained and submitted for cytopathologic analysis. A low dose post procedure CT was performed to assess for complications. All procedures were performed by a single cardiothoracic radiologist.

Results: Six lesions in six patients were identified (3 men, 3 women, with a mean age of 59.3). Lesion location for the 6 lesions was as follows: 2 left upper lobe, 2 left lower lobe, 1 right middle lobe, and 1 anterior mediastinal. Mean lesion size was 5.3 cm (standard deviation of 1.54). Mean distance of the lesions from the skin surface was 0.6 cm (standard deviation of 1.00). The greatest distance from the pleural surface to the lesion was 2.4 cm. Technical success of percutaneous biopsy utilizing the EMN system was 100% (6/6) as determined by diagnostic pathology. In our patient population, the smallest lesion was 7 mm. Histopathologic analysis for the 6 biopsied lesions resulted in the following pathology: 2 non small cell lung cancers, 1 synovial cell carcinoma, 1 biopsy resulting in benign lung tissue, 1 metastatic renal cell carcinoma, and 1 biopsy indicative of malignancy (melanoma). No EMN procedural complications were identified.

Conclusions: Although a small sample size, preliminary results indicate that EMN guidance for percutaneous thoracic biopsy is safe and yields a high success rate. EMN may provide an alternative approach for CT-guided thoracic biopsy in select patients and circumstances. With continued utilization, EMN may provide additional benefits such as reduced procedure time and radiation dose when compared to conventional CT-guided thoracic biopsy procedures.

Poster 27: Prospective Evaluation of Cone Beam CT Vessel Identification and Display Software Versus Digital Subtraction Angiography during Hepatic Arterial Embolization

K.T. Brown, G. Avignon, J.C. Durack, L. Brody, W. Alago, H. Yarmohammadi, R.H. Siegelbaum, J.P. Erinjeri, S.B. Solomon

Objectives: The aim of this study was to prospectively assess and quantify the potential benefits of an automated vessel analysis and 3D roadmapping software package to facilitate identification of vessels supplying a hypervascular region of interest in the liver from cone-beam studies performed during hepatic arterial embolization (HAE).

Methods: Between February and July 2014, 35 patients with unresectable hypervascular hepatocellular carcinoma or liver metastases with at least one hyper-vascular lesion planned for selective HAE, underwent arterial phase cone-beam CT (A-CBCT) with contrast injection from the common or proper hepatic artery. Target vessels for embolization were initially identified on conventional digital subtraction angiography (DSA) and subsequently on A-CBCT utilizing the study software package by a technologist. A 3D rendering of the computed vessels was superimposed on live 2D fluoroscopy to provide a road map for embolization. After the procedure, physicians completed surveys recording their experience with the software and perceived benefits of its use. Radiation exposure and contrast media related to A-CBCT acquisition were recorded and compared to total procedure levels.

Results: At least one additional target vessel was identified by the software compared to DSA alone in 13 of 30 evaluable cases (43%). An embolization plan based on DSA alone was modified based on software findings in 10 of 30 cases (33%), and its use increased operator confidence in procedural technical success in 25 of 30 cases (83%). In 15 of those cases (50%), physicians reported that the use of the software and live 3D road mapping reduced the number of DSA acquisitions necessary for HAE. A-CBCT contributed to 11% of the total x-ray exposure and 18% of the total contrast media volume utilized.

Conclusions: A-CBCT software designed to facilitate analysis of arterial supply to hypervascular tumors with live 3D road mapping capabilities increased relevant vessel detection and operator confidence during HAE. Further studies may clarify the contribution to oncologic efficacy in relation to patient radiation dose exposure and contrast volume.

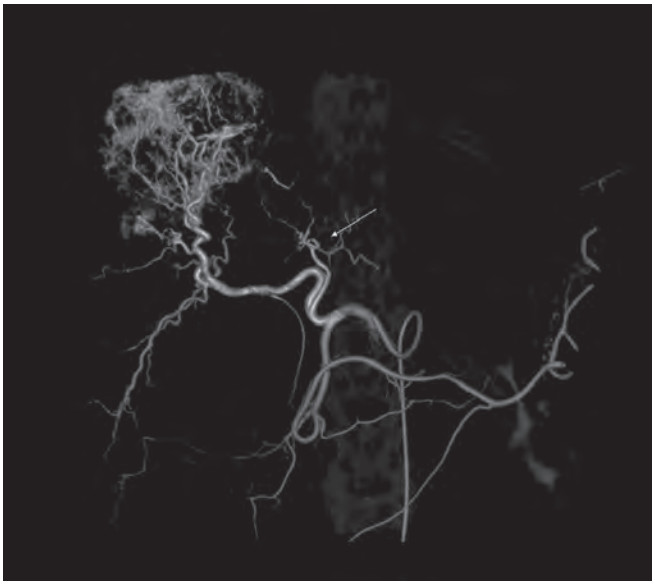

Segment 4/8 lesion where FlightPlan for Liver highlighted a vessel coming from the left side, which appeared to be a true feeder and was not seen on initial DSA, even thought it was suspected from pre-op imaging

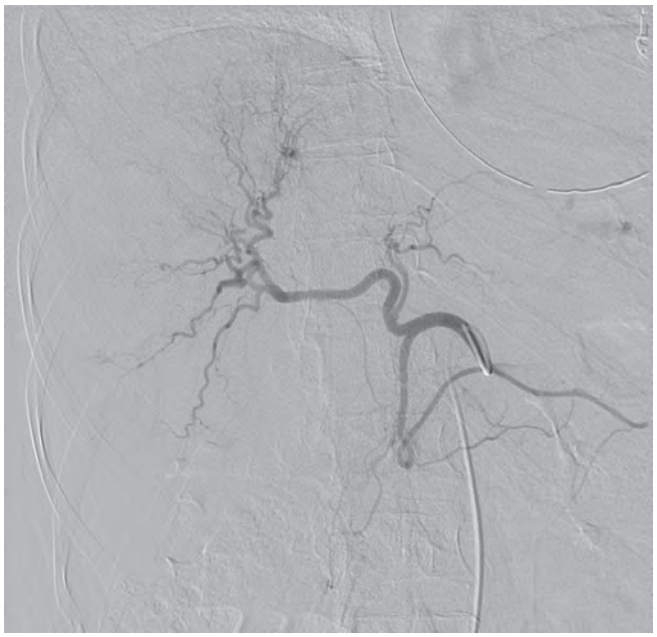

Corresponding DSA image from the Common Hepatic Artery

Poster 28: Accuracy Testing of a Needle Placement Robot for Biopsy and Radiofrequency Ablation under CT Fluoroscopy Guidance: Validation with Phantom Study

H. Won, N. Kim, G. Kim, J. Seo, H. Kim

Objectives: Purpose of this study is to evaluate accuracy of a needle placement robot for biopsy and radiofrequency ablation (RFA) with abdominal phantom including various sizes of simulated lesions.
Methods: A robot which has been jointly developed by Asan Medical Center and Hyundai Heavy Industries Co., Ltd. was used. This robot is a master-slave robotic system and includes needle path planning system and needle-inserting robot arm with pre-scanned diagnostic CT and CT fluoroscopy guidance. For evaluation of robot accuracy for needle placement, a commercially available abdominal phantom (Model 057A, CIRS, US) was used. And the phantom was scanned by a Sensation 16 MDCT (Siemens, Germany). The liver part of the phantom contains multiple spherical simulated tumors of three different size spheres. Various needle insertion trials with two nodule sizes (10 mm and 20 mm in diameter) and four insertion angles (0, 15, 30 degrees in transverse plane, and 20 degrees in caudocranial plane) were performed. In addition, seven time trials on each nodule with 0 degree in transverse plane were performed to see reliability of this robot. To assess accuracy, CT scan was performed after each trial with needle in situ.
Results: The overall error was 1.61±0.87 mm, which was calculated by the distance from planned trajectory before insertion to actual needle trajectory after insertion. There is no difference among insertion angles and nodule size. Standard deviations of seven trials on two nodules (10 mm and 20 mm in diameter) with vertical (0 degree) insertions are 0.47 and 0.21 mm, respectively.
Conclusions: CT-compatible needle placement robot for biopsy and RFA shows relatively acceptable accuracy, which could be used for 1 cm nodule RF ablation under CT fluoroscopy guidance.

Fig. 1 CT fluoroscopy guided needle placement robot for biopsy and radiofrequency ablation made by Asan Medical Center and Hyundai Heavy Industries Co., Ltd.

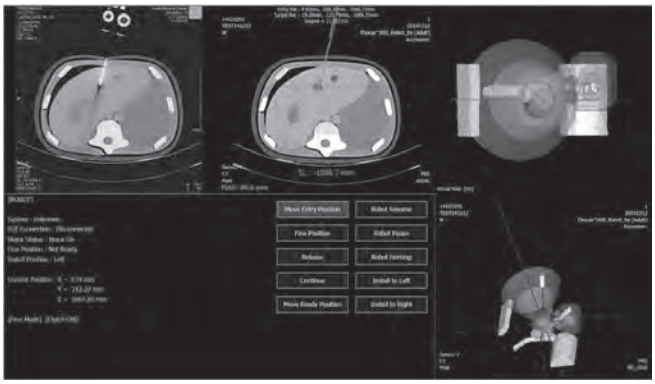

Fig. 2 A screen shot of CT fluoroscopy guided needle placement robot. Top left is CT fluoroscopy image. Top middle is planner screen. Top right and bottom right is 3D view of planning.

Poster 29: Can Planning Software be Used to Confirm Complete Thermal Coverage During Percutaneous Microwave Ablations?

T. Hoffman, A. Kalia, G. McLennan, C. Martin

Objectives: The purpose of this study is to evaluate how closely the post-treatment tumor ablation margins estimated by recently approved planning software correlate with actual post-procedural image findings correlating with cell death. To determine if using planning software on intraprocedural CT or cone beam CT images can confirm a complete inclusion of the target tumor in the predicted zone of lethal energy during percutaneous microwave ablations
Methods: One lung and two liver microwave ablations using computed guidance were performed. Planning software (Emprint Procedure Planning Software; Covidien, Boulder, CO) was used to plan the needle placement and was applied to the CT images obtained during the ablation. The maximum and minimum distance from the edge of the tumor to the lethal edge of the calculated ablation zone was measured in 3 planes of the final procedural CT images.
Results: There was complete overlap of the projected lethal ablation zone and the tumor in all 3 procedures. The maximum distance to the edge of the lethal zone was 9.0 mm. The minimum distance to the edge of the lethal zone was 4.0 mm.
Conclusions: Based on this limited series, the predicted ablation zones can be overlayed with imaging obtained during the ablations. Further follow-up is required to determine if this information correlates with complete response to ablation.<!— Copyright (c) 2006 Microsoft Corporation. All rights reserved. —><!— OwaPage = ASP.webreadyviewbody_aspx —><!—Copyright (c) 2006 Microsoft Corporation. All rights reserved.—>

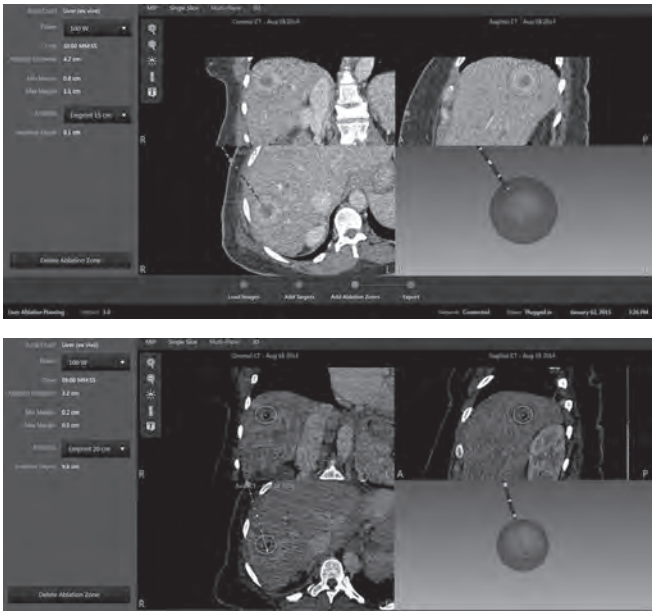

Poster 30: CT-Guided Microwave Ablation for Hepatic Caudate Lobe Tumors: A Puncture Route via the Left Lobe of Liver and its Clinical Application in 12 Patients

F. Gao, G. Wang, F. Zhang

Objectives: To evaluate the clinical value and safety of the puncture route via the left lobe of liver in treating hepatic caudatelobe tumors by computed tomographic (CT) guided microwave (MW) ablation.
Methods: A total of 12 tumors located in the hepatic caudate lobe in 12 patients including 9 cases of hepatocellular carcinoma (HCC) and 3 cases of colorectal liver metastasis (CLM) were percutaneously treated in 14 MW ablation sessions byusing the puncture route via the left lobe of liver. Follow-up contrast materialenhanced CT scans were reviewed and ablation was considered a success if no contrast enhancement was detected in the treated area on the CT scan obtained at 1 month. The local control rate of 3, 6, 12, 24 and 36 months, as well as local tumor progression rate, tumor-free rate were also assessed. Months are counted from the first time of MW ablation and the median duration of follow-up was 23.0 ± 9.3 months (range, 11-36 months).
Results: In total, 12 lesions were all treated. The ablation success rate was 83.3% (10 of 12 tumors). Two lesions were ablated for the second time 1 month later because of tumor residual. The local control rate of 3, 6, 12, 24, 36 months was 83.3%, 75.0%, 58.3%, 25.0%, 16.7% respectively. The local tumor progression rate of 3, 6, 12, 24, 36 months was 8.3%, 16.7%, 33.3%, 75.0%, 83.3% respectively and the tumor free rate of 3, 6, 12, 24, 36 months was 75.0%, 66.7%, 50.0%, 25.0%, 16.7% respectively. A small amount of hepatic sub- capsular hematoma was found in 1 patient which was automatically absorbed. Mild right upper quadrant pain developed in 2 patients and lasted for about 1 month. Severe complications such as massive bleeding or thermal damage of bile ducts did not occur.
Conclusions: CT-guided MW ablation using the puncture route via the left lobe of liver is feasible, effective and safe in treating hepatic caudate lobe tumors.

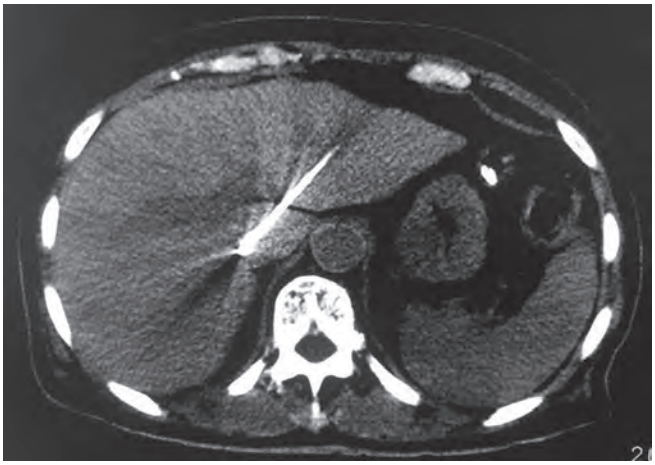

A MW probe was percutaneously inserted into the tumor via the left lobe of liver and positioned against the lesion's deepest margin.

Table. Patients' characteristics summary

Characteristic	
Age (years)	
Average	55-71
Mean ± SD	63.1 ± 4.9
Sex	
Male	9
Female	3
Diagnosis	
HCC	9
CLM	3
Tumor diameter (cm)	
Average	0.9-2.3
Mean ± SD	1.7 ± 0.4
≤1	1
>1, ≤2	9
>2	2
ECOG PS	
0	7
1	3
2	2

Note: HCC = Hepatocellular carcinoma; CLM = colorectal liver metastasis

Poster 31: Percutaneous Lung Biopsy: 7-Years Experience with an Augumented Reality System

R.F. grasso, R. Cazzato, G. Luppi, E. Faiella, F. Giurazza, B. Beomonte Zobel

Objectives: Percutaneous lung biopsies (PLBs) performed for the evaluation of pulmonary masses require image guidance to avoid critical structures. A new CT navigation system (SIRIO) for PLBs was validated. We herein review our 7-year experience with such system
Methods: The local Institutional Review Board approved this retrospective study. Image-guided PLBs in 788 patients were performed with SIRIO. The procedures were reviewed in terms of number of CT scans, patients' radiation exposure and procedural time. Comparison was performed with a group of 288 patients undergoing standard CT-guided PLBs. Sensitivity, specificity and overall diagnostic accuracy were assessed in both groups.
Results: SIRIO-guided PLBs showed a significant reduction in procedure time, number of required CT scans and the radiation dose administered to patients (P< 0.001). In terms of diagnostic accuracy, SIRIO proved to be more accurate for small-sized lesions (<20mm) than standard CT-guidance.
Conclusions: Long-term experience with SIRIO proved it to be a reliable and effective when performing CT-guided PLBs, especially for sampling small lesions

Poster 32: Early Elevated Tissue Stiffness Detected by Elastography Hints Local Thermal Damage during Irreversible Electroporation Ablation

K. Huang

Objectives: Irreversible electroporation (IRE) is a nonthermal ablation technique that induces permanent cell membrane damage and death. Elastography used to be introduced to monitor ablation effect in the liver, and the stiffness change of ablation zone will develop one hour later.
Methods: 6 Lanyu pigs underwent IRE ablation of the liver and were imaged with ultrasound and elastography. Central and peripheral temperature of ablation zone were monitored, too. Histologic evaluation of cell death by triphenyltetrazolium chloride staining was performed. Within these animals, a total of 270 electric pulses were given on 18 areas of livers in 3 animals, and 90 pulses were given on 18 areas in other 3 animals.
Results: Elastography showed that liver ablated by IRE did not exhibited significantly increased tissue stiffness till one hour after ablation in 90 pulses group. The local temperature is 38-40. The local temperature increased to 52-57 in 270 electric pulsed group, and the stiffness increasing was also noted 10-20 minutes after IRE ablation.
Conclusions: IRE ablation does not led to increased tissue stiffness immediately, however, when repeated IRE ablation over an area results in local hyperthermia, the thermal effect will increase tissue stiffness detectable by elastography within 20 minutes and indicative of malpractice. Elastography may be used to monitor IRE ablation of the liver in the future.

Poster 33: Vessel Occlusion During Microwave Ablation of Hepatocellular Carcinoma: Impact of Vessel Size, Proximity and Type

J. Chiang, M. Cristescu, M. Lee, A. Moreland, J. Hinshaw, F. Lee, C. Brace

Objectives: Microwave energy provides faster heating to greater temperatures than other thermal modalities, allowing for more effective treatment near large vessels. However, some studies have identified a potential for heat-induced vascular occlusion during microwave ablation (MWA). In animal models of normal liver, vascular occlusion was dependent on vessel size, vessel-applicator spacing, and most significantly, vessel type. The purpose of this study was to determine whether the same factors predict vessel occlusion during microwave ablation of HCC in human patients
Methods: Microwave ablations of primary HCC performed at a single center between 01/2011 and 05/2014 were retrospectively reviewed. Ablations were performed using a 2.45 GHz system with gas cooling and a maximum power of 195 W divided among one to three antennas. Pre-, intra- and post-procedural CT or MR images were each reviewed by one of two radiologists. All vessels within the ablation zone were tabulated and characterized by type, size and distance from the microwave antenna. Logistic regression analysis was used to correlate these metrics with vessel patency on immediate post-ablation scans.
Results: A preliminary cohort of n=124 HCC ablations adjacent to n=167 hepatic vessels among n=95 patients was analyzed. Mean (±SD) tumor diameter was 21.2 ± 8.4 mm. Mean generator output was 109.8±41.4 W (45-195 W) for 5.9±2.5 min, which produced a mean ablation zone diameter of 38.9±10.1 mm. There was no difference in ablation settings or adjacent tumor size among vessel types. Occlusion was noted in 15.0% (6/40) of hepatic veins, 39.7% (26/57) of portal veins and 14.3% (10/70) of hepatic arteries. Both vessel-antenna spacing and vessel-size were predictors of hepatic vein occlusion (P=0.0878 and P=0.0364, respectively), while only vessel size

predicted portal vein occlusion (P=0.0011). There was no association between hepatic artery occlusion and vessel-antenna spacing or vessel size. Hepatic arteries occluded at a higher rate than in previous animal studies, likely due to substantial differences in flow and mechanics between HCC arterial supplies and normal hepatic arteries in the tumor-free lab model.
Conclusions: As seen in animal studies, small vessel size and close proximity to MW antennas were independent predictors for occlusion of certain vessel types, with portal vein occlusion occurring more frequently than hepatic vein occlusion. Improved characterization of these occlusion rates among various vessel types can lead to better patient-specific antenna placement strategies in microwave ablation procedures.

Poster 34: Supradiaphragmatic Computed Tomography and Infradiaphragmatic Ultrasound Guidance for Microwave Ablation of Hepatic Dome Tumors

F. Gao, J. xue, V. Khanna, D. Lee, A. Sharma

Objectives: To evaluate the success rate and safety of the supradiaphragmatic and infradiaphragmatic approaches guided by computed tomograph (CT) or ultrasonography (USG) for microwave (MW) ablation in treating hepatic dome tumors.
Methods: To reduce the risk of diaphragmic damage by MW ablation, we use CT guidance for supra diaphragmatic tumors and USG guidance for infra diaphragmatic tumors. In this study, 5 supra diaphragmatic tumors in 5 patients (Group A), including 4 of hepatocellular carcinoma (HCC) and 1 of colorectal liver metastasis (CLM), were ablated by CT guidance. Another five infra diaphragmatic tumors in another 5 patients (Group B), including 3 of HCC and 2 of CLM, were ablated by USG guidance. Follow-up contrast CT or magnetic resonance imaging (MRI) were reviewed and ablation was considered a success if no contrast enhancement was detected in the treated area at 1 month.
Results: In total, 10 lesions were ablated. The ablation success rate was 90% for all the patients (100% in group A, 80.0% in group B), and there was no difference between the two groups (P = 0.292). In all patients, hepatic sub-capsular hematoma, pneumothorax diaphragmatic paralysis, perforation, fistula formation or rupture did not occur.
Conclusions: CT and USG guidance have a high success rate for the MW ablation of hepatic dome tumors via either supradiaphragmatic or infradiaphragmatic approach. Both are safe and depending on the situation of tumors.

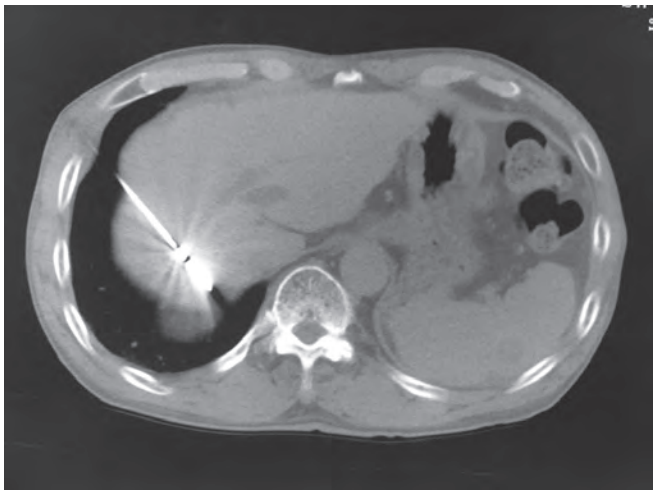

Poster 35: Percutaneous Pulmonary Fiducial Marker Placement Using CT Guidance: Our Single Center Experience

S. Gilani, V. Khanna, D. Lee, E. Mathes, D. Waldman

Objectives: 1. Discuss indications for and complications associated with CT-guided pulmonary fiducial marker (PFM) placement. 2. Review the existing literature on CT-guided PFM placement including data on technical success and complications. 3. Present the procedural protocol, technical success, and challenges encountered at our institution.
Methods: From 2011-2014 55 PFMs were placed in 47 consecutive patients (32 females, 15 males; average age 65.7 years ± 12.7) using a CT guided approach. We retrospectively reviewed pre- and intra-procedural imaging to determine technical success and complication rates. We classified complications as per the Society of Interventional Radiology guidelines.
Results: At our institution, PFMs are placed to guide radiosurgery. Over the course of four years we placed 55 markers in 47 consecutive patients with a diagnosis of primary or secondary lung malignancy with the majority of tumors measuring less than 3 cm in diameter. In each patient PFM marker placement was preceded by core biopsy of the lesion using a 17-gauge outer cannula with an 18-gauge biopsy needle. The same outer coaxial needle was used to deploy the PFM. PFM placement was technically successful in 92.7% of cases with four markers deployed at a distance greater than 2 cm beyond the tumor margin. Self-limiting pneumothorax (SIR Class B) was seen in eight patients (17.0%) while a major pneumothorax requiring chest tube placement (SIR Class D) was seen in one patient (2.1%). Four patients (8.5%) had self-limiting pulmonary hemorrhage (SIR Class A). Six patients had greater than one PFM placed of whom two developed self-limiting pneumothoraces (33.3%).
Conclusions: Prior data on CT-guided PFM placement demonstrate pneumothorax rates as high as 71% with all known studies reporting the complication occurring in over half of cases. Self-limiting hemorrhage rates of 13%-45% have been reported. Our retrospective review reports a 19.1% occurrence rate of pneumothorax, the majority of which were self-limiting, and only one patient requiring a thoracostomy tube. We attribute our significantly lower rate of pneumothorax to the careful review of pre-procedure imaging including assessment of background lung parenchyma, and to deployment of the PFM through the same outer cannula as the core biopsy needle limiting multiple passes through the pleura. Our rate of self-limiting pulmonary hemorrhage (8.5%) falls within the previously reported rates of such. We also demonstrate that the placement of more than one PFM within a lesion has no significant difference in complication rates. We conclude that CT-guided PFM placement is a safe and effective means of pulmonary lesion localization prior to radiosurgery.

Poster 36: Technical Development of Yttrium 90 Glass Microspheres: A Minimally Embolic Device Engineered to Treat Hepatocellular Carcinoma

W. Mullett

Objectives: The goal of radioembolization for liver cancer is maximize dose and limit toxicity. During transarterial radioembolization (TARE) radioactive particles that are injected into tumor via hepatic artery become trapped and emit lethal radiation. Yttrium-90 glass microspheres (^{90}Y, TheraSphere®) are a minimally embolic device engineered for the treatment of HCC. This is an overview of technical development/design features of ^{90}Y glass microspheres, which are presently approved for use under an FDA HDE.
Methods: Key optimized design considerations for the 90Y glass microspheres are choice of radionuclide, microsphere stability/uniformity+specific activity and dose preparation/delivery approach. 90Y radionuclide plays an important role in dose delivery. 90Y is a high-energy β-emitter with a suitable half life (t1/2) and long particle penetration distance. Optimal radiation penetration ensures complete tumor dose coverage. Incorporating 90Y isotope into glass matrix yields highly radioactive, stable microspheres. Y2O3/Al2O3/SiO2 are melted and formed into spheres of uniform size/shape. The stable Y2O3 (40% of glass formulation) is converted to 90Y by neutron bombardment, creating a high potency of 2500 Bq/microsphere at calibration. As 90Y is integrated into the microsphere glass matrix and not surface bound, there is a low level of 90Y leaching. In addition, a low number of microspheres minimizes stasis risk and the stability of 90Y glass microspheres minimizes systemic exposure. As glass microspheres possess a high specific activity per microsphere, clinicians investigated the relationship between high radiation dose to tumor and patient outcomes. Garin showed that survival in unresectable HCC was stratified (27 months >205 Gy; 9.75 months <205 Gy; dose to tumor), emphasizing importance of high tumor dose+delivery efficiency. Minimally embolic 90Y also permits possible retreatment. Padia (2013) illustrated radiation uptake in the local region of target tumor which demonstrated retreatment possibilities 1 mo post-treatment.
Results: NA
Conclusions: The overarching goal of TARE is maximize tumor dose with minimal toxicity. 90Y glass microspheres enable direct delivery of optimized, localized radioactive dose to tumor tissue via the vasculature and are minimally embolic and contained in a highly stable matrix.

Poster 37: Tc-99m MAA Liver Perfusion Scan Prior to Y90 Radioembolization: Lung Shunt Fraction and Beyond?

R. Tong, M. Kohi, D. Olorunsola, K.P. Kolli, A. Taylor, J. LaBerge, R. Kerlan, N. Fidelman

Objectives: To determine if Technetium-99m (Tc-99m) macroaggregated albumin (MAA) imaging can be used to predict Yttrium-90 (Y90) treatment response in addition to calculate the lung shunt fraction (LSF) in patients with hepatocellular carcinoma (HCC).
Methods: In this single center retrospective study, 39 consecutive patients (mean age 65.4 years, 32 men, 7 women) with HCC who underwent Tc-99m MAA liver perfusion scans prior to Y90 radioembolization with resin (27 patients) or glass (12 patients) microspheres from 2009 to 2014 were reviewed. Pre- and post-treatment imaging (contrast-enhanced multiphase CT or MRI) were used to assess treatment response based on modified Response Evaluation in Solid Tumors (mRECIST) criteria. Data regarding adverse events (AE) were derived from the electronic medical

record. Either Fisher's exact or Chi square tests were used to correlate treatment response and post procedure AE with LSF.

Results: The median LSF was 7.6% (range 2.3%-22.4%). Post treatment scans were obtained a median of 36 days (range 28-89 days) with follow-up clinical assessment after Y90 radioembolization. Radiographic tumor response rates for patients with LSF at or below median of 7.6% were complete response (CR) in 1 patient (6%), partial response (PR) in 5 patients (27%), stable disease (SD) in 6 patients (33%), and progressive disease (PD) in 6 patients (33%). Patients with LSF above 7.6% demonstrated SD in 13 patients (65%) and PD in 7 patients (35%). Radiographic response to Y90 radioembolization was significantly better ($P<0.05$) for patients with LSF <7.6%. LSF <7.6% also correlated with a lower risk of developing post treatment abdominal pain ($P<0.05$).

Conclusions: Patients with a LSF <7.6% were significantly more likely to have a better radiographic response to Y90 radioembolization and less likely to develop post-procedure abdominal pain.

Poster 38: Validation of the Hong Kong Liver Cancer Staging System: A North American Study with 890 TACE Patients

J. Sohn, R. Duran, F. Fleckenstein, Y. Zhao, H. Lee, L. Zhao, S. Sahu, R. Schernthaner, M. Lin, J. Geschwind

Objectives: The Hong Kong Liver Cancer (HKLC) staging system is a newly developed hepatocellular carcinoma (HCC) staging system that has gained significant attention because it addresses some of the limitations of the current staging system (Barcelona Clinic Liver Cancer [BCLC]). The HKLC staging, in the original study cohort, offered not only better prognostic classification but also provided treatment recommendations more consistent with the current practice of HCC management, specifically with expanded role of TACE. However, HKLC was built primarily on a hepatitis B, Asian patient cohort. The purpose of this study is to evaluate the performance of HKLC in a North American cohort where the disease etiology is much more heterogeneous and primarily involves hepatitis C patients.

Methods: This retrospective, single center study included HCC patients who received TACE treatment at our institution between 2000 and 2013. 968 patients were reviewed and 890 were found to have both lab and imaging reports available to calculate HKLC and BCLC stages. Overall survival was defined as from the date of first TACE to the date of death or last known follow-up date. The performance of the staging systems was assessed and compared through three statistical measures: homogeneity (outcome similarity within stage), survival discrimination, and monotonicity of gradient (outcome worsening with increasing stage). The staging systems were evaluated through Kaplan-Meier (KM) estimate and then through Cox model with likelihood ratio (LHR) test, linear trend (LT) test, Harrell's C, and Akaike's information criterion (AIC).

Results: Unlike the original HKLC study, our patient cohort had more heterogeneity in HCC etiologies: 132 (14.8%) hepatitis B, 427 (48.0%) hepatitis C, 254 (28.5%) alcoholic, 60 (7.8%) NASH, 60 (6.7%) cryptogenic (some patients had more than one etiology). Both staging systems classified survival with high significance ($P<0.001$). However, HKLC performed better across all statistical measures. Median overall survival (MOS) is shown in table 1 and KM estimates are shown in figure 1. LHR test demonstrated greater homogeneity for HKLC (LHR: 201; $P<0.001$) than BCLC (LHR: 119; $P<0.001$). Both AIC and Harrell's C showed stronger survival discrimination by HKLC (C=0.71, AIC=6242) than BCLC (C=0.64, AIC=6320). Gradient monotonicity was better observed in HKLC (LT: 193; $P<0.001$) than in BCLC (LT: 111; $P<0.001$).

Conclusions: While both HKLC and BCLC staging systems were able to classify survival, the HKLC staging system outperformed the BCLC staging system as a prognostic classification system across all statistical measures. This is the first, as we know it, validation of HKLC in a predominately hepatitis C North American population.

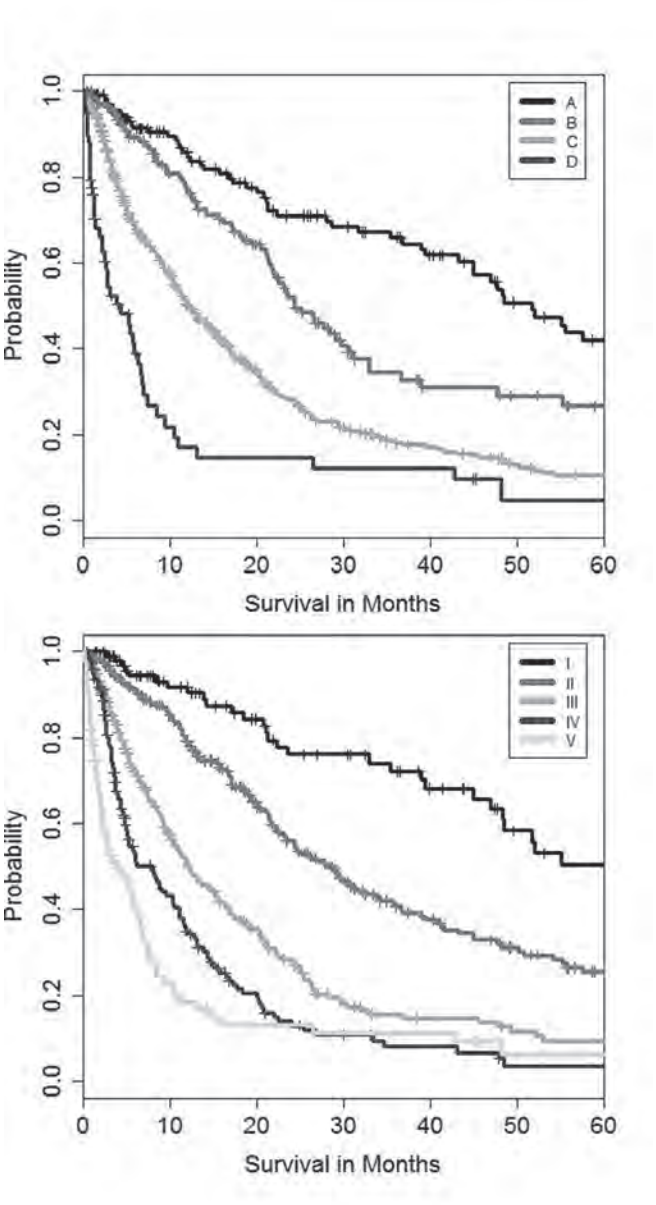

Top: Kaplan-Meier curve of BCLC; Bottom: Kaplan-Meier Curve of HKLC

Median Overall Survival (months) for BCLC and HKLC Stages

BCLC stage	A	B	C	D	
BCLC MOS	51.6	24.3	12.1	4.3	
HKLC stage	I	II	III	IV	V
HKLC MOS	62.6	28.0	12.2	8.0	3.8

Poster 39: Safety and Feasibility of Selective Internal Radiation Therapy Planning Using a Left Transradial Access without Conscious Sedation

V.V. Patil, R.S. Patel, N.E. Tabori, E. Kim, R.A. Lookstein, F.S. Nowakowski, A.M. Fischman

Objectives: To determine the safety and feasibility of SIRT planning utilizing transradial access with only local anesthesia without conscious sedation.

Methods: Single-center retrospective review of all angiography/mapping cases for Y90 treatment planning performed via transradial access and local only anesthesia (i.e. no intravenous sedation) was performed from December 2013 to December 2014. A total of 6 cases were identified via radiology information system (RIS) search and included in analysis. Technical success was defined as successful administration of mapping radiotracer to the liver as confirmed by post-procedure SPECT/CT scan.

Results: Technical success was achieved in 100% of cases. 5 patients were male and 1 patient was female. In 5 of 6 patients, coil embolization of visceral vessels was performed during the procedure, which included 4 gastroduodenal arteries, 1 right gastric

artery, and 1 branch of right hepatic artery. In all 6 patients, subsequent Y90 radioembolization was successfully performed. No major or minor complications were seen.
Conclusions: This pilot study demonstrates the safety and feasibility of performing SIRT planning angiography and coil embolization via a transradial approach utilizing local anesthesia only. Local only anesthesia allows for early patient discharge and avoids the risks associated with sedation, which are particularly significant in at-risk patients with comorbid obesity or obstructive sleep apnea.

Poster 40: Hepatocellular Carcinoma Promotion by Endoplasmic Reticulum Stress Transducer BBF2H7

Y. Zhang, K. Chayama

Objectives: The tumor suppressor p53 is reported to be functional inactivated in Hepatocellular Carcinoma (HCC). Internal and external environmental stress brings about p53 instability and might lead to HCC formation. Endoplasmic reticulum (ER) stress occurs in several liver diseases, including HCC. So far, how effectors of ER stress cause HCC is not well studied. Here we show that ER stress transducer BBF2H7 contributes to cell survival, by promoting ubiquitin-dependent p53 degradation and diminishing p53 phosphorylation. This new mechanism of p53 modulation could help us understand about how ER stress is involved in HCC formation.
Methods: Paired tumor and non-tumor liver tissues were stained by BBF2H7 antibody. Effects on the cell cycle and apoptosis by BBF2H7 were detected using FACS. Expression of p53 and its downstream targets were checked by both Real-Time PCR and western blot in either BBF2H7 overexpressed or knocked down HepG2 cells. Dual luciferase reporter assay was performed to test how BBF2H7 modulates p53 transcriptional activities. Nuclear abundance of p53 affected by BBF2H7 was also identified by immunostaining.
Results: 8 out of 10 stains showed a comparatively higher BBF2H7 expression in HCC tissues than in non-tumor tissues. FACS results indicated that BBF2H7 regulated apoptosis but not cell cycle. Real-Time PCR results showed that BBF2H7 overexpression increased MDM2 and BCL-2 expression, but p53, Cyclin D and Cyclin E mRNA levels were not changed. Protein levels of both p53 and phos-p53 were decreased by BBF2H7 overexpression, but only p53 protein could be restored by blocking proteasome activity. The anti-apoptosis genes BCL-2 and BCL-xL were up-regulated by BBF2H7, while Pol.δ cofactor PCNA was not affected. Strikingly, p53 transcriptional activity was drastically reduced by BBF2H7 overexpression. Contrary to the case of overall p53 protein, p53 transcriptional activity could barely be recovered by proteasome inhibitor. The impairment of p53 nuclear abundance by BBF2H7 might be the reason behind this.
Conclusions: These findings reveal a new mechanism in which p53 can be destabilized by ER stress transducer BBF2H7, and also imply that BBF2H7 has full potential to trigger HCC carcinogenesis through impairing p53 transcriptional activity.

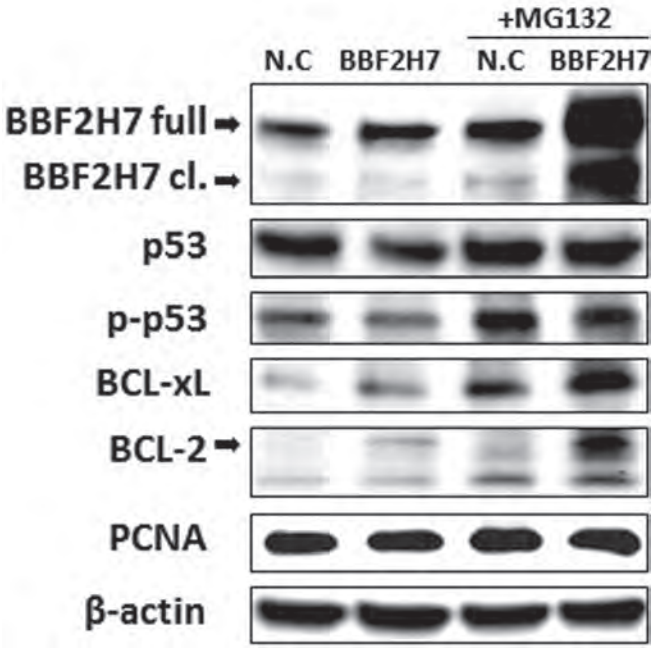

HepG2 cells were transient transfected by either empty vector or BBF2H7 plasmid. The cells were treated by MG132 (1 μM) 36H post-transfection, and were harvested 48H post-transfection. The whole cell lysates were blotted by indicated antibodies.

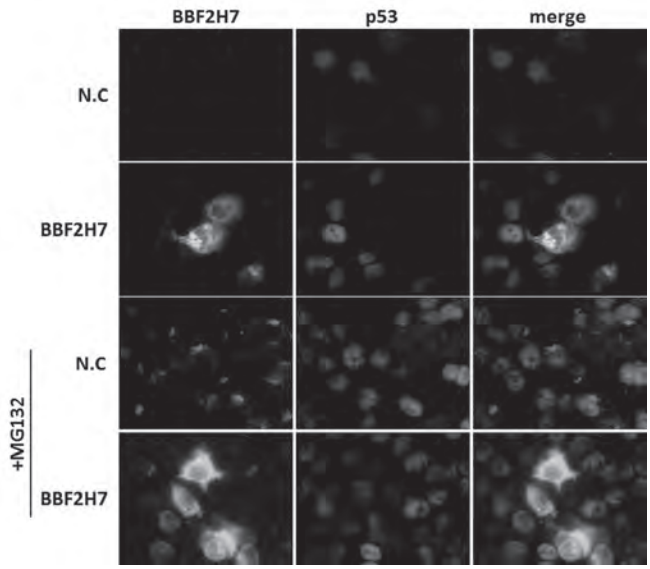

HepG2 cells were treated as described in Fig.1. 48H post-transfection, the cells were collected and stained with BBF2H7 and p53 antibodies.

Poster 41: Retrospective Review of Radiofrequency Ablation of 555 Hepatic Tumours: Assessment for Complications and Local Progression Rates and Determination of Possible Risk Factors

C. Too, P. Nho, R. Lo, F.G. Irani, K. Tay, S. Chan, A. Gogna, K. Damodharan, A. Patel, B. Tan

Objectives: A single centre, retrospective review of 555 hepatic lesions which underwent radiofrequency ablation (RFA), with focus on complications, local tumour progression (LTP) rates and determination of possible risk factors.
Methods: From January 2009 to October 2012, 555 hepatic tumours in 337 patients were treated with RFA. Using hospital computerised records, the following data was captured: patient demographics, preprocedural laboratory results, Child status, type, location and size of tumour, development of tumoural seeding, complications and LTP. Possible risk factors for LTP were identified.
Results: 483 (87.0%) were hepatocellular carcinomas (HCC), 52 (9.4%) were colorectal metastases and 20 (3.6%) were other tumours. Mean tumour size: 2.1 cm (SD 1.05 cm, range 0.4-6.8 cm). Mean follow up duration was 387 (SD 331.4, range 0-1368) days. 416 (74.9%) lesions had no local tumour progression at last imaging. Using Cox regression, the following factors were significant ($P < 0.05$) in predicting LTP: size (RR 1.3), hilar location (RR 4.0), age (RR 0.98), colorectal metastases (RR 2.1). Dome location (RR 1.8) showed a trend towards significance ($P = 0.053$). The following factors were not significant: sex, Child's status, platelets, INR and hepatic segment. 70 patients (20.8%) had minor complications which only required observation while 7 patients (2.1%) had significant complications which required further interventions. Only 1 case of tumour seeding was detected.
Conclusions: RFA of liver tumours is safe and effective, with a low significant complication rate of 2.1%. In our study, 74.9% of patients showed no tumour progression at last follow-up. The following factors significantly contributed to higher risk of developing LTP: hilar locations, larger lesion size and colorectal metastasis. Dome location of the tumour trended toward significance as well.

Poster 42: Percutaneous Cryoablation of Subcapsular Hepatocellular Carcinoma Using 17-guage Ultra-thin Cryoneedle

J. Won, K. Kim, M. Kim, D. Lee, S. Park, S. Lee

Objectives: To report our early experience of percutaneous cryoablation (PCA) of subcapsular hepatocellular carcinoma (HCC) using 17-guage ultra-thin cryoneedle.
Methods: Sixteen patients with subcapsular located single HCC who were not surgical candidate underwent PCA under the US, fluoroscope or CT guidance. The size of each tumor was 11 to 48mm (mean: 19.6). All the HCCs were located within 0.5cm from the liver capsule and six of them were abutting adjacent organ such as gall bladders (n=3), colon, stomach and kidney. Ablation was done using one to four 17-guage cryoneedle (IceRod, Galil Medical, Yokneam, Israel). Each session of ablation consisted of freezing - thawing –freezing cycles. Follow up CT scans were taken immediately, 1, 3, 6 months after the PCA. We evaluated the clinical efficiency and safety of PCA.
Results: All procedures were successful and the pain score was 0 to 2 (negligible). There was 2 cases procedure related complication; one with self resolved pneumothorax and one with gastric spasm. On immediate CT scans, all 16 cases (100 %) showed

complete necrosis. During the early follow up (≤ 6 month), there was 1 case (6.3%) of local recurrence of HCC without other complication such as tumor seeding.
Conclusions: PCA using ultra-thin cryoneedle was effective and safe for the treatment of subcapsular HCC.

Poster 43: Microwave Ablation of HCC Using 915 MHz Internally Cooled Synchronous Wave Antenna

S. Contractor, S. Chivi, J. Thomas, U. Shahid

Objectives: Microwave devices use either a single 2.45GHz arge diameter antenna or 915mHz devices that can utilize multiple antenna to allow amplification of the burn zone using lower wattage. Device limitations with the 2.45 GHZ or non internally cooled antennas include skin burns due to shaft heating and non spherical burn areas. We report our experience with a 915mHz generator with an internally cooled antenna that uses synchronous wave technology to allow spherical burns, and eliminates the risk for skin burns.
Methods: 31 patients with 52 lesions were treated under CT guidance over an18 month period. 36 sessions of ablation were performed. 22 patients had a single lesion, 6 had 2 lesions and 3 had 3 lesions. Lesion sizes ranged from 1.3 cm to 9 cm, mean 3.4 cm, median 3 cm. 4 lesions were directly abutting a major hepatic vessel and 3 lesions were directly sub capsular. 50 lesions were either LIRADS 5A/B and 2 lesions were LIRADS 4A. Lesions were evaluated at 1, 3 and 6 months post ablation using the mRECIST criteria. Tumor pathology from liver explants was used in 3 patients that had a subsequent liver transplant.
Results: 47 lesions showed either complete or partial response by mRECIST criteria at 6 months, 4 lesions stable disease and 5 showed progressive disease. For small HCCs (diameter <3 cm) complete necrosis was obtained in 100%. Surgical explants showed complete necrosis of the ablated lesions with a spherical zone of ablation and at least a 0.5 cm margin in all 3 patients that had a subsequent transplant. The treated lesions adjacent to major vessels (4) also showed complete response with no evidence of vessel injury. 1 patient with a subcapsular lesion developed a pneumothorax that was treated expectantly. None of the treated patients experienced skin burns. All ablations were done under general anesthesia with same day discharge, 3 patients experienced post procedural pain necessitating hospital admission.
Conclusions: A consistent spherical burn volume and ablation outcomes similar to previous published reports seen, 100% response rates for lesions less than 3 cm. Device eliminates the risk of skin burns.

Poster 44: Local Recurrence after Radiofrequency Ablation of Hepatocellular Carcinoma: Treatment Choice and Survival Analysis

M. Kuang, B. Liu, W. Hu, M. Lin

Objectives: The aim of this study is to evaluate and compare the outcomes of these multidisciplinary treatments for RFA-related local recurrence and define a logical management algorithm for those patients.
Methods: From May 2008 to June 2013, a total of 112patients with HCC were detected local recurrence after RFA. Among them, 94 patients received sequential treatments in our hospital, including salvage resection (SS) (n=24), salvage liver transplantation (n=2), repeated RFA (n=62), and TACE alone (n=6).We compared the survival outcomes of patients treated by salvage surgery (SS), RFA, and TACE.
Results: The median follow-up after treatment was 32 months. After treatments of local recurrence, 82 of 94 patients (87.2%) were cured. The overall survival (OS) rates of all patients were 78.9% at 1 year, 53.3% at 3 years, and 37.3% at 5 years. In subgroup analysis, the OS rates were 73.6% and 51.4% at 1 and 3 years in patients after RFA, and those were 93.3% and 69.1% in patients after SS, and those were 41.7% and 20.8% in patients after TACE, respectively(P=0.016). Tumor response was the only factor significantly associated with overall survival of patients in multivariate analysis (P=0.001).
Conclusions: Re-treatment with complete response improves the survival of patients with post-RFA local recurrence. Repeated RFA is the first treatment choice. SS as the most radical treatment should be considered when RFA failed or is inapplicable.

Poster 45: Transarterial Chemoembolization for Hepatocellular Carcinoma using Lipiodol as the Sole Embolic Agent: 15 Year Single-Institution Experience

J.J. Morrison, Y. Jahangiri Noudeh, J. Loo, K. Kolbeck, J. Kaufman, F. Keller, R. Barton, K. Farsad

Objectives: Transarterial lipiodol chemoembolization (TACE) for hepatocellular carcinoma (HCC) is classically followed by gelatin-sponge particle (GSP) embolization. Embolization with GSP may occlude hepatic arteries, either hindering subsequent treatment or stimulating formation of collateral arterial supply. We present a single institution retrospective analysis of patients with HCC treated with lipiodol TACE without subsequent GSP embolization to assess efficacy as measured by survival.
Methods: An IRB-approved database of 530 patients treated by conventional TACE without GSP embolization between 1998-2013 was evaluated for those treated for HCC. Exclusion criteria included patients treated with surgery, systemic chemotherapy, external beam radiation, alternative liver directed therapy, or thermal ablation. Two patients were also excluded from the analysis due to acute demise from renal failure. A total of 147 patients who met the inclusion and exclusion criteria were analyzed for survival. One, 2 and 3-year survival rates were calculated with Kaplan Meier life tables and Kaplan Meier survivor function graphs stratified to baseline Childs-Turcotte-Pugh (CTP) classification and Barcelona Clinic Liver Cancer (BCLC) stage. Survival rates in subcategories of measured risk factors were compared using the log rank test.
Results: The majority of patients (66%) had HCV disease. Median follow up time was 11.9 months (range 0.4-133.6). Survival stratified by CTP class and BCLC stage is summarized in Table 1. Median survival of all treated patients with CTP A disease was 17.3 months, and for all patients treated with BCLC stages A and B was 15.5 and 15.3 months, respectively. Median survival was highest for patients with CTP A and BCLC A disease (24.4 months) and significantly longer than for those with either BCLC C disease (P ≤ 0.02) or CTP C class (P < 0.0001) (Table 2).
Conclusions: TACE using lipiodol as the sole embolic agent without additional GSP embolization is an effective treatment for HCC, particularly for patients with compensated liver disease, comparable to published standards. Eliminating additional GSP embolization may reduce procedure time and complexity, and may facilitate repeat treatments.

		Median OS (mo)	1-year OS	2-year OS	3-year OS	P value
CTP class	A (n=37)	17.3	64.9%	33.8%	21.0%	<0.0001
	B (n=91)	12.4	51.6%	26.1%	15.1%	
	C (n=18)	3.1	11.1%	0	0	
BCLC	A (n=64)	15.5	60.9%	38.2%	21.8%	
	B (n=48)	15.3	60.4%	20.9%	15.3%	<0.0001
	C (n=16)	5.9	18.8%	11.2%	0	
	D (n=18)	3.1	11.1%	0	0	

Table 1. Median overall survival (OS) by CTP class and BCLC stage.

	BCLC			
CTP	A	B	C	D
A	24.4 (n=17)	16.6 (n=15, p=0.09)	6.0 (n=5, **p=0.02**)	-
B	14.4 (n=47, p=1.00)	15.3 (n=33, p=0.08)	5.9 (n=11, **p=0.001**)	-
C	-	-	-	3.1 (n=18, **p<0.0001**)

Table 2. Median overall survival (months) as function of BCLC and Child-Pugh. P values compare outcomes with CTP A/BCLC A patients.

Poster 46: Treatment of Hepatocellular Carcinoma with Combination TACE+MW Ablation versus TACE Monotherapy: A Lesion-by-Lesion Analysis

A. Smolock, M. Cristescu, M. Woods, J. Pinchot, T. Ziemlewicz, M. Lubner, P. Dalvie, C. Brace, J. McDermott, J. Hinshaw, M.C. Brunner, O. Ozkan, F. Lee

Objectives: Combining TACE and thermal ablation appears to improve HCC treatment results due to a synergistic tumoricidal effect. However, there are no studies of TACE+MW using equipment available in the United States or Europe. The purpose of this study was to compare HCC treatment response after TACE monotherapy vs. TACE combined with MW ablation.
Methods: Our interventional oncology database was retrospectively reviewed for cases of TACE and combination TACE+MW between 2008 and 2014. TACE was performed using a combination of chemotherapeutic agents (doxorubicin, mitomycin C, and cisplatin) mixed with lipiodol. MW ablation was performed using 1-3 antennas and powers up to 140 W. For combination therapy cases, TACE was performed at a target time of two weeks before MW ablation. Local tumor progression (LTP) and disease response according to mRECIST criteria were evaluated using serial post-procedure contrast-enhanced CT or MRI. Data was analyzed with Student's t-tests and Fisher's exact tests.
Results: TACE monotherapy was performed on 65 tumors in 45 patients (36 M, 9 F; mean age 63.4 ± 8.9 years). Combined TACE and MW ablation was performed on 27 tumors in 24 patients (22 M, 2 F; mean age 61.9 ± 7.3 years). Overall, LTP was significantly lower when using combination therapy compared to TACE monotherapy (11.1% vs 60%, P<0.0001). Likewise, complete response (CR) was higher in the combination group (88.9% compared to 38.5% in the TACE monotherapy group, P<0.0001). When stratified by size, the difference in LTP and disease response was

most pronounced for 3-4 cm tumors (see Table 2). There were no major complications in either treatment group.

Conclusions: The results of this study suggest that combination therapy utilizing both MW ablation and TACE is an effective and safe treatment for HCC. Specifically, combination therapy appears to lower local tumor progression rates and improve disease response in individual tumors compared to TACE monotherapy in all size ranges.

Table 1

	TACE	TACE+MW	p
n	65	27	
size (cm)	3.3±1.9	3.6±1.4	0.3719
MELD	7.4±3.6	9.3±1.9	0.0192
follow-up (mo)	6.7±7.6	10.8±7.8	0.0219

Descriptive measures of the treatment groups.

Table 2

	HCC overall		HCC <3cm		HCC 3-4cm		HCC >4cm	
	TACE	TACE+MW	TACE	TACE+MW	TACE	TACE+MW	TACE	TACE+MW
n	65	27	35	7	10	10	20	10
LTP % (n)	60 (39)	11.1 (3)	51.4 (18)	0 (0)	60 (6)	0 (0)	75 (15)	30 (3)
p	<0.0001		0.014		0.0108		0.045	
mRECIST response								
CR % (n)	38.5 (25)	88.9 (24)	45.7 (16)	100 (7)	40 (4)	100 (10)	25 (5)	70 (7)
PR % (n)	29.2 (19)	11.1 (3)	20 (7)	0 (0)	40 (4)	0 (0)	40 (8)	30 (3)
SD % (n)	26.2 (17)	0 (0)	25.7 (9)	0 (0)	20 (2)	0 (0)	30 (6)	0 (0)
PD % (n)	6.2 (4)	0 (0)	8.6 (3)	0 (0)	0 (0)	0 (0)	5 (1)	0 (0)
p	<0.0001		0.1265		0.0108		0.0635	

Local tumor progression and mRECIST response after treatment.

Poster 47: Laser Ablation in Liver: In Vitro and In Vivo Experiment

X. Xie

Objectives: Objective To evaluate the ablation zone and temperature changes caused by laser ablation in vitro and in vivo. Methods Single needle single point laser ablation was performed in vitro porcine liver using 5W and 7W-power, and in vivo rabbit liver using 5W-power. All energy outputs are 1800J. Evaluate the ablation zone in vitro and in vivo, and temperature changes during the 5W-power laser ablation process. Conclusion Laser ablation can cause coagulation necrosis in vitro and in vivo liver tissue; ablation range increases with increasing power; Laser ablation is more concentrated and can be used in the ablation of tumor localized in critical sites.

Methods: Methods Single needle single point laser ablation was performed in vitro porcine liver using 5W and 7W-power, and in vivo rabbit liver using 5W-power. All energy outputs are 1800J. Evaluate the ablation zone in vitro and in vivo, and temperature changes during the 5W-power laser ablation process.

Results: Results Coagulation caused by laser ablation was classes oval and was divided into the black carbonized area and brown white necrotic area from the inside out; the mean ablation range obtained by 5W and 7W-power laser ablation in vitro liver experiments was 1.9cm × 1.2cm × 1.2cm and 2.5cm × 1.5cm × 1.5cm, respectively; the mean carbonation range was 1.1cm x 0.5 cm x 0.5cm and 1.4cm × 0.7cm × 0.7cm, respectively. The average maximum temperature using 5W-power was 243.57 ° C, 62.47 ° C and 34.27 ° C in the ablation center, 5mm far from the center and 10mm far from the center, respectively, in vitro liver experiment; and 62.26 °C and 44.35 ° C, respectively, in vivo liver experiment.

Conclusions: Conclusion Laser ablation can cause coagulation necrosis in vitro and in vivo liver tissue; ablation range increases with increasing power; Laser ablation is more concentrated and can be used in the ablation of tumor localized in critical sites.

Poster 48: ShearWave Elastography Evaluation for Differential Diagnosis of Focal Liver Lesion

X. Xie

Objectives: ShearWave Elastography evaluation for differential diagnosis of focal liver lesion

Methods: From Feb 2012 to Aug 2013, a total of 148 patients (101 males, 47 females, mean age 48.7 years, range 17.0–90.0 years) with 151 lesions(mean diameter: 5.6±3.2 cm, range 1.0-15.4 cm)including hepatocellular carcinoma(HCC, n=75), intrahepatic cholangiocarcinoma(ICC, n=14), metastasis liver cancer(MLC, n=24), hemangioma (n=31), focal nodular hyperplasia(FNH, n=11) were studied. Mean, max and standard deviation SWE values of both lesion and adjacent liver parenchyma were measured. All parameters were expressed as kPa. Compared the difference between malignant and benign group as well as between each two groups, and ROC curve was used to determine the optimal cut-off point for differential diagnosis malignant from benign lesions.

Results: Mean, max and standard deviation SWE value of malignant lesions were higher than those of benign ones(45.40 ± 20.83 Vs 18.12 ± 11.80, 77.75 ± 40.67 Vs 23.55 ± 13.82, 12.08 ± 9.01 Vs 2.75 ± 1.85) (P<0.001). Mean, max and standard deviation SWE value of HCC (38.63 ± 11.75, 64.64 ± 30.05, 9.61 ± 5.97) was less than those of ICC (57.86 ± 15.45, 113.68 ± 8.07, 14.45 ± 7.70) (P<0.01) and MLC (59.28 ± 33.00, 100.7 ± 52.46, 18.23 ± 13.60) (P<0.01), whereas no significant difference was found between MLC and ICC for all three parameters. Max and standard deviation SWE value of FNH (37.52 ± 12.78, 3.54 ± 1.96) were less than those of HCC (P<0.001), although mean SWE value did not show significantly different. Mean (30.62 ± 11.93) and max SWE value of FNH were higher than those of hemangioma (13.68 ± 8.07, 18.89 ± 10.79) (P<0.001), whereas standard deviation did not show significantly difference. All lesions were stiffer than adjacent liver parenchyma (P<0.001). Adjacent liver parenchyma of HCC was stiffer than which of MLC, hemangioma and FNH (P<0.05). For differentiation malignant from benign FLLs, area under ROC curve of mean, max and standard deviation SWE value of lesion were 0.909, 0.957, 0.956, respectively. Taking 24.82(mean), 39.28(max), 5.35(standard deviation) as cut-off point, sensitivity and specificity were 93.81% and 76.19%, 90.57% and 85.00%, 84.62% and 92.50%, respectively.

Conclusions: SWE could quantitatively analyze elasticity characteristics of FLLs, especially max and standard deviation SWE value could provide more information for differential diagnosis between malignant and benign lesions as well as between HCC and other types of tumour.

Poster 49: Percutaneous Microwave Ablation for Hepatocellular Carcinoma: Safety and Efficacy of a 4-Year Experience Treating 150 Tumors

T. Ziemlewicz, J. Hinshaw, M. Lubner, S.A. Wells, C. Brace, M. Alexander, P. Agarwal, F. Lee

Objectives: Microwave ablation has demonstrated promise in preliminary studies evaluating treatment of hepatocellular carcinoma (HCC). The purpose of this study is to evaluate a 4-year experience in 102 patients with hepatocellular carcinoma (HCC) treated with a high-power, gas-cooled MW device at a single center.

Methods: Between December 2010 and September 2014 150 treatment-naive HCCs were treated in 111 sessions in 102 BCLC stage A patients via a percutaneous approach utilizing US and/or CT guidance. There were 84 male and 20 female patients with mean age of 62.0 years (range 48-82). All procedures were performed with a high-powered, gas-cooled microwave system (Certus 140, Neuwave Medical, Madison, WI). Mean power per antenna was 73 Watts (range 35-140 Watts) with mean of 1.7 antennas (range 1-3 antennas) used per case for a mean total ablation time of 5.1 minutes (range 1-12.5 minutes).

Results: Tumors ranged in size from 0.5 to 4.2 cm (mean 2.1 cm) and median follow-up was 15 months (range 3-48 months). Technical success was achieved in 99.3% 149/150 of tumors in a single session with a tumor requiring 2 treatments due to inadequate needle length along the planned path at the initial procedure. Primary treatment effectiveness was 94.0% (141/150), 93.9% (124/132) for tumors < 3 cm, 100% (16/16) for tumors 3-4 cm, and 50% (1/2) for tumors > 4 cm. Of the 9 tumor progressions, 3 were treated with repeat ablation, 2 were noted at explant pathology, and 4 were treated with intra-arterial therapy as they were abutting an adjacent critical structure precluding more aggressive ablation (1 tumor), or multifocal HCC had developed in the interval (3 tumors). Distant intrahepatic progression occurred in 23.5% of patients during the follow-up period with 9 patients undergoing repeat ablation, 11 developing multifocal disease treated with intra-arterial or systemic therapy, and 3 not undergoing further treatment due to compromised liver function. A single major complication occurred (0.9%), a pneumothorax following needle placement that was successfully treated during the course of the procedure with a pleural blood patch. There was no procedure related mortality. Overall survival is 80.4% with most deaths related to end stage liver disease (n=12) or multifocal HCC (n=5).

Conclusions: Treating hepatocellular carcinoma using percutaneous microwave ablation is safe with effectiveness comparable or improved from radiofrequency ablation when compared with historical controls.

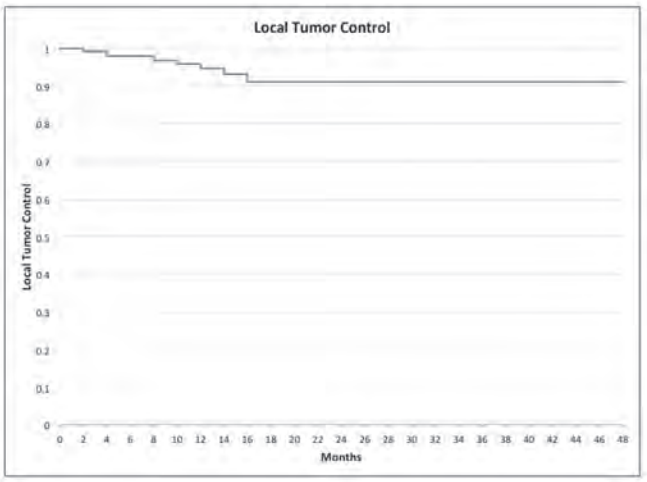

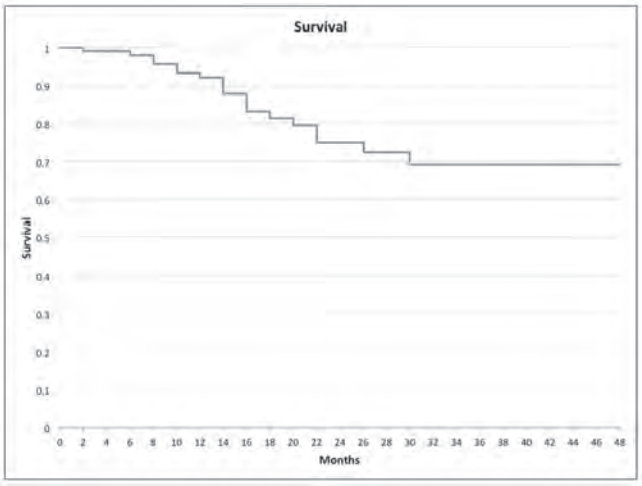

Poster 50: Hepatitis C is an Independent Predictor of Increased Sedation Requirements during Trans-Arterial Chemoembolization

T.J. Ward, T. Techasith, D.S. Wang, N. Kothary, J.D. Louie, G.L. Hwang, D.Y. Sze

Objectives: Trans-arterial chemoembolization (TACE) is routinely performed under moderate sedation on a heterogeneous patient population with a wide range of tolerance and ability to metabolize sedative agents. We performed multivariate analysis of factors predictive of sedation requirements during TACE.
Methods: TACE procedures performed for the treatment of HCC under moderate sedation between August 1, 2013 and July 31, 2014 were retrospectively reviewed. Sedatives were titrated to minimize pain and anxiety while maintaining the patent's ability to cooperate with breathing instructions. Stepwise multiple linear regression analysis was performed on factors potentially predictive of administered fentanyl and midazolam doses. Variables tested included age, sex, height, weight, body-mass index, outpatient narcotic or benzodiazepine use, etiology of liver disease, largest tumor size, number of treated lesions or segments, chemotherapy dose, drug carrier for TACE, and number of previous TACE. Independent t- and χ-2 tests were performed on continuous data and categorical data.
Results: 246 procedures were reviewed. 72% of patients were male, mean age was 64.8 ± 10.1. Mean dose of fentanyl was 147 ± 68; range 25-450 mcg. Parameters that correlated with fentanyl dose included outpatient benzodiazepine use, hepatitis C (HCV), weight, and male sex (adjusted R2=0.18). Mean dose of midazolam was 2.4 ± 1.2; range 0.5-7.0 mg. Parameters that correlated with midazolam dose included outpatient benzodiazepine use, male sex, HCV, weight, and outpatient narcotic use (adjusted R2=0.22). HCV proved to be an independent predictor of higher dose requirements. No significant differences were found in outpatient narcotic (21.4% vs 17.4%; P=0.43) and benzodiazepine (3.8% vs 9.6%; P=0.07) use between patients with HCV and other etiologies. Mean fentanyl and midazolam doses in patients with HCV (162 ± 70 mcg, 2.6 +/- 1.2 mg) were significantly higher than those with other etiologies (131 ± 63 mcg, 2.2 ± 1.2 mg; P<0.001, P=0.003).
Conclusions: Hepatitis C liver disease is an independent predictor of increased sedation requirements during TACE, and interventional oncologists should be prepared to accommodate this proactively.

Poster 51: Safety and Effectiveness of Irreversible Electroporation for Perihilar Hepatocellular Carcinoma as an Outpatient; The Canadian Experience

R. Beecroft

Objectives: To determine the safety (as an outpatient procedure) and short term efficacy of irreversible electroporation (IRE) in the treatment of hepatocellular carcinoma (HCC) in perihilar location (< 5 mm from main right / left biliary ducts or portal veins) that prohibits thermal ablations.
Methods: Over 17 month period, 6 patients (average age 62.5 years, range 52-72 years) with perihilar HCC (average size 1.6 cm [1.1-1.9 cm]) by diagnostic imaging criteria that were situated in close proximity (<5 mm) to central biliary structures and/or central portal veins, and for whom it was felt thermal ablation was contraindicated given risks of thermal injury, underwent IRE. Efficacy was assessed with contrast CT immediately following IRE, then CT or MRI 1 month post IRE, then every 3-4 months, with clinic visits.
Results: Technical success 100%. Primary treatment effectiveness (or local recurrence free survival) 100 %, average follow-up 7.2 months (0-17months). Complications 0%; specifically no biliary or vascular related complications (i.e. no vascular thrombosis or biliary dilatation). All patients were discharged home the same day, with no readmissions. 50% (3) patients developed HCC remote from the site of IRE post ablation which were intrahepatic and treated with RFA in 2, and the third was referred for systemic therapy for pulmonary metastatic disease.
Conclusions: IRE for perihilar HCC demonstrates good short term efficacy, is safe with regards to biliary and vascular structures, and can be performed as outpatient.

Poster 52: High Risk TACE in Liver Cancer Patients with Portal Vein Thrombosis

M. Mizandari, T. Azrumelashvili, N. Habib

Objectives: To present the experience of portal vein thrombosis (PVT) patients embolization including the technique of the portal vein recanalization by a novel endovascular radiofrequency (RF) catheter for portal vein thrombosis
Methods: The recanalization procedure was performed to 5 patients with liver cancer, complicated with PVT; the tumor thrombus caused the main portal vein (MPV), left pertal vein (LPV) and right posterior portal vein (RPPV) occlusion -1 case, right portal vein (RPV) - 3, RPV and LPV partial occlusion - 1 case. DEB TACE has been performed to 4 patients and lipiodol TACE in rest case. PV Percutaneous recanalization was performed in 2 cases; it was fulfilled to reconnect the peripheral LPV with MPV in one case and to recconect the right anterior portal vein (RAPV) with PV confluence in the other. The recanalization was performed using an endovascular bipolar radiofrequency device; Using both sedation and local anaesthesia, an 18G puncture needle accommodating a 0.035 inch guidewire was introduced into a tributary of the portal vein through which the guide wire was introduced through the thrombus into the portal vein confluence/SMV after manipulation by 5 FR diameter guide catheter under the guidance of digital subtraction angiography (DSA). The endovascular radiofrequency device was inserted into the thrombus. The device was then connected to a radiofrequency generator for radiofrequency ablation (RFA) at 10 watts for a duration of 2 minutes followed by vascular stent placement. The procedure was completed by portography. TACE was performed using conventional technique
Results: Post RFA portography showed significant improvement of the portal vein patency with restoration of blood flow into the liver; no intra- or postprocedure complications were observed . All patients tolerated the TACE procedure well; in one case postembolization abscess formation was documented, managed by percutaneous drainage.
Conclusions: Selected liver cancer patients with PVT might be successfully treated by TACE. The endovascular RFA and stenting is a safe and efficient technique, which can be used as a bridge to TACE procedure.

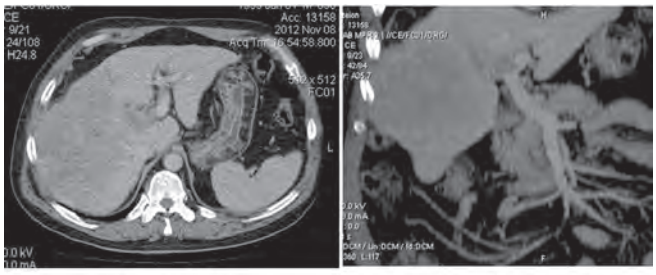

Thrombus in MPV Thrombus in LPV

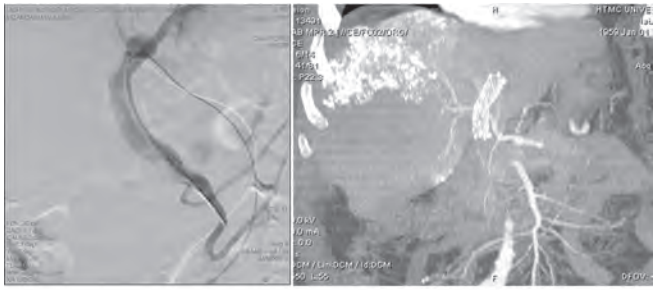

Portography after thrombus recanalization by RFA and stent placement

CT after lipiodol TACE, stent is Identified by arrow

Poster 53: Safety and Efficacy of Percutaneous Cryoablation for Treatment of Hepatocellular Carcinoma; Initial Experience

S. Lee, J. Won, K. Kim, M. Kim, S. Park, D. Lee

Objectives: To evaluate the efficacy and safety of percutaneous cryoablation for the treatment of hepatocellular carcinoma (HCC)
Methods: Between Sep 2013 and Nov 2014, 21 cryoablation for HCCs were conducted in 21 patients. The patients mean age was 64.7 years (range 49-77). Follow up period of patients was 166.5 days (range 20-422). Average of 1.9 cryoablation probes (range 1-4) were used to achieve at least 5mm of safety margin. All procedures were conducted under US (n=19) or CT (n=2) guidance. Size and location of tumor and adjacent organ, complication rate, initial treatment success, and local tumor recurrence were evaluated.
Results: Average of maximum diameter of tumor was 19.7mm (range 10-45mm). Location of tumors were as follows; 13 subcapsular (capsular abutting), 4 exophytic, and 4 intrahepatic. Adjacent organ of subcapsular or exophytic lesion were stomach (n=5), colon (n=2), kidney (n=3), gallbladder (n=3), diaphragm (n=1). Complete tumor ablation was achieved in all patients. Local tumor recurrence occurred in one patient (4.7%). No peritoneal seeding metastasis occurred. Procedure related complication occurred in 4 patients (19.5%) and was managed conservatively; small hemoperitoneum (n=2), right pleural effusion (n=1), segmental portal vein thrombosis (n=1). There was no severe complication requiring additional treatment. No adjacent organ injury occurred in subcapsular or exophytic HCCs.
Conclusions: Percutaneous cryoablation is safe and effective treatment for HCC, even for exophytic or subcapsular tumor.

Poster 54: Effect of Neoadjuvant Locoregional Therapy on Outcomes of Orthotopic Liver Transplant for Hepatocellular Carcinoma

G.J. Nadolski, N. Harrison, E. Mills-Robertson, T.P. Gade, M.C. Soulen, S.J. Hunt

Objectives: Patients with hepatocellular carcinoma (HCC) who are listed for liver transplant (OLT) commonly receive neoadjuvant locoregional therapy (LRT) to treat the tumor while awaiting OLT. A retrospective cohort study was performed to compare transplant related outcomes of patients with HCC listed for OLT treated with LRT to those who do not receive LRT.
Methods: Review of the OTTR database was used to identify patients evaluated in multidisciplinary liver tumor clinic listed for OLT with HCC (1998-2010). Number and size of tumors, severity of liver disease, type of LRT, OLT waitlist time and outcome, and date of death were recorded. Survival from time of HCC diagnosis was analyzed using Cox proportional hazard ratios.
Results: 373 patients met inclusion criteria; 206 received LRT (Group 1) and 167 did not (Group 2). Results are summarized in Table 1. Median length of follow up was 1900 days. In Group 1, type of LRT included 148 TACE, 28 RFA, 17 TACE plus RFA, and 13 other. Severity of liver disease and number of HCC were similar. Tumors in the LRT group were slightly larger at time of diagnosis (30 vs 27 mm; p=0.02). Median time on wait list was significantly longer in the LRT group (132 vs 76 days; P<0.01). Proportion of patients transplanted did not differ (79% vs 83%, LRT vs no LRT; P=0.4). As a whole, intention to treat overall survival from HCC diagnosis did not differ between groups (1895 vs 1952 days, LRT vs no LRT, HR 0.95; p=0.7). However, in patients with largest tumor diameter ≥38 mm, LRT was associated with a significantly longer median overall survival of 1838 days compared to 900 days for those who did not receive LRT(HR=0.42, CI=0.22-0.79, P<0.01).
Conclusions: Despite longer OLT wait list times and slightly larger tumors, patients with HCC on the OLT wait list treated with LRT have similar transplantation rate and overall survival compared to listed HCC patients not treated with LRT. Subgroup analysis suggests patients with larger tumor diameters have improved survival with LRT.

Table 1

	Median Age (years)	Male Gender	Calculated MELD @ diagnosis	Mean longest diameter @ diagnosis (mm)	Median number of tumors	Median time on Wait List (days)	Frequency of Transplantation	Median OS from Diagnosis (days)
LRT (N=206)	56±8	174 (84%)	10±4	30±0.8	1±0.8	132±253	163 (79%)	1895±1285
No LRT (N=167)	55±8	135 (81%)	12±6	27±0.9	1±0.7	76±182	137 (83%)	1952±1555
p value	p=0.7	p=0.4	p=0.6	p=0.02	p=0.09	p<0.01	p=0.4	p=0.7

Poster 55: Does Drug Eluting Beads Size Correlate with Degree of Tumor Necrosis? : A Retrospective Study from Single Institute Experience

V. Klungboonkrong, J. Bullen, S. Bennett, B. Kapoor, I. Haddadin, A. Levitin, H. Koji, M. Fujiki, B. Eghtesad, D. Kelly, C. Quintini, F. Aucejo, L. Yerian, D. Allende, X. Liu, A. Bennett, D. Patil, T. Plesec, R. Tuthill, G. Amanjit, G. McLennan

Objectives: To determine the difference in percent tumor necrosis between three bead size categories used to treat hepatocellular carcinoma in patients awaiting liver transplant.
Methods: From 1/1/2007 through 6/30/2014, a retrospective study of 46 patients with hepatocellular carcinoma receiving drug eluting beads to downstage or bridge to transplant was performed. The percent tumor necrosis was evaluated from surgical pathology reports and categorized by ranges of 0-25%, 26-50%, 51-75% and 76-100%. Wilcoxon rank sum test was used to assess pairwise differences in tumor necrosis percentage among the three bead size categories and to compare the tumor necrosis percentage between single and combined size beads.
Results: Beads used were 70-150 μm in 7 patients, 100-300 μm in 21 patients and 300-500 μm in 11 patients. Seven patients had multiple sizes. 71.4% of patients who received 70-150 μm beads had >50% necrosis while only 52% & 45% did in the 100-300 μm & 300-500 μm groups. This was not statistically significant (P = 0.999 for 70-150 vs 100-300 and P = 0.776 for 70-150 vs 300-500). 85.7% of patients receiving combined therapy had > 50% necrosis but, compared to patients with single size beads, this was not statistically significant (P = 0.184). A sample size estimate based on a one-way ANOVA with bead size category as the independent variable and tumor necrosis percentage as the dependent variable suggests that a study with 180 subjects per group would have 80% power to detect a difference similar to the one observed in this sample among the bead size categories with respect to tumor necrosis percentage.
Conclusions: Tumor necrosis percentage tended to be higher in patients receiving bead size 70-150 microns and in patients receiving combined size beads. However both results were not statistically significant due to limited sample size. Further study with at least 180 subjects per group would allow comparison of tumor necrosis between different sizes of beads used for DEB.

Poster 56: Safety of Drug-Eluting Beads Chemoembolization in Patients with Pre-existing Transjugular Intrahepatic Portosystemic Shunt

A. Pirasteh, K. Rief, A. Shenoy-Bhangle, S. Ganguli, S. Kalva

Objectives: Transarterial chemoembolization with drug-eluting beads (DEB-TACE) has been shown to be at least as effective as and safer than conventional TACE, especially in high risk populations with inoperable hepatocellular carcinoma (HCC). Many cirrhotic patients with symptomatic sequelae of portal hypertension undergo a transjugular intrahepatic portosystemic shunt (TIPS) placement, which results in significant shunting of the portal venous blood flow in to the systemic veins with associated compensatory increase in the hepatic arterial blood flow to the normal liver parenchyma. In theory, this suggests an increased theoretical risk of post-TACE hepatic dysfunction. This study was designed to retrospectively assess the safety of DEB-TACE in this population.
Methods: Records of patients with a patent TIPS who underwent DEB-TACE for inoperable HCC from 2005 to 2014 at two institutions were reviewed. Patient demographics, number of procedures, extent of embolization (lobar vs segmental), 30-day mortality, and post-procedure adverse events classified based on Common Terminology Criteria for Adverse Events (CTCAE V4.03) were recorded.
Results: Ten patients (6 male, average age 59) with a patent TIPS underwent 14 DEB-TACE procedures. TIPS to TACE period range was 4 days to 17 years. The underlying liver disease included hemochromatosis (n=2), chronic hepatitis B (n=2), combined chronic hepatitis C with alcoholic cirrhosis (n=2), alcoholic cirrhosis (n=3), and non-alcoholic steatohepatitis (n=1). Patients belonged to Child-Pugh class A or B. Number of procedures per patient ranged from 1-4, with a median of 1 TACE per patient. Four patients underwent lobar embolization (7 procedures), and the rest were segmental (Table 1). Median post-procedure hospital stay was 2 days (range 2-8) for lobar TACE and 2 days (range 1-2) for segmental TACE. There were no deaths within 30 days of the procedure. One patient who underwent lobar embolization required a 5-day hospitalization for acute necrotizing pancreatitis, upper GI bleed, and liver toxicity – CTCAE grades 4, 3, and 4, respectively. Another patient who underwent lobar

embolization required an 8-day hospitalization for grade-4 liver toxicity. One patient who underwent segmental embolization experienced a normal post procedure stay, however was admitted two weeks later for sepsis and a hepatic abscess. Less severe adverse events which did not result in prolonged hospital stay are listed in Table 1.

Conclusions: Segmental DEB-TACE is a well-tolerated option for non-operative HCC in patients with pre-existing TIPS; complications are more likely to be seen in the setting of lobar embolization. Three of 10 patients had significant adverse events requiring prolonged hospitalization or readmission, two of which had undergone lobar embolization. These patients were successfully managed with supportive measures and discharged home. The study limitations include its retrospective nature, a small cohort, and lack of a comparable group of patients without TIPS who underwent the similar procedure.

Table 1: Patient Information, Procedure Details, and Adverse Events

Patient	Age / sex	Number of TACE	Lobar vs Segmental	Hospital stay post each TACE (days)	Significant Adverse Events (CTCAE grade)
1	39 / M	1	Segmental	1	Transient elevation of alkaline phosphatase (1)
2	56 / M	1	Segmental	2	None
3	52 / F	1	Lobar	5	- Necrotizing pancreatitis (4) - Liver toxicity (4) - Upper GI bleed (3)
4	71 / F	1	Segmental	1	- None immediate - Hepatic abscess two weeks post procedure (3)
5	56 / M	1	Segmental	1	- Transient bilirubin rise (2) - Transient, mild transaminitis (1)
6	74 / F	4	Lobar x 4	2,3,2,2	None
7	50 / F	1	Lobar	8	Liver toxicity (4)
8	60 / M	2	Segmental x 2	2,2	None
9	70 / M	1	Lobar	2	Transient azotemia (2)
10	64 / M	1	Segmental	2	None

Poster 57: Effect of Oral Antiviral Treatment on the Prognosis of Hepatitis B Virus-Related Hepatocellular Carcinoma after Radiofrequency Ablation Therapy: A Propensity Score Analysis

T. Kang, H. Rhim

Objectives: Recent studies showed that antiviral treatment improves the clinical outcomes of the patients with chronic hepatitis B. This study was aimed to investigate the effect of oral antiviral treatment on the prognosis of hepatitis B virus (HBV)-related hepatocellular carcinoma (HCC) after radiofrequency ablation (RFA) therapy.

Methods: Between January 2003 and December 2010, 228 patients who did not receive antiviral treatment prior to ablation were treated with RFA for a single HBV-related HCC. We divided the patients into two groups, patients with antiviral treatment (n=125) or patients without (n=103), based on whether antiviral treatment was received after RFA. After propensity score matching, long–term recurrence-free and overall survival were compared between both groups. Tumor recurrence was defined as intrahepatic distant and extrahepatic recurrence. We also assessed risk factors for HCC recurrence and overall survival after RFA in matched data.

Results: The cumulative recurrence-free survival rates at 5 year were 14.7% for non-antiviral treatment group and 43.8% for antiviral treatment group, respectively (P<0.001). The overall survival rates at 5 year were 77.2% for non-antiviral treatment group and 93.5% for antiviral treatment group, respectively (P=0.002). A multivariable analysis showed that risk factors for HCC recurrence were a lower level of albumin (hazard ratio (HR)=0.62, P=0.010), tumor size (HR=1.40, P=0.014), and HBeAg positive (HR=1.54, P=0.029). Overall survival were associated with Child-Pugh class B (HR=2.85, P=0.004), and tumor size (HR=1.59, P=0.036). In addition, post-RFA oral antiviral treatment was significantly associated with tumor recurrence and overall survival, respectively (HR=0.32, P<0.001, and HR=0.31, P=0.001).

Conclusions: Use of oral antiviral treatment induced a favorable outcome in terms of tumor recurrence and overall survival in patients with HBV-related HCC after RFA therapy.

Table 1. Baseline characteristics of all patients (n=228).

	All patients (n=228)	Post-RFA antiviral treatment (-) (n=103)	Post-RFA antiviral treatment (+) (n=125)	P-value
Age (years)	55.1 ± 8.9	55.2 ± 8.9	55.0 ± 8.9	0.856
Gender				0.328
women	58 (25%)	23 (22%)	35 (28%)	
men	170 (75%)	80 (78%)	90 (72%)	
Tumor size (cm)	2.2 ± 0.7	2.1 ± 0.6	2.2 ± 0.7	0.464
Platelet count (x10³/mm²)	111.0 ± 46.9	111.9 ± 48.5	110.2 ± 45.7	0.792
Prothrombin time (INR)	1.22 ± 0.15	1.21 ± 0.14	1.23 ± 0.16	0.347
Albumin (g/dL)	3.6 ± 0.5	3.6 ± 0.5	3.6 ± 0.6	0.557
Total bilirubin (mg/dL)	1.0 ± 0.6	1.0 ± 0.6	1.0 ± 0.6	0.721
AST (U/L)	49.2 ± 28.3	43.1 ± 21.9	54.2 ± 31.8	0.002
ALT (U/L)	45.2 ± 38.9	36.9 ± 32.3	52.1 ± 42.5	0.003
Log_{10}HBV DNA (IU/mL)	4.1 ± 2.6	2.8 ± 2.6	5.3 ± 2.0	<0.001
AFP (ng/mL)				0.007
<20	104 (46%)	57 (55%)	47 (38%)	
≥20	124 (54%)	46 (45%)	78 (62%)	
HBeAg (N, %)				<0.001
negative	144 (63%)	80 (78%)	64 (51%)	
positive	84 (37%)	23 (22%)	61 (49%)	
Liver cirrhosis (N, %)				0.953
absence	38 (17%)	17 (17%)	21 (17%)	
presence	190 (83%)	86 (83%)	104 (83%)	
Child-Pugh class (N, %)				0.661
A	193 (85%)	86 (83%)	107 (86%)	
B	35 (15%)	17 (17%)	18 (14%)	

Abbreviations: RFA, radiofrequency ablation; INR, international normalized ratio; AST, aspartate aminotransferase; ALT, alanine aminotransferase; HBV, hepatitis B virus; AFP, alpha-fetoprotein; HBeAg, hepatitis B virus envelope antigen

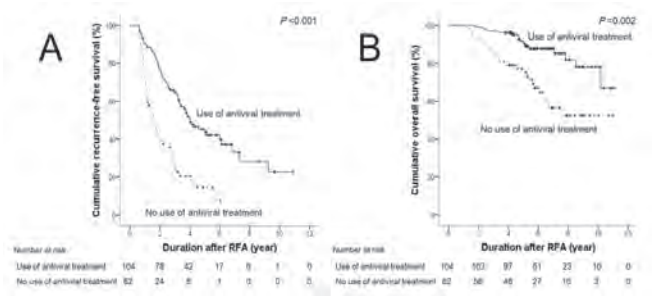

The difference of recurrence-free survival (A) and overall survival (B) according to post-RFA antiviral treatment after propensity score matching.

Poster 58: A Prospective Study of Smaller Caliber Drug-Eluting Beads in Transarterial Chemoembolization: Preliminary Results of Tumor Response and Safety for the Treatment of Hepatocellular Carcinoma

S. Sahu, R. Duran, R. Schernthaner, E. Funai, F. Fleckenstein, Y. Zhao, J. Sohn, M. Lin, J. Geschwind

Objectives: Drug-eluting beads transarterial chemoembolization (DEB-TACE) is commonly used for the treatment of unresectable hepatocellular carcinoma (HCC) and beads typically are 100-700 μm in size. Recently, there has been a growing interest in smaller caliber beads (70-150 μm) which can potentially penetrate deeper into the tumor. In this ongoing prospective clinical study, we examined the safety and efficacy of novel, small caliber drug-eluting beads after the first DEB-TACE.

Methods: In this HIPPA compliant, IRB approved, single center prospective trial, 23 patients with HCC were included and underwent DEB-TACE using 70-150 μm doxorubicin-eluting beads (M1, BTG, Surrey, United Kingdom). Inclusion criteria was the following: adequate hematologic function (absolute neutrophil count ≥ 1500/mL, hemoglobin ≥ 9.5 g/dL, platelet count ≥ 50,000/mL, and INR < 1.5), adequate hepatic function (total bilirubin ≥ 3.0 mg/dL and AST and ALT ≤ 8 x the upper limit of normal), serum creatinine ≤ 2.0, BCLC A-C, Child-Pugh A-B, ECOG 0-2 and intra-arterial treatment naïve. Tumor response was assessed by modified Response Evaluation Criteria in Solid Tumors (mRECIST), European Association for the Study of the Liver (EASL), and volumetric tumor enhancement [quantitative EASL (qEASL)] on T1-weighted contrast-enhanced MR at baseline and 1 month post M1 DEB-TACE. qEASL response was defined as ≥65% decrease in volumetric tumor enhancement. Toxicities after the first DEB-TACE were reported using CTCAE V4.0.

Results: The median age was 62 years (range, 34-80) and 20 (87%) patients were men. The number of patients with BCLC A/B/C were 6 (26.1%)/10 (43.5%)/7 (30.4%), Child-Pugh A/B were 18 (78.3%)/5 (21.7%), and ECOG 0/1/2 were 15 (65.2%)/7 (30.4%)/1 (4.3%). Baseline mean mRECIST, EASL, and qEASL were 6.1 ± 3.9cm, 12.6 ± 12.1cm2, and 62.1 ± 34.5%, respectively. After M1 DEB-TACE, mRECIST, EASL, and qEASL decreased to 2.7 ± 2.2cm, 10.6 ± 16.4cm2, and 30.0 ± 27.7%, respectively. Tumor response was seen in 10 (43.5%) patients according to mRECIST and EASL (9/10 patients were the same) and 9 (39.1%) patients using qEASL. There were no serious adverse events. 2 patients had grade 3 toxicities which included elevated AST and hyponatremia. 3 patients had toxicities 30 days after the first DEB-TACE that were probably device related [hypoalbuminemia (n=2), luekopenia (n=1), anemia (n=1), elevated AP (n=2)] and 2 patients had toxicities that were possibly device related [headache (n=2) and weight loss (n=1)].

Conclusions: Smaller caliber beads for DEB-TACE are well tolerated and have good short-term tumor response on preliminary analysis.

Poster 59: Prognostic Effect of Arterioportal Shunt in Radioembolization Using Yttrium-90 Resin Microspheres for Hepatocellular Carcinoma with Portal Vein Thrombosis - a Single Center Study

E. Jung, Y. Kim, S. Cho

Objectives: The aim of this study was to analyze a prognostic effect of the arterioportal (AP) shunt in Yttrium-90 (Y90) radioembolization for hepatocellular carcinoma (HCC) with portal vein thrombosis (PVT).
Methods: A total of 20 patients with HCC and PVT were treated with Y90 radioembolization between 12/2008 and 04/2014. Each target lesions were divided in two groups which tumors with or without AP shunts. The HCCs in same areas of the AP shunt were considered as same lesion, and the HCCs without AP shunt in same patient were considered as same lesion. Radiological tumor response of the target lesions was assessed using modified Response Evaluation Criteria in Solid Tumors (mRECIST). Uni/multivariate analyses were performed.
Results: Eleven target lesions were with AP shunts and 14 target lesions were without AP shunt. Target lesions with AP shunts show 6 (54.5%) partial response (PR), 2 (18.2%) stable disease (SD) and 3 (27.3%) progressive disease (PD). Target lesions without AP shunt show 1 (7.1%) complete response (CR), 7 (50.0%) PR, 3 (21.4%) SD and 3 (21.4%) PD. Disease control rates (CR+PR+SD) of target lesions with or without AP shunts were 72.7% and 78.6%, each (P=0.420).
Conclusions: The presence or absence of the AP shunts in the target lesions was not a significant prognostic factor in patients with HCC and PVT. But prospective study with more number of the patients is possible, the result could be changed.

Poster 60: Use of an Anti-Reflux Microcatheter During DEB-TACE after Failed Response to Initial DEB-TACE: Early Experience at Single Center

G. Sivananthan, M. Edwards, R.A. Lookstein, E. Kim, R.S. Patel, F.S. Nowakowski, N.E. Tabori, A.M. Fischman

Objectives: The Surefire anti-reflux microcatheter (ARM) (Surefire Medical, Westminster, CO) has been shown to increase tumor penetration by changing tumor interstitial pressure during chemoembolization (1,2). The purpose of this study is to evaluate tumor response following drug eluting bead transarterial chemoembolization (DEB-TACE) utilizing an ARM after failure to achieve objective response during initial DEB-TACE with a standard microcatheter.
Methods: From 5/2013 to 11/2014, 8 patients with BCLC B HCC that had utilized an ARM during DEB-TACE to increase tumor penetration were identified. Of these, 5 patients (mean age 65+-6.89 years) had received prior DEB-TACE with failure to achieve objective response (CR+PR) by mRECIST criteria. Patient demographics, tumor characteristics, technical parameters, tumor response using mRECIST criteria and adverse events were reviewed. All patients underwent DEB-TACE using 100-300 (n=4) or 300-500 (n=1) LC Beads (BTG, Surrey, UK) loaded with 50 mg of doxorubicin.
Results: Baseline tumor characteristics included a single target lesion in each patient and mean lesion size 2.4 +- 0.9 cm. 100% technical success was noted with the ARM during DEB-TACE (5/5). 80% of patients with stable disease after initial DEB-TACE had a radiologic response (partial or complete response) after DEB-TACE with ARM. There remaining patient had no change in response after DEB-TACE with ARM. There was no progressive disease in this cohort. 2/5 patients had post embolization syndrome relieved by oral narcotics. There was no change in total bilirubin, Child Pugh Score, ascites or encephalopathy after DEB-TACE with ARM.
Conclusions: DEB-TACE with ARM is feasible and safe. In patients failing to respond to initial DEB-TACE, use of an ARM was moderately successful at achieving objective response. Further larger scale studies are needed.

Poster 61: Efficacy of Y-90 Radioembolization for BCLC Stage C Hepatocellular Carcinoma

R. Schenning, J. Harrison, Y. Jahangiri Noudeh, K. Kolbeck, J. Kaufman, K. Farsad

Objectives: Patients with advanced hepatocellular carcinoma (HCC) have few therapeutic options according to current treatment algorithms. The Barcelona Clinic Liver Cancer (BCLC) staging system recommends that patients with advanced HCC (BCLC stage C) be treated with systemic sorafenib, supported by the results of the SHARP trial (Llovet et al., NEJM 2008). At our institution, we often treat patients with advanced HCC and preserved liver function with transarterial Y90 radioembolization as an alternative to sorafenib due to better tolerated systemic toxicity. We examined the efficacy of this approach by reviewing our experience.
Methods: An IRB-approved single institution database of patients treated with Y90 radioembolization was retrospectively reviewed for patients treated for HCC from September 2004 to March 2014. Exclusion criteria included history of systemic sorafenib therapy, prior transarterial chemoembolization (TACE), prior ablation, and living patients without at least 6 months clinical follow-up. Patients treated for BCLC stage C disease were evaluated for survival. Patients who underwent Y90 to the dominant disease burden with subsequent TACE to non-dominant disease were also included in the analysis. The primary outcome was overall survival. Six-month, 1-year and 2-year survival rates were calculated using a Kaplan-Meier life-table, and the Wilcoxon test was used to compare survival between different groups of patients.
Results: 93 patients were treated with Y90 radioembolization for HCC. Median follow-up time was 11.2 months (1.4 – 46.6 months). 50 patients who met study criteria were treated for BCLC stage C disease, of whom 35 (70%) had underlying hepatitis C-related liver disease. BCLC C patients were further categorized into those with Child-Pugh A (n=33) and Child-Pugh B (n=17) class liver disease. Patients were treated with Y90 radioembolization alone (n=25) or radioembolization in combination with subsequent liver-directed therapies to non-dominant disease (n=25). Median overall survival was 14.8 months, with 6-month, 1-year, and 2-year survival rates of 74.0%, 51.4% and 20.4%, respectively. Patients with underlying Child-Pugh class A liver disease demonstrated significantly improved survival relative to patients with Child-Pugh class B liver disease (median survival, 6-month, 1-year and 2-year survival rates: 15.7 months, 81.8%, 60.2% and 24.1% in CP class A vs. 7.8 months, 58.8%, 34.1% and 12.8% in CP class B; P=0.047). Survival rates were not significantly different between patients treated with Y90 alone vs. Y90 with additional liver-directed therapy to non-dominant disease (P=0.299).
Conclusions: Y90 radioembolization is an effective treatment for patients with advanced (BCLC C) HCC and compensated liver disease. Our results are comparable to those reported for systemic therapy with sorafenib and support Y90 radioembolization for advanced HCC as an alternative therapy for patients unable to tolerate the systemic toxicities of sorafenib.

Poster 62: Baseline Evaluation of Hepatocellular Carcinoma: Does Tumor Burden Measured by 3D Quantitative Tumor Enhancement Analysis on MRI Predict Overall Survival?

F.N. Fleckenstein, R. Duran, J. Chapiro, R. Schernthaner, J. Sohn, S. Sahu, Y. Zhao, L. Zhao, M. Lin, J. Geschwind

Objectives: To evaluate in a preliminary study if assessment of tumor burden at baseline can predict overall survival in patients with hepatocellular carcinoma (HCC) treated with transarterial chemoembolization (TACE).
Methods: 27 patients (22 male, mean age 66 ±10 years) with 41 HCC lesions treated with TACE were retrospectively included. All patients were naïve to therapy and underwent baseline multiphasic contrast-enhanced MRI. A whole liver semi-automatic segmentation software was used on the unenhanced phase of the MR to measure liver volume. Volumetric tumor enhancement (VTE) values of tumor lesions were obtained on the arterial phase of the MR using 3D semi-automatic software. VTE (expressed in cm^3) was converted to z-scores through normalization (nVTE). Furthermore, VTE values were related to each patient's whole liver volume, thus calculating the relative tumor burden (RTB). Overall survival time was defined as date of baseline MRI to death. Univariate Cox regressions with log-rank test were created for nVTE and RTB.
Results: 19 patients (70%) had single lesions, 3 patients (11%) had 2 lesions and 5 patients (19%) showed 3 or more lesions. Mean liver volume was 1836.5cm^3 (range, 988.5 to 3887.9cm^3). Mean VTE was 121.9cm^3 (range 2.2-505.2cm^3) resulting in a mean RTB of 6.0±5.3% (range, 0.18-18.1%). Mean overall survival of the cohort was 30.9 months (range, 3-78 months). The Cox regression for survival prediction showed a highly significant correlation between tumor burden and overall survival (nVTE (HR 2.83; P<0.001) and RTB (HR 1.25; P<0.001)).
Conclusions: These preliminary results showed a highly significant correlation between total tumor burden and overall survival. 3D quantitative tumor enhancement analysis on baseline MRI could be a strong predictor of overall survival and a new staging marker at diagnostic of HCC. Work is underway with a larger patient cohort.

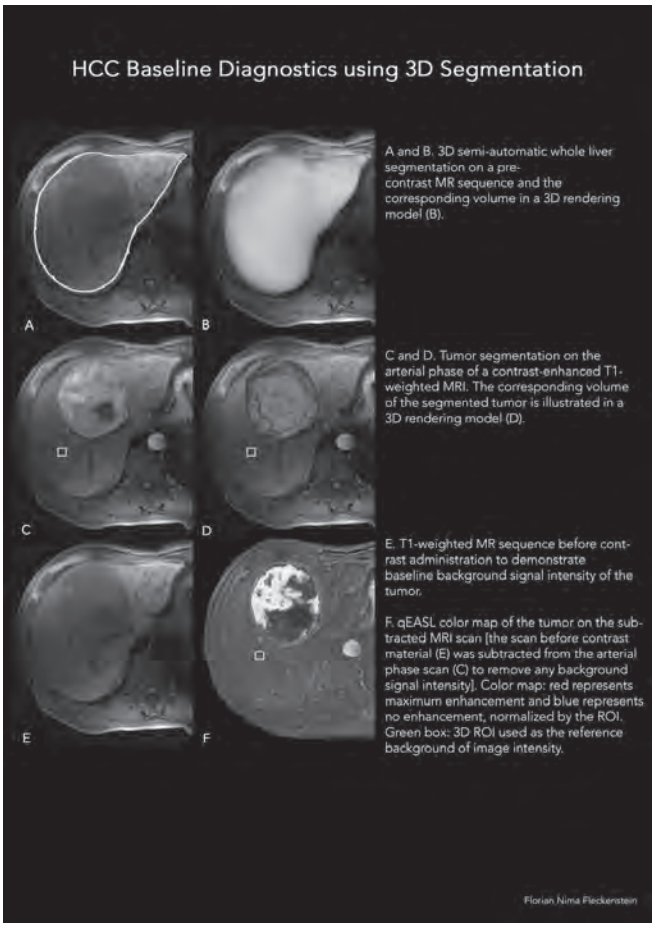

Poster 63: The Clinical Value of Radioembolization for Portal Vein Thrombosis in Hepatocellular Carcinoma: Effectiveness and Safety in 12 Patients

F. Gao, J. xue, V. Khanna, A. katz, D. Lee, D. Waldman, A. Sharma

Objectives: To retrospectively evaluate the effectiveness and safety of yttrium-90 (Y-90) radioembolization for portal vein thrombosis (PVT) in treating hepatocellular carcinoma (HCC).

Methods: We reviewed 94 cases of HCC treated with transarterial radioembolization at our institute from August 2010 to October 2014 . Of these cases we found 15 patients had PVT, 3 of these patients were lost to follow up. 12 patients with follow up imaging were included for the study. These 12 HCC patients with PVT were treated by 13 sessions of transarterial radioembolization using Y-90 microspheres. Of the 12 patients, 3 had main PVT, 6 had right PVT, 2 had left PTV and 1 had main PVT with right and left PVT. Follow-up contrast-enhanced computed tomograph (CT) or magnetic resonance imaging (MRI) were reviewed. Objective response was assessed by mRECIST. The local control rate of 3, 6 and 12 months, as well as local tumor progression rate were also assessed. Months are counted from the first time of Y-90 treatment and the median duration of follow-up was 11.2 months ± 10.1 (range, 3-35 months).

Results: In total, all patients were treated. The proportion of complete response (CR), partial response (PR), stable disease (SD) and progressive disease (PD) were 0 (0/12), 25.0% (0/12), 41.7 (5/12), 33.3% (4/12) at 3 months; 0 (0/12), 8.3% (1/12), 41.7 (5/12), 33.3% (3/12) at 6 months; and 0 (0/7), 0 (0/7), 57.1 (4/7), 14.3% (1/7) at 12 months. The local control rate of 3, 6 and 12 months was 25.0%, 8.3% and 0 respectively. The local tumor progression rate of 3, 6, and 12 months was 33.3%, 8.3% and 8.3% respectively. Mild fatigue was found in 1 patient who was relieved 2 weeks later. Mild right upper quadrant pain developed in 1 patient and lasted for about 1 week. Severe complications such as upper gastrointestinal ulcer/hemorrhage, or liver failure did not occur.

Conclusions: Y-90 radioembolization is effective and safe for portal vein thrombosis (PVT) in treating hepatocellular carcinoma (HCC). Y90 increases the survival of HCC patients with PVT, however, more cases are need to authenticate it.

The local control rate, local tumor progression rates of transarterial radioembolization with Yttrium-90 microspheres

Time (months)	number of patients	CR	PR	SD	PD	Local control rate (%)	local tumor progression (%)
3	12	0	3	5	4	25 (3/12)	33.3 (4/12)
6	6*	0	1	4	1	14.3 (1/7)	14.3 (1/7)
12	5**	0	0	4	1	0 (0/7)	14.3 (1/7)

* Six patients were excluded at 6 months of follow-up time. Of the 6 patients, 1 patient died 6 months after Y-90 radioembolization and the other 5 were followed up less than 6 months.

** One patient died 10 months after Y-90 radioembolization and was excluded at 12 months of follow-up time.

CR = complete response; PR = partial response; SD = stable disease; PD = progressive disease

Poster 64: Long-Term Therapeutic Outcomes of Radio Frequency Ablation for Subcapsular versus Non-Subcapsular Hepatocellular Carcinoma

T. Kang, H. Lim

Objectives: Recent clinical guidelines for management of hepatocellular carcinoma (HCC) have not recommended the radiofrequency ablation (RFA) for subcapsular tumordue to a higher risk of incomplete ablation or major complications. However, these guidelines were mainly based on retrospective studies with insufficient sample size and follow-up. We retrospectively compared the long-term therapeutic outcomes of RFA for HCC n a subcapsular versus non-subcapsular location.

Methods: Between January 2006 and March 2011, 508 patients (396 men, 112 women; age range, 30-80 years) with a single HCC were treated with ultrasonography-guided percutaneous RFA as a first-line treatment. We divided the patientsinto two groups, subcapsular (n=227) or non-subcapsular group (n=281), based on whether the index tumor was abutting the liver capsule or not. After propensity score matching, there were 163 matched pairs of patients in both groups. We evaluated the association of subcapsular location and the long-term therapeutic outcomes of RFA including local tumor progression (LTP) andoverall survival (OS)using the matched data and assessed the major complication rate in overall data for safety analysis.

Results: In the matched groups, the 3- and 5-years cumulative LTP rates were estimated as 18.8% and 20.9%, respectively, for the subcapsular group, and 13.2% and 16.0% for the non-subcapsular group. The corresponding OS rates were 90.7% and 83.2% in the subcapsular group, and 91.4% and 79.1% in the non-subcapsular group, respectively. The hazard rates for LTP (HR [hazard ratio] = 1.37, 95% confidence interval (CI) = 0.81 – 2.33, P = 0.244) and OS (HR = 0.86, 95% CI = 0.50 – 1.50, P = 0.604) were not significantly different between two matched groups. In addition, there was no significant difference in both groups in terms of major complications rates (P>0.05).

Conclusions: The difference in long-term therapeutic outcomes of RFA for HCC was not significant between the subcapsular and non-subcapsular groups.

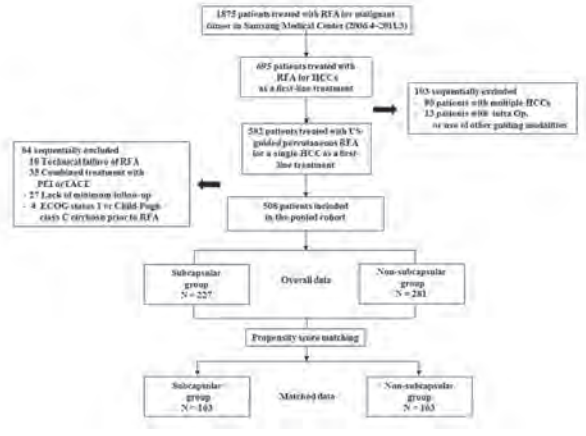

Flow diagram for the study.

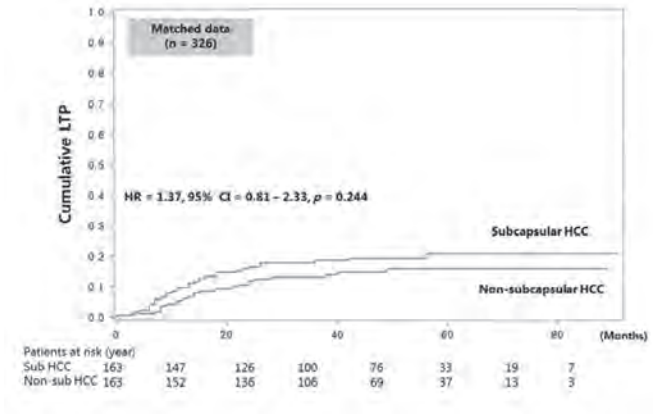

Cumulative LTP ratecurves after propensity score matching according to the subcapsular tumor location.

Poster 65: Feasibility Study of Transcatheter Arterial Chemoembolization for Hepatocellular Carcinoma with Epirubicin Drug-eluting Beads in Japan

H. Ishii, Y. Arai, M. Sone, S. Sugarawa

Objectives: To evaluate the safety and efficacy of transcatheter arterial chemoembolization (TACE) with 75mg Epirubicin drug-eluting beads (DEB) for intermediate stage hepatocellular carcinoma (HCC) as a feasibility study prior to planning of randomized trial for Epirubicin DEB versus conventional TACE in Japan.
Methods: Eight patients with intermediate HCC were enrolled into this study, and all the patients received TACE with 75mg Epirubicin DEB. After four weeks, tumor response was assessed as the primary endpoint by CT or MRI, based on modified Response Evaluation Criteria in Solid Tumors. Adverse events (AEs) after treatment were evaluated as the secondary endpoint based on Common Terminology Criteria for Adverse Events version 4.0.
Results: Complete response was not observed, but partial response was obtained in 4 patients, and the response rate was 50%. There was no patient with grade 4 or higher adverse events. Grade 3 thrombocytopenia occurred in 1 patient. One patient experienced grade 3 increase in AST, ALT and bilirubin level. All adverse events were well managed with medical cares. There was no procedure-related death.
Conclusions: DEB-TACE with 75mg epirubicin was effective in 4 out of 8 patients without severe adverse events. Based on these results, we will conduct further randomized control trial comparing epirubicin DEB-TACE and conventional TACE in Japan.

Poster 66: Comparative Effectiveness Analysis of Drug-Eluting Bead Transarterial Chemoembolization (DEB-TACE) versus ^{90}Y-Radioembolization for Hepatocellular Carcinoma

J.M. Ludwig, M. Xing, K. Kim

Objectives: Objective: Meta-analysis to compare treatment effectiveness of chemoembolization with drug eluting beads (DEB-TACE) versus Yttrium-90 radioembolization (^{90}Y) for the treatment of hepatocellular carcinoma (HCC)
Methods: Studies comparing conventional chemoembolization (cTACE) vs. ^{90}Y radioembolization or DEB-TACE were identified using a PubMed Library Database search with the following keywords: ("hepatocellular carcinoma" and/ OR "HCC" and/ OR "hepatic tumor" and/ OR "liver cancer") and ("TACE" and/ OR "transarterial chemoembolization" and/ OR "DEB-TACE" and/ OR "drug eluting beads" and/ OR" chemoembolization" and/ OR "90Y" and/ OR "radioembolization"). Articles were excluded if they dealt with liver metastasis or other primary liver tumors than HCC. Studies were not excluded if a part of the study population was pretreated with other modalities like e.g. hepatectomy, RFA or cTACE, since this is often observed in the clinical setting. Studies with a concurrent Treatment like e.g. Sorafenib were excluded. Meta-analysis of adjusted indirect comparison method by Bucher et al. was used to analyze the comparative effectiveness between DEB and Y90 (1). The difference of patients' baseline characteristics between two interventions were accessed by Wilcoxon rank sum test. Mean imputation and information from related observations were used to impute missing data in patients' baseline characteristics. Sensitivity analysis with stratification was also performed for primary outcome analyses. All statistical analyses were conducted in STATA.
Results: A total of 7 studies on DEB-TACE vs. cTACE (660 patients with 331 in DEB-TACE group) and 7 studies on ^{90}Y-radioembolization vs. cTACE (1405 patients with 405 in ^{90}Y-radioembolization group) were selected. Comparing baseline characteristics of DEB-TACE vs. ^{90}Y-radioembolization cohorts a BCLC stage D (0 vs. 2 patients; P=0.0241) difference was obvious. Age, sex, gender, BCLC stage A-C, Child-Pugh stage and tumor size did not prove to be statistical different. Comparison of ^{90}Y-radioembolization and DEB-TACE revealed a 1-yr survival benefit for DEB-TACE with a pooled estimate of survival rate of 79% compared to ^{90}Y-radioembolization (54.8%) (Odds ratio (OR): 0.57 (95 % CI: 0.355 - 0.915; p=0.02) for DEB-TACE. No relevant heterogeneity between studies for the 1-yr comparison could be found (I-squared: 0%). No statistical significant benefit for DEB-TACE vs. ^{90}Y-radioembolization could be found for the 2-yr (61% vs. 34%; OR: 0.650 (95% CI: 0.294 - 1.437) and 3-yr survival (56.4% vs. 20.9%; OR: 0.713 (95% CI: 0.210 – 2.548). Due to significant heterogeneity of DEB-TACE vs. cTACE studies evidence for the 2- and 3-yr survival is limited. The pooled estimate for median overall survival for DEB-TACE and ^{90}Y-radioembolization are 22.6 and 14.7 months respectively. The analysis of reported mRECIST response rate did not show a significant difference (OR: 0.713 (95% CI: 0.125 - 4.080). Both treatment modalities were proven to be safe and efficacious, with multiple procedures demonstrating low rates of adverse events and treatment-associated death. Both treatment modalities showed low hospitalization rate.
Conclusions: This meta-analysis of 736 patients treated with ^{90}Y-radioembolization or DEB-TACE showed a 1-year survival benefit for DEB-TACE in comparison to ^{90}Y-radioembolization but no survival benefit for the 2- and 3- year survival could be revealed. In conclusion both, DEB-TACE and ^{90}Y-radioembolization are considered safe and efficacious treatments for HCC. Large randomized controlled trials are greatly warranted to further compare the two treatment modalities.

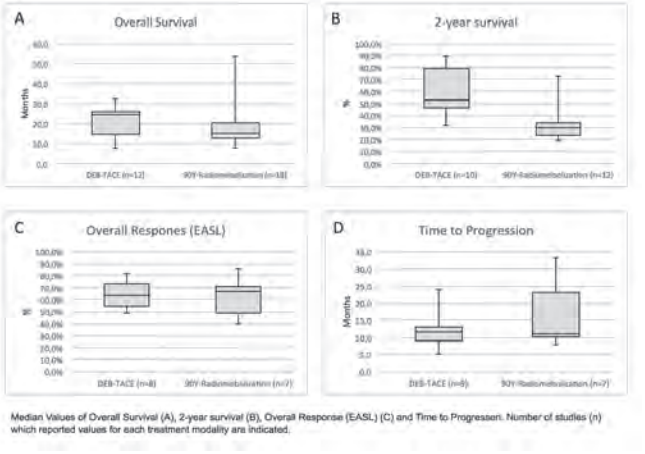

Median Values of Overall Survival (A), 2-year survival (B), Overall Response (EASL) (C) and Time to Progression. Number of studies (n) which reported values for each treatment modality are indicated.

Poster 67: Meta-Analysis of Percutaneous Radiofrequency Ablation versus Hepatic Resection for Treatment of Hepatocellular Carcinoma

J.B. Jia, M. Xing, K. Kim

Objectives: To analyze the comparative effectiveness of radiofrequency ablation (RFA) versus hepatic resection (RES) in overall survival (OS) for the treatment of hepatocellular carcinoma (HCC) in patients with Child Pugh Class A liver cirrhosis.
Methods: A comprehensive literature search was performed and 8 studies were found comparing the OS and DFS of RFA and RES: 1 non-blinded randomized control trials and 7 population-based case series (Table-1). The analysis was limited to patients with Child Pugh Class A liver cirrhosis. 510 HCC cases treated with RFA and 649 treated with RES are included in this analysis.
Results: The median 1-, 3-, and 5-year OS rates for the RFA and RES groups were, 95.8%, 72.1%, 52.0% and 93.0%, 73.4%, 57.0% respectively. There was a significant difference between the RFA and RES groups in 1-,3-, and 5-year OS (P=6.9E-4, P=1.4E-6, P= 4.3E-4). Of the 4 studies measuring complication rates, RFA had a significantly lower number of complications (p=1.1E-11). 3 studies examined hospitalization length, and the RFA groups consistently had shorter lengths of stay ranging from 3-9 days with the RES group ranging from 9-20 days.
Conclusions: Meta analysis of 1,159 patients demonstrates significantly different OS by RFA vs RES for HCC. RFA consistently has lower complication rates and hospital lengths of stay than RES.

Study	Level of Evidence	N	Solitary tumor (%)		Overall Survival RFA (%)			Overall Survival RES (%)		
			RFA	RES	1-year	3-year	5 year	1-year	3-year	5 year
Vivarelli (2004)	3i	113	58.2	83.5	82	43		88	71	
Hong (2004)	3i	148	100	100	100	73		98	84	
Cho (2005)	3i	160			96	80		98	77	
Chen (2006)	1ii	161	100	100	96	71		93	73	
Guglielmi (2007)	3i	133	60	76	86	44	28	90	72	57
Santambrogio (2009)	3i	152	100	100	86	66	41	93	85	54
Nanashima (2010)	3i	147	100	100		80	63		81	59
Peng (2012)	3i	145	100	100	99	88	72	91	71	62

Table 1. Study and patient characteristics and summary of OS

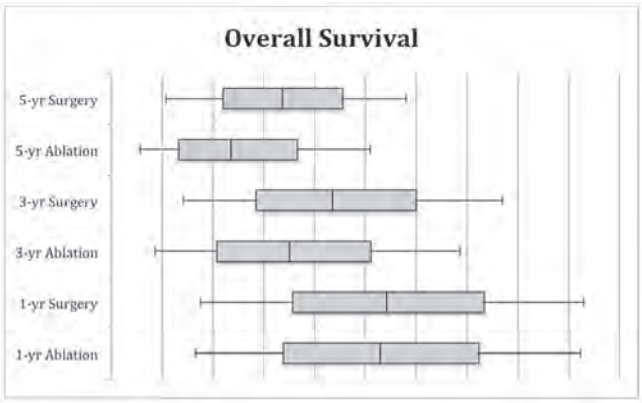

Figure 1. Results of meta-analysis

Poster 68: MRI Imaging Features of Hepatocellular Carcinoma (HCC) Correlating with Response to First Transarterial Chemoembolization (TACE)

A.K. Iranmahboob, N. Lamparello, S. Rice, J. Gross, D.S. Sridhar

Objectives: Although TACE remains a mainstay of non-operative HCC treatment, response rates vary widely. Attempts have been made to identify pre-procedural HCC imaging features predicting response to TACE. Our study evaluates MR appearance of HCC as correlated to outcome of first TACE.
Methods: All patients who underwent TACE for HCC in the setting of viral hepatitis from 2008 to 2012 at a single tertiary-care university hospital were identified. After excluding those without pre- or post-TACE MRI, 65 HCCs in 47 patients were characterized on pre-TACE MRI by size, arterial and portal venous enhancement, and tumor margins. Lesions previously treated or below 1 cm in size were excluded. Post-TACE followup imaging was assessed independently by a separate reviewer using mRECIST criteria
Results: Complete response (CR) after first TACE was seen in 60% of patients in our study. Tumor margins correlated significantly with response: well-circumscribed lesions had a higher rate of CR after first TACE (P<0.012), and ill-defined/infiltrative lesions had a higher rate of progression of disease (PD) after TACE (P<0.03). HCCs with washout on portal venous phase had a slightly higher rate of CR versus those without (64% vs. 50%). Response rates did not vary significantly based on tumor size in our series of predominantly small and intermediate sized tumors (mean 2.5 cm, median 2.3 cm, range 1.0 - 7.7 cm). The correlation of arterial enhancement and response could not be well-assessed due to the predominance of arterially hyperenhancing lesions in our series (95.4%).
Conclusions: In our series, 60% of patients had complete response to first TACE. Of the HCC MR imaging features reviewed, tumor margins correlated significantly with response to first TACE, with significantly higher complete response rates after first TACE in well-circumscribed tumors and higher progression of disease rates in ill-defined tumors. A trend toward higher complete response rates in tumors with portal venous washout was observed. Further study of imaging predictors of response to TACE for HCC could improve treatment selection and prognostication.

Response Rates by Imaging Feature

	Arterial		Portal Venous		Margins	
	Hyperenhancing	Non-enhancing	Non-hypoenhancing	Hypoenhancing	Well-circumscribed	Ill-defined/Infiltrative
CR	55.4 % (36)	4.6 % (3)	13.8% (9)	46.2 % (30)	46.2 % (30)	13.8 % (9)
PR/SD	26.2 % (17)	0.0% (0)	12.3 % (8)	13.8 % (9)	13.8 % (9)	12.3 % (8)
PD	13.8 % (9)	0.0% (0)	1.5 % (1)	12.3 % (8)	4.6 % (3)	9.2 % (6)
Total	95.4 % (62)	4.6 % (3)	27.7 % (18)	72.3 % (47)	64.6 % (42)	35.4% (23)

CR = complete response, PR = partial response, SD = stable disease, PD = progression of disease

Poster 69: Is Microwave Ablation Superior to Radiofrequency Ablation for Hepatic Lesions? A Meta-Analysis

Y. Huo, G.D. Eslick

Objectives: To evaluate the efficacy and safety of microwave ablation (MWA) compared to radiofrequency ablation (RFA) for hepatic lesions using meta-analytical techniques.
Methods: A search of Medline, EMBASE, PubMed, Cochrane and Google Scholar databases was done. Meta-analysis of overall survival (OS), local recurrence rate (LRR), disease free survival (DFS) and adverse events (AEs) were performed.
Results: Overall, 16 studies involving 2,062 patients were included. MWA was found to have significantly better 6 years overall survival compared to RFA (OR: 1.47, 95% CI 1.09-1.99). The two ablative techniques had similar one to five-year overall survival, DFS, LRR and adverse events. MWA was reported to be was significantly cheaper than RFA ($1200 vs $2000), have a lower number of treatment sessions (1.7 vs 2.6), and associated with a shorter overall treatment duration (average: 78 vs 102.9 minutes).
Conclusions: MWA may yield greater benefit in terms of long-term survival and short-term costs compared to RFA, however randomized controlled trials are warranted to confirm these findings.

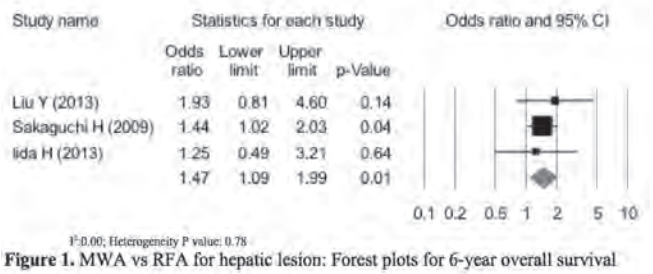

Figure 1. MWA vs RFA for hepatic lesion: Forest plots for 6-year overall survival

Figure 1. MWA vs RFA for hepatic lesion: Forest plots for 6-year overall survival

Table 1. MWA versus RFA for hepatic lesions: a meta-analysis of survival, complete ablation and adverse events.

End Point	Study number	Odds Ratio	95% Confidence Interval		Significance *P*	I^2	Heterogeneity P
			Lower	Upper			
Overall survival							
1 year	10	1.02	0.88	1.18	0.79	0.00	0.99
2 year	10	1.01	0.87	1.18	0.88	0.00	0.98
3 year	8	0.97	0.80	1.17	0.73	0.00	0.91
4 year	7	1.00	0.82	1.22	0.98	0.00	0.69
5 year	5	0.99	0.77	1.28	0.93	2.69	0.39
6 year	3	1.47	1.09	1.99	0.01	0.00	0.78
Disease Free Survival							
1 year	8	0.95	0.77	1.17	0.64	0.00	0.99
2 year	6	0.99	0.76	1.31	0.96	0.00	0.95
3 year	6	1.05	0.80	1.36	0.74	0.00	0.71
4 year	6	0.91	0.67	1.25	0.56	10.64	0.35
5 year	2	0.71	0.43	1.17	0.18	0.00	0.54
Complete ablation	10	0.98	0.85	1.14	0.83	0.00	1.00
Adverse events							
Treatment associated deaths	1	0.47	0.02	12.17	0.65	10.64	0.35
Bile duct injury	4	2.73	0.74	10.13	0.13	0.00	0.53
Liver decompensation	2	2.92	0.43	19.56	0.27	0.00	0.38
Peritoneal haemorrhage	2	3.26	0.35	30.05	0.30	0.00	0.95
Post-interventional pain	4	1.70	0.91	3.19	0.10	61.86	0.05
Subcapsular haematoma	5	1.00	0.29	3.49	1.00	0.00	0.63
Fever (>38^0 C)	4	1.21	0.88	1.66	0.24	0.00	0.49
Skin burn	4	1.20	0.30	4.74	0.79	0.00	0.53
Pulmonary effusion	6	1.33	0.70	2.52	0.38	11.41	0.34

Poster 70: Combined Radiofrequency Ablation and Sorafenib in the Treatment of Postsurgical Recurrent Hepatocellular Carcinoma

M. Kuang, B. Liu, C. Jiang, X. Xie, M. Lin, Y. Wang

Objectives: To retrospectively evaluate the clinical efficacy of radiofrequency ablation (RFA) combined with sorafenib in the treatment for postsurgical recurrent hepatocellular carcinoma (HCC).
Methods: From January 2008 to June 2014, 45 patients (40 men, 5 women; mean age, 47.6 ± 11.2 years; age range 27-72 years) with postsurgical recurrent HCC were treated by combined RFA and sorafenib, due to concurrent portal vein thrombosis or extrahepatic metastases, or uncontrollable multiple intrahepatic recurrences by transarterial chemoembolization. Within 1 week after RFA, patients started taking

continuous sorafenib 400 mg bid without breaks until unacceptable toxicities or disease progression. The adverse effects and survival outcomes for all the patients were assessed.
Results: No ablation-related major complications occurred. The most common adverse events related to sorafenib were hand-foot skin reaction (45/45, 100%) and diarrhea (43/45, 95.6%). During a median follow-up of 16.2 months (range, 4-44 months), Twenty-six patients (26/45, 57.8%) died of tumor progression. The median overall survival (OS) after the combined treatment was 22.8 ± 2.5 months. The 1-, 2-, and 3-year cumulative OS rates were 62.0%, 33.9% and 33.9%, respectively. The 1-, 2-, and 3-year OS rates were 76.5%, 40.1%, and 40.1%, respectively, in the patients without portal vein thrombosis or extrahepatic metastases (n=17), and 52.2%, 28.7%, and 28.7%, respectively, in the patients with portal vein thrombosis or extrahepatic metastases (n=28) (P=0.109).
Conclusions: The combination of RFA and sorafenib is an acceptable treatment for postsurgical recurrent HCC.

Poster 71: Central Vein Stenosis in Breast Cancer Patients after Totally Implantable Venous Access Port Placement

M. Song, T. Seo, E. Kang, H. Yong, J. Seo, Y. Choi

Objectives: To evaluate risk factors for central vein stenosis after placement of the totally implantable venous access ports (TIVPs) and the clinical relevance of this condition in breast cancer patients.
Methods: TIVPs were placed in 191 women with breast cancer via the internal jugular vein (IJV) from January 2009 to December 2012 (mean age, 51.42 years) by left- (n=102) and right-side (n=89) approaches. Medical records were retrospectively reviewed. The presence of significant central vein stenosis, tip location of the catheter, and retrosternal space were evaluated on chest CT images. Statistical analysis was performed.
Results: Central vein stenosis developed in 1 and 14 patients after placement via the right and left IJV, respectively. Differences in the cumulative incidence of central vein stenosis were statistically significant between left- and right-side approach groups (log rank test P-value: 0.009). In Cox regression analysis, the hazard ratio for central vein stenosis was 9.441 (P = 0.031) in the left-side approach. The distance between the sternum and the left innominate vein was found to be significantly and independently related to the development of central vein stenosis (P = 0.026). The hazard ratio of distances between the sternum and left innominate vein < 16 mm was 10.133 (1.319-77.841).
Conclusions: The incidence of central vein stenosis in breast cancer patients was higher after placement of TIVPs via the left IJV. An ipsilateral approach may be favorable in patients with right breast cancer and a retrosternal space less than 16 mm in length.

Poster 72: State-of-the-Art Imaging Biomarkers for Assessing Treatment Response to Intra-Arterial Therapies in Primary and Metastatic Liver Cancer

V. Gowdra Halappa, O.M. Teytelboym, S. Chan, I.R. Kamel

Objectives: Assessing response to intra-arterial therapies in hepatic malignancies is crucial for guiding patient management since treatment response has been identified as an independent predictor of survival. Purpose of this exhibit is 1) To review various criteria to assess response to intra-arterial therapies including WHO, RECIST, mRECIST, EASL with emphasis on their strengths and limitations 2) To demonstrate the value of volumetric multiparametric MRI including Diffusion Weighted Imaging(DWI) and Dynamic Contrast Enhanced-MRI(DCE-MRI) for evaluation of treatment response in hepatic malignancies
Methods: 1. Review criteria currently used to assess treatment response to liver cancer treated by intra-arterial therapies. 2. Discussion of limitations of WHO, RECIST, mRECIST and EASL criteria. 3. Assessing response to treatment utilizing quantitative 3D functional maps using diffusion-weighted MRI (DWI) and dynamic-contrast enhanced MRI (DCE-MRI) 4. Describe our experience using 3D volumetric quantification of DWI and DCE-MRI in assessing tumor response to intra-arterial therapies. 5. Present examples of treatment response for various primary and metastatic hepatic malignancies.
Results: This exhibit will review imaging biomarkers for assessing response to intra-arterial therapies including volumetric multiparametric functional MRI with DWI and DCE- MR with various case examples of primary and metastatic liver tumors treated by intra-arterial therapies and monitoring their response to treatment.
Conclusions: Monitoring treatment response plays a crucial role in the era of targeted drug delivery where various treatment options exist. Accurate quantification of response to therapy helps in further management and improved decision making, thus potentially improving quality of life in patients with advanced liver cancer. This review highlights the drawbacks of current anatomical metrics (i.e. tumor size) and advantages volumetric functional MRI for assessing early treatment response.

Poster 73: Intra-Procedural Cone-Beam CT During DEB-TACE Can Predict Early Tumor Response in Patients with HCC

S. Sahu, R. Duran, R. Schernthaner, J. Sohn, Y. Zhao, F. Fleckenstein, M. Lin, J. Geschwind

Objectives: Understanding how intra-procedural findings relate to short term (1 month) tumor response is important for making early and informed treatment decisions in patients with hepatocellular carcinoma (HCC). This is particularly challenging in patients undergoing drug-eluting beads transarterial chemoembolization (DEB-TACE) as the beads are radiolucent. The purpose of this study was to investigate whether intraprocedural contrast patterns as seen on C-arm cone-beam computed tomography (CBCT) can predict early tumor response on magnetic resonance (MR) imaging in patients with HCC treated using DEB-TACE.
Methods: A retrospective analysis of patients with HCC who underwent DEB-TACE between 2010-2014 at a high-volume tertiary center was performed. Inclusion criteria was the following: 1) intra-arterial therapy naive 2) intra-procedural CBCT before bead delivery (with contrast injection) and CBCT after bead delivery (without contrast injection) 3) baseline and 1 month follow-up MR imaging. The longest enhancing length (1D), product of the longest enhancing bi-dimensional length (2D), and volume of enhancing tissue (3D) of the target lesions were measured on both CBCTs. Blinded to the CBCT measurements and using MR imaging, patients were classified as responders or non-responders according to mRECIST**,** EASL, and quantitative EASL (qEASL, a 3 dimensional criteria). A decrease in volumetric enhancement of ≥ 65% was defined as qEASL response. To assess whether 1D, 2D, and 3D measurements on CBCT could predict mRECIST**,** EASL, and qEASL response, respectively, on 1 month MR, univariate and multivariate linear regression modeling was conducted. Multivariate modeling involved forward step-wise Akaike information criterion (AIC) and the following control variables: BCLC stage, Child Pugh class, cirrhosis, sorafenib therapy, age, etiology of liver disease, gender, ethnicity, and alcohol abuse.
Results: The study included 47 patients [38 (80.9%) men; median age 62.4 years (range, 34-88.8)] with 51 target lesions. BCLC stage A/B/C/NA was seen in 11 (23.4%)/8 (17.0%)/25 (53.2%)/3 (6.4%) patients. The majority had hepatitis C [32 (68.1%)].17 (36.2%) patients were treated with 70-150 μm LC-Bead M1 beads and 30 (63.8%) with 100-300 μm beads**.** 12 (25.5%) patients were on sorafenib. After DEB-TACE, mRECIST and EASL response were seen in 16 (31.4%) lesions and qEASL in 22 (43.1%) lesions. Using univariate and multivariate analysis, neither 1D nor 2D enhancement on CBCT could predict mRECIST or EASL response on MR. However, 3D enhancement on CBCT before bead delivery and CBCT after bead delivery were predictive of qEASL response in univariate (= 0.01, P<0.001; = 0.01, P<0.001, respectively) and multivariate (= 0.01, P=0.01; = 0.01, P<0.001, respectively) models.
Conclusions: 3D tumor enhancement on intraprocedural CBCT before or after bead delivery can predict early 3D tumor response in HCC patients treated with DEB-TACE.

Poster 74: Analysis of Contract Material Delivered During Thermal Ablation: Is Iodine Trapped in the Ablation Zone?

P. Wu, C. Brace

Objectives: Post-ablation contrast enhanced CT imaging (CECT) is widely used to improve visualization of thermal ablations due to attenuation contrast between the zone of coagulation and normally perfused liver. However, it is not clear whether iodinated material delivered during thermal ablation becomes trapped in the ablation zone and potentially reduces ablation visualization or whether it might be expelled due to material diffusion processes. The objective of this study was to use CT imaging to analyze the behavior of iodinated contrast material delivered during microwave ablation.
Methods: Microwave ablations were created in the livers of four swine by applying 100W for 5 minutes. Contrast enhancement was produced using one of three material delivery protocols: (1) no material delivered during ablation (control), (2) material delivered continuously during ablation (125ml 300mg/ml iohexol at 0.3ml/s), and (3) material delivered concurrently with euthanasia (300mg/ml iohexol, 2ml/s), leaving a saturated, unperfused liver. Five samples per protocol were collected. CT data were acquired before, during 15s intervals and after ablation using a thin-slice protocol (0.625mm thickness, 80kVp, 250mA). CT volumes were analyzed using co-registration, multi-planar reformatting along the microwave antenna, and two-dimensional projection through the ablation zone. The resulting slice was cropped to an ROI centered around and including the ablation zone plus a margin of normal liver, and then attenuation values were transformed to a polar coordinate system to construct an average attenuation profile through the ablation zone and normal liver. CT attenuation and CNR between each radial location and the background normal liver were calculated for all timepoints before, during and after ablation. Ablation zones were excised and sliced along the axis of the antenna. Ablation dimensions were correlated to CT data.
Results: On average, attenuation decreased by 12.5-57 HU inside of the ablation zone, with the greatest decrease noted in the gaseous central zone. While gas was visible in Group 1 (no contrast material), the gaseous zone did not correlate well to

the ablation zone measure at gross pathology. In group 2, attenuation increased in the background liver as expected. However, average attenuation inside of the ablation zone decreased less than 44.8-77 HU when compared to group 1, indicating that contrast material was being trapped in the ablation zone (Fig 1). Despite the trapping of material, the ablation zone remained highly visible with a mean CNR of 2.08, which average decreased attenuation more than 40.3-70 HU compare to iodine-laiden liver. Ablations were larger and contained a more substantial gaseous zone in group 3 due to the lack of perfusion. Comparisons between groups indicated that contrast remained trapped in the ablation zone after the gas dissipated and the ablation cooled.
Conclusions: While contrast material can become trapped inside of the treatment zone when delivered during thermal ablation, even greater accumulation in the normally perfused liver facilitated improved ablation zone conspicuity overall.

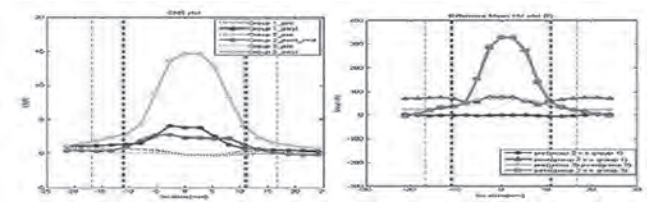

CNR and attenuation profiles from each group. Vertical dashed lines correspond to the ablation zone diameters measured at gross pathology.

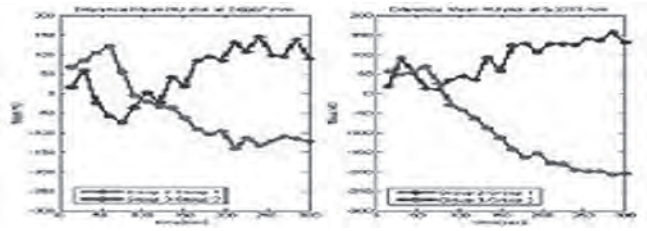

Poster 75: Post-Radioembolization PET/MR: A Score to the Future

B.O. Safar, R. gurajala, S. Shah, S. Srinivas, K. karuppasamy

Objectives: •Review the epidemiology of liver cancer •Discuss the current pathway for patients going for Y-90 radioembolization •Illustrate the role of imaging in the pre- and post-embolization decision making •Review our first case of post-radioembolization PET/MR •Summarize the potential pros and cons of post-radioembolization PET/MR and identifies potential indications and research directions
Methods: We are presenting a case of post-radioembolization Yttrium-90 PET/MR for a 42-year-old male with history of diffuse metastatic burden of the liver from a primary adenocarcinoma of the colon which has been resected. His liver metastases are resistant to two lines of chemotherapy. Referred to the interventional radiology clinic for Y-90 treatment of the liver metastases considering failing role of chemotherapy and constant symptomatology (pain in the right upper quadrant). His liver function testes are preserved and he was functionally active (ECOG 1).
Results: Post-radioembolization PET/MR images: - Customized protocol with limited sequences including (T1, T2 and diffusion weigted images) - The fused PET/MR images are comparable to PET/CT images (the current standard) - The Diffusion images and the calculated ADC maps were utilized to evaluate treatement response on the previously treated lesions.
Conclusions: The current post-radioembolization imaging standard is PET/CT, however PET/MR is definitly a potential tool that can be utilized to evaluate post-embolization particle distribution and treatment response for selected group of patients.

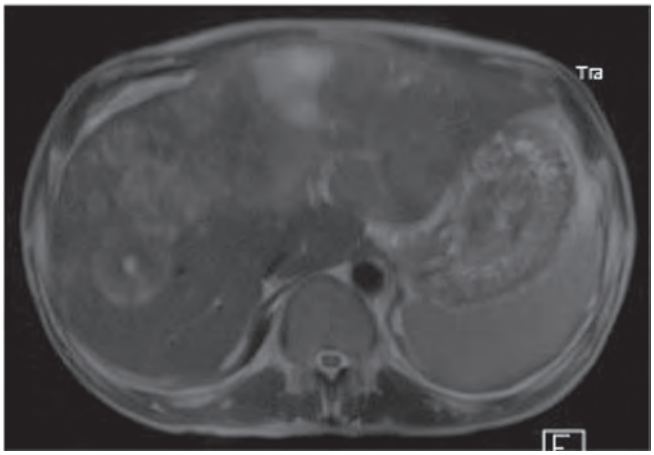

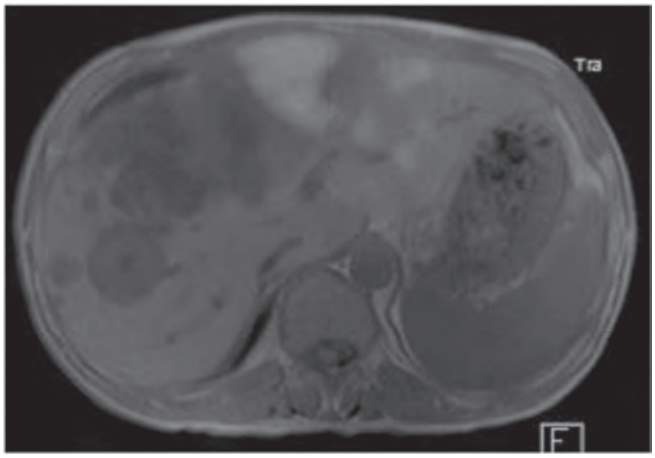

Poster 76: Creating an Ultrasound Phantom for Interventional Procedures Using Ultrasound Gel Standoff/Stepoff Pads and Other Off-the-Shelf Supplies

K. Stewart

Objectives: To demonstrate the feasibility of creating an off-the-shelf ultrasound phantom to aid in training personnel to perform ultrasound guided vascular access and biopsies with supplies commonly available in most hospitals and radiology practices.
Methods: By stacking ultrasound gel standoff/step off pads two to three high and placing tubing or other objects in between the layers (with additional ultrasound gel if desired) an easily made ultrasound phantom can be constructed to practice ultrasound guided vascular access and biopsies. Many people performing vascular access practice desire visual feedback in the form of fluid return from their needle in addition to the visual feedback of seeing the needle within the simulated vessel on the ultrasound display screen. This can be achieved by attaching a syringe (we use a 60 ml) to a three way stopcock and then connecting the three way stop cock to secondary IV tubing. The bag spike end of the secondary IV line (the portion normally inserted into a bag of normal saline) can then be connected to surgical tubing (1/8-1/4 inch thick tubing). Other tubing, including oxygen tubing, may be inserted over the end if surgical tubing is unavailable, but many of the other tubing in hospitals is not as soft for needle access. Surgical tubing is inexpensive and if unavailable in the hospital is available at most medical supply stores. The system is then filled with water from the syringe and the end of the surgical tubing is clamped using mosquito or Kelly forceps. The system is lightly pressurized with the syringe and the roller clamp on the IV tubing is used to maintain the pressure. The surgical tubing is then placed in between the layers of the ultrasound gel pads. Vascular access can then be practiced using a 20 gauge or other needle. When the needle enters the tubing positive return of fluid from the end of the needle verifies positioning within the tubing. As the tubing wears out from use it can be advanced further with the clamp moved up and a new portion of the tubing can be used for further practice. We use water in the tubing to avoid staining or soiling clothing or the surrounding area but red or blue food coloring can be used if desired. Very little pressure is needed in the system for fluid return in the needle, too much pressure can result in unwanted streams of fluid in the direction the needle is pointed (usually towards the user).
Results: An easily built ultrasound phantom can be made from ultrasound gel pads and other supplies commonly found in hospitals and radiology departments. These phantoms can be constructed enabling physicians and trainees to practice ultrasound guided vascular access and biopsies.
Conclusions: Many people and especially trainees desire practice in simulated environments before performing procedures on actual patients. Simulation can also be used to refine skills by enabling physicians and other healthcare providers to repetitively practice skills in a controlled environment. Ultrasound phantoms can be purchased or made but convenience, cost, and availability may limit their use. By being able to construct ultrasound phantoms from ultrasound gel pads and other materials that are readily available to physicians at very low costs make the use of phantoms to practice ultrasound guided vascular access and biopsies very convenient and easily accessible for use.

Poster 77: Computed Tomography–Guided High-Dose-Rate Brachytherapy Ablation of Neuroendocrine Liver Metastases: Initial Experience with 20 Patients

F. Collettini, A. Schippers, B. Gebauer

Objectives: The purpose of this study was to analyze our initial experience with computed tomography–guided high-dose-rate brachytherapy (CT-HDRBT) ablation of neuroendocrine liver metastases (NELM).

Methods: Data from 20 consecutive patients with 38 unresectable NELM treated by CT-HDRBT were reviewed. Treatment was performed by CT-guided applicator placement and high-doserate brachytherapy with an iridium-192 source. Tumour response was evaluated by Gd-EOB-DTPA-enhanced liver magnetic resonance imaging (MRI) performed before, 6 weeks after, and then every 3 months after treatment. Endpoints included local tumour control (LTC), progression-free survival (PFS) and overall survival (OS).
Results: Patients were available for MRI evaluation for a mean follow-up time of 29.53 months. Mean tumor diameter was 2,5 cm (range:0.7-11 cm). One major complication (liver abscess) was observed. Two (10 %) local recurrences were observed after a local tumor control of 2 and 37 months, respectively. Kean LTC was 29.3 months. Fifteen patients (75%) experienced a systemic tumor progression during the follow up period. Mean PFS was 14.7 months (range: 2–56 months). Nine patients died during the follow-up period. Mean OS was 32 months.
Conclusions: CT-HDRBT is a safe and effective minimally invasive therapeutic option to attain long-term local tumor control in patients with unresectable NELM.

Poster 78: Artificial Ascites for Pain Relief during Microwave Ablation of Subcapsular Liver Tumors

L. Tselikas, A. Hakime, F. Deschamps, T. de Baere

Objectives: To compare post-procedure pain of subcapsular hepatic metastasis treated with microwave ablation (MWA) with and without artificial ascites.
Methods: During a 2-years period, 41 patients underwent microwave ablation (MWA) of 52 peripheral liver metastases including 20 patients (10 men and 10 women, mean age: 62 ±9.3 years old) who underwent microwave ablation of 27 metastasis without artificial ascites (group 1), and 21 patients (12 men and 9 women, mean age: 63.5 ±9.9) years old) who underwent MWA of 25 metastasis with artificial ascites (group 2). Patient's pain assessment cores (10-point visual analog scale (VAS)) at 6h, 24h, and 4 days after the MWA procedure were compared among groups, as well as 24 hours (h) cumulative morphine dose was also compared among groups. Complications were reported. Statistical significance was evaluated by Fisher's exact test and Student's t-test.
Results: Pain VAS were 8.6 ±2.7, 3.9±1.4 and 0.6±1.2 at 6h, 24h, 4 days respectively for group I and 0.8±1.9, 0.3±0.9 and 6.6±3.5 for group II. Pain VAS were significantly different at 6h, 24 h and 4 days between the two groups ($p<0.0001$). The average 24h dose of morphine was 5.8±2.2 mg in group-I and 0.2±0.6 mg in group-II ($P<0.0001$). Complications occurred in 2 patients from group-I (10%), including one bilio-pleural fistula and one minor cutaneous burn. One patient (9.5%) in group-II developed a lobar infarction. No bleeding and no procedure-related death were reported.
Conclusions: Artificial ascites prevents immediate post-procedural pain, which re-appears intensively 4 days later.

Poster 79: Case-Control Retrospective Comparison of the Incidence of Cholecystitis using Standard Microcatheter Techniques Versus Flow-Directed Catheter (Surefire)

R.L. Hardman, T. Enniss, R. O'Hara

Objectives: Cholecystitis is a known complication of yttrium-90 radioembolization of the liver. The incidence of clinically significant cholecystitis is low, with reported rates of less than 1%. Many practitioners will treat a hepatic artery that supplies the cystic artery in its distribution, as long as the cystic artery is smaller than 2.5 mm. The use of a flow directing catheter, Surefire (Surefire Medical Inc, Westminster, CO), may increase the risk of cholecystitis.
Methods: Retrospective review was made of all patients undergoing radioembolization from October 2013 to December 2014. Patient with at least 30 days follow up were included. Patients who underwent radioembolization with a Surefire device were compared to those who underwent radioembolization without flow directed treatment. The incidence of clinical cholecystitis is compared.
Results: 88 radioembolization procedures were performed on 56 patients between October 2013 to December 2014. Thirteen patients were excluded from evaluation as they had cholecystectomy prior to radioembolization. 38 of the treatments included the cystic artery in the treatment field, 36 of these treatments were from the right hepatic artery. A Surefire device was used in 9 of the treatments. There was no clinical cholecystitis in any of the patients that underwent treatment with a standard microcatheter (0%). There was clinical cholecystitis in three of the nine patients that had treatment with a Surefire device (33%, P=0.0006).
Conclusions: Flow directed catheters are frequently used to increase drug penetration into tumors and in situations were harmful visceral branches cannot be embolized. Flow directed catheters decrease the arterial pressure distal to the device, leading to increased tumor treatment perfusion. This pressure change may increase yttrium dose to the gallbladder. Embolization of the cystic artery also must be used with caution as this also can lead to ischemic cholecystitis. In this retrospective cohort, the incidence of acute cholecystitis was significantly higher in the Surefire group compared to standard microcatheter techniques or published incidence rates.

Poster 80: Survival Outcomes of Patients with Liver Disease Following Treatment with Glass- Versus Resin-Based Yttrium-90 (Y-90) Radioembolization

T.R. James, R. Morgan, A. Robinson, M. Smith, K. Werth, T. Brown, J. Hill, S. DeBacker, Z. Collins

Objectives: Determine survival outcomes of patients with liver disease undergoing glass- or resin-based Y-90 radioembolization of unresectable hepatic malignancies at a tertiary care teaching institution.
Methods: A retrospective analysis was performed on 126 patients who underwent Y-90 radioembolization treatments with glass- or resin-based particles for unresectable primary hepatocellular carcinoma (HCC), colorectal, neuroendocrine, or other liver metastases between 2008 and 2013 at a tertiary care institution. The impact of liver disease on patient survival at 365 days was evaluated for both glass- and resin-based radioembolization treatments. Patients were classified in a binary manner as either having or not having liver disease based on the presence of any of the following diagnoses: Hepatitis B, Hepatitis C, unspecified hepatitis, cirrhosis, alcoholic liver disease, or non-alcoholic fatty liver disease. Time-to-death was defined as the duration of time (in days) between initiation of treatment and death due to any cause. Subjects lost to follow-up were censored at the date of last contact. Kaplan-Meier curves, log-rank tests, and hazard ratios were used to compare and describe survival between groups.
Results: A total of 217 Y-90 treatments were performed on 126 patients, with 136 (63%) using glass particles and 81 (37%) using resin particles. Fifty-one patients (40%) had primary HCC and 46 (37%) had metastatic colorectal cancer, while 11 patients (9%) had neuroendocrine and 18 (14%) had other primary liver metastases. Two-thirds of all patients were male with a median age of 62 years at first treatment. Forty-seven patients (37%) were classified as having chronic liver disease, with 37 (79%) treated with glass particles and 10 (21%) treated with resin particles. Mean survival in patients with liver disease who were treated with glass particles was 230 days (overall survival =16%) compared to 257 days for those treated with resin particles (overall survival =49%).
Conclusions: The therapeutic benefit of glass- and resin-based Y-90 therapies in the setting of unresectable hepatic malignancies has been well documented in both literature and clinical practice. However, there is limited research on outcomes of patients with comorbid clinical conditions, including liver disease. Although formal significance tests could not be conducted on patient survival due to the small sample size for the resin population, these initial results suggest that radioembolization with resin particles as compared to glass particles, may yield a survival benefit in patients with coexisting liver disease.

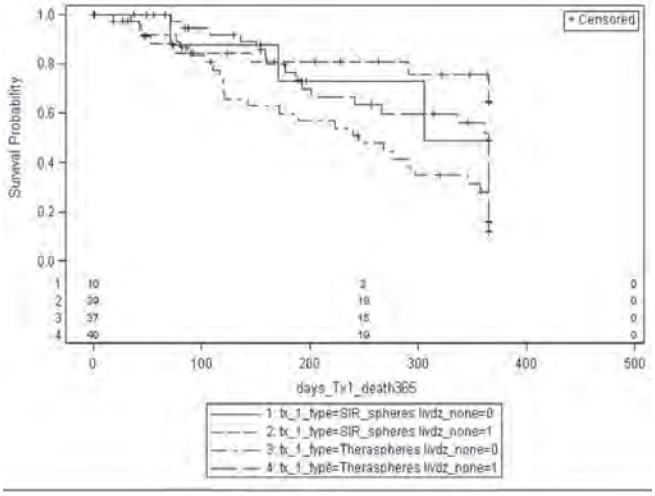

Figure 1: Kaplan-Meier Survival Curves by treatment and presence of liver disease. Resin/diseased (solid, $n = 10$), resin/non-diseased (short dash, $n = 39$), glass/diseased (dot-dash, $n = 37$), and glass/non-diseased (long dash, $n = 40$) are displayed. Mean survival in subjects with liver disease treated by glass-based Y-90 was 230 days (OS = 16%), compared to 285 days for glass-based Y-90 in non-diseased subjects (OS = 12%), 304 days for resin-based Y-90 in non-diseased (OS = 64%) and 257 days for diseased subjects treated with resin-based (OS = 49%).

Poster 81: Intraoperative US - Guided Thermal Ablation Combined with Surgical Resection for the Treatment of Colorectal Cancer Liver Metastases (CRClm)

L. Carmignani, M. Fedi, S. Riccadonna, A. Pagliari, M. Lupi, L. Vannucchi, M. Di Lieto, S. Giannessi, P. Pacini

Objectives: A retrospective analysis from a perspective hepatobiliary surgical database was performed with the aim to check the outcome and to assess the potential advantages of matching surgery and intraoperative thermal ablation.
Methods: From January 2011 to June 2014, 71 patients (43 male, 28 female), age 35 - 79 years (median of 64), with only CRClm, were selected for partial liver resection. 29/71 patients (41%) who were not candidates for potentially curative surgery alone because of the high number of lesions (6 - 19) and the bilobar involvement, underwent hepatic resection combined with intraoperative US-guided radiofrequency (RFA) or microwave (MWA) ablation (Fig. 1). Follow up was performed with Contrast Enhanced CT (CECT) at 1, 3, 6, 12 months and than on a yearly basis.
Results: Local recurrence rate at the ablation site, overall survival rate, disease-free survival rate and hepatic disease-free survival rate were evaluated for patients who underwent both surgery and ablation. There were no post-operative significant complications, mortality rate and in situ recurrence rate were 0% each. At the last follow-up (12/2014) 6 patients are dead for disease progression, 15 patients have no evidence of disease (Fig. 2), 8 patients are alive with disease. The median follow-up for survivor patients was 19,9 months (6 - 48). The median survival rate was 20,1 months (3 - 48). The 1 –, 2 –, 3 – and 4 – year survival rates were 83,3%, 77,8%, 69,5% and 54,7% respectively. The median hepatic disease-free survival was 16,5 months (1 - 48). The median disease-free survival was 13,6 months. There was a trend worse survival for patients with a K-ras gene mutation (P<0,01).
Conclusions: Intraoperative US-guided RFA/MWA joined with hepatic partial resection is a feasible and safe procedure for patients with CRClm. Combined techniques allow to increase the therapeutic opportunities for patients with advanced and/or bilobar disease (i.e. expanding the indications for the "two stages hepatectomy") and consent to reach an effective clearance of disease. The outcome for these patients is however affected by the biological features of the tumor and the need for adjuvant therapy.

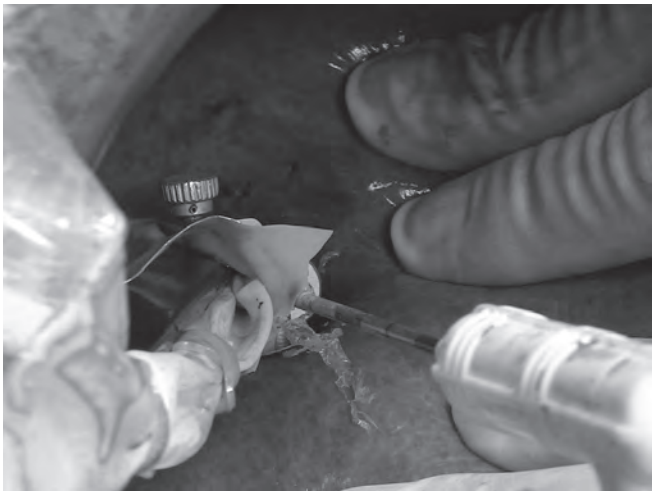

Intraoperative US - guided liver MWA

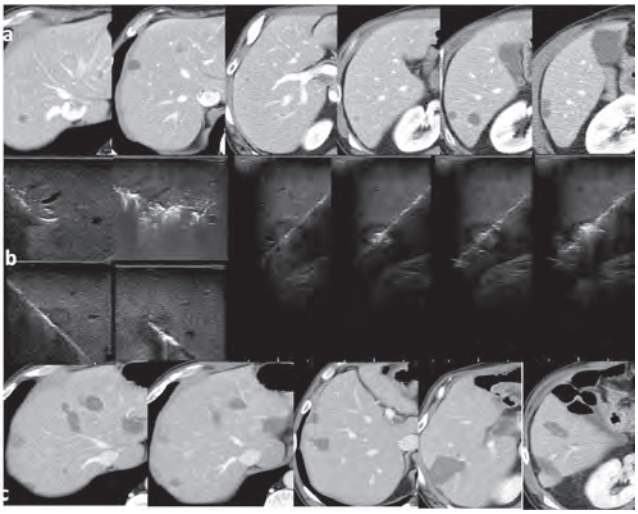

Male (06/05/1955)
04/2011 - right hemicolectomy + chemoterapy (Capecitabine + Oxalipatin);
08/2011 - 11 liver metastases scattered in several segments (Folfiri + Bevacizumab);
a) *01/2012* - CECT: good response with a reduction of the maximum diameter of the lesions (< 3 cm);
b) *02/2012* - wedge resections of 6 nodules + intraoperative US guided MWA of 5 nodules;
c) *05/2014* - CECT*:* no evidence of recurrent disease at the two year follow up.

Poster 82: Can Whole Liver Enhancement Patterns Predict Therapy Response and Survival in Patients with Neuroendocrine Liver Metastases Treated with Transarterial Chemoembolization?

S. Sahu, R. Duran, R. Schernthaner, J. Sohn, M. Lin, J. Chapiro, J. Geschwind

Objectives: Neuroendocrine liver metastases (NELM) are usually multiple, of varying size, and affect both liver lobes. However therapy response assessment after transarterial chemoembolization (TACE) can be challenging in patients with diffuse, bi-lobar neuroendocrine liver metastases (NELM) using conventional guidelines (RECIST, mRECIST, and EASL). We propose a new approach that assesses the entire liver. The purpose of this study was to determine whether volumetric changes in whole liver enhancement on multi-phasic contrast-enhanced MR imaging (MRI) can predict early tumor response and survival in patients with diffuse, bi-lobar NELM after the first TACE.
Methods: This IRB approved retrospective study included 51 patients (28 men; median age, 58.3 years) with extensive NELM who underwent their first TACE (conventional or drug-eluting beads) between Jan 2000 – Apr 2014. All patients were locoregional therapy naïve. MRI studies were performed 3-4 weeks before and after TACE. Using prototype semi-automatic 3D software, the whole liver was segmented in the hepatic arterial phase,by two independent readers and the volumetric liver enhancement was measured. Response to TACE was defined as a decrease in volumetric enhancement by ≥ 65%. Median overall survival (OS) was calculated from the date of TACE to death or last known alive date. Inter-reader agreement for liver volumes derived from the segmentation software was assessed via the two-way random intraclass correlation (ICC). Volumetric enhancement before and after TACE were compared with the paired *t-test* and Kaplan-Meier survival curves for responders and non-responders were compared using the log-rank test.
Results: There was high inter-reader agreement for liver volumes derived from whole liver segmentation before and after TACE [ICC 0.999 (95% CI: 0.998-0.999) and ICC 0.998 (95% CI: 0.997-0.999), respectively]. Mean volumetric liver enhancement decreased significantly after TACE from 49.7% to 26.5% (P<0.001) in all patients. 17 (33.3%) patients were responders and 34 (66.7%) were non-responders. Median OS was 1.7 years (95% CI: -3.9-7.5) and 1 and 2 year survival rates were 66.7% and 39.2%, respectively. Responders had a significantly better prognosis than non-responders (median OS: 4.4 years vs. 1.0 year, respectively; log-rank test, P<0.001).
Conclusions: Quantitative volumetric liver enhancement can be used as a surrogate biomarker for early tumor response and survival in patients with extensive neuroendocrine liver metastases after the first session of TACE.

Poster 83: Bland Hepatic Arterial Embolization and Radioembolization of Neuroendocrine Hepatic Metastases: A Single Institution Experience

M. Cristescu, M. Woods, J. Fallucca, P. Dalvie, J. McDermott, O. Ozkan, J.W. Pinchot

Objectives: Hepatic metastases from neuroendocrine tumors contribute significantly to both morbidity and mortality. As a result, aggressive liver-directed therapies are considered for those with unresectable lesions refractory to standard-of-care therapy. To date, no compelling data exist confirming superiority of one arterially-directed interventional strategy over another. The purpose of this study was to compare efficacy and toxicity of bland embolization (TAE) and radioembolization in patients with neuroendocrine metastases to the liver.
Methods: This study was IRB-approved and HIPAA-compliant. A retrospective review identified all patients with chemo-refractory, unresectable hepatic neuroendocrine metastases managed by TAE or radioembolization at a single institution from July 2005 to October 2014. Toxicity was assessed according to National Cancer Institute Common Toxicity Criteria for Adverse Events, version 4.0. Progression free survival (PFS) for each treatment group was estimated using Kaplan-Meier analysis. Comparisons were performed using Kruskal-Wallis and log-rank tests. Post-treatment 3 month radiological response was assessed using RECIST (v 1.1) criteria.
Results: A total of 27 patients with unresectable hepatic neuroendocrine metastases refractory to first-line systemic treatment underwent 48 transarterial embolization procedures: 12 patients received bland embolization with tris-acryl gelatin microspheres or PVA and 15 patients received ^{90}Y radioembolization with glass microspheres. Patient characteristics were well-matched between treatment groups. Four of 27 patients (15%) were lost to follow up. The mortality rate at 30 days was 3.7%. Estimated 2-year PFS rates were 41% (95% CI [0.21, 0.79]) and 51% (95% CI [0.28, 0.91]) in the TAE and radioembolization groups, respectively. The median progression-free survival was 15.5 months and 24.7 months in the TAE and radioembolization groups, respectively (P=0.658). Age, gender, scope of liver involvement, and concomitant treatment with somatostatin analogues were not associated with changes in PFS, whereas elevated baseline serum chromogranin A and urinary 5-HIAA levels were associated with shorter PFS in both treatment groups. Clinical and laboratory toxicities of grade III or worse in severity occurred after 5% of TAE treatments and 11% of radioembolization treatments. No radiation-induced liver failure occurred. Post-treatment 3 month radiological response using RECIST (v.1.1) demonstrated complete response, partial response, stable disease, and progressive disease in 0, 16, 25, and 50% of TAE patients, respectively, and 7, 13, 40, and 33% of radioembolization patients, respectively.
Conclusions: Radioembolization is an efficacious substitute for TAE in patients with hepatic neuroendocrine metastases, in keeping with published consensus guidelines asserting its role in this regard. Although not statistically significant, these data reveal a trend toward improved progression free survival with an acceptably low acute toxicity profile for radioembolization.

Poster 84: Retrospective Evaluation of Trans-Arterial Radioembolization (TARE) for Treatment of Liver Dominant Metastatic Pancreatic Cancer

A.Y. Kim, K. Unger, M. Pishvaian

Objectives: The aim of our study is to retrospectively evaluate the efficacy of TARE in the management of patients with liver dominant metastatic pancreatic cancer.
Methods: Eight patients were treated with TARE for liver-dominant pancreatic cancer from 2/2012 to 12/2014. Electronic chart review was performed for this group of patients to assess response.
Results: Five male and 3 female patients were treated for liver dominant metastatic pancreatic cancer. Three patients had extra-hepatic disease with evidence of pulmonary, ovarian and omental disease on pretreatment imaging. The average age was 64 (51-77). The mean total bilirubin and albumin was 0.44 (0.3-0.7) and 3.7 (2.3-4.4), respectively. All patients had adequate performance status (ECOG 0 or 1) at the time of Yttrium-90 delivery. Five of 8 patients were alive at the time of analysis. The median overall survival from diagnosis of liver metastases to time of analysis is 23.4 months (11.5-50 months). The median time of survival from TARE is 6.3 months (1-9.5 months). The median survival for the five surviving patients from time of treatment is 8.2 months (6-9.5 months). The mean local and systemic progression free survival (PFS) was 3.8 and 3.4 months, respectively. Per RECIST criteria, partial response (PR) was seen in one patient 2 months post treatment. Three patients demonstrated stable disease (SD) at initial follow-up. Of these patients, one died prior to the 2nd follow up scan, one demonstrated PD and the third continues to have SD at 9 months post treatment. Two patients demonstrated progression of disease (PD) at first follow-up, 2 and 3 months post treatment, respectively. One patient expired prior to any follow up imaging and one patient has not had his first follow up imaging at time of data analysis. Pre and post procedure CA 19-9 values were available for 3 patients. The patient who demonstrated partial response to therapy demonstrated a decrease of CA 19-9 from 124 to 20 post treatment. A patient who demonstrated SD on imaging had a decreased of CA 19-9 from 76,587 to 9050. The third patient who demonstrated progression on initial imaging had an elevation of CA 19-9 from 4722 to 7263.
Conclusions: The current standard of care for treatment of metastatic pancreatic cancer is with systemic chemotherapy. The median overall survival with FOLFIRINOX is 11.1 months and 8.5 months with gemcitabine and nab-paclitaxel. Patients in our retrospective evaluation demonstrated a much superior overall survival of 23.4 months. Even when excluding the single outlier who survived for 64 months, the overall survival for the rest of this cohort is 17.4 months. Moreover, the median survival from treatment is currently 6.3 months with 5 patients still alive. Our data suggests that the addition of TARE to systemic chemotherapy may be promising in patients with liver-dominant metastatic pancreatic cancer. A prospective trial is currently being developed for further evaluation.

Poster 85: Delayed-Arterial Phase Cone-Beam CT Shows Improved Identification of Colorectal Liver Metastasis Compared to DSA During Intra-Arterial Therapy

R. Schernthaner, R. Duran, M. Lin, H. Lee, J. Sohn, Y. Zhao, S. Sahu, F. Fleckenstein, L. Zhao, J. Geschwind

Objectives: Improved identification of colorectal liver metastasis (CRCLM) during intra-arterial therapy could help in better tumor targeting. The purpose of this study was to evaluate whether dual-phase cone-beam CT (CBCT) can better visualize CRCLM compared to digital subtraction angiography (DSA), with reference to pre-interventional baseline contrast-enhanced magnetic resonance imaging (CE-MRI) of the liver.
Methods: From January 2010 to October 2014, 1728 patients with primary or secondary liver cancer were treated with intra-arterial therapy at our institution. Out of 140 patients with CRCLM, 13 underwent intra-procedural dual-phase (early and delayed arterial phase (EAP- and DAP-)) CBCT and were included in this retrospective study. Dual-phase CBCT was acquired just before treatment, after a single injection of contrast agent with the microcatheter in the tumor-feeding arteries. Three patients were excluded (n=1 substantial tumor progression between baseline and time of therapy, n=2 no pre-interventional MRI), resulting in a final study cohort of 10 patients (4 men; mean age 59). In 8 patients, radio-embolization was performed and the remaining two patients were treated with drug-eluting beads. The degree of visibility of each CRCLM was graded on a three rank scale (complete, partial and none) on dual-phase CBCT and all DSA images acquired during the procedure and compared to CE-MRI. Lesions < 5 mm diameter or outside the CBCT's field of view were excluded from evaluation. Statistical analysis was performed with McNemar's test.
Results: At total of 46 CRCLM lesions were included. The combined sensitivity of DSA for the complete or partial depiction of CRCLM lesions was 41.3% only, whereas EAP- and DAP-CBCT had significantly higher sensitivity at 84.8% and 95.7%, respectively (P<0.001). There were only two lesions (4.3%) that were visible on DSA but not on EAP-CBCT; both of these lesions were mainly necrotic and showed only subtle and delayed enhancement on DSA. However, both lesions were completely depicted by DAP-CBCT. Conversely, out of the 27 lesions not visible on DSA, 22 (81.5%) and 25 (92.6%) could be identified on EAP- and DAP-CBCT images, respectively; only two lesions (7.4%) in the left liver lobe were not depicted by EAP- and DAP-CBCT because they were masked by streak artifacts caused by the adjacent contrast-filled catheter. EAP-CBCT showed no additional lesions compared to DAP-CBCT, whereas DAP-CBCT identified five more lesions (p=0.063) than EAP-CBCT. With regards to complete lesion visibility, EAP- and DAP-CBCT yielded a significantly higher sensitivity of 43.4% (P=0.007) and 91.3% (P<0.001), respectively, compared to DSA (15.2%). Complete delineation of lesions was achieved significantly better with DAP-CBCT compared to EAP-CBCT (P<0.001).
Conclusions: Dual-phase CBCT significantly improved the identification of CRCLM during intra-arterial therapy compared to DSA. The delayed arterial phase portion of dual phase CBCT yielded the highest sensitivity and we suggest its use as a standard imaging technique during intra-arterial therapy of patients with CRCLM to allow better lesion visualization, which could allow for improved targeting.

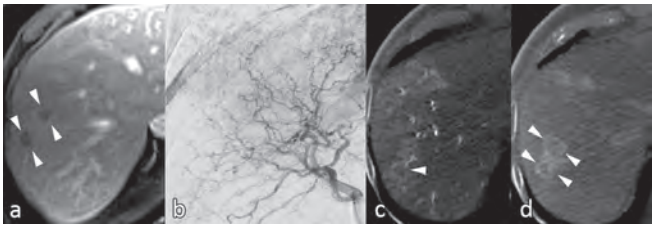

(a) MRI shows 2 CRCLM in segment 7/8 (arrows), both not visible on DSA (b). (c) On early-arterial phase CBCT, the medial rim of the dorsal lesion is not depicted (arrow). (d) On delayed-arterial phase CBCT, both lesion are completely depicted (arrows).

Poster 86: Liver Metastases from Renal Cell Carcinoma: Early Response Assessment after Intraarterial Therapy using 3D Quantitative Tumor Enhancement Analysis on MRI

F.N. Fleckenstein, R. Duran, J. Chapiro, R. Schernthaner, J. Sohn, S. Sahu, Y. Zhao, M. Lin, J. Geschwind

Objectives: Liver metastases from renal cell carcinoma (RCC) are not uncommon in the course of the disease. However intraarterial therapy (IAT) is rarely performed in these patients and data about tumor response is scarce. This study assessed whether response after one session of IAT using volumetric tumor enhancement (quantitative EASL (qEASL)) on magnetic resonance imaging (MRI) can evaluate tumor response and predict overall survival (OS).
Methods: 9 patients (5 male, mean age 64±8 years) with metastatic RCC to the liver treated with IAT (TACE, n=8 and Y-90 radioembolization, n=1) were retrospectively included between 2005 and 2013. All patients were naïve to locoregional therapy and underwent multiphasic contrast-enhanced MRI 3-4 weeks pre- and post-IAT. The target lesions (n=9) were segmented in the arterial phase using 3D semi-automatic software that could measure the qEASL, expressed in cubic centimeters (qEASL[cm3]) and as a percentage of the tumor volume (qEASL[%]). Partial response (PR) and progressive disease (PD) were defined as a ≥65% decrease and a ≥73% increase in qEASL, respectively. Stable disease (SD) was between these thresholds. Complete response (100% qEASL decrease) and PR were classified as responder (R), SD and PD as non-responder (NR). The Wilcoxon signed-rank test was used to compare pre- and post-IAT MRI. For OS analysis, Kaplan Meier curves with log-rank test and a Cox proportional hazard model were created.
Results: When using qEASL[%], target lesions showed a significant mean decrease of from 63.4 to 36.8% ($P<0.05$). 4 patients had a PR and 5 SD. A trend in OS prediction could be seen between R and NR (mean 29.2 vs. 9.8 months, (log rank test $P=0.10$) HR: 0.36 (95%CI: 0.029-1.09). Mean qEASL[cm^3] decreased from 102.75 to 80.79cm^3 ($P=0.0547$). 3 patients had PR and 6 SD. Mean OS was 31.7 vs. 10.7 months, (log rank test $P=0.20$); HR: 0.40 (95%CI: 0.075-1.46).
Conclusions: Despite the small sample size, qEASL showed promising results with a trend towards survival prediction in patients with RCC metastatic to the liver. Further studies with a larger patient cohort are warranted to see if quantitative tumor response can help guide treatment decisions early in the course of therapy.

Poster 87: Single-Center Experience of Selective Internal Radiation Therapy as a Salvage Treatment for Small Cell Lung Cancer Hepatic Metastases

V.S. Sotirchos, W. Shady, E.G. Violari, M.C. Pietanza, N. Pandit-Taskar, R.K. Do, M. Gonen, J.A. Carrasquillo, L. Brody, W. Alago, R.H. Siegelbaum, H. Yarmohammadi, F.E. Boas, C. Sofocleous

Objectives: To evaluate the safety and efficacy of selective internal radiation therapy (SIRT) for the treatment of chemotherapy refractory small cell lung cancer (SCLC) hepatic metastases.
Methods: An IRB waiver was obtained to retrospectively review treatment parameters and clinical outcomes of patients receiving SIRT to address progressing SCLC hepatic metastases. Kaplan-Meier methodology was used to calculate overall survival (OS) after SIRT. Response to treatment was documented by evaluating changes in size (RECIST 1.0) and metabolic activity (PERCIST) of the target lesions within the treated hepatic volume. Complications and toxicities within the first 30 days post-SIRT were evaluated according to the NCI Common Terminology Criteria for Adverse Events v3.0.
Results: From August 2010 to June 2014, 12 patients (median age: 64 years) with biopsy proven SCLC received a total of 17 sessions of SIRT at a median of 11 months after primary diagnosis. The mean corrected dose per session was 26.8 mCi. Stasis was observed before administration of the full intended dose in 3/17 sessions. Bilobar disease was treated either in two separate sessions (n=5) or with a superselective approach of the target lesions within one session (n=3). Median OS from the time of initial SIRT was 4.4 months (95% CI: 3.6-6.6). Response to SIRT was evaluated after 4-8 weeks. Of the 11 patients with available CT exams, seven patients exhibited partial response to SIRT, three had stable disease and one patient disease progression. Of the 10 patients with available PET/CT exams, nine had evidence of response within the treated liver volume. The majority of patients (83%) experienced mild (grade 1-2) clinical toxicities within the first 30 days, including a case of acute cholecystitis (grade 2) developing after prophylactic coil embolization of the cystic artery during mapping. One patient developed significant hyponatremia (grade 4) 5 days after SIRT. All patients resumed systemic chemotherapy post-SIRT to address disease progression in the liver or in other sites.
Conclusions: SIRT for SCLC liver metastases was relatively well-tolerated, providing in the majority of cases an initial response. Additional studies are necessary to demonstrate any potential benefit of SIRT in comparison to other treatment options for this disease in the salvage setting.

Poster 88: Percutaneous Microwave Ablation of Hepatic Metastases with High-Powered, Gas-Cooled Antennas: An Update with 20 Month Mean Imaging Follow-Up

J. Hinshaw, T. Ziemlewicz, M. Lubner, S.A. Wells, C. Brace, L. Sampson, M. Alexander, F. Lee

Objectives: Oligometastic disease to the liver is a leading indication for thermal ablation. Microwave (MW) ablation has several advantages over Radiofrequency (RF) ablation including faster heating, higher temperatures, decreased variability in different tissue types, and larger ablation zone sizes. The purpose of this study was to retrospectively review the intermediate term results in the first 44 patients with hepatic metastatic disease treated with a high-power, gas-cooled MW device at a single center.
Methods: Between December 2010 and November 2013 we treated 84 hepatic metastases (Primary: 31 colon, 14 carcinoid, 11 melanoma, 8 sarcoma, 4 breast cancer, 3 renal cell carcinoma, 6 neuroendocrine tumor, 3 ovarian cancer and 1 each endometrial cancer, pancreatic cancer, gastrointestinal stromal tumor and squamous cell carcinoma from lung) in 44 different patients via a percutaneous approach utilizing US and/or CT guidance. Four patients had ablation at more than one setting. There were 26 male and 18 female patients with mean age of 61 years (range 35-84). All procedures were performed with a high-powered, gas-cooled microwave system (Certus 140, Neuwave Medical, Madison, WI) utilizing 1-3 (average 2.3 ± 0.7) 17-gauge antennas. Antenna power and ablation time was determined by the performing physician based on lesion size, location, and monitoring findings. Follow-up imaging was generally performed immediately post-ablation and at 1, 3, 6, 9, and 12, 18, 24, 36 months with contrast-enhanced CT or MRI.
Results: Tumors ranged in size from 0.5 to 6.0 cm (mean 2.2 cm). Mean imaging follow-up was 20.0 months and median imaging follow up was 18.9 months. Mean clinical follow up was 22.4 months. All treatments were technically. Local tumor progression occurred in 11.9% of tumors (10/84), with a rate of 60% (3/5) for tumors ≥ 4 cm, 16.7% for tumors between 3 and 4 cm (2/12) and 7.5% (5/67) for tumors <3 cm. One of the patients underwent successful reablation of the LTP, but the other 9 patients all had progressive disease at the time that the LTP was identified and therefore, did not have additional ablation. There were two major complications (4.2%): pulmonary embolus two days post-procedure (successfully treated with anticoagulation) and a pleural effusion within one week of the procedure (requiring thoracentesis x 2). No minor complications other than post-procedural pain were encountered. There were no procedure related mortalities. 10 patients have died of progressive metastatic disease giving an overall survival of 77.3%, at a mean f/u of 22.4 months. 38.6% (17/44) of patients have no evidence of disease with a mean follow up in those patients of 20.7 months. 15.9% (7/44) of patients were treated with palliative intent and had other sites of known disease at the time of the ablation. Mean power was 75 W (range, 25-140 W) and mean ablation time was 6.3 minutes (range, 1-19 minutes).
Conclusions: Intermediate follow up after treatment of hepatic metastatic disease with a high-powered, gas-cooled microwave ablation system shows that MW is associated with local control rates and patient survival that is comparable to other ablation modalities and potentially even surgery with an excellent safety profile. Continued study is warranted to determine efficacy and survival with longer-term follow-up.

Poster 89: A Single-Incision Technique for Placement of Implantable Venous-Access Ports in Medial Pocket via the Axillary Vein

M. Song, T. Seo, Y. Kim, S. Cho, H. Chung, S. Hwa

Objectives: To evaluate the technical feasibility and safety of a single-incision technique for placement of implantable venous-access ports in medial pocket via the axillary vein.
Methods: Celsite Discreet ports (6.5F, B.Braun) were placed in 425 patients between May 2012 and August 2013 using a single-incision technique and medial pocket via the axillary vein. Patients included 281 men and 144 women with a mean age of 59.4 years. Ports were placed via the left and right axillary veins in 334 and 91 patients, respectively, after making a single vertical incision without subcutaneous tunneling and pocket medial side to incision. Axillary vein punctures were directed medially at the incision site under ultrasound guidance. We retrospectively reviewed success rates, problems, procedure times, and immediate and delayed complications of the procedure.
Results: All single-incision port placements were technically successful. Problems occurring during the procedure included advancement of the wire or catheter into an unintended vein (n=59), kinking at the cuff-catheter junction (n=10), bleeding via the puncture tract (n=5), bending of the peel-away sheath (n=3), and puncture of the axillary artery (n=3). All technical problems were overcome with additional manipulation. The only immediate complication was puncture site hematoma in two patients. Central venous thrombosis was observed in 3 patients. In 9 patients, ports were removed due to systemic infection during follow-up period.
Conclusions: The single-incision technique for port placement in medial pocket via the axillary vein was a feasible and safe procedure with high technical success and low risk of complications.

Poster 90: The Track Embolization Technique to Improve Safety of Image-Guided Percutaneous Solid Abdominal Organ Biopsy

S. Mittal, A. Fadl, A. Rahman, O. Shoaib, A. Baadh, N. Georgiou, M. Hon, J.C. Hoffmann

Objectives: To describe the procedural steps of the track embolization technique used during percutaneous image-guided solid abdominal organ biopsy to decrease risk of complications. Procedural outcomes will be presented in a large cohort of patents. The procedural steps of this technique differ from the track embolization technique which can be used in the lung/thorax, and these specific differences will be described in detail.
Methods: Our track embolization technique involves embolization of the biopsy track with active Surgifoam injection via the trocar as it is withdrawn. This is a variation of a technique used during percutaneous lung biopsy described separately, with multiple important technical differences. Procedural steps will be detailed. In addition, this retrospective study presents outcomes in 297 consecutive solid abdominal organ biopsies (liver, spleen, and kidney) performed at a single, tertiary care institution from October 2011 through November 2014. Patients were evaluated for signs/symptoms of bleeding, including hypotension, tacchycardia, and drop in hemoglobin/hematocrit in the first 36 hours post procedure.
Results: The track embolization technique was technically successful in all procedures, with appropriate Surgifoam deposition in the biopsy track in all cases. In this patient population, there was no hemorrhage, pseudoaneurysm, or other vascular injury diagnosed after percutaneous image-guided biopsy. No episodes of hemodynamic instability or upgrade in patient condition occurred in the study population. This compares well to published rates of vascular complication in the radiology literature ranging from 2 to 12%, particularly in more vascular organs such as the liver, spleen, and kidneys. No complications occurred in any of the procedures.
Conclusions: Track embolization with active Surgifoam injection can be used during image-guided percutaneous biopsy of solid abdominal organs to decrease complication rates.

Poster 91: Incidence and Significance of Nontarget Embolization following Transarterial Treatment of Hepatic Malignancy

B.J. Newgard, K.T. Brown, G.I. Getrajdman

Objectives: To determine the significance of post-treatment non-target embolization (NTE) as identified on immediate post-embolization CT following transarterial treatment of hepatic malignancy.
Methods: All hepatic arterial embolizations (HAE) performed between November 18, 2013 and August 26, 2014 for the treatment of primary or metastatic liver disease and in which an immediate post-procedure CT was performed were reviewed. All images were reviewed to evaluate for NTE. Patient demographics and length of hospital stay following embolization were noted. Note was also made of complications related to the embolization procedure or associated NTE.
Results: A total of 138 cases were reviewed during the above time period, all of which were bland particle HAE. 42 of these cases had evidence of NTE on the post-procedure CT (42/138, 30%). Of the 42 patients with NTE, 35 involved the gallbladder (35/42, 83%). The mean length of hospital stay for patients with NTE and without NTE was 3.8 +/- 1.7 days (range 2 to 8 days) and 3.8 days +/- 2.4 days (range 2 to 22 days), respectively (P = 0.99). There were two complications in the NTE group (2/42, 5%) related to the embolization procedure including one patient who developed acute ischemic cholecystitis following NTE of the gallbladder that required percutaneous cholecystostomy and ultimately cholecystectomy. The other complication was an incident of contrast-induced nephropathy. In the group without NTE, there were six patients (6/96, 6%) with complications including one death occurring in a patient with hepatic failure. The other complications included a hepatic abscess requiring percutaneous drainage, acute pancreatitis, pneumonia, and two patients with GI bleeds.
Conclusions: Non-target embolization following transarterial hepatic embolization is identified on post-procedure CT in up to 1/3 of patients but is not associated with longer hospital stay or a higher complication rate.

Poster 92: Periprocedural Evaluation and Management of Nurse Practitioner-Led Thoracentesis and Paracentesis in the Oncology Patient

J. Anuran-Torres, S.J. Kim-Saechao

Objectives: This presentation will focus on the evaluation and management process involved in nurse practitioner led drainages, specifically paracentesis and thoracentesis, in the oncology patient.
Methods: Nurse practitioners are increasingly involved in procedures historically performed by physician proceduralists in the oncology setting. This presentation will focus on the evaluation and management process involved in nurse practitioner led drainages, specifically paracentesis and thoracentesis, in the oncology patient. Discussion will include periprocedural evaluation of patients prior to intervention, as well as safety techniques to minimize complications during and after the procedure.
Results: N/A; not a research study
Conclusions: N/A; not a research study 3 objectives to be obtained by the end of session: 1. Elaborate on the top 3 risks and complications associated with paracentesis and thoracentesis. 2. List the preprocedure laboratory testing utilized in evaluate the patient. 3. Evaluate the safety profile of drainages while on anticoagulants.

Poster 93: Pressures Obtained during Transjugular Liver Biopsy Predict Cirrhosis

A. Star, M.P. Chapman, H. Bohorquez, D.A. Devun, D. Kay, D. Kirsch

Objectives: Our institution currently performs over 200 transjugular liver biopsies (TJLB) annually, during which pressures are routinely measured. The question is, what do the pressures mean? How do these pressures play a role in clinical management? A review of the literature reveals that the clinical relevance of pressures obtained during TJLB remains poorly understood. Consequently, we decided to attempt to answer that question by performing a retrospective study investigating the relationship between pressures and clinical outcomes.
Methods: We included all TJLB performed at our institution between 2009 and 2012 with recorded pressures and histopathologic fibrosis staging (N=424 biopsies). For free hepatic pressure, the catheter was situated freely in the lumen of the hepatic vein. For hepatic wedge pressure, the catheter was advanced until it was wedged against the liver parenchyma within the hepatic vein. The transhepatic gradient was calculated as the difference between the wedge and the free hepatic pressures. The clinical outcome we investigated was cirrhosis, as defined by the histopathology of the biopsy sample, scored as Scheuer stage 4 or 3-4 fibrosis. For our analysis, we chose to establish threshold clinical parameters for hepatic wedge pressure and transhepatic gradient which would allow us to predict cirrhosis in transplant and non-liver transplant patients. We accomplished this by employing a Receiver Operating Characteristic (ROC) analysis. We performed subgroup analysis on the two patient populations included in our study (liver transplant group N=313, non-liver transplant group N=111).
Results: We found that wedge pressure ≤25.5 has a 96% NPV for cirrhosis in liver transplant patients. (See Table.) Our data also shows that a transhepatic gradient ≤6.5 has a 96% NPV for cirrhosis in liver transplant patients. In addition, wedge pressure >25.5 has 84% specificity for cirrhosis in liver transplant patients. For the non-liver transplant subgroup, our data shows that a transhepatic gradient >8.5 has a 85% PPV for cirrhosis, and a transhepatic gradient of ≤8.5 has a 71% NPV for cirrhosis. In addition, a transhepatic gradient of >8.5 is 87% specific for cirrhosis in non-liver transplant patients.
Conclusions: Our data suggests that pressures measured during TJLB are able to reliably and accurately rule out cirrhosis in liver transplant patients. Moreover, our study establishes a new clinically relevant threshold of 6.5 for transhepatic gradient and 25.5 for wedge pressure for cirrhosis in liver transplant patients. In non-liver transplant patients, our data suggests that elevated transhepatic gradient as measured during transjugular liver biopsy is able to accurately and precisely predict cirrhosis. Moreover, our study establishes a new clinically relevant threshold of 8.5 for transhepatic gradient for cirrhosis in non-transplant patients.

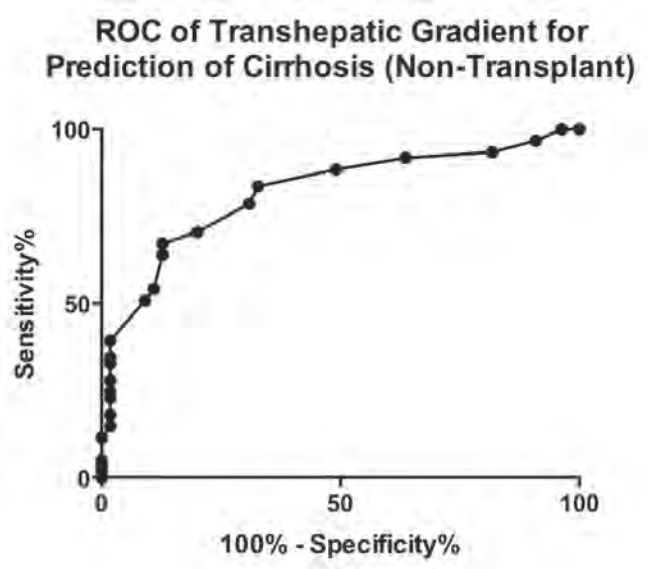

Prediction of Cirrhosis by Transjugular Intrahepatic Pressure Measurement

		Area Under ROC Curve	Diagnostic Threshold Pressure (mmHg)	Sensitivity	Specificity	Likelihood Ratio	PPV	NPV
Transplant Patients	Wedge Pressure	0.66	>25.5	0.54	0.84	3.39	0.19	0.96
	Transhepatic Gradient	0.67	>6.5	0.62	0.75	2.48	0.14	0.96
Non-Transplant Patients	Wedge Pressure	0.72	>25.5	0.52	0.74	2.06	0.70	0.58
	Transhepatic Gradient	0.82	>8.5	0.67	0.87	5.28	0.85	0.71

Poster 94: Transradial Access for Peripheral Interventions: Analysis of Technical Failure Etiology

V.V. Patil, V.B. Amin, R.S. Patel, N.E. Tabori, E. Kim, R.A. Lookstein, F.S. Nowakowski, A.M. Fischman

Objectives: Transradial access (TRA) for peripheral interventions has recently seen increasing adoption across many centers worldwide. There is limited data on etiologies of TRA failure, particularly for repeat access. In this study, failure mode analysis is performed to delineate causes of TRA failure in both initial TRA and repeat TRA patients.
Methods: Retrospective review of 941 consecutive TRA procedures performed in 639 patients between April 2012 and September 2014 at a high volume academic medical center was conducted. Data collected included: technical success (defined as use of TRA for the intended intervention) and etiology of unsuccessful TRA. Poisson confidence interval for rate of failure was calculated and X2 test was used to compare first-time TRA failure rate with repeat TRA failure rate.
Results: TRA failure was 3% (28/941). 8 of 28 (28.6%) failures were in patients in whom a previously successful TRA was performed (7 patients had 1 prior successful TRA, 1 patient had 2 prior successful TRAs). Failure rate for first-time TRA is 3.1% (20/639, 95% confidence interval 1.9-4.8). Failure rate for subsequent TRA is 2.9% (8/275, 95% confidence interval 1.3-5.7). There is no difference between the failure rates of the two groups (P=0.86). Failure mode analysis revealed Barbeau D classification as the most common etiology of failure, accounting for 21% (6/28) of failures. Radial artery occlusion, small radial artery size and radial loop were the next most common etiologies, with 4 patients in each category. See Table 1.
Conclusions: Technical success of TRA for peripheral interventions is high and failure is uncommon (3% failure rate). Failure mode analysis reveals Barbeau D classification as the most common etiology. Failure rates are not statistically significant for first-time TRA patients as compared to repeat TRA patients.

Failure Mode Analysis of TRA Access

Etiology of Failure	Mode
Barbeau D	6
Small Radial Artery	4
Radial Loop	4
Radial Artery Occlusion	4
Hematoma Precluding Catheterization	3
Catheter Not Long Enough	3
Brachial Artery Stenosis	1
Subclavian Artery Stenosis	1
Unknown	2

Poster 95: Increased Rate of Replacement for Percutaneous Gastrojejunostomy Tubes Placed Ensuent to Another Form of Enteral Access vs. Those Gastrostomy Tubes Placed as the First Enteral Percutaneous Access

M. Warren, M. Osher, A. Croake, L. Bergmann, L. Vance

Objectives: Gastrojejunostomy (GJ) tubes are an important vehicle for providing enteral feeding. A patient that suffers from severe gastroesophageal reflux, has altered anatomy, or has gastric outlet obstruction may require a gastrojejunostomy tube. The purpose of our study was to determine if there is a higher rate of failure among primarily placed gastrojejunostomy tubes vs. gastrojejunostomy tubes replacing an existing percutaneous enteral access site.
Methods: After obtaining institutional review board approval, a retrospective review of all image guided percutaneously placed gastrojejunostomy (GJ) tubes over the last five years at our community hospital was performed. Patients were placed into two categories: those receiving a GJ tube as their first enteral access, or as a subsequent access after previous percutaneous enteral entree into the gut. A total of 11 patients had GJ tubes placed as their first enteral access. The average age of primary GJ access was 63. A total of 6 patients required GJ tube placement subsequent to a prior percutaneous enteral access. The average age of these patients was 68.
Results: Of the 11 patients with GJ placement as their first enteral access 3 failed. One due to obstruction-lasting on average 3 months, one to fracture-lasting 1 month, and one for an unknown reason-lasting 2 months. Of the 6 patients with a GJ tube placed ensuant to another form of enteral access 4 tubes failed. Two GJ tubes failed due to obstruction-lasting 2 and 1 weeks, another GJ from dysfunction-lasting 1 week, and another GJ was replaced for an unknown reason-lasting 4 months. The first two failed GJ tubes replaced gastrostomy tubes, and the last two failures replaced jejunostomy tubes. The two GJ tubes that did not fail were placed subsequent to gastrostomy tubes. Our findings reveal a relative risk of requiring GJ tube replacement after a prior enteral access vs. primary GJ tube placement is 2.09 (95 % Confidence Interval of 0.65-6.67; P = 0.21)
Conclusions: Although this is a limited study, our findings demonstrate a 2.09 times higher risk of GJ tube replacement in patients who received a GJ after a previous form of enteral access vs. those patients with GJ tube as their first enteral access into the gut. When a GJ tube is indicated it should be placed as the first means of enteral feeding in order to reduce the future increased risk of needing replacement if one is eventually placed after a previous means of enteral access.

Poster 96: Endoluminal Radio Frequency Ablation with Subsequent Stenting in Biliary, Pancreatic Duct and Portal Vein Occlusions

M. Mizandari, N. Habib, T. Azrumelashvili

Objectives: Malignant block recanalization percutaneous technique is presented
Methods: 113 biliary, Wirsung duct and PV recanalization procedures has been performed to 97 patients; Unresectable biliary block - 81 (cholangiocarcinoma 26, pancreatic cancer 24, gallbladder cancer 9, liver hilum metastatic invasion 8, papilla of Vater tumor 7, hepatocellular carcinoma 5, common bile duct metastatic invasion 1, pancreatic metastasis - 1), Unresectable Wirsung duct block - 5 (all pancreatic cancer) and symptomatic PV tumor thrombus - 11 (HCC- 10, Liver sarcoma-1) cases. 10 to 15 Watts for 2 minutes was applied using bipolar endoluminal RF device (Habib™ EndoHPB, EMcision Ltd., London, UK), placed in duct or PV blocked area using guidewire technique via percutaneous biliary\Wirsung drainage fistula or via direct US guided percutaneous PV puncture. Procedure finishes with metal stent placement. Safety drainage catheter was repositioned in biliary&Wirsung duct cases.
Results: Biliary&Wirsung patency has been restored in 95 (97.9%) of 97 procedures; in 2 (2.1%) cases guidewire conduction failed; 4 patients generated stent occlusion in 7 and 8 months after RFA&stenting requiring percutaneous drainage. PV procedures were fulfilled completely 7 (63.6%) cases; in 1 (9.1%) case RF device could not be introduced and procedure was completed by stent positioning withour RFA processing, in 3 (27.3%) cases recanalization procedure could not be performed because guidewire conduction failure; PV patency restoration has been achieved in 7 (63.6%) cases. There was no 30 day mortality, hemorrhage or pancreatitis following biliary and Wirsung duct RFA&stenting; in 1 case of PV thrombus processing significant intraabdominal bleeding was documented and patient died because of polyorganic failure.
Conclusions: Endoluminal RFA&stenting is safe and effective in biliary&Wirsung duct block recanalization; it might be successfully used for PV malignant thrombus recanalization in selected patients. Procedure track ablation and/or coil embolization should be recommended in PV cases to avoid possible bleeding problems

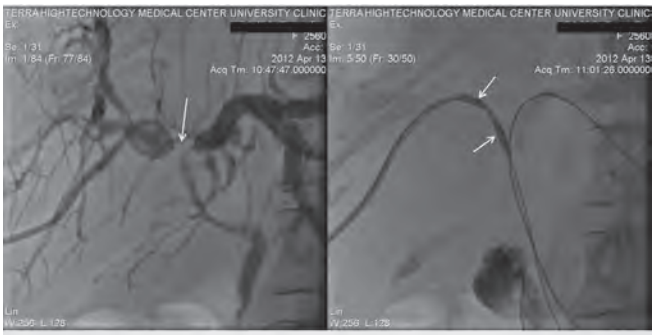

Klatskin tumor, bilateral biliary drainage. Contrast injection shows the tumor block in HD confluence (arrow)

Wires are conducted through the block. Right duct is processed by 8 Fr diameter bipolar endoluminal RF device; electrodes are identified by arrows

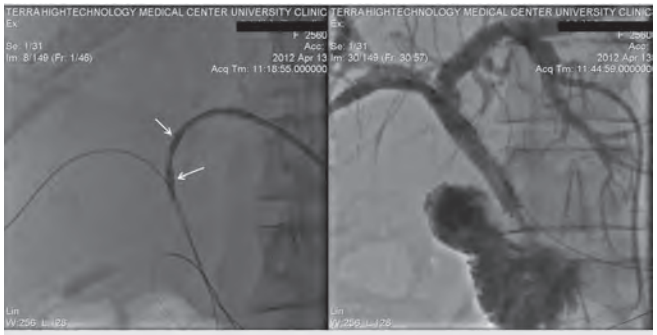

Left duct is processed by 8 Fr diameter bipolar endoluminal RF device; electrodes are identified by arrows

Biliary patency has been restored

Poster 97: Spectrum pf Percutaneous Image-Guided Pancreatic Duct Internventions on Pancreatic Head Tumor Patients - Indications, Technique & Devices

M. Mizandari, N. Habib, T. Azrumelashvili

Objectives: Percutaneous image-guided pancreatic duct (PD) drainage and subsequent second- line procedures (duct recanalization and endoluminal biopsy) are presented

Methods: Thirteen patients with pancreatic head tumor underwent percutaneous image-guided PD drainage. Puncture of the PD was performed using either ultrasound (7) or computed tomography (6) guidance using 22 to 18G needles. PD neck segment was accessed in 2 cases, body segment - in 7 and the tail segment - in 4 cases. Hydrodissection was used to create the safe needle route in 2 CT guidance cases. Transgastric and tranhepatic puncture route was used in 4 and 3 cases respectively. A fixed tip "Pig-Tail" drainage catheter was placed under the real-time fluoroscopy guidance. All second line procedures (metal stent placement - 2, endoluminal RFA & metal stent placement - 4, endoluminal biopsy- 1) were performed under fluoroscopy guidance using the PD drainage fistula. Endoluminal RFA was performed using a novel 5 Fr diameter RF device, metal stent placement was achieved using a conventional technique. Endoluminal biopsy was performed using a forceps device. After PD recanalization safety drainage catheters were repositioned and kept closed for a week prior to removal.

Results: PD drainage was successful in all 13 cases; in post-biopsy pancreatic fistula case practically non-dilated PD was accessed. Clinical improvement was documented by the gradual reduction in clinical symptoms and improved blood test results. The amount of received pancreatic juice was between 300 -900 ml/day. Three cases who had had recent onset of diabetes showed a dramatic improvement in hyperglycemic control with complete cessation of medication in 2 cases and a significant dose reduction in 1 case. Second-line procedures were fulfilled in 6 (85.7%) of 7 cases; in 1 (14.3%) case the procedure completion was impossible due to guidewire conduction failure. Endoluminal biopsy enabled to get tissue material safely; in all 5 PD recanalization cases the safety drainage catheters were withdrawn in a week. All patients tolerated the procedure well, there was no 30-day or hospital mortality.There were no observed technique specific complications, such as hemorrhage, vessel perforation or infection, even in the cases where the transgastric route was used.

Conclusions: Percutaneous image-guided PD drainage and spectrum of second-line procedures (stenting, endoluminal RFA&stenting, endoluminal biopsy) appears to be a safe and effective in pancreatic head cancer patients management; drainage procedure might be considered for symptomatic PD occlusion as an alternative to retrograde stent placement and EUS guided antegrade drainage and stenting. PD recanalization and endoluminal biopsy using PD drainage fistula is safe and efficient.

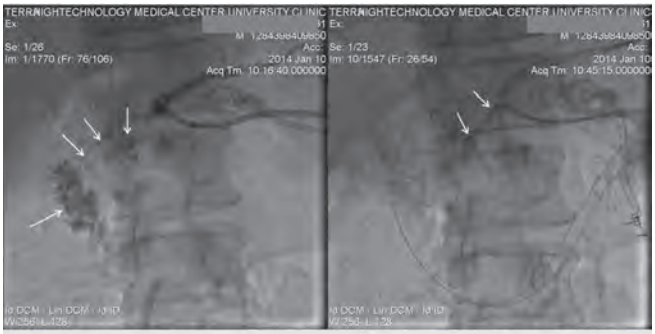

Wirsung duct is decompressed by drainage; Contrast injection allows to see the PD duct Stenotic segment and duodenum (arrows)

5 Fr diameter endoluminal bipolar RF device is positioned for PD stenotic segment processing; arrows Identify device electrodes

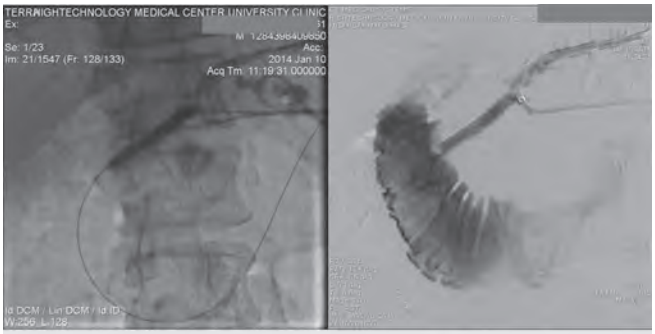

6 mm balloon expandable metal stent is implanted in PD stenotic segment after RF processing

PD restored patency is documented by contrast injection using repositioned drainage catheter

Poster 98: Post Transarterial Radioembolization (TARE) Dosimetry: Implementation and Limitations

M.T. Alshammari, P.L. Esquinas, H. Ma, C.F. Uribe, D. Liu, A. Celler

Objectives: **Learning Objectives:** To define the terms: activity, quantitation, and dosimetry. To review the techniques which are currently used to estimate post TARE dosimetry. To compare the precision of dosimetry based on Bremsstrahlung SPECT/CT and 3D TOF PET/CT post Y-90 and to correlate them with pretreatment Tc99 MAA SPECT/CT. To review the challenges and strategies to achieve accurate quantitative Y-90 imaging.

Methods: **Background:** Although techniques have been established to calculate TARE administered activity (e.g. empiric, medical internal radiation dose (MIRD) single compartment, partition model and body surface area), image dose determination of segmental or intratumoral activities is not possible. With the increasing interest in post implantation dosimetry as a surrogate to tumoral response, further refinement of the imaging and image quantification is necessary.

Results: **Teaching Points:** Conventional imaging methods have limited accuracy and resolution, resulting in the inability to calculate or predict tumoral doses. Quantification of activity distribution from Y-90 3D TOF PET images faces a number of challenges including: low statistics of true coincidences and large number of random coincidences, resulting in significant noise in the reconstructed images. Similarly, imaging of Y-90 Bremsstrahlung radiation is very difficult, images have poor resolution and currently there are no methods to quantify activity distributions that would be easily transferable to the clinical settings. For both PET and SPECT, we are investigating methods to improve quantitative accuracy of image reconstructions as this can potentially lead to better dosimetry estimates.

Conclusions: **Conclusion:** Current methods of activity determination involve the use of variables and factors that do not relate to actual tumor physiology, or volume. The establishment of accurate, reproducible post TARE dosimetry can serve as a verification technique of dosimetry to tumour, and have the potential to avoid suboptimal administration.

Poster 99: Endovascular Treatment of Hemorrhage after Radiofrequency Ablation for Hepatic Malignancy

D. Hyun, S. Shin, S. Cho, K. Park, H. Park, Y. Do

Objectives: To evaluate imaging findings and endovascular treatment results for bleeding after radiofrequency ablation (RFA) of primary or secondary hepatic malignancy

Methods: Twelve consecutive patients (mean age, 65.5 yrs; 8 males and 4 females) who underwent RFA and transarterial embolization for bleeding control were included in this study from January 2003 to December 2014. Liver function (Child-Pugh score), coagulation status, tumor characteristics (primary vs. secondary, size, number, and location within the liver), and ablation process were analyzed. Onset of bleeding (immediate vs. delayed), CT and angiographic findings, and embolization method were reviewed. Treatment results included technical success (defined as hemostasis on completion angiogram), clinical success (defined as neither recurrence within 30 days nor mortality), and complication. Institutional review board approval was not required.

Results: RFA and tract ablation were performed for the treatment of HCC (mean size, 1.6 cm) in 9 patients and hepatic metastasis from colon cancer (mean size, 1.9 cm) in 3 patients. Tumors were located in subcapsular area (n=4), adjacent to middle hepatic vein (n=1) and portal vein (n=1), and central area (n=6). Coagulation status was normal in all patients. Immediate bleeding occurred in 11 patients with delayed bleeding in one patient. CT finding (available in 7 patients) consisted of peritoneal contrast extravasation (n=3), hemoperitoneum (n=1), and intraparenchymal contrast leakage (n=3). Angiography was performed in 10 patients and positive findings included contrast extravasation (n=5), arteriportal shunt (n=1), arteriovenous shunt (n=1), and arteriobiliary shunt (n=1). Technical success rate was 100%. Clinical success rate was 100%. No complication happened.

Conclusions: Endovascular treatment is effective and safe for control of post-RFA bleeding. Embolization should be considered in patients with unstable vital sign or peritoneal contrast leakage on CT.

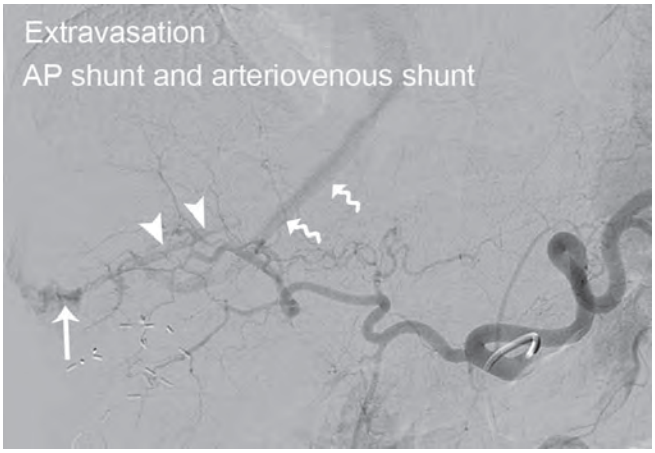

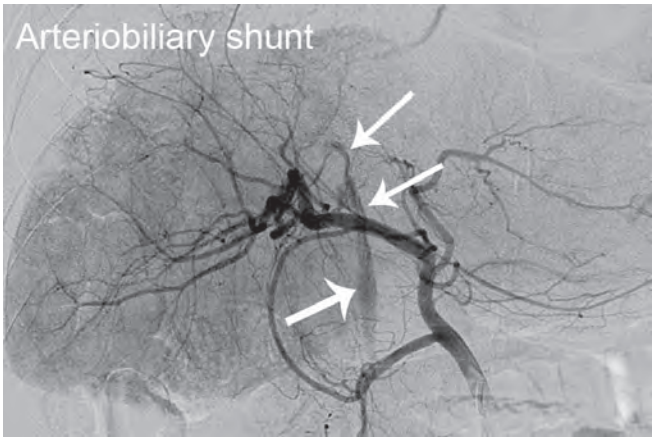

Poster 100: Ex-vivo Ovine Liver Model Simulating Respiratory Motion and Blood Perfusion for Validating Image-Guided HIFU Systems

X. Xiao, M. Domschke, I. Karakitsios, A. Melzer

Objectives: The effect of moving organs and blood perfusion on image guided procedures such as focused ultrasound is challenging therefore we have developed ex-vivo ovine liver phantoms to simulate respiratory motion and blood perfusion. The simulator was used to validate ultrasound image-guided HIFU treatment when the target tissue was moving.

Methods: The respiratory liver motion simulator consists of a physical ovine liver, agar-gelatine block surrounding the liver, a medical air balloon which is connected to a lung ventilator, and two water balloons which are used to move the phantom back to its original position. The whole setup was MR compatible, including the ventilator which is used to provide simulation of respiratory motion. The movement generated by the simulator was analysed via an MR compatible ultrasound system, and this real-time motion information was used to guide a dynamic high intensity focused ultrasound system (Exablate 2100 system, 0.55MHz) to steer its focus to follow this motion (Figure 1). The blood perfusion for ovine liver is built as well. A heart lung machine (HL30, Maquet, Germany) was used to provide perfusion in via the portal vein and out from the hepatic veins of the ovine liver with some minimal losses due to leakage in the tissue . The machine provides continuous and pulsatile saline water flow with rates of 220 millilitre per minute. X-ray angiography images were made to visualise the vessel prior to scanning with the MR and ultrasound doppler. The perfused vessel was then scanned in the 1.5 T Signa HDxGE (GE, USA) and ultrasound wireless scanner (ACUSON Freestyle, SIEMENS, GERMANY).

Results: Mean displacement between expiration and inspiration was up to 30 mm along superior-inferior direction. The setup also allowed motion in left-right direction by reducing the width of the phantom block. After establishing the saline water perfusion, the vessels of the ovine liver provides a large contract from the background in x-ray and MR scan (FRFSE-XL, TE=8.7, TR=400). And a clear pulse was observed in the ultrasound colour Doppler (Figure 2).

Conclusions: The ovine liver movement generated by the respiratory simulator is comparable to that of a human liver in vivo. This model could be used to test the influence of motion on image guided focused ultrasound therapy. The successful re-creation of physiological flow in the peripheral arteries of ovine liver has provided a model for testing the influence of blood flow rate on the image guided focused ultrasound sonication. Therefore the phantom provides a low-cost option for validating ultrasound and MR image-guided focused ultrasound treatment.

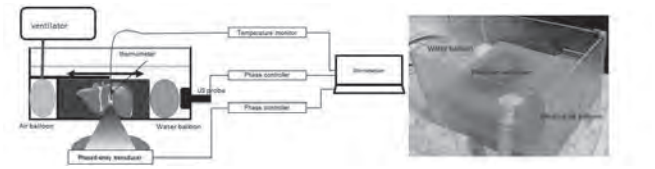

Illustration and photo of respiratory liver motion simulator, ovine liver is embedded into 3% agar-gelatine phantom

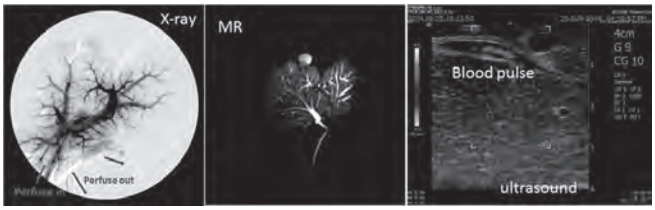

x-ray scan, and MR scan and ultrasound scan results of the ovine liver phantom

Poster 101: Novel Method for Rapid Percutaneous Biliary Leak Management using an MVP and an Epoxy Resin

A. Agbay, F. Moeslein

Objectives: Biliary leaks are a common complication after hepatic and biliary surgery, with the rate of post-operative occurrence reportedly ranging from 0.8 - 12%. These leaks are associated with significant patient morbidity, as they may result in formation of bilomas, fistulas, biliary peritonitis or sepsis. Traditional therapy for these leaks involves biliary decompression, either by endoscopically placed stents or via percutaneous drainage. While many leaks resolve with treatment, persistent leaks are clinically challenging to manage. The Micro Vascular Plug (MVP) (Reverse Medical, Irvine, CA) is a microcatheter deployable device incorporating a membrane along its leading edge designed for rapid vascular occlusion. The following cases illustrate a novel method for rapid percutaneous biliary leak management using an MVP and an epoxy resin.

Methods: Patient 1- 77 y/o M with metastatic renal cell carcinoma, including hepatic metastasis treated with chemoembolization and radiofrequency ablation in 2010. In 2013, he presented with recurrent low-grade fevers and was found to have developed left-sided ductal dilation secondary to biliary structuring. His was initially treated with biliary stenting for the following 8 months, but with no resolution of the intrahepatic biliary stricture. We elected to ablate the obstructed ducts by deployment of a 5 mm MVP device and Onyx. Patient 2- 46 y/o M with PMH of metastatic colon cancer status post hepatic wedge resection for metastatic disease in segment 3. Post-opera-

tively the patient developed a biliary leak at the resection site, which was treated for 7 months with internal-external biliary drainage with no resolution of symptoms. We elected to treat him definitively using MVP device and cyanoacrylate glue to selectively ablate the damaged duct.
Results: Both patients failed months of standard methods of biliary management prior to undergoing biliary occlusion. Both ablations were performed as single sessions with complete removal of the biliary drains at the termination of the case. At the time of submission, both patients had complete resolution of symptoms and no immediate or delayed complications from the procedure.
Conclusions: In this technique, the MVP device serves as a dual-purpose embolic platform and protection device for biliary intervention. Given the expense, morbidity and quality of life issues related to traditional long duration biliary intubation, this technique should be considered as a lower cost, low risk alterative for the management of biliary leaks.

Poster 102: Application of Colonic Stents for Malignant Obstruction of the Inferior Vena Cava

J. Ng, O. Ahmed, D.S. Wang, R. Shah, L. Hofmann

Objectives: To describe the novel use of self-expanding colonic stents to treat malignant obstruction of the IVC.
Methods: All patients (n=56) who underwent IVC stenting for malignant obstruction between 2007 and 2014 were retrospectively reviewed. Of these, nine patients (5 male, 4 female, age range: 28-75) underwent stenting of the IVC with a nitinol self-expanding colonic stent (Wallflex®) for severe malignant intrahepatic IVC obstruction. Four of these patients underwent primary stenting with a steel endovascular stent (Wallstent®) that migrated intraprocedurally; these were then subsequently secured using a colonic stent. The etiology for obstruction included primary hepatic malignancy (44%) and hepatic metastatic disease (56%). Primary sources of hepatic metastatic disease included colonic, pancreatic, duodenal, and neuroendocrine tumors. Three patients had concurrent IVC tumor thrombus. Presenting symptoms included lower extremity edema (89%), worsening ascites (33%), or abdominal distention (22%). All stents were deployed in the intrahepatic IVC. Additional modifications included one stent extending into the right atrium to secure a migrated stent, two stents extending into the right atrium for intra-atrial thrombus, and one stent placed across the right atrium into the SVC to secure a migrated stent.
Results: 10 colonic stents were placed in 8 procedures; 6 stents were utilized in response to a migration event. The technical success rate was 100%. 1 patient presented with in-stent thrombosis at 3 days due to cancer infiltration through stent interstices and was treated successfully with a covered stent. No other major or minor complications occurred. The average pre- to post-stent cavoatrial gradient was reduced from 16.5 mm Hg to 5.5 mm Hg.
Conclusions: Colonic stents may represent a technically feasible treatment option for malignant obstruction of the IVC. They may also have utility in the management of intra-procedural migration of traditional IVC stents.

Poster 103: Percutaneous Cryoablation for Schwannomas: A Promizing Treatment

B. richioud, A. Kalenderian, M. Cuinet, F. Pilleul, G. Vaz, P. Thiesse

Objectives: To evaluate efficacy and safety of percutaneous cryoablation for schwannomas.
Methods: Two women were treated for painful lesions (11mm and 24mm) of the right buttock, corresponding to documented schwannomas of the iliohypogastric nerve (lateral cutaneous branch). US-guided percutaneous cryoablations were performed under general anesthesia.
Results: In both cases, the MRI showed a progressive reduction of the pseudo-nodular, hyper T2 but non-enhancing scar, which completely disappeared at 6 months. Patient 1 presented persistent pain during 3 weeks, requiring anti-inflammatory treatment. For patient 2 during the 6 month follow-up, T2 weighted images showed a significant oedema in the surrounding soft tissues, and pain intensity remained the same, sometimes even increased, despite the escalation of analgesics and anti-inflammatory treatments. At 6 months we decided to perform a percutaneous nerve infiltration upstream and the patient was quickly relieved, with an almost complete disappearance of pain in 5 days. Neurologically, both patients described mild paresthesia in the treated area after the procedure, which disappeared in one month. There were no neurological symptoms downstream.
Conclusions: Tumor lesions of peripheral nerves are divided into pseudo-tumors and true tumors. Among pseudo-tumors, several series are available on cryoablation for traumatic neuromas and Morton neuromas. To our knowledge however, no cases of percutaneous cryoablation is reported for the treatment of true tumors as schwannomas, neurofibromas or nerves malignancies. Thus our experience appears original and positive, although larger studies are needed. Note however that systematic prescription of anti-inflammatory treatment immediately after the cryotherapy would probably be relevant, which details remain to be clarified.

Poster 104: Prognostic Significance of Metastatic Lymph Node Ration in Gastric Cancer

I.F. Kayali, R. Habiboglu, S. Cakar, H. Sayan, F. Cetinyokus, S. Ozyurt, E. Aydinkarahaliloğu, Y. Lehimcioğu, N. Aslan

Objectives: The survival in gastric cancer patients is still poor, and lymph node metastasis is considered one of the most important prognostic factors. This study was carried out to determine the prognostic significance of metastatic in gastric cancer patients.
Methods: We retrospectively reviewed the data of 179 patients who were irradiated curatively at Ankara Numune Training and Research Hospital Radiation Oncology Clinic. Of the patients, 137 (76.5%) had histologically proven lymph-node metastasis. All patients were irradiated 180 cGy/ fraction,totally 4500 cGy. The prognostic value of the metastastic node ratio, defined as the ratio of the number of metastatic lymph nodes over the total number of resected lymph nodes, and the pN classification was assessed. N ratio categories were determined as follows; N ratio >0.20 :50 pts. 36.49%; N ratio 0.20 – 0.39 :42 pts. 30.65%; N ratio 0.40-0.59:17 pts. 12.40%,N ratio 0.60-0.89: 13 pts. 9.48%,N ratio 0.80-1: 15 pts. 10.94%.
Results: After a median follow-up of 26 ± 4 months (1–44 months), the 1 year, 2 year and 3 year overall survival of the patients were 73,69%, 50,14%, 38,29% respectively. For pN0;1 year and 2 and 3 year survival rates are 88% and 75% and 75% respectively (median survival 37±4 months). For pN1; 1year and 2 and 3 year survival rates are 74% and 52% and 32% respectively (median survival 25±2 months). For pN2; 1 year and 2 and 3 year survival rates are 80% and 56% and 56% respectively (median survival 28±3 months). For pN3; 1 year and 2 year survival rates are 58% and 33% respectively(median survival 14±2months). Statistically pN was found to be significant(P=0.015). For metastatic lymph node/resected lymph node ratio the survival rates are shown in the table. The ratio was found to be statistically significant for the survival (P =0,007).
Conclusions: It has been previously suggested that the number of metastatic lymph nodes is a prognostic factor for gastric cancer. Lymph node ratio category has advantages in providing a more precise prognostic value than the pN category [4]. Therefore, the addition of the n ratio to the N category defined by the JCGC may be a useful strategy in the N-staging classification of gastric cancer. The metastatic lymph node ratio is a simple and useful independent prognostic factor and should be considered as an important component in the lymph node category.

Poster 105: The Nottingham Prognostic Index for Primary Breast Cancer Patients Treated in a Single Institution

I.F. Kayali, R. Habiboglu, N. Aslan, S. Cakar, Y. Lehimcioğu, F. Cetinyokus, H. Sayan, E. Aydinkarahaliloğu, S. Ozyurt

Objectives: In breast cancer, prognostic factors can be defined as clinical and molecular factors. Among clinical factors lymph node status, tumor size, histological grade, reseptor status, menopausal status and the age of the patient can be included. In 1982 Galea MH et.al. constructed a prognostic index for patients with primary, operable breast cancer.[1] One of prognostic factors known as Nottingham Prognostic Index (NPI), which is combination of known prognostic factors such as tumor size, grade and axillary node status, is recently in usage in some European countries in clinical practice in prediction of breast carcinoma patients' survival. Therefore, the aim of this study was to verify, according to our experience, the prognostic significance of Nottingham Prognostic Index (NPI) in breast carcinoma patients in association with other prognostic factors.
Methods: In the study 64 patients were included. The age of the patients was between 25 and 69 years (median 46 years). The histology was ductal carcinoma in 51 patients (80%). It was grade I in 8 patients (12,5%), grade II in 28 patients (43.8%), and grade III in 16 patients (25%). In 12 patients (18.8%) the grade was missing. The following data for each patient were collected: age, tumor size, histological grade, axillary lymph node status, overall survival, . The Nottingham Prognostic Index (NPI) was calculated from the pathological information and patients were grouped according to the standard NPI index into: good prognostic group, moderate prognostic group, and poor prognostic group
Results: The followup time was between 5 and 134 months (median 26 months). The overall survival rate for 5 years is 75% and for 10 years is 34%. We found that patients in the good prognostic group survived longer than the patients in the poor prognostic group. This was not statistically significant because of the inhomogeneous distribution of patients among the groups
Conclusions: Although the search for single independent prognostic factors in breast cancer has often produced conflicting results, the use of prognostic indexes, especially when compiled using traditional parameters, is a useful aid to the clinician, since they can provide a reliable indication of how individual tumours will evolve [4] and the NPI was found to allow clinicians to accurately predict prognosis [5] and gives a better definition of the prognostic profile for each patient. It seems that other prognostic factors in combination with NPI prognostic groups in our group of patients may have

practical clinical relevance for the management of patients with breast carcinoma if number of patients is enlarged.

Poster 106: The Impact of Radiotherapy on Serum Tumor Necrosis Factor Alpha in Head and Neck Cancer Patients

I.F. Kayali, R. Habiboglu, S. Ozyurt, N. Aslan, H. Sayan, F. Cetinyokus, E. Aydinkarahaliloğu, Y. Lehimcioğu, S. Cakar

Objectives: The purpose of this study is to evaluate the effect of radiotherapy on serum TNF alpha levels in patients with head and neck cancers.
Methods: In this study 45 patients aged 28 to 73 (median age 50 years) with head and neck malignities were included. Curative radiation therapy was performed to all of the patients. The total dose was between 5600 and 7000 and was given 200 cGy/fraction, 5 days a week, from all portals by cobalt 60 teletherapy unit. Primary tumor site and the neck (if needed) were irradiated. It was laryngeal carcinoma in 36 patients (80%). The TNF alpha levels were measured before the initiation of the radiotherapy and after the therapy was completed.For the measurement TNF-α ELISA was used. For statistical evaluation Wilcoxon test was used.
Results: In 20 patients (44,4%), the levels of TNF-α were decreased at the end of the radiotherapy compared to pre-RT values. In 26 patients there was an increase in the TNF-α values. There was no statistical significance between the pre-RT and post-RT values. There was no correlation between the stage and the TNF-α levels, and also no correlation was determined between the localization and the TNF-α levels.
Conclusions: During the past few years, several of the primary mediators of inflammatory response have been isolated, and it has become clear that certain host proteins can, of themselves, cause injury through direct and indirect effects on host tissues, and through their effects on host metabolism. Prominent among these proteins is a macrophage-derived hormone known as cachectin. Cachectin is produced by all types of macrophages thus far tested, including macrophages of pulmonary, hepatic, and bone marrow origin. Several other cell types have also been reported to produce cachectin. These include T lymphocytes. In part through its effects on vascular endothelial cells, cachectin can induce a coagulopathic state localized to certain vascular beds, leading to hemorrhagic necrosis of various tissues. This effect is particularly pronounced in certain tumor vessels, such that the hormone was originally recognized by its ability to provoke the hemorrhagic infarction of transplantable neoplasms, and was termed " tumor necrosis factor (TNF)". Cachectin is directly cyctotoxic to endothelial cells, and it also reported that tumor necrosis factor causes an endothelial cell rearrangement TNF has also a variety of other actions including fibroblast proliferation, activation of macrophages and NK cells, and induction of interleukin-1 production. In addition to enhacement of host immune response, TNF is also directly cyctotoxic to tumor cell lines in vitro. Cell killing by TNF is associated with the production of hydroxyl radicals within the sensitive cell lines resulting in oxidative damage to DNA and subsequently DNA fragmentation. The oxidative damage produced by TNF may enhance cellular damage produced by ionizing radiation and suggest that an additive or synergistic interaction may ocur between these two agents. Radiation treatment may also cause depression of bone marrow, tissue damage and deterioration of general condition. It must stressed that macrophages are radioresistant cells. The exact cause of TNF alpha changes during RT is not known. In most of the studies in the literature it was determined that there was an increase in the TNF alpha levels but in our study the changes of the levels were not statistically significant.

Poster 107: Primary Sarcoma of the Breast

I.F. Kayali, R. Habiboglu, N. Aslan, S. Ozyurt, F. Cetinyokus, H. Sayan, S. Cakar, E. Aydinkarahaliloğu, Y. Lehimcioğu

Objectives: Primary sarcomas of the breast are extremely rare with less than 1% of all malignant tumours of the breast reported in literature. Leiomyosarcomas are much more less common, being a subgroup of sarcomas of the breast and was first described 25 years ago, and yet few published reports exist.
Methods: We describe herein a case of primary leiomyosarcoma of the breast in a 25-year-old woman. Left modified radical mastectomy was performed to the patient because of infiltrating ductal carcinoma. Radiotherapy and chemotherapy were given as adjuvant therapies. During the follow-up at 11th month, left axillary total mass excision was performed due to mass existance in left axillary. The pathology revealed high grade malign mesenchymal tumor, leiomyosarcoma.
Results: The patient died after follow-up time of 27 months.
Conclusions: As primary leiomyosarcoma of the breast is very rare it represents a diagnostic and a therapeutic challenge. It constitutes a specific clinicopathologic entity and, therefore should be differentiated from the two main entities in differential diagnosis, cystosarcoma phyllodes and metaplastic carcinoma. Is is believed that breast sarcomas are comparable to soft-tissue sarcomas seen elsewhere An analysis of more cases with a longer follow-up duration is necessary to develop an optimum mode of treatment for leiomyosarcomas at this specific site

Poster 108: Cryoablation of the Breast Cancer in Metastatic Patients. Preliminary Experience

C. Pusceddu, B. Sotgia, N. Ballicu, R. Fele, G. Amucano, L. Melis

Objectives: The aim was to evaluate the safety and efficacy of breast cryoablation (CRA) as local therapy for patient with metastatic breast cancer.
Methods: Thirty-nine breast lesions, mean size 2,1 (range 1 - 6,7 cm) in twenty-nine consecutive patients, mean age 51 (36-81) with core-needle biopsy-proven breast carcinoma and metastases were enrolled in this study. Twenty-three patients had one lesion, 4 patients had two lesions, 1 patient had three lesions and 1 patient had five lesions. The metastases were located in the bone (24 patients), lung (2 patients), liver (2 patients) and lymph-nodes (1 patient). Under local anaesthesia and mild conscious sedation, the tumour and surrounding breast tissue were ablated with percutaneous CT-guided CRA. Cryoablation consisted of 2 cycles each of 10 minutes of freezing followed by a 4-min active thawing phase and a 4-min passive thawing phase for each one. Twenty-four patients underwent one CRA session, four patients 2 CRA sessions and one patient underwent 3 CRA sessions.
Results: All CRA sessions were successfully completed and all breast tumours were ablated. Morbidity consists in transient and mild ecchymotic changes and post-procedural oedema seen in ten cases. The therapeutic outcomes were evaluated by contrast-enhanced CT or MRI at 2-, 6-, 12-, and 18-month interval. The absence of tumour enhancement CT or MR image was considered to indicate complete tumour necrosis. During the mean follow-up of 15 months (6- 28 months) 26 patients had shown complete response to the treatment. Only 3 patients out 29 (10%) had shown relapse close to the treated lesion. These patients were treated with a second CRA procedure. A patient died for liver tumour progression after 16 months.
Conclusions: CRA of metastatic breast cancer is a safe and effective method which allows local control of the disease.

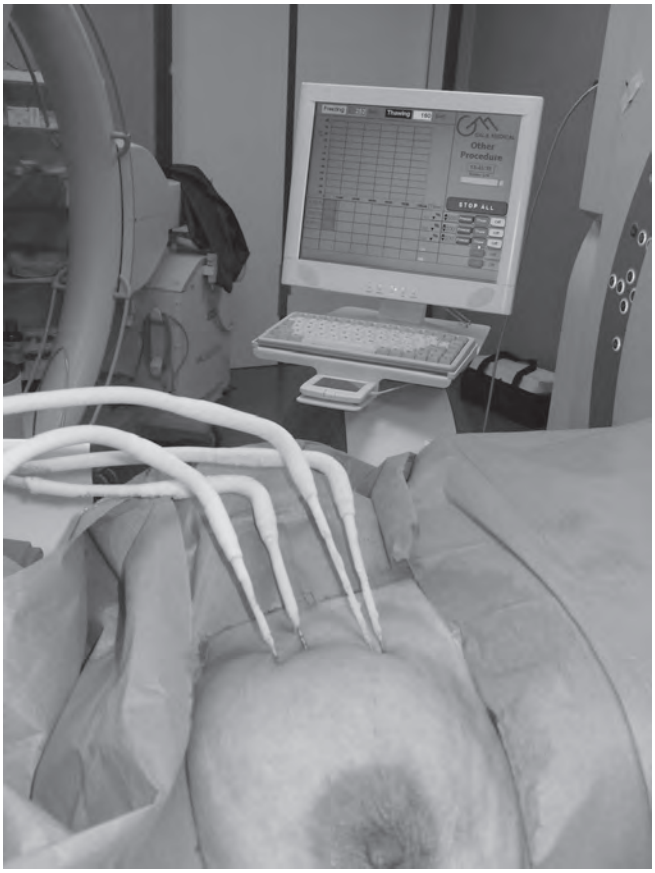

Cryoablation treatment of the right breast cancer during the freezing fase.

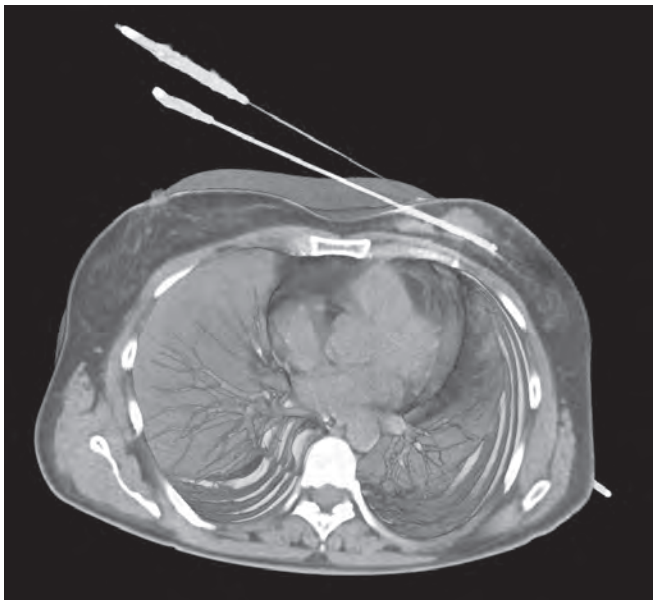

The volumetric CT reconstruction shows the correct positioning of the cryoprobes before the ablation.

Poster 109: Vitamin D Deficiency: In Breast Cancer Patients and in Healthy Women

I.F. Kayali, R. Habiboglu, S. Cakar, S. Ozyurt, N. Aslan, H. Sayan, F. Cetinyokus, Y. Lehimcioğu, E. Aydinkarahaliloğu

Objectives: Numerous observational studies have reported an inverse association between vitamin D status and breast cancer risk. The aim was to determine serum vitamin D levels in breast cancer patients and healthy women.
Methods: Forty breast cancer patients and equal number of healthy females were recruited in this case control study. Serum vitamin D [25 hydroxyvitamin D (25(OH) D)] levels were evaluated before the initiation of radiotherapy in the breast cancer arm. In the brast cancer group the age was between 25 and 72 years (median 48 yrs.), and in control group it was between 17 and 67years (median 38 yrs).
Results: In breast cancer group there was only patient with serum level of vitamin D above 25 ng/mL and she was using vitamin D supplement daily. Serum vitamin D levels in braest cancer patients group were < 3 ng/mL in 3 patients. The vitamin D level range was between <3 ng/mL and 25. 44 ng/mL (median 5.87 ng/mL) In control group, 4 women had serum levels of vitamin D above 25 ng/mL. The vitamin D level range was between < 3 ng/mL and 30.10 ng/mL (median 7.95 ng/mL).
Conclusions: Vitamin D is essential for the formation, growth, and repair of bones and for normal calcium absorption and immune function. It is obtained primarily through exposure of the skin to ultraviolet radiation in sunlight, but it can also be obtained from some foods and dietary supplements. Vitamin D deficiency is a potentially modifiable risk factor that may be targeted for breast cancer prevention and treatment Low serum levels of vitamin D are common at breast cancer diagnosis and are associated with a poorer prognosis in terms of overall survival and distant disease free survival particularly in postmenopausal females. Also in breast cancer patients it was found that 94% women with serum levels of vitamin D less than 20 ng/ml were likely to develop metastases and 73% were likely to die of advance disease. Thus breast cancer patients must undergo an evaluation of serum vitamin D levels Also greater awareness of the insidious consequences of vitamin D deficiency in healthy women is needed. Annual measurement is a reasonable approach to monitoring for vitamin D deficiency.

Poster 110: Does Glutamine Effect Depressive Mood in Cancer Patients?

I.F. Kayali, R. Habiboglu, F. Cetinyokus, H. Sayan, S. Cakar, Y. Lehimcioğu, E. Aydinkarahaliloğu, N. Aslan, S. Ozyurt

Objectives: Fatigue and depression aren't eating problems in themselves, but they can affect a patient's interest in food and their ability to shop and prepare healthy meals. So, depression can be considered a common cause of nutritional problems in patients with cancer and those undergoing treatment. We aimed to evaluate the changes in depressive mood by glutamine in this study.
Methods: We enrolled 72 cancer patients in this study. Of the patients 44 (61.1%) were female and 28 (38.9) were male. The Beck Depression Inventory was performed to each patients before the initiation of glutamine and at the end of 4th week of nutrition. All of the patients received radiotherapy.
Results: The results are given in the table 1 and 2.
Conclusions: Good nutrition practices can help cancer patients maintain weight and the body's nutrition stores, offering relief from nutrition impact symptoms and improving quality of life. Nutrition impact symptoms are those symptoms that impede oral intake. They include, but are not limited to, anorexia, nausea, vomiting, diarrhea, constipation, stomatitis, mucositis, dysphagia, alterations in taste and smell, pain, depression, and anxiety. Early recognition and detection of risk for malnutrition through nutrition screening followed by comprehensive assessments is increasingly recognized as imperative in the development of standards of quality of care in oncology practices

Table 1. Beck depression inventory scores before nutrition

	female	male	total number	%
Minimal depression	24	12	36	50
Mild depression	12	12	24	33,4
Moderate depression	8	4	12	16,6
Severe depression	0	0	0	0

Table 2. Beck depression inventory scores at the end of 4th week of nutrition

	female	male	total number	%
Minimal depression	28	12	40	55,5
Mild depression	12	12	24	33,3
Moderate depression	4	4	8	11,2
Severe depression	0	0	0	0

Poster 111: HU to Iodine Concentration Conversion (HUTICC) Formula

J. Thomas, J. Vetter, J. Swietlik, K. Karaoglu, O. Ozkan

Objectives: To establish a formula that allows for the quantification of Iodine concentration in liver lesions post Transarterial Chemoembolization (TACE) using non-contrast CT imaging.
Methods: In this study Hounsfield Units (HU) were measured using a set of tubes with gradually increasing amounts of Lipiodol mixed into pig's blood. First, HU of 10 mL of pig's blood by itself was measured, which has a HU value similar to a human liver. Then 0.1 mL of Lipiodol was added to the 10 mL of pig's blood, and again the HU was measured. This step was repeated 14 times with incremental amounts of Lipiodol. Since Lipiodol contains Iodine, at a concentration of 475 mg/mL, determination of the iodine concentration for each of the mixtures was possible. Finally, the HU and Iodine concentration values were used to create a formula that expressed the relationship between HU and Iodine concentration in a tumor using least squares method.
Results: The HU values from the pig's blood/Lipiodol mixtures ranged from 67 HU for 10 mL of pure pig's blood, up to 1090 HU for 1.5 mL of Lipiodol added to the original 10 mL pig's blood. The values of Iodine concentration in each of the mixtures ranged from 4.70 mg/mL to 61.96 mg/mL. Using the Linest Function of Excel, a relationship between HU and Iodine concentration was determined to have a slope of 16.82 and a constant of 64.44. Knowing the slope and constant allows for creation of the HU to Iodine Concentration Conversion (HUTICC) Formula. A plot of the line created by the HUTICC formula compared to real data points demonstrates the fit. HUTICC Formula: HU = Iodine Conc x 16.82 + 64.44
Conclusions: Using the HUTICC Formula it is possible to determine the concentration of iodine within lesions in the liver after treatment with TACE. The HUTICC formula may allow for future research to look for a possible correlation between Lipiodol concentration post TACE and patient outcomes, as well as the possibility of using 3D volumetric software to derive the content of chemotherapeutic agents that accumulate in a target lesion. Finally, one should know that the formula gives a rough estimate to compare temporal changes, not the absolute values.

Poster 112: Proximal Compared with Distal Gastric Cancer: Is There Any Difference on Survival?

I.F. Kayali, R. Habiboglu, S. Cakar, F. Cetinyokus, S. Ozyurt, Y. Lehimcioğu, H. Sayan, N. Aslan, E. Aydinkarahaliloğu

Objectives: Epidemiological studies show a continuing rise in the prevalence of proximal gastric carcinoma and the prognosis of patients with this carcinoma is poorer than that of patients with more distally located gastric carcinomas. There are indications that some features of gastric carcinoma are changing, with a possible impact on prognosis. Interest in leading prognostic determinants of proximal gastric carcinoma in comparison with distal gastric carcinoma led us to compare the prognosis of proximal gastric carcinoma patients with those of patients with distal gastric carcinoma.
Methods: We assessed 71 eligible patients with gastric carcinoma who had received curative radiotherapy. The age of the patients was between 34 and 82 (median 58 age). Of the patients 17 were female and 54 were male. The localization of the tumor was proximal in 13 patients (18.3%) and distal in 58 patients (81.7%). Before radiotherapy all of the patients had underwent surgery; 35 subtotal gastrectomy (49.3%) and 36 total gastrectomy (50.7%) were performed. As concomittant chemotherapy; 67 patients received 5FU (5 flouro urasil), 1 patient received CFF (cisplatin, 5 flouro urasil, folinic asid) and 1 patient received FUFA (5 flouro urasil, folinic asid) where

there was no concomittant chemotherapy for 2 patients. Radiotherapy was given as 180 cGy/frk., total dose 4500 cGy.

Results: The follow-up was between 4.7 – 66 months (median 18 months, mean 20 months). For all gastric carcinoma patients, when not classified according to the localization of the tumor, 1 year survival was 74 %, and overall survival was 44%. For proximal gastric carcinomas the survival for 1 year was 61% and the overall survival was 30%. In distal gastric carcinomas the 1 year survival was found to be 78% and overall survival was 48%. The median follow-up was 15 months for proximally localized carcinomas where it was 26 months for distally localized carcinomas.

Conclusions: Though it was not statistically significant it was found to be a difference in survival between proximal gastric carcinomas and proximal gastric carcinomas in our study. Pacelli F et al indicated that; at multivariate survival analysis proximal location was found to be independently associated with poor survival. The multivariate model shows the proximal location as an independent predictor of lesser favorable outcome in gastric cancer. The major determinants of the poor prognosis of proximal gastric carcinoma with respect to distal gastric carcinoma rely both on the more advanced age and tumor stage at the moment of clinical presentation and on the higher postoperative morbidity for proximal gastric carcinoma patients. This state was supported by Piso P. et al. They had found that proximal gastric carcinoma and distal gastric carcinoma represent the same tumor entity, and prognosis is similar, but due to more advanced tumor stages, the long-term survival is worse for patients with proximal gastric carcinoma than for those with distal gastric carcinoma . Left retroperitoneal lymphadenectomy may be indicated for of proximal gastric carcinoma . In the study where Rohde H et al. compared proximal with distal adenocarcinoma of the stomach reported that the differences in long-term prognosis are based primarily on poorer short-term survival for proximal gastric carcinoma, particularly for TNM stages Ib and II without residual tumour. The poor prognosis of proximal gastric carcinoma's being mainly due to its more advanced stage at diagnosis compared with that of more distally located gastric carcinoma was suggested by Kim DY et. al and it was underlined that early detection is important for improving the prognosis of patients with proximal gastric carcinoma .

Poster 113: Radiation Induced Skin Reactions In Adult Cancer Patients

I.F. Kayali, R. Habiboglu, N. Aslan, H. Sayan, F. Cetinyokus, Y. Lehimcioğu, S. Cakar, E. Aydinkarahaliloğu, S. Ozyurt

Objectives: A great number of patients treated with radiotherapy experience a skin reaction, which may range in severity from a mild erythema to moist desquamation. This damage can be dose-limiting. The purpose of this paper was to evaluate the radiation induced acute skin reactions.

Methods: In the study 172 patients were evaluated. The age of the patients was between 21 and 84 (median 56). There were 122 male and 64 female patients.The applied dose range was between 10 Gy and 70 Gy (median 50 Gy). The intend of therapy was curative in 108 patients (62.79%) and palliative in 64 patients (31.39%). The localization of the therapy portals used were as follows: 43 chest wall, 38 cranium, 34 pelvis, 16 abdomen, 15 supraclavicular fossae and larynx, 8 toracal vertebrae, 4 lomber vertebrae, 4 larynx, 4 mantle, 3 upper extremity and 3 lower extremity. Burrow solution was used for moist desquamation and starch was used for dry desquamation.

Results: Totally in 69 patients (40.11%) skin reactions were seen. Grade I skin reaction was observed in 57 patients (33.13%) and grade 2 skin reaction was observed in 12 patients (6.97%). No grade 3 skin reaction was detected. In 2 patients (1.16%) there was a need for a treatment gap. Dry desquamation was observed in 48 (27.90%) patients, moist desquamation was reported in 4 patients (2.32%) and dry and moist desquamation together were seen in 7 patients

Conclusions: The management of the skin reactions varies between centres and is often based on personal preference and historical practices rather than clinical evidence. We found the number of patients having skin reactions as 69 which can not be ignored. Factors can be identified for radiotherapy induced skin reactions and therapists must be aware of these factors and be familiar with management of this side effect

Poster 114: The Impact Of Radiotherapy on Outcome of Paranasal Sinus and Nasal Cavity Tumors

R. Habiboglu, I.F. Kayali, S. Ozyurt, N. Aslan, H. Sayan, F. Cetinyokus, S. Cakar, E. Aydinkarahaliloğu, Y. Lehimcioğu

Objectives: Malignant neoplasmas of the paranasal sinuses and nasal cavity are rare and present usually in advanced tumor stage due to the lack of early clinical symptoms. The purpose of this study is to evaluate the impact of radiotherapy on paranasal sinus tumors

Methods: Twentysix patients, who were treated in Ankara Numune Education and Research Hospital Radiation Oncology Clinic were included to the study. There were 7 female (34.6%), and 19 male (65.4%) patients. The age of the patients was between 32 years and 87 years (median 54 years). The types of surgery performed were as follows: total maxillectomy in 5 patients (19%), partial maxillectomy in 9 patients (34%), mass resection in 3 patients (11.5%). Nasal cavity localisation was detected in 13 patients where maxillar localisation was present in 23 patients. The distribution to the stages was as follows: 17 patients in Stage II, 11 patients in Stage III, 8 patients in Stage IV. The external radiotherapy was performed to the patients. The follow-up duration was between 1 – 161 months (median 22.5 months). The follow-up time was between 1 month and 161 months (median 40.3 months. The statistical analysis was done by Statistical Package for Social Scienses (SPSS for MS Windows Release 6.0, Chicago, Illinois, USA) To analyse survival long-rank statistics were used.

Results: Comparison between operation plus radiotherapy vs radiotherapy alone was done. Although there was numerical difference between them, no statistical significance was detected because of the number of patient in each group. The same was obtained when nasal cavite vs maxillar localisation was compared. Though there was numerical difference, no statistical significance was seen. When distribution of the stages was taken into account, again the small nmber of patients in each group made the results statistically insignificant. The survival rates found in our study were 42% for 2 years, 26.9% for 5 years, and 10.3 for overall. Mean survival was found to be 44,051 ± 9,525 and median survival to be 21 ± 4,462.

Conclusions: Malignancies of the nasal cavity and paranasal sinuses represent a wide spectrum of histologies, tissues of origin, and anatomic primary sites. The inherent difficulty in generalizing treatment approaches is obvious, given the numerous variables associated with the broadly-based term, paranasal sinus malignancy. Nevertheless, the majority of epithelial and salivary malignancies of this region (ie, squamous cell carcinoma, adenocarcinoma, adenoid cystic carcinoma, sinonasal undifferentiated carcinoma, and esthesioneuroblastoma) require surgical intervention as part of any treatment regimen. Recent trends have broadened the indications for chemotherapeutic and radiotherapeutic options in the management of advanced paranasal sinus malignancy. Nonepithelial malignancies, including the wide variety of sarcomas arising in this region, most commonly require multimodality treatment including chemotherapy, radiation, and/or surgery for definitive treatment. Moreover, the proximity of the nasal cavity and paranasal sinuses to structures including the orbit, dura, brain, cranial nerves, and carotid arteries mandates careful radiologic and neurologic evaluations throughout the course of the disease. Surgical advances now permit complex tumor removal and reconstruction surrounding these structures resulting in functional and cosmetic improvements when compared to earlier techniques. However, additional clinical trials are necessary to systematically evaluate the locoregional control, organ-preservation strategies, and survival related to the variety of treatments currently available.

Poster 115: Primary Osteosarcoma of the Skull

R. Habiboglu, I.F. Kayali, E. Aydinkarahaliloğu, N. Aslan, S. Cakar, F. Cetinyokus, H. Sayan, Y. Lehimcioğu, S. Ozyurt

Objectives: Osteosarcoma is the most common primary malignancy of bone and it is an aggressive neoplasm composed of spindle cells producing osteoid . It primarily affects the long bones, particularly after radiation or chemotherapy for other neoplasms; however, 6-7% present in the head and neck. An osteogenic sarcoma of the skull is rare, particularly as a primary tumor The incidence of primary osteogenic sarcomas of the skull is about 1 to 2% of all skull tumors . Spreading lesions to the central nervous system is uncommon, in addition plain film features are misleading due to the lock of evidence of osseous involvement of the calvaria .

Methods: CASE DESCRIPTION: A 31-year-old female was initially evaluated because of a large mass that had been growing for 3 months. The patient had been experiencing frequent headaches for about 1 year before being seen by the neurosurgeon. A magnetic resonance imaging (MRI) scan revealed 28 mm x 45 mm x 22 mm a large mass, involving the scalp and having pressure effect on left superior frontal gyrus. The patient subsequently underwent surgery. Pathology evaluation of the specimen revealed osteosarcoma, with dural invasion and permeation to the adjacent bony structure. As postoperatively imaging studies showed residual disease, chemotherapy (cisplatinum and adriamycin) was initiated. After the 4th cyclus of chemotherapy, 6600cGy radiotherapy was performed

Results: She is still alive on the 4th month of follow-up.

Conclusions: Osteogenic sarcoma, in general, has a bad prognosis . Osteosarcomas of craniofacial region have a better prognosis than those of the skeletal bones, and distant metastasis is rare. Local recurrence is the most significant factor contributing to poor outcome. Complete excision with negative margins is the key to a better outcome. Adjuvant therapy may be an option in cases of incomplete excision. Advances in target chemotherapy may diminish the significant morbidity associated with these lesions .

Poster 116: Multicenter Clinical Series Evaluating Radiofrequency Ablation (RFA) in the Treatment of Painful Spine Metastases

S. Bagla, J.B. Smirniotopoulos, D. Sayed, J.S. Bower, I. Lekht, B.A. Gregory

Objectives: Vertebral body metastases (VBM) represent the most common etiologies of chronic pain, fractures, and spinal cord compression in patients with metastatic bone disease. Palliation with radiation Pain relief can be protracted with limited response rates. RFA of VBM has been reported as safe and effective in retrospective studies. The purpose of this prospective multicenter study is to assess pain palliation, degree of disability and improvement in quality of life in patients with vertebral metastatic tumors following percutaneous RFA.
Methods: 50 patients with painful thoracolumbar spine metastases were prospectively enrolled in a multicenter registry during a 13 month period at 8 US centers. Target lesions were treated with RFA and with cement augmentation at the discretion of the operator. Inclusion criteria: pain in a thoracolumbar vertebral body concordant to the metastatic lesion. Pain, disability and quality of life were evaluated at baseline, prior to discharge, day 3, 7, 30, and 90 using the following validated scales Numerical Pain Rating Scale (NPRS), Oswestry Disability Index (ODI), the Functional Assessment of Cancer Therapy General -7 (FACT-G7) and Functional Assessment of Cancer Therapy Quality of Life Measurement in Patients with Bone Pain (FACT-BP). Adverse events were monitored throughout this time interval.
Results: 50 patients (26M/24F, Age Mean 61.0 ± 12.6) underwent treatment of 69 levels (30 thoracic, 39 Lumbar). Technical success was achieved in 100% of the cases (mean time 51.3 min,14-133). Cement augmentation was performed in 96% of reported levels (66/69). Breast, lung and renal cancer comprised over 50% of tumor etiology. Statistically significant improvement in mean scores for pain, disability and cancer specific health related quality of life from baseline to all intervals (day 3, day7, day 30, day 90. NRPS improved from a baseline of 5.9 to 3.6, 3.5, 2.7 and 2.1 (P<0.0001),. ODI improved from a baseline mean of 52.9 to 45.2, 45.9, 41.2, and 37.0 (P<0.02). FACT-G7 baseline mean 10.9 to 15.0, 16.1, 15.9, and 16.2 (P=0.008). FACT-BP baseline 22.6 to 33.0, 35.3, 37.3, and 38.9 (P<0.001). There were six adverse events reported during the course of this study including pain related to progression of the primary or other metastatic disease (n=3), a ruptured disc (n=1), neuropathic pain that was present prior to the procedure and intermittent after the procedure (n=1) and syncope (n=1). No complications were deemed as related to the RF ablation or cement augmentation procedures.
Conclusions: This multicenter clinical series found that radiofrequency ablation with/without vertebral augmentation is a safe, effective, and durable treatment for patients with painful metastatic vertebral body tumors. This study also found that the disability and quality of life is improved for these patients following RFA/VA treatment.

Poster 117: IVC Filter Retrievals in Oncology Patients in an Academic Healthcare System

M.J. Magnetta, A. Nickerson, D. Zhang, E.G. Santos Martin, K.M. McCluskey, K. Kim

Objectives: To investigate the IVC filter retrievals and post retrieval clinical outcomes in oncology patients.
Methods: A retrospective review of 187 consecutive patients with implanted IVC filters over 12 months was investigated. Records were surveyed to assess for IVC filter removal and cancer diagnoses. Using Stata/SE13.1, Chi-squared test was applied to compare the outcomes of cancer patients versus non-cancer patients. Types of cancer were also recorded. Mean time to explant were calculated and compared using a Students t-test. Post retrieval outcomes in cancer patients including recurrent DVT and PE were studied.
Results: Oncology patients accounted for 24.6% of patients studied. 85% of IVC filters placed were temporary models (Table 1). Half of IVC filters placed were retrieved in the follow-up period (Table 2). The median time to filter removal was 58 days in oncology patients and 53 days in non-oncology patients (P=0.80). In oncology patients with IVC filter removal, 0 developed new VTE after IVC filter removal. In the oncologic patients, there were 39 solid-tumor cases and 8 blood cancer cases.
Conclusions: IVC filters in cancer patients can be safely removed as non-cancer patients. There were no recurrent DVT or PE on cancer patients after filter removals within the 1-year study period.

Comparing rates of permanent and temporary IVC filter usage in oncology and non-oncology patients.

	Oncology	Non-oncology	Total
Permanent IVC Filter	12 (26.1%, 40.0%)	18 (12.8%, 60.0%)	30 (16.0%)
Temporary IVC Filter	34 (73.9%, 21.7%)	123 (87.2%, 78.3%)	157 (84.0%)
Total	46 (24.6%)	141 (75.4%)	187

Oncology patients were more likely to have permanent filters placed than non-oncology patients (Pr=0.033).

Comparing rates of removed and not removed temporary IVC filters in oncology and non-oncology patients.

	Oncology	Non-oncology	Total
Removed	12 (44.4%, 18.5%)	53 (50.5%, 81.5%)	65 (49.2%)
Not removed	15 (55.6%, 22.4%)	52 (49.5%, 77.6%)	67 (50.8%)
Total	27 (20.5%)	105 (79.5%)	132

Oncology patients were equally as likely as non-oncology patients to have their IVC filters removed (Pr=0.56).

Poster 118: Clinical Application of Combined Therapy with Thermal Ablation and Intra-Arterial Chemoembolization in Advanced-Stage Cancer

Y. Jeon

Objectives: To evaluate the practical feasibility and clinical benefits of combined therapy with thermal ablation and intra-arterial chemoembolization in the palliative treatment of advanced cancer patients.
Methods: We studied 45 advanced cancer patients (from January 2009 to September 2014, 20 males and 25 females) who were unable to control with standard treatments. All patients underwent locoregional treatments using combined therapy of thermal ablation (radiofrequency ablation and/or cryoablation) and intra-arterial chemoembolization to control their clinical problems. Thermal ablation and intra-arterial chemoembolization were performed simultaneously, consecutively, or alternatively for target lesions. Patients' current problems, clinical benefits and complications were evaluated with the consulting oncologists. The consulting purposes for the procedures could be categorized into 3 groups according to the clinical manifestations and clinical situations —'Rescue' (control of lesions and symptoms, impossible with other treatment modalities, n=23: control of pain and discomfort in 16, control of rapidly growing lesions in 5, old age in 1, refusal of chemotherapy in 1), 'Supporting' (adjuvant to consolidate main treatments, n=19), and 'Bridging' (improving patients' performance status to take systemic treatments, n=3). Post-procedural clinical benefits were evaluated in 5–10 days and 30 days, including assessment for clinical improvement, laboratory and radiological changes.
Results: Clinical benefits concurred with oncologists were obtained in 18 patients in the rescue group (78%), 14 in the support group (74%), and 2 in the bridging group (67%). Results were all statistically significant (P<0.05). Complications developed in 5 patients (major in 1).
Conclusions: Combined locoregional treatment of thermal ablation and intra-arterial chemoembolization is safe and helpful for advanced cancer patients to control disease progression and symptom palliation. And it can be a meaningful treatment option in the palliation of advanced cancer patients.

Poster 119: A model for co-designing clinical decision support to advance more efficient IO imaging

R.A. Holayter, O. Ozkan, K.S. Lee, D. Moberg, S.B. Busarow, P. Dalvie, J. Pinchot, M.C. Brunner

Objectives: There is great variability in the way that non-specialists initially image patients with cancer[1] and consequently the resources they utilize. While the VA spends less per patient than CMS on cancer-related medical imaging[1], in part related to its universal electronic health record (CPRS) with integrated clinical decision support (CDS), this entity, like CMS[2], has ongoing difficulty with provider response to CDS for diagnostic ordering, particularly medical imaging[3, 4, 5, 6, 7]. We present a model to help improve and evaluate VA primary care provider compliance with multidisciplinary pre-IO diagnostic imaging clinical pathways by "co-designing" this CDS in partnership with these providers.
Methods: Using a convergent mixed-methods approach organized by the RE-AIM framework[8], formative evaluation during provider education and roll-out of solid tumor imaging workup pathways informs CDS design to prompt the appropriate transition to more efficient, evidence-based imaging workup and staging. Quantitative data obtained throughout the course of the study tracks CDS implementation with sufficient power to detect significant differences in ordering patterns over the life of the project. Semi-structured interviews of 10-15 participants conducted during the first one third of the study (Phase 1) are repeated during the last two thirds after initiating co-designed CDS (Phase 2). After each wave of provider interviews, (via email) a Delphi method[9] virtual consensus panel convenes: including two referring providers, the interview leader (providing input from the interviews), a medical oncologist, a surgical oncologist, a radiation oncologist, an interventional oncologist, and a CPRS operational expert. The Delphi team then reviews and further refines the proposed CDS to reach a consensus regarding the CDS design.
Results: In an academic IO referral service (which provides similar services to the Madison VA) we found inefficient medical imaging evaluations in 36% of 50 consecutive patients.
Conclusions: Enhanced provider compliance with multidisciplinary pre-IO imaging pathways due to the co-design process will improve evidence-based diagnostic IO

imaging and subsequent therapeutic intervention. [1]McWilliams, JM,et al. Geographic Variation in Cancer-Related Imaging: VA Health Care System Versus Medicare. *Ann Intern Med* 2014;161:794-802. [2]Medicare Imaging Demonstration Evaluation Report to Congress. [3]Fung CH, et al. Variation in...CCR's in an integrated healthcare system. *Am J Manag Care* 10(11 Pt 2): 878-885, 2004. [4]Georgiou A, et al. The impact of CPOE systems on medical-imaging services: a systematic review. *J Am Med Inform Assoc* 18(3): 335-340, 2011. [5]Roshanov PS, et al. Can CDS systems improve practitioners' diagnostic test ordering behavior? *Implement Sci* 6:88, 2011. [6]Rothendler J. Factors Influencing Success of CCR's in the VA, EN Rogers Memorial Veterans Hospital, 2014. [7]Saleem JJ, et al. The next-generation EHR: perspectives of key leaders from the VA. *J Am Med Inform Assoc* 20(e1): e175-177, 2013. [8]Glasgow RE, et al. Evaluating the public health impact ...: the RE-AIM framework. *Am J Public Health* 89(9): 1322-1327, 1999. [9] Delbecq A, et al. *Group techniques ...: a guide to nominal group and Delphi processes,* Scott, Foresman, 1975.

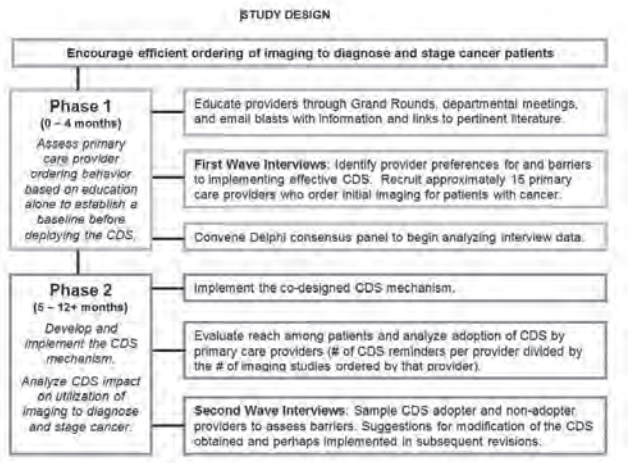

Poster 120: Combination Radiofrequency Ablation and Cementoplasty of Painful Supra-acetabular Metastases

A.N. Wallace, J.W. Jennings

Objectives: To evaluate the feasibility, safety and palliative efficacy of radiofrequency ablation (RFA) and cementoplasty of painful supra-acetabular metastases.
Methods: Institutional review board approval was obtained to retrospectively review the records of 10 patients with supra-acetabular metastases treated with combined RFA and cementoplasty during a 28-month period. Ablations were performed under CT-guidance with a navigational bipolar electrode. In some cases, this electrode allowed the posterior acetabulum to be ablated from an anterior approach, thus avoiding the sciatic nerve (Figure 1). High-viscosity polymethylmethacrylate cement was instilled under CT-fluoroscopy. The primary tumor histology, number and duration of ablations, and volume of instilled cement were recorded for each case. Pain scores before and 1-week after the procedures were measured with the numerical rating scale (NRS; 10 point scale). Procedure-related complications, including thermal nerve injury and intra-articular cement extravasation, were also recorded.
Results: Patient, tumor, and procedure characteristics and changes in pre- and post-procedure pain scores are listed in Table 1. All procedures were technically successful. The mean number of ablations performed of each lesion was 7.7 +/- 3.6, and the mean total ablation time was 12:56 (range, 6:45 to 35:55). The mean volume of cement instilled during each procedure was 15 +/- 7.5 ml. Patients reported a mean pre-procedure pain score of 6.8 +/- 2.4 and a mean pain score 1-week after the procedure of 3.7 +/- 1.8. Six of 9 patients (67%) reported an at least 2-point pain score reduction. There were no instances of thermal nerve injury. There was one case (10%, 1/10) of minimal, asymptomatic intra-articular cement extension into the posterior hip joint.
Conclusions: Combined RFA and cementoplasty of supra-acetabular metastases is feasible, safe and has the potential to produce rapid pain relief.

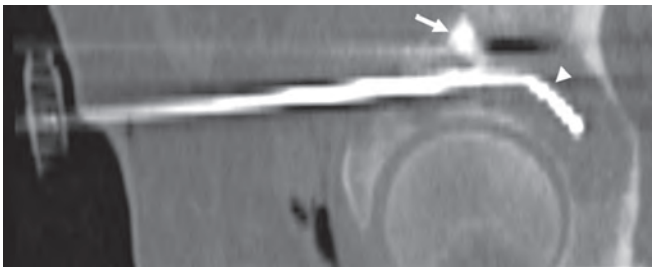

69-year old man with gastrointestinal adenocarcinoma and left supra-acetabular metastasis causing debilitating pain. Cementoplasty of the anterior acetabulum was performed (white arrow), which partially relieved his pain for 4-weeks. His pain subsequently worsened and repeat imaging demonstrated increased osteolysis of the posterior acetabulum. Sagittal reformatted CT shows the navigational radiofrequency ablation probe (white arrowhead) curving into the posterior aspect of the acetabulum from an anterior approach.

Patient, Tumor, and Procedure Characteristics and Pain Scores

Pt. No. / Age (y) / Sex	Tumor Histology	# Ablations Performed	Total Ablation Time	Volume of Cement (ml)	Pain (NRS) Pre-procedure	Post-procedure	Change
1 / 69 / M	GI	2	6:45	15	9	3	-6
2 / 59 / W	Breast	6	8:51	13	7	2	-5
3 / 72 / M	HCC	8	7:25	10	4	1	-3
4 / 49 / M	NSCLC	15	21:08	25	8	2	-6
5 / 34 / M	Melanoma	8	10:04	6	4	3	-1
6 / 64 / W	Breast	7	9:38	7	9	4	-5
7 / 30 / W	Angiosarcoma	8	8:43	9	3	4	+1
8 / 68 / W	RCC	12	35:55	30	8	8	-
9 / 64 / M	RCC	3	13:27	20	10	5	-5
10 / 34 / M	Hemangiopericytoma	8	7:33	13	NA	NA	NA

Abbreviations: GI = gastrointestinal adenocarcinoma, HCC = hepatocellular carcinoma, NA = not available, NRS = numerical rating scale, NSCLC = non-small cell lung cancer, RCC = renal cell carcinoma

Poster 121: Percutaneous Image-Guided Cryoablation: Another Treatment Option on Desmoid Tumors

A. Bouhamama, F. Pilleul, B. richioud

Objectives: Desmoid tumor is a benign tumor that causes significant morbidity and mortality depending on its site and size. The treatment of desmoid tumors used to be very aggressive using large resection surgery or radiotherapy. The aim of this study is to evaluate the effectiveness of percutaneous cryotherapy on extra abdominal desmoid tumors.
Methods: Between 2012 and 2013, 10 patients diagnosed with desmoid tumor underwent percutaneous cryoablation (11 procedures in 10 patients). For each patient, the disease free survival (DFS), the overall survival and the radiological progression according to RECIST criteria were calculated.
Results: 6 patients underwent cryoablation as a first invasive treatment. 4 patients had already undergone surgery. One patient was lost to follow up. The mean follow up was 10,2 months. The mean DFS was 5.1 months. At the end of the follow up, 8 patients were considered as stable disease (SD) according to RECIST criteria.
Conclusions: Percutaneous image-guided cryoablation allows less invasive treatment than surgery and leads to significant local control on extra abdominal desmoid tumors.

Poster 122: Feasibility, Safety and Early Effectiveness of CT and MRI-Guided Percutaneous Ablation as Second-Line Treatment for Symptomatic Vascular Anomalies: Initial Results

S.M. Thompson, M.R. Callstrom, M. McKusick, D.A. Woodrum

Objectives: To determine the feasibility, safety and early effectiveness of percutaneous image-guided ablation as second-line treatment for symptomatic soft tissue vascular anomalies.
Methods: An IRB-approved retrospective review was undertaken of all patients who underwent percutaneous image-guided ablation as second-line therapy for treatment

of symptomatic soft tissue vascular anomalies (VA) during the period from January 1, 2008 to May 20, 2014. US/CT- or MRI-guided and monitored cryoablation or MRI-guided and monitored laser ablation were performed under general anesthesia. Clinical follow-up began at one month post-ablation.
Results: Eight patients with nine VA were treated with US/CT (N=4) or MRI-guided (N=2) cryoablation or MRI-guided laser ablation (N=5) for moderate to severe pain (N=7) or diffuse bleeding secondary to hemangioma-thrombocytopenia syndrome (N=1). The median maximal diameter was 9.0 cm (6.5 to 11.1 cm) for VA undergoing cryoablation and 2.5cm (2.3 to 5.3 cm) for VA undergoing laser ablation (P<0.02). Seven VA were ablated in one session, one VA initially treated with MRI-guided cryoablation for severe pain was re-treated with MRI-guided laser ablation due to persistent moderate pain and one VA was treated in a planned two-stage session due to large VA size. At an average follow-up of 19.8 months (range 2 to 62 months), 7 of 7 patients with painful VA reported symptomatic pain relief. There was no recurrence of bleeding at five years post ablation in the patient with hemangioma-thrombocytopenia syndrome. There were two minor complications and no major complications.
Conclusions: Image-guided percutaneous ablation is a feasible, safe and effective second-line treatment option for symptomatic vascular anomalies.

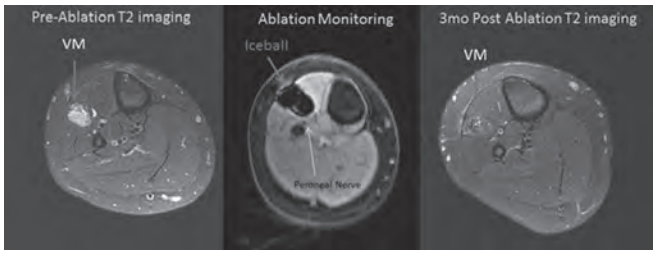

Poster 123: Reducing Medical Errors in Interventional Oncology by Improving Communication - A Call to Action

M.J. Magnetta, K. Kim

Objectives: To review the importance of communication in IO. To propose a method to improve IO communication.
Methods: Background: In 1999, the Institute of Medicine released a report entitled "To Err is Human." The report stated that between 44,000-98,000 people per year are harmed by medical error. One review in 2013 suggested that the true number of premature deaths associated with preventable harm in hospitals is more than 400,000 per year. In analysis of 2,455 sentinel events reported to the Joint Commission, the primary root cause of 70% of events was found to be communication error. In 75% of these cases, the patient died. Radiation oncology literature suggests communication failures account for a number of near misses with a total error rate in all encounters of 0.2-0.4% - much higher than in other high-stakes fields like aviation and nuclear power. Despite these statistics, to our knowledge, no data has been published regarding medical error from communication failure in interventional oncology.
Results: Discussion: The objective of interventional oncology (IO) is to improve quality and length of life of our patients. One part of this is acting to reduce the staggering human cost of medical communication error through research and quality improvement initiatives. IO providers are part of complicated communication networks composed of many stakeholders (Fig. 1). Due to the complexity of our communication networks, failure of team members to provide updated, pertinent information to all stakeholders is commonplace. Information technology (IT) is capable of helping in this arena by leveraging human decision making with the memory and routing ability of computers. In the most successful applications, IT used to disseminate information is developed in conjunction with those who will be using the tools to ensure relevance. To ensure success, objectives should bet set and measurements made. IO providers interact with patients, families, environmental service personnel, technologists, nurses, residents, referring providers and administrators. The people in all roles should be encouraged to speak-up in the face of error. In medical culture, error is often seen as personal failure. In reality, error is multifactorial and often related to systems issues. In a number of organizations, a "culture of safety" has been established through training and implementation of "safe words" to ensure concerns are accurately and freely relayed.
Conclusions: Using a multidisciplinary approach, interventional oncologists should become involved in the development of unobtrusive healthcare IT communications methods and initiatives to develop a safe culture in our departments. These projects should be actionable, evidence-based and reported in literature. Our patients lives depend on it.

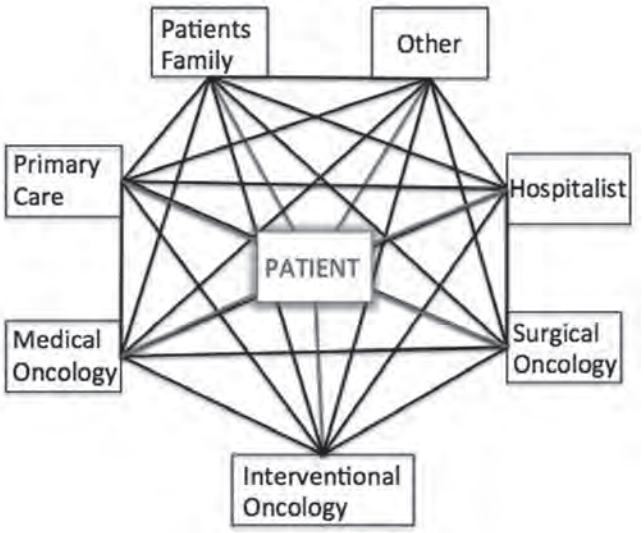

A diagram of a healthcare communications network for an oncology patient. Red lines represent direct communication with the patient. Black lines represent communications with various hospital services. With 7 services in the care of a single patient, 40,320 2-way communications are possible. In reality, many others are involved in patient care of oncology patients including other consultants, Chaplin's, etc.

Poster 124: Retrospective Comparative Study of Absolute Ethanol Versus N-Butyl-2-Cyanoacrylate (NBCA) in Percutaneous Portal Vein Embolization (PVE)

S. Sugawara, Y. Arai, M. Sone, H. Ishii

Objectives: To evaluate the efficacy of absolute ethanol and NBCA in preoperative PVE retrospectively.
Methods: From May 2013 to October 2014, twenty-five patients (18 males, 7 females; median age 71.5 years [range, 43-78]) underwent PVE (14 ethanol, 11 NBCA) in a single center. As the primary endpoint, change of non-embolized liver volume ratio (NEL ratio) was calculated by CT before and 4 weeks after PVE. Volume change of embolized and non-embolized liver (ELV and NELV), indocyanine green retention rate at 15 minutes (ICG-15), and adverse events were evaluated as the secondary endpoint.
Results: The increase of NEL ratio was significantly higher in ethanol group than NBCA group (14.1% vs 9.9%, P=0.021). ELV decreased significantly more in ethanol group than NBCA group (-198.9ml vs -102.3ml, P=0.01). The increase of NELV did not show significantly different (134.9ml vs 90.1ml, P=0.944). There was no significant difference of ICG-15 change between both groups. In ethanol group, grade 3 to 4 (CTCAE ver.4) transient elevation of aspartate aminotransferase and alanine aminotransferase occurred in 12 (85.7%) and 10 (71.4%) patients, while elevation in transaminase was slight in NBCA group. Hepatic necrosis was observed in 1 patient (7.1%) in ethanol group, but no additional treatment was required.
Conclusions: PVE with absolute ethanol showed greater increase of NEL ratio than NBCA. Difference of change in ELV and NELV and adverse events in both groups may be caused by ethanol-induced parenchymal liver damage.

Liver volume change after PVE

	Ethanol	NBCA	p value
Embolized liver volume change	- 198.9 ml (-342.1 - -103.0)	- 102.3 ml (-277.6 - -15.3)	0.01
Non-embolized liver volume change	+ 134.9 ml (36.1 - 190.5)	+ 90.1 ml (34.0 - 278.9)	0.944
Non-embolized liver volume ratio change	+ 14.2% (8.0 - 21.7)	+ 9.9% (2.1 - 15.0)	0.021

Poster 125: Transforming Interventional Oncology: Principles Needed in the New ACO

J.B. Jia, M. Xing, K. Kim

Objectives: To review the effects the Affordable Care Organization (ACO) will have on Interventional Oncology (IO) and to explore methods to adapt.
Methods: Background: Currently, America spends $3.8 trillion on healthcare and this is projected to grow at a rate of 5.8%, reaching more than $5 trillion in 2022. IO treatment specifically is expensive with high profit margins. The national median cost of outpatient treatment with yttrium-90 is $34,683 with hospitals' profiting $16,465 and physicians reimbursed $4,169. The goals of the ACO are to provide coordinated high-quality care while cutting costs. The payment system will move toward a value-based system with rewards for curtailing the growth in health care costs and

meeting high performance standards. The current IO model is fee for service and with rocketing health care costs this is unsustainable. If IO continues on its current path, it will likely become irrelevant. However, if adaptations are made, it can remain a pillar in oncology treatment and provide more effective care.

Results: Discussion: To ensure longevity and to increase its value in the new healthcare system, there are a number of action points that IO needs to address. *Incorporation into the Cancer Center service line*. Cancer Care is a multidisciplinary operation however IO is not often fully incorporated. Interventional Oncology belongs in the modern Cancer Center service line, as it offers less invasive therapies and unique expert knowledge and options. This would result in better-coordinated and improved care. To join the Cancer Center would also allow interventionalists to play a larger role in patient management, ensuring longevity. *Outpatient clinic model.* An integral part of joining the cancer center service line with an enlarging role in cancer care, is development of a clinic infrastructure to allow for follow-up and long-term care. This will likely also decrease preventable post-procedural complications. *Quality metrics.* Value and reimbursement needs to transition to quality based rather than volume based. IO should utilize quality metrics to ensure that practitioners are performing at a high caliber with percentage incentives and penalties. Important metrics that should be monitored are survival, complication rate, readmission rate, hospital length of stay, and patient satisfaction. *Regulation of costs*. With the new healthcare system, a large influx of new patients is expected. As such, IO needs to reexamine workflow and resources so the demand can be met while controlling costs.

Conclusions: IO is a dynamic field with advancements in technology and the promise of more elegant cancer treatment options. However, thought needs to be put into its integration into the larger health care system. Here at the cusp of the new ACO model is the time that IO needs to organize itself for future returns. IO has a lot to offer to cancer care, so the field needs to make the correct steps now; incorporating into the cancer center service line, creating an outpatient clinic structure, and regulating costs and quality metrics; for the benefit of its future physicians and patients.

Poster 126: Evaluating the Effectiveness of Microwave/RF Ablation for Focal Disease Control as Compared with Conventional Chemotherapy

T.D. Hodgkiss, M. Pagni

Objectives: The primary objective of this study was to evaluate the effectiveness of microwave/RF ablation technology in extending life as compared to chemotherapy when only focal recurrent disease is present.

Methods: This was a retrospective study and data was collected by researching electronic medical records and PACs on 25 male and female subjects (39 lesions) undergoing thermal (radiofrequency and microwave) ablation for biopsy proven metastatic disease.

Results: No evidence of disease was observed in 54.1% of the lesions at 3 months, 40.6% of lesions at 6 months, 50.0% of lesions at 9 months and 60.0% at 12 months. Progressive disease was observed in 29.7% of the lesions at 3 months, 31.1% of lesions at 6 months, 36.4% of lesions at 9 months and 26.7% at 12 months. Partial Response was observed in 5.4% of the lesions at 3 months, 9.4% of lesions at 6 months, 4.5% of lesions at 9 months and 6.7% at 12 months. Stable disease was observed in 10.8% of the lesions at 3 months, 18.8% of lesions at 6 months, 9.1% of lesions at 9 months and 6.7% at 12 months. Of those subjects who had disease progression, the average time to progression in these subjects was 168.8 +/- 115.4 days. The complication rate for these subjects was 10.3% with the complications being reported as a small pneumothorax, hematoma (5.7 x 7.2cm), a small aortic pseudoaneurysm and a RLE DVT.

Conclusions: Microwave/RF ablation appear to be effective in terms of disease recurrence, disease progression time, and complications as compared to conventional second to sixth line chemotherapy. The duration of response seen in this patient population was very favorable with survival rates improved in comparison to conventional chemotherapy alone. (L.C. Hanker, 2012) (Krishnansu S. Tewari, 2014) Sixty-percent of the lesions showed no evidence of disease/complete response at 12 months. Time to progression of disease was also favorable and improved in comparison to chemotherapy alone. When stratifying by initial tumor size, it appears that time to progression of disease becomes shorter as the initial tumor size is larger so it appears that this therapy is most effective on the smaller tumor sizes.

Duration of Response

	3 months (n=37)	6 months (n=32)	9 months (n=22)	12 months (n=15)
NED/CR (No evidence of disease/complete response)	20 (54.1%)	13 (40.6%)	11 (50.0%)	9 (60.0%)
PD (Progressive Disease)	11 (29.7%)	10 (31.3%)	8 (36.4%)	4 (26.7%)
PR (Partial Response)	2 (5.4%)	3 (9.4%)	1 (4.5%)	1 (6.7%)
SD (Stable Disease)	4 (10.8%)	6 (18.8%)	2 (9.1%)	1 (6.7%)

Poster 127: Percutaneous Cryoablation of Clinical T2 Renal Masses: Technical Feasibility, Complications and Short Term Outcomes

G.D. Schmit, M. Moynagh, R.H. Thompson, S.A. Boorjian, T. Curry, T.D. Atwell

Objectives: To evaluate technical challenges, complications and outcomes with percutaneous cryoablation of large (> 7cm) renal masses.

Methods: 12 patients underwent percutaneous cryoablation for treatment of renal tumors measuring greater than 7cm between December 2004 and June 2013. Technical success, procedural complications (Clavien-Dindo classification system), renal function and oncologic outcomes were evaluated for each patient.

Results: Median patient age was 75 years (range 46 – 84) and median patient Charlson Comorbidity Index (CCI) was 5 (range 4 - 9). Median maximal tumor diameter was 8.4cm (range 7.2 – 9.7). All cryoablation procedures were technically successful in a single treatment session. Two patients (17%) experienced major (> Grade 2) complications related to significant post-procedural hemorrhage. There were no procedure-related deaths. Median change in estimated glomerular filtration rate (eGFR) within 7 days following cryoablation treatment was 11 mL/min (range 7-14). One patient with baseline stage IV chronic kidney disease and a major cryoablation bleeding complication required temporary dialysis in the periprocedural period. No local tumor recurrence was identified in the 11 patients with greater than 3 months imaging followup (median 14 months, range 4-49).

Conclusions: Percutaneous cryoablation of large (> 7cm) renal masses is technically feasible in well selected patients who are poor surgical candidates. Comprehensive multidisciplinary periprocedural management is important given the medical complexity of these patients and the high risk of complications with cryoablation of large renal tumors.

Poster 128: Placental Growth Factor is a Prognostic Marker in Patients with Refractory Colorectal Liver Metastases Treated with DEBTACE in a Multivariate Analysis

M. Schermaul, J. Koch, R. Dappen, H. Wilke, D. Strumberg, A. Bachinger, S. Wnendt, M. Stahl, S. Pluntke

Objectives: TACE with irinotecan loaded drug-eluting beads (DEBIRI) has shown activity in colorectal liver metastases. Among factors potentially interfering with its effectiveness is a hypothetical neoangiogenic reaction due to ischemia. In this trial we evaluate the changes in serum level of placental growth factor (PlGF).

Methods: Patients with predominant and life threatening colorectal liver metastases, which were refractory to all drugs approved for metastasized colorectal cancer and documented tumor progression during or shortly after the last chemotherapy, were prospectively treated with irinotecan loaded drug eluting beads with a size of 100 -300 µm. Therapy was delivered by a temporary catheter placed in the liver arteries. Usually each lobe of the liver was treated two times with an interval of 4 weeks. Each treatment of one liver lobe was performed with one vial of the 100-300 µm DC-beads loaded with 100 mg irinotecan. Blood samples to measure the serum level of PlGF were taken before TACE and at day 7, 14 and 21 after the first treatment.

Results: Complete blood samples were taken from 35 patients (22 male/ 13 female, median age 64 years). 51 % of patients had an increased baseline level of PlGF above ULN. The increased baseline level were found in patients with a bevacizumab-therapy within the last 9 weeks (P=0.0006). The shorter the interval between the last treatment and the time point of baseline the higher were the PlGF-Level (P=0.0015). Patients with increased baseline-level of PlGF have shorter overall survival (P=0.0139.) In a multivariate analysis of the survival time we found significant impact from PlGF-baseline-level (P=0,0005), the count of the previous therapies (P=0,0045) and a previous Bevacizumab therapy (P=0,0014).

Conclusions: In a multivariate Cox regression on the survival time a low baseline level of PlGF (P=0.0031), a bevacizumab pretreatment within the last 9 weeks (P=0.0144), a negative nodal status (P=0.0071) and a low number of liver metastases (P=0.0308) are predictive markers in a salvage patient population undergoing a treatment with DEBTACE. PlGF is an alternative neoangiogenesis factor, indicating a resistance against an antiangiogenic therapy targeting the VEGF and linked to a bad prognosis. If the presence of elevated PlGF level could be used to exclude patients from a salvage treatment with DEBTACE should be investigated in future trials.

Poster 129: Consistent and Predictable Spherical Ablation Shape in Both Liver and Lung: Performance of the Emprint™ Ablation System with Thermosphere™ Technology in an In Vivo Porcine Model

K. Howk, C. Ladtkow, D. Peterson, A. Cafaro

Objectives: Thermal ablation has been evaluated for the management of inoperable tumors in both the lung and the liver. However, first-generation systems are challenged by inconsistent and elongated ("hot dog") ablation zones, largely due to variations in tissue properties, which increases the risk of both local recurrence and burns to adjacent structures. The Emprint™ Ablation System with Thermosphere™

Technology was designed to produce a predictable, spherical ablation zone not distorted by variations in tissue environment. The purpose of this preclinical study was to assess ablation zone size and shape at various time and power doses in both liver and lung.

Methods: The Emprint™ Ablation System with Thermosphere™ Technology (Covidien, Boulder, CO) was evaluated at 45W, 75W, and 100W over a range of time settings (1:00-10:00 minutes) in liver and lung tissue of male domestic swine. Following ablation, animals were euthanized for tissue collection and gross measurement of ablation zone width and height. Ablation shape was defined as the ratio of height and width, with a value of 1 indicating a perfect circle. All measurements were inclusive of the hyperemic zone.

Results: A total of 53 liver and 73 lung ablations were successfully completed in 16 animals. In liver, the average ablation width at 45W, 75W, and 100W, respectively, ranged across time settings from 2.3-2.7 cm, 2.3-3.5 cm, and 2.3-3.9 cm. At 5 minutes, the average ablation widths were 2.7 cm, 3.3 cm, and 3.8 cm, respectively. Similarly, in lung, the average ablation width at 45W, 75W, and 100W, respectively, ranged from 2.3-3.1 cm, 3.0-3.7 cm, and 3.2-4.0 cm. At 5 minutes, the average ablation widths were 2.8 cm, 3.7 cm, and 4.0 cm, respectively. The average ablation shape was 0.9 (range 0.8-1.0) for liver and 0.8 (range 0.8-0.9) for lung with no remarkable difference based on duration of ablation. Ablation zone size and shape was most predictable at 100W. Figure 1 depicts ablation zone width and height at 100W power over time. Ablation zone shapes were relatively constant across time settings.

Conclusions: In porcine liver and lung, ablation with Thermosphere™ Technology produced predictable and consistent ablation zone sizes and shapes, regardless of tissue type. Future studies are envisioned to confirm the technology performs similarly in clinical practice.

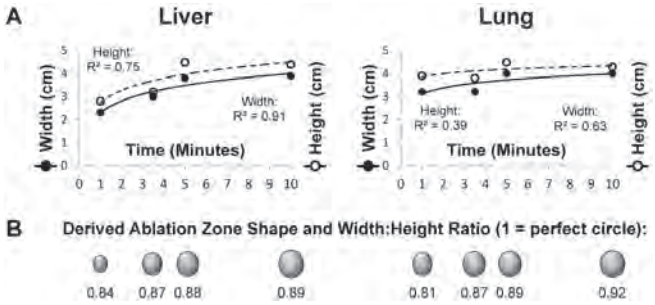

Figure 1: (A) Ablation zone height and width across time at 100 Watts in liver and lung. (B) Derived ablation zone shape. Circles depict 2-dimensional ablation zone for each timepoint derived from natural logarithmic regression; width:height ratio is shown below where 1 corresponds to a perfect circle.

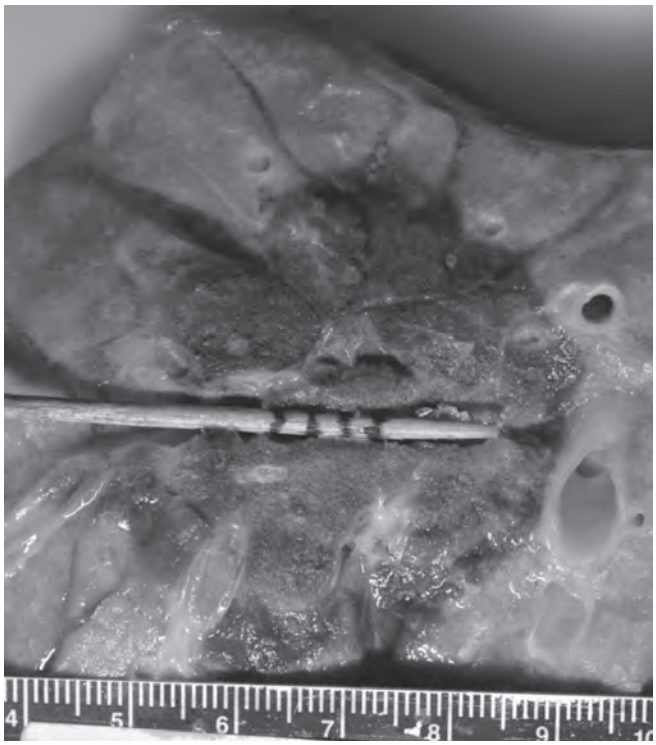

Figure 2. Representative image of a lung ablation at 10 minutes, 100 Watts.

Poster 130: Magnetic Resonance Guided Coaxial Electrochemical Ablation – Initial Investigations of a Novel Technique

B.H. Ge, C.N. Weber, G.J. Nadolski, T.P. Gade, S.J. Hunt, M.C. Soulen, M. Itkin

Objectives: Electrochemical ablation is a pH mediated percutaneous ablation technique utilizing direct current (DC) electricity. Advantages over thermal ablation include sharp margins, decreased non-target injury, and immunity to heat sink effects. Disadvantages historically included long ablation times and difficulty monitoring ablation. We test a coaxial design to rapidly create a size adjustable ablation under magnetic resonance (MR) monitoring.

Methods: A 32 volt DC generator supplied an 18 gauge platinum anode centered within a cage consisting of ten 16 gauge nitinol cathodes. Safety, feasibility, and ablation rate was calculated for six trials of 3, 4, 5, and 6 cm diameter ablations (n = 24) on ex vivo bovine liver. Ablations were repeated on eight normal swine livers in a 1.5 T MRI system with VIBE T1 monitoring sequences (TR/TE 5.0/2.2 ms, FA 15o, FOV 200 mm; Matrix 196x320; slice 3 mm) at 3 – 5 minute intervals. Post ablation outcomes were verified by gross pathology.

Results: The maximum anode ablation temperature (61 C) was achieved within 10 minutes. No heat was produced at the cathodes and current scatter was less than 0.05 mA. Local pH was 3.2 at the anode and 13.8 at the cathode. All ablations were contained within the cathode cage with heat and pH mediated coagulation at the anode and pH mediated liquefaction at the cathode. Complete ablation was achieved within 15, 20, 35 and 40 minutes for 3, 4, 5, and 6 cm diameters respectively with T1 and T2 signal changes on MR corresponding to ablation zones on gross pathology.

Conclusions: The coaxial design considerably improved electrochemical ablation rates with times similar to current thermal techniques. The ablation system's MR compatibility allows for active monitoring and real-time adjustments.

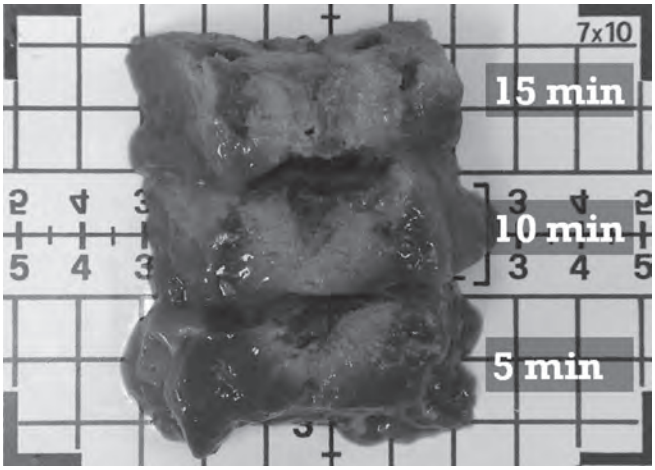

Figure 1 - Ex Vivo Bovine Liver: Serial ablation of 3 cm diameter, 2 cm thick ex vivo bovine liver at 5, 10, and 15 minutes demonstrate complete ablation by 15 minutes (32 V, 1.2 – 1.8 A). Notice the central zone of coagulation about the anode and peripheral liquefaction about the cathodes.

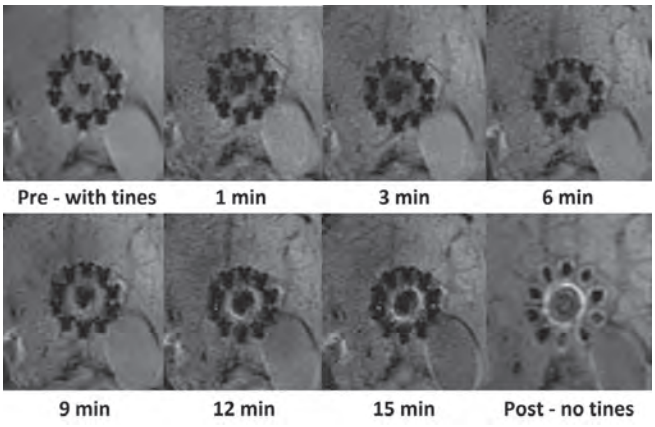

Figure 2 - In Situ Swine Liver: Ablation progress was monitored in real-time using VIBE T1 sequences along the short axis of the cathode cage. Sequences were performed before, during (3 minute intervals), and after ablation with the tines removed. In this example of a 3 cm ablation zone, T1 hypointense signal was seen to propagate circumferentially from the central anode towards the cathode with a leading edge of T1 hyperintense signal. Similar changes were seen at the cathode tines. Complete ablation was achieved when the signal changes coalesce.

Poster 131: Performance of the Emprint™ Ablation System in an In Vivo Porcine Lung Model: Correlation between Computed Tomography and Gross Measurements

K. Howk, C. Ladtkow, D. Peterson, A. Cafaro

Objectives: Image-guided thermal ablation is becoming increasingly accepted as a minimally invasive option for the coagulation (ablation) of inoperable lung tumors. Studies have evaluated the relationship between device settings and ablation zone size ex vivo and in vivo (via gross measurements). However, in order to support clinical applications it is necessary to demonstrate that ablation zones measured grossly relate to ablation zones measured via computed tomography (CT), as in the clinical setting. The purpose of this study was to evaluate the correlation between gross in vivo and CT measurements.
Methods: An ablation system (Emprint™ Ablation System with Thermosphere™ Technology, Covidien, Boulder, CO) was evaluated in a porcine lung model. Variable power (45W, 75W, 100W) and time (0 – 10 minutes) settings were evaluated to correlate ablation zone sizes measured by gross examination and CT. After surgical access and ablation zone creation, a subset of target zones underwent unenhanced CT imaging. The animals were then euthanized for tissue collection and gross measurement of ablation zone width and height. All gross measurements were inclusive of the hyperemic zone. Analyses were conducted to assess the correlation and agreement between ablation measurements made via the gross method and the CT image method.
Results: A total of 73 lung ablations were successfully completed in 16 male domestic swine. At 100W power, ablation width and height increased over time according to both gross and CT measurements (Figure 1). Average measurements obtained by CT imaging were largely equivalent to the gross measurements and remained approximately the same as ablation time increased. For the shortest ablation times, CT measurements were smaller compared to gross measurements.
Conclusions: Ablation zones created with Thermosphere™ Technology demonstrated a strong correlation between CT imaging dimensions and gross in vivo measurements. This result supports both clinical practice and future clinical studies by providing confidence that desired ablation zone sizes correlate with what is measured via CT immediately post-ablation. When shorter ablation times were used, CT measurements underestimated gross measurements. More work should be done to understand this reduced correlation at short times to further quantify the relationship.

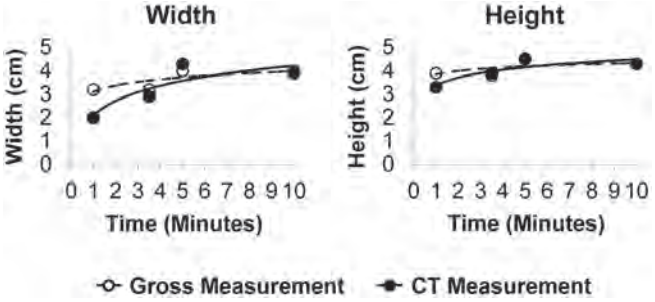

Figure 1. Ablation zone width and height across time at 100W power.

Poster 132: Feasibility of Bedside Post-Procedure Patient Pain and Access Site Preference Assessment Using IPad Technology: A Pilot Study of Patients Undergoing Transarterial Interventional Oncologic Procedures

V.V. Patil, R.S. Patel, D.V. Scasserra, N.E. Tabori, E. Kim, R.A. Lookstein, F.S. Nowakowski, A.M. Fischman

Objectives: To determine the feasibility of post-procedure patient pain level and access site preference assessment using iPad technology after radial and femoral access for transarterial interventional oncologic procedures.
Methods: In this single-center study performed at a high volume academic medical center, 56 patients undergoing arterial interventions were given a post-procedure survey via a bedside iPad in the IR recovery unit. Surveys were available in English, Spanish and Mandarin. Patient demographic data as well as information regarding the type of procedure performed was recorded. The survey included semi-quantitative assessments of intra and post-procedural access site pain levels (1-no pain, 10-severe pain). Wilcoxon test was performed using SPSS Statistics 21 (IBM Corp, Armonk, New York).
Results: Survey respondents reported having various arterial procedures including TACE (29%), Y90 (37%), and MAA injection (34%). Of the 56 patients, 12 (21%) had common femoral artery (CFA) access and 44 (79%) had left radial artery (RA) access. CFA access patients reported an access site-specific intra-procedural pain score average of 3.0 (median = 1) and post-procedure 2.3 (median = 1). RA access patients reported an access site-specific intra-procedural pain score average of 2.6 (median = 2) and post-procedure 1.7 (median = 1). Comparing the two groups, there was no significant difference in intra-procedure pain score (P=0.91) or post-procedure pain score (P=0.86). 33 patients reported having had both types of access in the past. Of those 33 patients, 27 (82%) preferred radial and 2 (6%) preferred CFA access. 4 (12%) patients reported no preference for TRA or CFA access.
Conclusions: Post-procedure survey data acquired via iPad is feasible in a recovery unit setting. Early pilot data gathered in this setting indicates no significant difference in patient reported pain levels. A strong patient preference for RA access is noted in patients who had undergone both types of access.

Poster 133: Computed Tomography Guided Placement of High Activity, Low Dose Rate (HALDR) Brachytherapy seeds

M. Warren, P. McLaughlin, E. Abu-Isa, M. Osher, D. Semaan, D. Lincoln

Objectives: The trend to fewer, high dose per fraction stereotactic treatments for primary and salvage therapy has grown rapidly in the last decade. Modern technologies are capable of delivering sculpted dose with rapid dose fall off, mimicking dose gradients associated with brachytherapy approaches. One approach that is seldom used but holds great promise employs ultra-simple implants using high activity sources. This technique would be well suited for retreatment from the normal tissue standpoint since dose is delivered over months at a low dose rate. Preliminary responses in refractory tumors suggest efficacy and safety, and a vast potential for combination therapy approaches. HALDR approach allows for CT or ultrasound guided implants to be delivered by small gauge needles to any part of the body.
Methods: HALDR brachytherapy is minimally-invasive, less disruptive in side effects, and requires a small time commitment to the procedure. For heavily pretreated solid tumors, seeds placed within the tumor under CT guidance, with an overnight stay for observation is far easier than heroic resections in a prior radiated field. Three clinical examples will be presented.
Results: Patient 1 is a 54 yo man with prostate cancer post prostatectomy treated with radiation for rising PSA. He later has a bladder neoplasm and under goes cystectomy. A small cell neoplasm of the bladder is found and subsequently treated with chemotherapy. 4 months after completion he develops a small cell metastasis adherent to the pelvic side wall. He is retreated with beam radiation and chemotherapy with a partial response. 4 months later the mass progresses and no further chemotherapeutic options remain. He underwent placement of 3 high activity I-125 sources by CT guidance delivering approximately 5 cGy/hr. He has a partial response by serial CT and continues with stable disease 36 months after implant. Patient 2 was a 50 yo woman with a head and neck sarcoma treated initially with neck dissection and post-operative radiation therapy and chemotherapy. 2 years later there is recurrence treated with partial resection, chemotherapy, and salvage external beam therapy. 1.5 years later she develops two discrete nodules in the neck ranging from 4-5 cm. She undergoes CT guided I-125 high activity seed implant with dramatic response of both lesions. 8 months later, she develops two other recurrences treated with high activity sources and again achieves excellent palliation for 6 months. Patient 3 is a 66 year old male with a pancreatic tail adenocarcinoma who had a PET CT that showed an SUV of 10.5. After treatment with chemotherapy he had minimal change in the size of the neoplasm and underwent CT guided placement of two external beam markers and two I-125 seeds (22.9 cGycm^2/hr for a total of 103 Gy). 19 days later a repeat PET CT demonstrated that the lesion had decreased in size and now had an SUV of 4.4.
Conclusions: CT guided placement of HALDR brachytherapy is a promising backup and alternative to hypofractionated SBRT approaches for salvage of refractory local-

ized solid tumors. In preliminary reports and experience such low dose rate therapy has been well tolerated even in patients treated with initial full dose with external beam and SBRT salvage, confirming the normal tissue sparing effects of low dose rate implants. Since most practitioners may employ this in very limited number of patients, an international registry may be necessary to further define the potential of this approach in anticipation of prospective trials.

Poster 134: Biomechanical Strengthening of Pre-Fractural Tumor-Induced Lesions at the Level of the Proximal Femur Using a New Implantable Device

F. Cornelis, T. Carteret, B. Lapuyade, F. Deschamps, F. Cornelis, T. de Baere

Objectives: Percutaneous cement augmentation using viscous cement can be done safely and minimally invasive to treat malignant bone lesions. Although its easy use, cement is not biomechanically relevant to prevent hip fracture (no bending resistance) since it creates micro-cracks and bone fracture. Standard osteosynthesis fixation is also performed to prevent fracture on malignant lesion and gives successful results in term of pain management and fracture prevention, however the use of metallic implant can be an issue for radiotherapy treatment. The purpose of this study is to evaluate the impact of a new prevention dedicated osteosynthesis device (PDOI) made of polymer implanted by minimal invasive approach and combined with bone cement to biomechanically strengthen pre-fractural tumor-induced lesions at the level of the proximal femur.

Methods: This study is an on-going prospective series of 10 PDOIs. To date, 8 patients were implanted for bone malignant lesions (PMBL) by interventional radiologists. Feasibility of the implantation procedure is evaluated per-operatively. Clinical evaluation includes Visual Analog Scale for Pain and Oxford Hip Score during a one year follow-up.

Results: Mean Age and BMI of patients were 62±7 years and 24±4 kg/m2 for PMBL. Mirel score was between 8 and 10 and the EGOG Functional status 1.14 (0-2). Mean duration of implantation were 101 (60-155) minutes. Four (4) patients were positioned in lateral decubitus, 4 supine. Mean cement quantity combined with the PDOI was 8 (3-10 cc). No major difficulty were reported during the implantation of the device and no severe adverse event was linked to the procedure. At 2 months, Visual Analog Scale (VAS) was 2.7 (2-3) and OHS-12 score was 29.8 (21-42). Average follow-up is 1.6 months (0-4.4) and no post-operative fracture was recorded.

Conclusions: Preliminary results of this prospective study demonstrated the feasibility of the implantation of this new PDOI by an interventional radiologist. This new treatment for pathological fracture prevention seems to be a promising alternative. Learning curve should improve the implantation duration. Further follow-up data are required to confirm this preliminary experience.

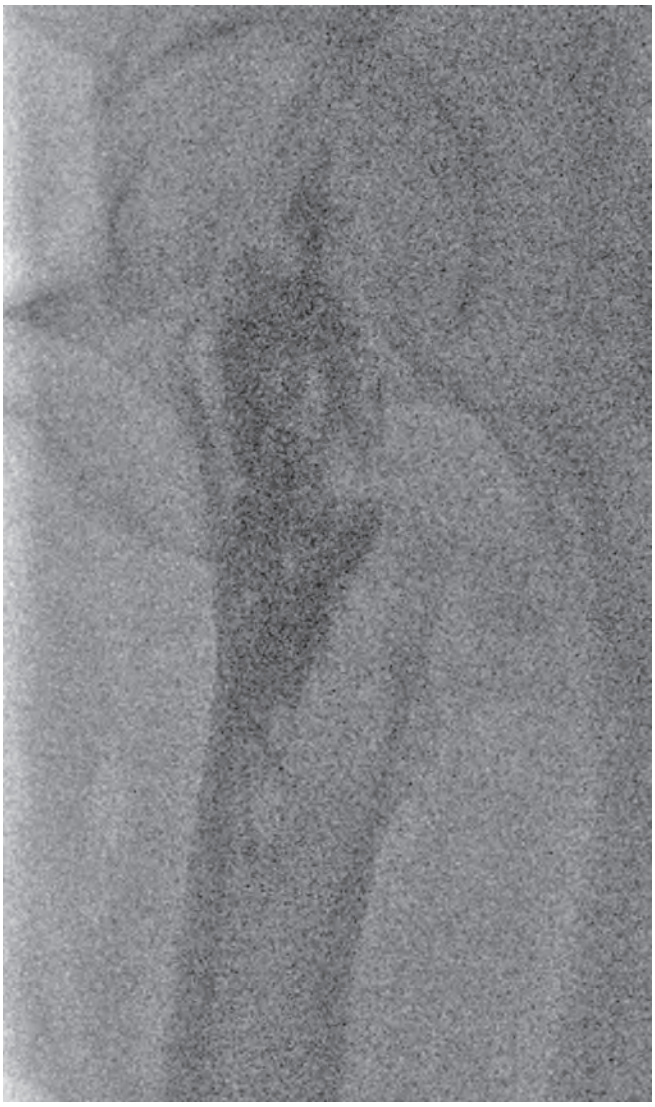

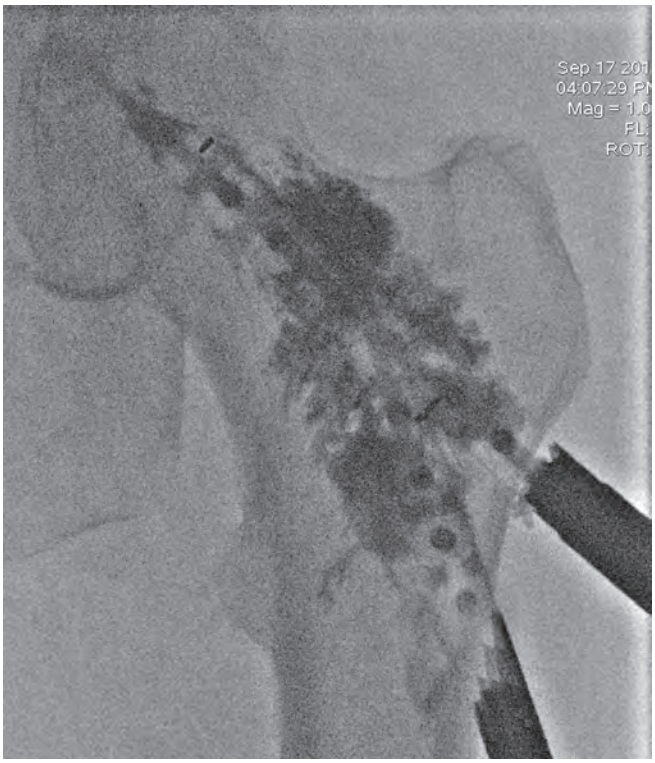

Poster 135: Combined Radiofrequency Ablation and Laser Ablation Blocking Hepatic Vascular of Dogs: In Vivo Experimental Studies

X. Xie

Objectives: Objective To explore the feasibility and experimental conditions of laser ablation in blocking great liver vessels of dogs and whether the volume of radiofrequency ablation could be expanded by blocking the blood vessels.
Methods: Methods Twelve UK Beagles was numbered as D1 ~ D12. Laser ablation was used to block the left hepatic blood vessels of D1 ~ D7 firstly, with the fiber exposed of 1.0cm and total power of 1800J. Laser ablation was end when color Doppler imaging showed no blood signal in the selected portal vein and hepatic artery. Contrast enhanced ultrasound (CEUS) was performed to assess the blood supply of the selected lobe of canine liver 30min after laser ablation. Right after CEUS was performed, single needle single point radiofrequency ablation was carried out in this lobe. The same procedure of radiofrequency ablation was performed in the left lobe of D8 ~ D12. The volume of radiofrequency ablation was measured using CEUS 6 days after ablation.
Results: Results When 7W-power was used, the selected liver lobe show no enhancement on CEUS after laser ablation. The average ablation volume was (87.6 ± 70.8) cm^3 in D1~D7 and (10.0 ± 2.0) cm^3 in D8~D12, the difference was statistically significant (P = 0.027).
Conclusions: Conclusion: Great liver vessels of dogs could be partially or completely blocked by using laser ablation, causing liver lobe to part or all of ischemia or necrosis; the volume of radiofrequency ablation could be expanded by blocking the blood vessels.

Poster 136: Use of the PhaSeal Transfer System during Chemoembolization to Prevent Unintentional Leakage of Chemotherapeutic Agents during Preparation and Delivery

S. Contractor, J. Thomas, U. Shahid

Objectives: The contamination of the work environment during drug delivery and transfer has been previously reported in the literature, and this is especially concerning given that inadvertent absorption of hazardous drugs has been shown. The Occupational Safety Administration and National Institute of Occupational Safety and Health guidelines recommend the use of closed-system-transfer-devices during handling of vesicant and chemotherapeutic agents. Currently, most IR practices utilize open transfer system devices to prepare and administer the chemo-embolic suspension, resulting in potential and actual contamination of the procedure field with these hazardous agents. There are available closed system transfer devices that could potentially eliminate this risk. Review the PhaSeal closed transfer system in the preparation and administration of ethiodized-oil-chemotherapy-agent-suspension during transarterial chemoembolization procedures, and outline instructions for use.
Methods: In our institution, we began to use the PhaSeal transfer system in the interventional radiology suite for tha past 9 months, and we present our experience with approximately fifty patients over a 6 month period. The transfer device consists of 3 components that have a leur lock connection and enable leak proof transfer of the chemotherapeutic drugs and Ethiodol during the preparation and administration of the chemo-embolic suspension(Fig 1). The chemotherapeutic and lipiodol is mixed using the closed transfer system of the device (Fig 2). The chemo-embolic suspension is injected into the microcatheter with a 3 cc syringe and the phaseal system. 50 hepatic chemoembolizations using chemotherapy (Doxorubicin and mitimycin with Lipiodol) were performed using this device to transfer and prepare chemoembolic cocktail
Results: All procedures were performed successfully with minimal learning curve for the device components. No procedure had any inadvertent spillage of chemotherapeutic- lipiodol suspension on to the procedure field or operator. The advantages of this system include the ability to "lock in" the suspension when not being injected, as well as the use of a single system to complete and entire procedure. A step by step illustration of the device and components along with use instructions will be discussed.
Conclusions: Closed system transfer devices allow leak proof preparation and administration of hazardous agents. The PhaSeal closed transfer system reduces the contamination of the procedure field. A basic knowledge of this device will enable the interventionalist to ensure a safe and effective workplace environment

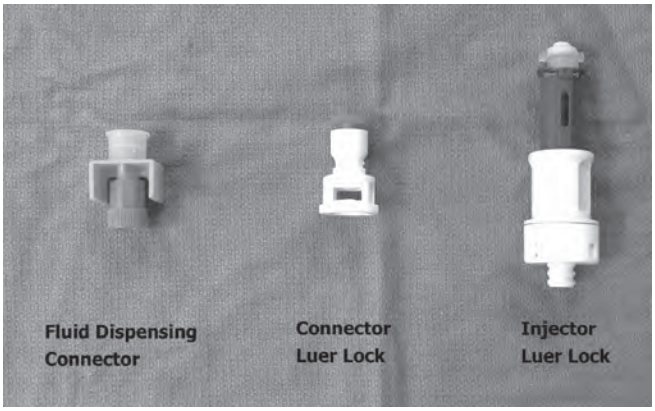

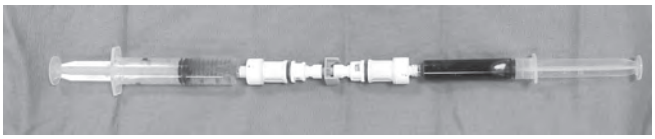

Poster 137: Sterile Evaluation of PACS Imaging Intra-Procedurally Using the Leap Motion Controller

K. Stewart, T. O'Neill, N. Akle

Objectives: To demonstrate the feasibility of reviewing prior imaging intra-procedurally during transarterial chemoembolization (TACE) procedures by physicians, while remaining sterile, using the Leap Motion Controller.
Methods: The Leap Motion Controller is a computer peripheral device which utilizes infrared cameras to enable touchless three-dimensional motion controlled computer interaction. A custom application, written using the Leap Motion application programming interface (API) detects hand movements and gestures and translates those motions into image manipulation commands that are sent to the picture archival and communications system (PACS) viewer. The custom software allows PACS to be controlled by hand movements instead of by a traditional computer mouse. The physician's hand does not come in contact with the device, but is placed in the air over the device. This allows the physician to maintain a sterile field while navigating through PACS. The Leap Motion device and the custom software were installed onto a computer running PACS for use in the interventional suite during TACE procedures. Physicians were given basic instruction on hand gestures used to control the device prior to the procedures and the device was made easily accessible to them in the interventional suite during the procedures. A post-procedure assessment of operator satisfaction with the device and software was conducted.
Results: Physicians were able to access prior images during TACE procedures, scroll through images within a series and change between series while staying sterile using the Leap Motion Controller. Operators were satisfied with their ability to review images in PACS and felt that it would be of benefit to them as they performed procedures. They also felt that the functionality could be further improved by adding additional features commonly used at the reading station.
Conclusions: Physicians often need to access prior imaging during procedures to evaluate anatomic relationships and variant anatomy to help guide their procedures. The Leap Motion Controller was used by physicians to review images while remain-

ing sterile as an alternative to scrubbing-out or relying on over-the-shoulder review with the technologists. Novel applications of new technology in interventional suites, operating rooms and other procedure rooms stand to benefit the physician performing the procedure by making intra-procedural imaging review easily accessible and more efficient.

Accessing imaging in PACS while maintaining a sterile field using the Leap Motion Controller.

Poster 138: A Novel Dual Infusion Protocol to Evaluate Differences in Embolic Therapies Among Different Infusion Catheters

R. Stanborough, A.C. Bourgeois, Y.C. Bradley, J. McElmurray, A. Pasciak

Objectives: The selection of infusion catheters for use in transcatheter liver-directed embolotherapy is largely dependent upon operator preference, device familiarity, and empiric evidence. This is at least partially attributable to the absence of standardized performance data of catheters for delivering liver-directed therapies. Recent studies have suggested differences in microsphere distribution may result from varying infusion catheters. Today, no clear objective evaluation method in human patients is documented. We present a novel same-day, dual infusion technique in which differences in embolic distribution among varying catheters can be directly compared.
Methods: This study was conducted with informed consent and IRB approval. An initial lobar infusion of 99mTc -MAA was administered to patients with a nominal activity of 100 MBq for the purposes of lung shunt fraction evaluation prior to yttrium-90 radioembolization. A second, same-day 600 MBq 99mTc-MAA infusion with identical technique was performed with a different microcatheter. Fluoroscopic images confirmed near-identical catheter placement. Differences in 99mTc-MAA distributions within tumor and non-target sites were evaluated via SPECT imaging on a qualitative and semiquantitative basis. Considering only the physical decay of the 99mTc, the maximum calculated residual activity from the first infusion was less than 15% of the second infusion activity, rendering the residual persistent activity negligible for the second image set.
Results: This method has been employed in several cases at our institution with reproducible alterations in MAA distributions among variable catheters, confirming its validity.
Conclusions: This dual-infusion method is conceptually a similar technique to that used in same-day renal and cardiac perfusion studies and could be employed for objective comparison of microcatheter performance in liver-directed therapy.

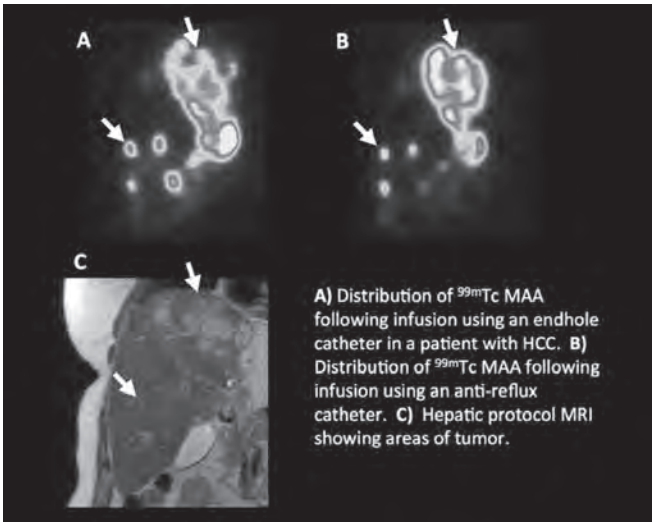

Poster 139: Toward a Robotic System for MRI-guided Focal Laser Ablation of Prostate

R. Seifabadi, Y. Chen, A. Squires, S. Xu, H. Agrawal, M. Bernardo, P. Pinto, P. Choyke, Z. Tse, B.J. Wood

Objectives: Over 225,000 people are diagnosed with prostate cancer annually in the US with around 30,000 deaths. Early diagnosis along with radical prostatectomy can reduce mortality rate in localized cancers. However, prostatectomy has been shown to overtreat the cancerous tissue, resulting in permanent sexual dysfunctions and incontinence. Prostate Focal Laser Ablation (FLA) is a localized treatment that destroys a predefined region of the prostate gland through precisely targeted heat which is performed under image guidance. MRI has been used as an imaging modality of choice as it provides excellent guidance for needle placements, thermometry, and damage visualization. Our study was to improve the precision of needle placements in prostate FLA using a robotic system integrated with Visualase® (a FDA approved system for FLA) since the positioning grid template of the Visualse system has a nominal accuracy of > 2.5mm.
Methods: System components: The proposed system comprises of robot hardware (including robot, holder, board, controller, and User Interface), MRI scanner, Laser ablation system (Visualase Inc.), and Navigation software (NIH OncoNav). **Robot Hardware:** Fig. 1 shows the robot in a rectangular shape, mimicing the FLA grid template (Fig. 1-b) and moves a needle guide in x nad y directions with sub-millimeter accuracy. The robot was 3D-printed with ABS plastic, assembled with brass screws and motorized with pneumatic motors and optical encoders. The robot controller (containing pneumatic valves and a microprocessor) is placed in control room. **Workflow:** 1) the robot together with the patient was setup inside the MRI scanner. 2) Images were acquired and streamed to OncoNav. 3) Registration was performed between the robot and the scanner coordinates. 4) Targets specified by the physician, were sent to robot controller software. 5) The robot aligned the needle trajectory for manual insertions. **MRI compatibility test:** The robot was introduced to the MRI isocenter, and tested with the conditions of the robot's power off (1), power on (2) and (3) the robot with both motors activated. Images of a saline phantom were taken in (1-3) and compared with the baseline (without the robot) to calculate the image Signal to Noise Ratio (SNR) reduction and image artifacts. **Calibration accuracy test:** Five MRI gadolinium spherical markers were embedded in the robot frame. After MRI scans, scanner-robot registration was performed. The robot moved the needle from its initial location to the target. A verification scan was taken to measure the distance between the target and the needle tip. **Open-air Targeting accuracy test**: A donut shape gadolinium marker was placed concentric to needle and the robot was commanded to different targets within a prostate phantom. The distance between the desired target and the actual location of the needle was measured in images as the targeting error.
Results: Maximum SNR reduction was 7.8%. No image artifact was observed. The fiducial registration error was 2.1 mm. The RMS targeting error was 1.17 mm (STD = 0.47 m m) for all targets (N=3).
Conclusions: Robotic FLA needle placement could reduce the targeting error compared to a conventional grid template approach.

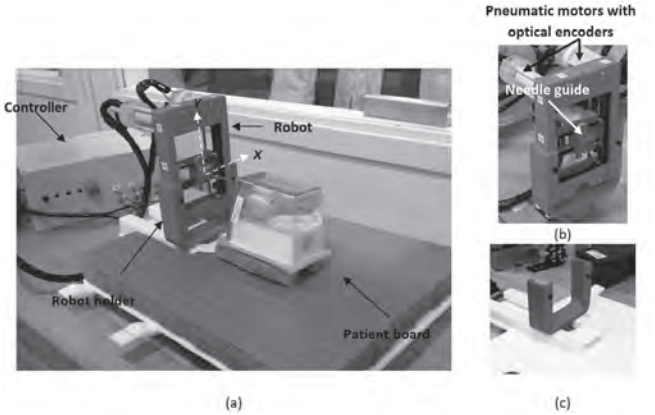

A pneumatic robot for FLA. (a) Robot hardware components, (b) Close-up view of robot, (c) robot holder.

Poster 140: Clinical Efficacy and Patency of Stents for Malignant Iliocaval Venous Obstruction

G. Kim, M. Kim, J. Won, S. Park, D. Lee, M. Shin

Objectives: To evaluate clinical efficacy and patency of the stents for symptomatic iliac vein or inferior vena cava (IVC) obstruction caused by tumor invasion or extrinsic compression.
Methods: From May 2003 to June 2014, 34 patients with malignant iliac vein or IVC obstruction underwent stent indwelling in our institution. We reviewed their electronic medical record, pre- and post-procedural CT scans, and angiograms retrospectively, and evaluated technical success (successful recanalization and restoration of venous return), clinical success (improvement of edema at discharge), patient-based and vessel-based reocclusion rate. We also assessed the difference of reocclusion rate between IVC and iliac stents using Fisher's exact test.
Results: The patients consisted of 18 men and 16 women, and their mean age was 63.1 years. They suffer from leg and/or trunk edema. The locations of the stents were IVC in 9, iliac veins in 19, and both IVC and iliac veins in 6 patients. Technical success rate was 100% and clinical success rate was 87.5%. follow-up CT scans were available in 21 patients and median follow-up period was 65 (7 – 3167) days. Patient-based reocclusion rate was 42.8% (9/21). Vessel-based occlusion rates were 12.5% (1/8) for IVC and 45% (9/20) for iliac vein. Fisher's exact test showed significant difference of reocclusion rate between IVC and iliac vein stents (P = 0.048).
Conclusions: Stent insertion for malignant iliac vein or IVC obstruction is technically feasible and can help to improve patients' symptoms. And IVC stent tend to remain patent than iliac vein stent.

Poster 141: Safety of Irreversible Electroporation in Liver Tumors

J.C. Tasse, A. Masrani, P. Smith, A. Chen, J. soni, B. Arslan

Objectives: Discuss Irreversible Electroporation (IRE) as a relatively new percutaneous tumor ablation technique that primarily uses electrical currents to induce tumor cell lysis and death. Describe benefits of IRE in patients that are not candidates for thermal ablation (cryoablation, radiofrequency ablation, microwave) due to tumor proximity to bowel or blood vessels. Present our limited short-term experience with this ablation method.
Methods: We performed an electronic chart review of all cases where IRE was used as an ablation method in our institution. All patients with at least one follow-up imaging exam were included. Procedural notes and potential complications were reviewed as well as all imaging to assess for lesion characteristics, procedure related complications and recurrences during follow-up. Complications that we evaluated for were: liver failure, hydrothorax, pneumothorax, tumor seeding, gastrointestinal hemorrhage, intra-hepatic abscess, non-target organ damage, cardiac arrhythmia or arrest and post ablation syndrome.
Results: Total of 7 patients underwent hepatic IRE between Jan 2013 and Aug 2014. Lesions ranged in size from 1.4 cm to 4.4 cm. Six out of eight patients were treated for hepatocelluar carcinoma (HCC) secondary to liver cirrhosis with goal to bridge to transplanatation. One patient was treated for colorectal carcinoma with solitary metastasis to the liver. Of the HCC patients follow up times ranged from 1-13 months. One patient was transplanted after 9 months and another patient expired due to liver failure, which was considered unrelated to the IRE ablation as the procedure was 5 months earlier. None of the lesions showed growth or persistent enhancement in the follow up period. For the CRC patient, follow up was 1 month. The patient had stable tumor size and resolution of its PET positivity, at 1 month follow-up. None of the patients had any complications related to the ablation procedure. They were all discharged after a 24 hour observation period to home.
Conclusions: Our limited short term experience with this new ablation method is very positive with no significant side effects and excellent outcomes. We feel this ablation method is very promising, especially for patients not eligible for thermal ablation due to proximity to neighboring bowel or blood vessels. Further studies with larger patient enrollment are needed to show continued safety and evaluate efficacy.

Poster 142: I-Mode: New Technology for Cool Tip Thermoablation Needles. Can it Improve the Area of Ablation in Liver Primary and Metastatic Disease?

T. Cabrera, V. Desmers, L. Boucher, C. Torres, K. Muchantef, D. Valenti

Objectives: Image-guided ablation is one of the leading therapeutic alternatives for malignant liver tumors, whether primary or metastatic, in patients unsuited for surgical resection. The thermal lesion size depends on the energy delivered and the interaction with the surrounding tissue. The ideal scenario is maximum energy delivery with minimal tissue charring tissue. The aim of this study is to compare the Cool-Tip RF Ablation System E Series i-mode with the regular Cool-Tip technology.
Methods: A review of our prospective database of patients treated by image-guided RFA from July 2013 to November 2014 was performed. Other ablation modalities were excluded. A total of 141 patients underwent RFA. In 25 patients the Cool-Tip system was used and in 25 patients the Cool-Tip RF Ablation System E series with i-mode energy deliver system was used. All patients were followed with a 3 week post-ablation CT scan and then imaging follow-up every 4 months with either MRI or CT. Short and long term imaging was reviewed retrospectively for assessment of thermal lesion size, borders, and residual tumor. Immediate complications and long term complications were analyzed.
Results: A total of 35 lesions in 25 patients were treated using the i-mode system and 30 lesions in 25 patients were treated with the conventional Cool-Tip system. In every case tract cauterization was performed. The mean follow up time was 105 days. Among the 25 patients treated with i-mode system, 1 had residual tumor that required a second treatment of RFA and 1 had significant disease progression at the ablation area and in the lungs. Two patients that underwent conventional Cool-Tip system had local and systemic progression. On the follow up images, the i-mode thermal lesion were larger (but not statistically significant) and had better defined borders.
Conclusions: There are continuous technical improvements in many of the energy delivery systems. In our study comparing the conventional Cool-Tip technique with the new i-mode progressive energy delivery, no statistically significant difference was identified, however the thermal lesions seems to be larger, and perhaps more importantly, with better defined borders using the i-mode. The oncological results were similar. Larger comparative studies would be helpful to further define the distinctions between these technologies.

Poster 143: Safety and Mid-term Efficacy of Percutaneous Image-Guided Irreversible Electroporation in Primary and Secondary Solid Tumors

J.C. Tasse, P. Smith, C. stuart, A. Chen, J. soni, B. Arslan

Objectives: Report our single institution experience and discuss mid-term follow-up results of percutaneous Irreversible Electroporation (IRE) in multiple types of primary and secondary lesions throughout the body.
Methods: Retrospective review of all patients undergoing IRE of solid tumors by interventional radiology between January 2013 and June 2014. IRE was performed using the Nanoknife system (Angiodynamics, Latham, NY) and all cases were performed using CT guidance with general anesthesia and cardiac synchronization. Biopsy was performed to confirm malignancy prior to ablation in all cases except HCC cases diagnosed by imaging criteria. Patient demographics, tumor characteristics and procedural outcomes were recorded. Complications were classified as major vs. minor per SIR criteria. Number of probes used and length of procedure were also recorded. Technical success was defined as successful placement of probes within the lesion as determined at preoperative planning and completion of all ablation cycles. Post-IRE follow up imaging (CT, MR and/or PET) were performed at various intervals for different tumor types as clinically indicated. Successful ablation was defined by lack of residual enhancement or growth or resolution of hypermetabolic activity of the treated lesion, compared to the patient's most recent imaging follow-up.
Results: A total of 24 tumors in 22 patients were treated with IRE during the defined time period. Mean age is 58 years (12-75) and average tumor size is 2.6 cm (1-5.6). Tumor type are 6 HCC and 2 metastatic colorectal adenocarcinoma of liver, 8 renal cell carcinoma and 1 pheochromocytoma of the kidney, 1 soft tissue Ewing sarcoma metasasis adjacent to the sacral plexus, 1 retroperitoneal colorectal adenocarcinoma metastasis, 1 adrenal leiomyosarcoma metastasis, 2 osteosarcoma metastases to lung and 2 ovarian granulosa cell abdominal wall metastases, Mean follow-up is 185 days (1-622 days). All cases were technically successful. No major complications were observed. Minor complications included paresthesia (1) and pain (13). Of the 8 hepatic lesions no residual enhancement was seen at mean follow up 145 days. 7/9 renal lesions showed no residual enhancement at mean-follow up of 180 days. 2 local renal recurrences were seen, both approximately 1 cm in size at 230 and 320 days. Both

lesions were successfully treated with subsequent cryoablation. One 3 cm soft tissue Ewing sarcoma metastasis adjacent to the sacral plexus showed no growth at 420 days. 1 retroperitoneal colorectal carcinoma metastasis showed no growth 312 days post-ablation. 1 adrenal leiomyosarcoma metastasis showed no growth 241 days post ablation. 2 metastatic osteorsacoma lung lesions were successfully ablated for debulking with intention to improve chemotherapy response. Additional IRE ablations with goal for pain relief were successful in a patient with 2 metastatic ovarian granulosa cell metastases to the abdominal wall.
Conclusions: Percutaneous IRE demonstrates favorable safety and efficacy in the treatment of solid primary and secondary tumors, not technically amenable for treatment with conventional ablation techniques.

Poster 144: A Contemporary Review and Clinical Experience of Tract Closure Devices after CT-Guided Percutaneous Lung Biopsy

J. Shah, S. Kantharia, J. Moseley, M. Oselkin, S. Honig, S. Sobolevsky, S. Corelli, D. Mobley

Objectives: Specific Objectives: 1. Review lung anatomy and physiology in the context of lung biopsy. 2. Discuss the various risk factors for pneumothorax. 3. Review the various methods and published data regarding the efficacy of sealing the biopsy tract.
Methods: Percutaneous transthoracic lung biopsy is a mainstay in the workup of pulmonary and pleural lesions due to the relative accessibility, high diagnostic yield, low cost, and relatively low risk. The most common complication of transthoracic needle biopsy is a pneumothorax, thought to be secondary to air leak via the needle tract in the lung. While the majority of pneumothoraces are clinically insignificant, they cause anxiety on the part of both the patient and interventional radiologist due to the risk of delayed presentation and subsequent respiratory decompensation. Up to 5% will require chest tube placement and subsequent hospitalization, transforming an otherwise brief outpatient procedure into an hospital admission. While they have yet to become standard of care, numerous techniques have been utilized to mitigate the risk of pneumothorax including hydrogel plug, gel foam pledget, isobutyl-2-cyanoacrylate, blood patch, and fibrin plugs.
Results: Content Organization: A. Pictorial review of anatomy, pathophysiology, and diagnostic imaging of needle biopsy and pneumothorax. B. Review of commonly employed methods to decrease the risk of a post procedural pneumothorax C. There is a growing body of literature that supports the postprocedure use of these indivudal techniques over no intervention. Review of the published literature on the efficacy of these methods
Conclusions: Given the high frequency of transthoracic needle biopsy and the potential risk of pneumothorax, it is prudent to be familiar with the availability of various tract closure techniques. Being familiar with these techniques and options allow interventional radiologist / oncologist to potentially decrease complications and reduce costs to patient and provider.

Poster 145: Percutaneous High-Energy Microwave Ablation (MWA) for the Treatment of Solid Thoracic Tumours: 105 Tumour Deposits Treated at a Single Centre

S. Bandula, Y. Egashira, T.A. Buchan, R.O. Illing

Objectives: High-energy microwave ablation (MWA) is being increasingly used as a minimally invasive alternative to surgery for the treatment of solid tumour deposits in the thorax, however relatively little data has been published on treatment outcomes. We report complications, technical success and technique effectiveness of MWA procedures performed at a single tertiary referral centre.
Methods: A local ethics committee approved the review. Prospectively collected data on patient and tumour characteristics, procedure technical success and computed tomography followup imaging were collected. Technique effectiveness was deemed to be lack of unexpected late local recurrence at the treatment site after a technically successful treatment.
Results: Between June 2012 and June 2014, 105 solid tumours in the thorax were treated with microwave ablation in 55 patients (mean age: 63 years; range: 12-89, 24 men and 30 women). In these patients the primary tumour origin was colorectal (n=20); sarcoma (n=24); lung (n=7); oesophagus (n=1); breast (n=1) and bladder (n=1). The mean(SD) tumour size was 14mm(6.7mm). Technical success was 96%, mean followup interval was 13.8 months (range; 1-28.5). Local tumor progression was observed in 2 out of 102 cases (2%) and occurred within 6 months of MWA. Pneumothorax requiring chest tube insertion occurred in 13 out of 77 sessions (17%). Of these 13, pneumothorax was intentionally induced in 3 patients during treatment, 5 were unintentional but inserted at the time of treatment and 5 were unintentional and inserted post procedure. There were no other major complications. Overall survival rate was 97.5% at 1 year and 77.5% at 2 years.
Conclusions: Microwave ablation of solid tumour deposits is safe and effective. This cohort compared very favourably to other modalities including radio frequency ablation. A prospective trial evaluating microwave ablation of solid tumour deposits versus stereotactic ablative body radiation (SABR) therapy is suggested.

Poster 146: Pre-Procedural Patient Evaluation in an Outpatient Interventional Radiology Clinic Improves Success Rates for CT-Guided Lung Biopsies

S. Abboud, Y. Ahmed, S. Partovi, T. Patel, J. haaga, D. Nakamoto, N. Azar

Objectives: The study aims to assess if a pre-procedural outpatient interventional (IR) clinic evaluation impacts procedure time (PT), radiation dose, technical success rate (SR), and pneumothorax (PNX) rate for patients receiving CT-guided lung biopsy CTLB. We hypothesize that patients evaluated in the radiology clinic prior to CTLB may have improved technical SR and reduced PT, radiation dose, and PNX rate compared to patients without pre-procedural clinic evaluations.
Methods: After receiving institutional review board approval, we randomly selected 50 patient that received CTLB after pre-procedural evaluation in our outpatient IR clinic and 50 patients that received CTLB during that same time period without pre-procedural IR clinic evaluations. Total PT, defined as time between first and last images acquired during the procedure, was collected for each patient, as well as dose-length product (DLP), presence of PNX detected during or immediately after the procedure, lesion size and distance from chest wall, and patient age. A procedure was defined as technically successful if a core needle biopsy or fine needle aspiration sample was obtained from the target lesion. Non-paired T test was used to compare patient age, DLP, PT, and lesion size and distance from the chest wall.Significance test for proportionswas used to compare SR and PNX rate between groups.
Results: Clinic and non-clinic patients were not significantly different in terms of age ($P = 0.65$), lesion size ($P = 0.36$), lesion distance from chest wall ($P = 0.89$), or DLP ($P = 0.18$). PT for Non-clinic patients (mean =38 minutes) was significantly shorter than for clinic patients (mean = 44 minutes) ($P = 0.035$). SRwassignificantly better for clinic patients (98%) than non-clinic patients (89%) ($P = 0.025$). No significant difference was found in PNX rate of clinic (22%) and non-clinic (24%) patients ($P = 0.41$). No patients in either group required chest tube placement for PNX.
Conclusions: Pre-procedural IR clinic evaluation may improve procedural success rate in patients receiving CTLB, but not necessarily reduce procedure time or radiation dose. The impact of pre-procedural outpatient radiology clinic evaluations on clinical outcomes for various IR procedures merits additional investigation.

Poster 147: Incidence of Major Cardiac Arrhythmias During Microwave Ablation of Lung Tissue Near the Heart: A Pilot Study in an In Vivo Porcine Model

G. Carberry, P. Mason, T. Warner, C. Brace, F. Lee

Objectives: Thermal ablation of primary and metastatic lung malignancies is an increasingly accepted treatment option for patients refractory to surgery. As a result of this, larger tumors and tumors in close proximity to the heart are being targeted for ablative therapy. While the incidence of cardiac arrhythmias has been studied with radiofrequency ablation and cardiac gated irreversible electroporation, little data exist on the arrhythmogenicity of microwave (MW) ablation near the heart. The objective of this pilot study is to evaluate the effect of antenna distance from the heart on the development of cardiac arrhythmias in a normal animal model.
Methods: This study was performed under approval from our institutional animal care and use committee and complied with National Research Council guidelines. Eleven open MW ablations adjacent to the pericardium were performed in two domestic swine following anesthesia and median sternotomy. A single PR MW antenna (Certus 140, NeuWave Medical, Madison, WI) was positioned directly against the pericardium, or within lung tissue 10 mm or less than 5 mm in distance from the surface of the pericardium, under direct visualization. Ablations were performed within lung tissue adjacent to all cardiac chambers except for the left atrium due to antenna positioning limitations associated with open thoracotomy. The emission zone of the antenna was aligned parallel to the pericardium and contact between the emission zone and pericardium was maintained throughout the cardiac cycle during each ablation. The MW generator power was set at either 50 or 65 W with ablation periods lasting from 30 to 60 seconds. ECG and Sp02 tracing were acquired during and after each ablation. A cardiologist interpreted the ECG tracings and all arrhythmias were categorized as major (ventricular tachycardia, ventricular fibrillation and heart block) or minor (nonspecific T-wave changes, ST-T elevation and transient supraventricular arrhythmias). Following the experiments, the heart and lungs were removed en bloc for pathologic analysis.
Results: No major arrhythmia developed when the emission zone of the antenna was positioned 10 mm from the pericardium. A major arrhythmia occurred in 6/9 ablations (67%) when the emission zone of the antenna was within 5 mm of the pericardium. The average length of time into an ablation before an arrhythmia developed was 64 seconds for a major arrhythmia and 18 seconds for a minor arrhythmia, suggesting focal thermal injury as opposed to cardiac electrical stimulation as the etiology for

arrhythmia. All major arrhythmias were preceded by a minor arrhythmia. Ventricular tachycardia occurred in four cases whereas ventricular fibrillation and heart block occurred in one case each. No bradycardic rhythm occurred to suggest vagal nerve stimulation. A major arrhythmia occurred with the MW antenna positioned next to all evaluated cardiac chambers.

Conclusions: 1. Positioning the MW antenna emission zone < 5 mm from the pericardium in an orientation parallel to the pericardium resulted in both major and minor arrhythmias. No arrhythmias were encountered when the emission point was 10 mm from the pericardium. 2. Major arrhythmias were preceded by minor arrhythmias. 3. Induction of arrhythmias appears related to focal thermal injury, not direct cardiac electrical stimulation.

Poster 148: Evaluation of Pain Reduction after Percutaneous Thoracic Cryoneurolysis in Chest Wall Metastatic Patients

A. Kalenderian

Objectives: To prospectively determine the safety and effectiveness of percutaneous cryoneurolysis for pain reduction, improvement in daily life activities, and reduction in the use of analgesic medications for patients with painful metastatic lesions involving chest wall.

Methods: From January 2012 to June 2014, 32 cryoneurolysis of chest intercostal nerves were performed on 12 patients (six men, six women; ages ranged, 17 to 79 years; mean age, 60 years). Median pre-operative EVA was 7 out of 10 (max 8, min 5) for worst pain in a 24-hour period. Inclusion criteria were neurological pain, failure of third level opioid treatment and high side effects, attested by the coverage-care of pain equip. Chest nerve roots incriminated of the pain were determined after clinical examination and confirmed by recent CT or MRI exams. During consultation, interventional radiologist asked patients to rate their worst, least and average pain in 24h with response from 0 to 10 (0, no pain; 10, pain has bad as you can imagine). Relief of pain through the use of pain treatment or medications was recorded on a 0%-100% scale (0%, no relief; 100% complete relief). Cryoneurolysis was done under CT guidance under general anesthesia or neuroleptanalgesia. A single cryoprobe (ice Rod® or ice sphere® -Galil Medical) was placed on each chosen chest wall root.

Results: Technical success was 100%. No major complication occurred. The median hospital stay was 2 days (1-4 days). At day 1, week 1, week 2, week 4, median EVA was respectively 1.5, 2.5, 3,3.5 of 10, and relative change from initial EVA : -77.25%, -61.05%, -55.07%, -47.72%. After the first month, median EVA was 5 of 10, with a median relative change of -38.87 % from the pre-operative EVA. Because of poor performance status and palliative state, median follow-up was 5 months (max 15.5 months, min 10 days).

Conclusions: Cryoneurolysis is a safe and effective method for palliation of pain due to metastatic disease involving chest wall. Pain reduction is sharper during the first month. Pain recurrence can be explained by disease progression itself in multi metastatic patients.

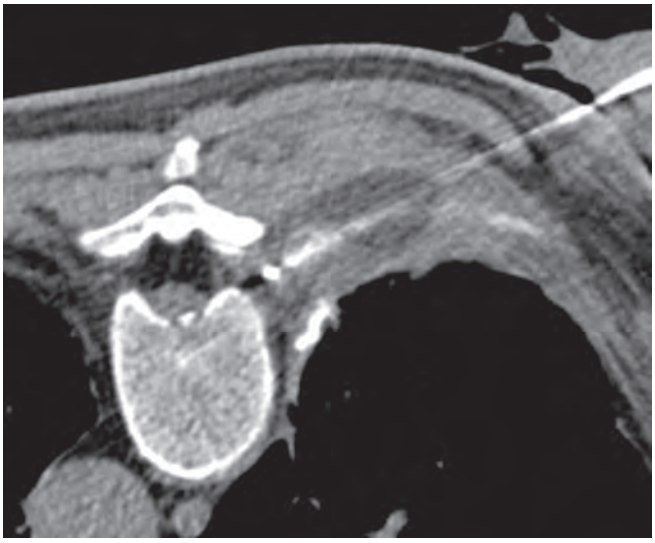

Poster 149: Interventional Radiology and Lung Cancer: From Diagnosis to Treatment

V. Gowdra Halappa, O.M. Teytelboym, S. Chan, I.R. Kamel, A. Brandis, S. Simmons

Objectives: Lung cancer is the leading cause of cancer deaths in the United States. Optimal care requires a multidisciplinary team including diagnostic radiologist, interventional radiologist, oncologist, surgeon, radiation oncologist and pathologist. Interventional radiologists have a crucial role in management of patients with lung cancer from diagnosis to treatment. Percutaneous ablation of primary and metastatic lung tumors by radiofrequency or cryotherapy represent a major advance in interventional oncology. The exhibit provides a comprehensive overview of diagnostic and therapeutic interventional radiology procedures, including post treatment evaluation in primary and metastatic lung cancer.

Methods: 1) Review percutaneous lung biopsy techniques 2) Review minimally invasive interventional oncology treatment procedures in primary and metastatic lung cancer including, a) Cryoablation b) Radiofrequency ablation c) Microwave ablation 3) Review efficacy, complications and post treatment evaluation of various techniques. 4) Provide practical tips for daily practice 5) Summary

Results: This exhibit reviews the role of interventional radiologist as part of the multidisciplinary team in diagnosis and treatment of lung cancer including percutaneous lung biopsy and minimally invasive treatment options like cryoablation, RFA and microwave ablation.

Conclusions: Interventional radiologist plays a crucial role within the multidisciplinary approach in diagnosis and treatment of lung cancer. The exhibit describes review of various minimally invasive procedures performed by interventional radiologists from lung biopsy to minimally invasive procedures including cryoablation, RFA, microwave ablation. The exhibit provides a comprehensive review of techniques, efficacy, complications and post treatment evaluation in primary and metastatic lung cancer.

Poster 150: Using 18F-FDG PET/CT Scan to Further Predict Lung Nodule Malignancy in Patients Prior to Percutaneous CT-Guided Core Lung Biopsy: A Retrospective Look at 128 Patients

R.H. Dunlap, E. Rotem

Objectives: To investigate the utility of 18F-FDG PET/CT scan prior to percutaneous CT-guided core lung biopsy in improving malignancy detection rates in patients with pulmonary lesions suspected of malignancy.

Methods: With a power calculation of 80%, 128 patients who underwent percutaneous CT-guided core lung biopsy for suspected malignancy at our center were included in the retrospective study. A case control model was used taking patients who had an 18F-FDG PET/CT scan prior to biopsy as cases and those who did not as controls. Historical data, radiographic lesion characteristics, and pathological diagnoses were extracted from patient records. Non-continuous and continuous variables were examined with chi-square and t-student analysis for statistical significance pertaining to malignancy detection. Logistical regression was used to remove confoudning variables.

Results: Of the 128 patients, 71.1% (n=91) had biopsy proven malignancy. The 34% (n=44) who had an 18F-FDG PET/CT scan with an 18F-FDG active lesion prior to biopsy were taken as cases. Among these cases, those without a previous biopsy and those with metastatic disease at the time of biopsy had a malignancy incidence of 82.9%(n=34) (P<0.01) and 100%(n=21) (P<0.01) respectively. Also in the case group, 85%(n=34) of non-calcified lesions and 67%(n=18) of primary lung processes were associated with malignancy (P<0.01 and P<0.01 respectively). Among controls, i.e the 66%(n=84) of patients who did not have an 18F-FDG PET/CT scan prior to biopsy, the average radius of the lesion and cigarette pack years were directly related to the incidence of malignancy (P< 0.01 and P<0.05 respectively). After logistical regression analysis, malignancy incidence was increased among those who had an 18F-FDG PET/CT scan prior to biopsy (B=2.112, P<0.01) as well as in those with increased number of cigarette pack years (B=0.027, P<0.05). Previous biopsy, calcification, metastatic status, and primary lung processes were found to be confounding variables influencing the incidence of malignancy.

Conclusions: The study found an increased incidence of biopsy proven malignancy in patients who had an 18F-FDG PET/CT scan prior to biopsy as well as in those with increased cigarette pack years. This translates into higher malignancy detection rates and less biopsies of benign lesions among patients who had an 18F-FDG PET/CT scan prior to biopsy. We propose that imaging patients with an 18-F FDG PET/CT scan prior to CT-guided core lung biopsy will improve the efficiency of the management of patients with identified lung lesions and avoid unnecessary biopsies.

Poster 151: Microwave Ablation of Lung Tumors: A Community Hospital Experience

S. Bagla, J.B. Smirniotopoulos

Objectives: To retrospectively evaluate the survival after ablation of primary and metastatic tumors of the lung performed in a community hospital setting.

Methods: The Institutional Review Board approved this retrospective study and informed consent was waived. 24 consecutive patients underwent 34 treatments of 34 target lesions. 17/24 of patients had primary non-small cell lung carcinomas and 7/24 patients had metastatic tumors to the lung. Clinical evaluation was performed at baseline, 30 days and 3 months, 6 months, 1 year, and 2 years. Response was assessed using Modified Response Evaluation Criteria in Solid Tumors (mRECIST) (n=29)

at 3 months and classified as: Complete Response (CR), Partial Response (PR), or Progressive Disease (PD). Complications were reported according to Society of Interventional Radiology Grading System.

Results: Overall mean tumor size was 1.96 cm (Primary N=19, mean 2.1cm, 1.2cm-4.5cm) and (Metastatic n=15, mean 1.8cm, 0.7cm–5.8cm). 33/34 treatments were technically successful with one unsuccessful case secondary to inability to place the probe safely through the tumor. Overall 30 day, 3 month, 6 month, 1 year and 2 year survival was: 100% (n=23/23), 100% (n=22/22), 95.5% (n = 21/22), 92.9% (n = 13/14) and 71.4% (n=5/7). Response rates for neoplasms were as follows: (Primary lung, n=15) CR 71.4%, PR 28.6%, PD 0.0%; (Metastatic, n=15) CR 53.3%, PR 40.0%, PD 0.07%. Four patients in the primary lung neoplasm group did not follow-up for response assessment, and one patient died prior to response assessment. Progression-free survival for the population with primary lung neoplasm was 70.6% at 12 and 24 months, with four episodes of progression at 1, 7, 10, and 12 months, and one death at four months. Recurrence-free survival was 82.4% at 12 and 24 months, with two recurrences at 1 and 5 months after therapy, and one death at four months. Progression-free survival for the population with metastatic disease to the lung was 71.4% at 12 months and 57.1% at 24 months, with two episodes of progression, both at 4 months after therapy, and 1 death at 17 months. The recurrence-free survival for this group was 85.7% at 12 months and 71.4% at 24 months, with one episode of recurrence at 10 months after therapy, and 1 death at 17 months. There were 11 complications (SIR grading A=1, B=1, C=9): 10 iatrogenic pneumothoraces (29%) with 9 thoracostomy tubes placed, all less than 24 hours in duration. One case of self-limited hemoptysis occurred and one case of self-limited neuralgia occurred.

Conclusions: Percutaneous Microwave Ablation (MWA) is a feasible and potentially safe technique for both primary and metastic neoplasms of the lung, with promising response rates.

Poster 152: Frequency of Driver Mutations in Patients Undergoing Lung Ablation for Lung Adenocarcinoma

E. Ziv, N. Ahmad, J.P. Erinjeri, E.N. Petre, C. Ridge, S.B. Solomon

Objectives: Driver mutations in lung adenocarcinoma have been well studied. The frequency of the most common mutations EGFR and KRAS are reported to be approximately 25% and 23%. These mutations confer variable sensitivity to treatment, and potentially different prognosis. Lung ablation represents an accepted modality for the treatment of primary lung cancer for non-surgical candidates. The mutation frequency of lung cancer patients treated with lung ablation has not been reported. Here we aim to determine the frequency of the most common driver mutations found in lung adenocarcinomas in patients undergoing lung ablation.

Methods: We identified a cohort of 24 patients undergoing lung ablation for primary lung adenocarcinoma and who underwent biopsies to assess for mutations in driver genes.

Results: Of the 24 patients, 11 (46%) were wild type (no driver mutations identified), 8 (33%) had KRAS mutations (either G12C or G12A), 5 (21%) had EGFR mutations (L858 or copy number loss) and 1 (4%) had a BRAF mutation (V600E). One patient had both an EGFR and a KRAS mutation. These frequencies are similar to published reports of frequency of driver mutations in the general population.

Conclusions: We have identified a cohort of patients with lung adenocarcinoma who have undergone lung ablation and who have had molecular studies to evaluate the mutation status of their tumors. The frequency of driver mutations in our cohort is similar to nationally reported frequencies.

Author Index

L

M

N

O

P

Q

R

S

T

U

V

W

X

Y

Z

NOTES

IO Central

Connecting the Interventional Oncology Community

Discover the one-stop resource for the Interventional Oncology community and network with world class leaders in IO. Visit *www.IO-Central.org* to access unique features designed to bring together physicians, researchers, industry, and members of the global IO community for online dialogue and learning.

Joining IO Central is **free of cost!**
www.IO-Central.org

- Discussion Forum
- IO News Feeds
- Industry Directory
- IO Event Calendar
- IO Video Library
- IO Insights Bi-monthly Newsletter
- Case of the Week Education Series
- IO University Education

IO Insights

Stay Up-to-date with the Latest Interventional Oncology News

IO Insights is now distributed **bi-monthly!**
Visit **www.io-central.org** to see the latest issue.

Targeted POWER You Can Trust

TheraSphere®

Power Where You Need It

Over 18,000 patients treated worldwide since 2005.[1]

While some cancers are in retreat, hepatocellular cancer is an ever-growing problem.[2] It is a challenge we must rise to meet. With ^{90}Y radioembolization, Interventional Oncology is doing exactly that, taking the fight directly to the tumor.[3–6]

At BTG we go even further.

TheraSphere® ^{90}Y glass microspheres are specifically engineered to carry far greater power than any other ^{90}Y liver-directed cancer therapy, delivering high doses of radiation to the tumor while sparing normal tissue.[3–5,7–9] The result is an ability to target an exact dose just where it's needed – all in a matter of minutes.[3–5,10] Now you can do more to maximize outcomes and to protect your patient's quality of life by limiting the battleground of treatment to the tumor.[3–5,9,11–12]

Experience the power of TheraSphere® and deliver hope where it's needed most.[3–5,7]

Imagine where we can go.

Humanitarian Device.
TheraSphere® is authorized by Federal Law for use in radiation treatment or as a neoadjuvant to surgery or transplantation in patients with unresectable hepatocellular carcinoma (HCC) who can have placement of appropriately positioned hepatic arterial catheters. The device is also indicated for HCC patients with partial or branch portal vein thrombosis/occlusion, when clinical evaluation warrants the treatment. The effectiveness of this device for this use has not been demonstrated.

References: 1. BTG, Data on file, March 27, 2015. **2.** Cancer Facts & Figures 2014. Available at http://www.cancer.org/research/cancerfactsstatistics/cancerfactsfigures2014/. **3.** Riaz A *et al. Int J Radiat Oncol Biol Phys* 2011;79(1):163–71. **4.** Hilgard P *et al. Hepatology* 2010;52(5):1741–9. **5.** Mazzaferro V *et al. Hepatology* 2013;57(5):1826–37. **6.** Garin E *et al. Int J Mol Imaging* 2011;2011:398051. **7.** Vouche M *et al. Hepatology* 2014;60(1):192–201. **8.** Kulik LM *et al. Hepatology* 2008;47(1):71–81. **9.** Walrand S *et al. J Nucl Med* 2014;55(8):1317–22. **10.** Package Insert – TheraSphere® Yttrium-90 Glass Microspheres – Rev. 12. Biocompatibles UK Ltd, a BTG International group company. Available at: http://www.therasphere.com/physicians-package-insert/TS_PackageInsert_USA_v12.pdf. **11.** Salem R *et al. Clin Gastroenterol Hepatol* 2013;11(10):1358–65. **12.** Steel J *et al. Psycho-Oncology* 2004;13(2):73–9.

11 Hines Road, Suite 200, Ottawa, Ontario, Canada K2K 2X1

www.therasphere.com

US-USTHSP-2015-0412a

BTG

btg-im.com